This is to certify that the

dissertation entitled

Kinetics and Mechanisms for Cationic Photopolymerizations of Divinyl Ethers

presented by

Eric W. Nelson

has been accepted towards fulfillment
of the requirements for

Ph.D degree in ChE

Alec Scranton
Major professor

Date 5/25/95

KINETICS AND MECHANISMS FOR CATIONIC PHOTOPOLYMERIZATIONS OF DIVINYL ETHERS

By

Eric W. Nelson

A DISSERTATION

Submitted to
Michigan State University
in partial fulfillment of the requirements
for the degree of

DOCTOR OF PHILOSOPHY

Department of Chemical Engineering

1995

ABSTRACT

KINETICS AND MECHANISMS OF CATIONIC PHOTOPOLYMERIZATIONS OF DIVINYL ETHERS

By

Eric W. Nelson

This research provided detailed pictures of the kinetics and mechanisms of a model cationic photopolymerization system, and resulted in the development of a host of analytical techniques which may now be used to characterize a broader set of cationic photopolymerizations.

In situ, time resolved fluorescence spectroscopy provided a means to characterize cationic photopolymerizations of vinyl ethers by monitoring the photosensitize intensity as a function of time. An observed reduction in fluorescence intensity was attributed to consumption of the photosensitizer, providing a means to monitor the production of active cationic centers.

The photosensitization mechanism for cationic polymerizations initiated by diaryliodonium salts photosensitized by anthracene was investigated using fluorescence and phosphorescence spectroscopy. Transient phosphorescence studies demonstrated that electron transfer occurred from the triplet state of anthracene to the initiator. The numerical solution of the photophysical kinetic equations indicated that ~95 % of the active cationic centers are produced by reaction of initiator with the triplet state.

In situ Raman spectroscopy was used to obtain complete conversion profiles as a function of time. The apparent kinetic constant for propagation, which comprises all types of propagating centers was determined. The Raman studies provided a direct measure of limiting conversion which is less than unity in these highly crosslinked polymerizations due to active center trapping.

Photo-differential scanning calorimetry (PDSC) experiments were used to determine effective kinetic constants for propagation and termination for unsteady-state divinyl ether polymerizations. The profile for the propagation rate constant exhibited a dramatic increase at the start of the reaction, plateaued, and then decreased as the reaction reached limiting conversion. The effective termination rate constant was found to be very low, with active center lifetimes approaching twenty minutes. Excellent agreement for the values of the kinetic rates constants was found with the Raman and PDSC experiments.

The temperature-dependent luminescence of tris(β-diketone) chelates of europium was used for *in situ* temperature measurements during cationic photopolymerizations of vinyl ethers. These molecular-level luminescent probes provided a real-time, noninvasive method for monitoring temperature during these high-speed polymerizations. *In situ* temperature profiles obtained using this novel technique verified the thermal effects during these highly exothermic photopolymerizations.

ACKNOWLEDGMENTS

I would like to express my appreciation to the many people that made contributions to this thesis.

First, I would like to thank my advisor, Professor Alec Scranton, for all his inspiration, encouragement and friendship during my stay at Michigan State University. Secondly, I am grateful to Jeffry Jacobs for all his assistance and the motivation he provided for completion of this work. Many of his contributions were the result of numerous discussions during the last three years.

The fluorescence and phosphorescence work in this thesis was performed in the *LASER* Laboratory, MSU Department of Chemistry. I would like to give special thanks Dr. Thomas Carter for all his assistance in experimental set-up and interpretation.

The Photo-Differential Scanning Calorimetry experiments were performed at the Department of Chemical Engineering, University of Colorado, Boulder in Professor Chris Bowman's laboratory. I am grateful for the assistance and encouragement of Dr. Bowman and Dr. Kristi Anseth with the PDSC work.

I thank professors Kris Berglund, Gary Blanchard, and Dennis Miller for serving on my thesis committee, and for making useful suggestions.

I would like to thank Arvind, Bharath, Julie, Kevin, Glen, Roger, Scott and Shail for making the laboratory and office both enjoyable and interesting. Special thanks go to Czarena Crofcheck and Brenda Becker for their work on the luminescence temperature probes and thermocouple studies.

I am grateful to the National Science Foundation (Grant No. CTS 9216939) for providing support of this research. I would also like to thank the Upjohn company for the fellowship which supported me during the last year of the project.

Finally, I would like to thank my family, friends and especially Beth Curtiss for all her encouragement, support and companionship during the completion of this work.

TABLE OF CONTENTS

LIST OF FIGURES

Chapter II.

Chapter IV.

Chapter V.

Chapter VI.

Chapter VII.

Chapter VIII.

CHAPTER I. INTRODUCTION

I.1. Issues for the Development of UV Curable Polymers

The emission of volatile organic components (VOCs) from curing inks, films and coatings is a leading cause of atmospheric pollution. Volatile organic solvents have traditionally been used to impart desirable viscosity and cure rate properties to ink and coating formulations. Typically, an ink or coating formulation must be sufficiently fluid to be easily applied (often onto a rapidly moving substrate through a series of transfer rollers), but must cure rapidly to a hard film. Historically, these processing demands have been met through the use of a rapidly evaporating organic solvent in the ink and coating formulations. Numerous studies have demonstrated that when these volatile organic solvents enter the atmosphere, they result in the formation of smog and air pollution. There is an urgent need for the development of high performance inks and coatings that will not emit VOCs to the atmosphere.

An improved, pollution-free formulation for inks or coatings must meet several stringent requirements. The cured ink or coating should exhibit good abrasion resistance, chemical resistance, flexibility, and excellent adhesion to the substrate. For applicability in a continuous web process, the formulation should have a shelf life of at least six mounts,[1] should be stable on the press, and cure very rapidly when initiated by the energy

source. Finally, to satisfy safety and environmental concerns, the formulations should be nontoxic, and should emit no volatile organic components. The required abrasion resistance and chemical resistance can be readily provided by a highly crosslinked polymer network. For this reason many traditional formulations consist of pigments and volatile solvents dispersed in multifunctional oligomers that form highly crosslinked networks upon curing. The improved formulations could be based upon highly reactive monomers of low enough viscosity that no organic solvent is necessary. If the monomers used in 100% reactive systems also have a low vapor pressure, they will emit no organic vapors during cure.

The curing of an ink or coating formulation to form a highly crosslinked polymer film could potentially be initiated by a variety of energy sources, including heat, electromagnetic radiation, and electron beam irradiation. Unfortunately, heat-initiated thermal systems typically require high temperatures to attain reasonable cure rates. The elevated temperatures not only lead to high energy costs, but could also result in significant distortions in substrate dimensions in many cases.[1] High-energy irradiation such as γ-radiation and electron beam radiation can lead to rapid cure rates in a variety of systems;[2-5] however, these techniques will most likely have very limited applicability because they would result in degradation of the substrate. Light-induced photo-polymerizations have many potential advantages for ink and coating formulations including very high reaction rates at room temperature, low energy requirements, and versatility since a wide variety of monomers may be initiated photochemically. With proper choice of wavelength and light source, degradation of the substrate can be avoided.

I.2. UV-Initiated Photopolymerizations

Photopolymerizations initiated by ultraviolet (UV) light have gained prominence in recent years for the rapid, pollution-free curing of polymer films (for reviews, see references 6-9). These solventless polymerizations proceed very rapidly with a fraction of the energy requirements of thermally cured systems, and create films with excellent properties. Ultraviolet light is a convenient energy source for photopolymerization because a variety of readily available compounds will initiate chain polymerizations upon absorption of UV light.[6-12] UV-sensitive photoinitiators are currently available for free-radical or cationic polymerizations. These photoinitiators are typically effective for a variety of incident wavelengths.[6-12] This feature is useful for UV-curable inks and coatings because the commonly used pigments may be strong absorbers of light in the visible and ultraviolet wavelengths, and an initiator which will be effective at a wavelength outside this window must be chosen.

Free-radical photopolymerizations were first reported in the literature nearly fifty years ago,[13] and are currently receiving considerable attention (for reviews see references 6-8,13). By far, the most widely used classes of monomers for UV-initiated free-radical photopolymerizations are multifunctional acrylates and methacrylates. These monomers polymerize very rapidly, and are easily modified on the ester group, allowing materials with a variety of properties to be obtained.[6] However, the acrylates are relatively volatile, and have an unpleasant odor.[6] Recently there has been growing concern over potential health hazards associated with the acrylates.[7,8,14] Several recent investigations have

demonstrated that free-radical polymerizations of multifunctional acrylates and methacrylates exhibit unusual kinetic behavior, including immediate onset of autoacceleration, the formation of heterogeneous polymers,[6,19-24] and the attainment of a maximum conversion significantly less than unity.[6,25-28] Finally, the free radical photopolymerizations are inhibited by oxygen and must be carried out under an inert atmosphere,[6,7,13] such as nitrogen.

UV-initiated cationic photopolymerizations differ greatly from free-radical photopolymerization and exhibit several advantages when compared with the free-radical photopolymerization discussed above. First of all, the cationic photopolymerizations are not inhibited by oxygen.[7,13,14,30] This feature provides a significant practical advantage for industrial processes since it is not necessary to blanket the system with nitrogen to achieve rapid cure rates. Secondly, in contrast to the free-radical polymerizations which experience a rapid decrease in polymerization rate when the light source is removed (due to radical-radical termination reactions), the cationic polymerizations will proceed long after the irradiation has ceased, consuming nearly all of the monomer.[13,33] Finally, cationic photopolymerization is a very versatile technique, and may be used to polymerize important classes of monomers, including epoxides and vinyl ethers.[14,30-35] Although these classes of monomers cannot be cured by free-radical polymerizations, they exhibit many desirable properties, including low volatility, good rheological properties and negligible toxicity. Cationic photopolymerizations of divinyl ethers proceed to completion in less than a minute when exposed to ultraviolet (UV) light.[14,30-35] However, fully formulated mixtures containing monomer and initiator are completely stable in the absence of UV light, eliminating the need for mixing immediately before

use. Furthermore, the cured polymer films associated with these monomers exhibit excellent clarity, adhesion, abrasion resistance, and chemical resistance.[13,14,34,35]

I.3. UV-Sensitive Initiators for Cationic Photopolymerizations

Despite the advantages of UV-initiated photopolymerizations discussed above, the technique has received considerably less attention than the analogous free-radical reactions. This fact may be attributed to the lack of suitable UV-sensitive cationic photoinitiators until recent years.[31,33] In fact, applicable photoinitiators for cationic polymerizations were not developed until the late 1970s, more than thirty years after free-radical initiators had been reported. Early photoinitiators for cationic polymerizations, first introduced in 1965, were aryldiazonium salts of complex metal halide anions.[31] Upon photolysis, these species produce an aryl halide, molecular nitrogen, and a strong Lewis acid capable of initiating cationic polymerization.[13,31] While the aryldiazonium salts were highly photoactive, they were also thermally unstable, which resulted in unacceptably short shelf lives for fully formulated systems.

Crivello and Lam reported two classes of thermally stable photoinitiators for cationic polymerizations: diaryliodonium and triarylsulfonium salts in 1976 and 1979, respectively (for a review of the development of these initiators, see reference 10). Upon photolysis, these compounds undergo irreversible photofragmentation in which the carbon-iodine or carbon-sulfur bond is cleaved to produce an aryliodinium or an arylsulfinium cation-radical capable of initiating cationic polymerization.[12] While the diaryliodonium and triarylsulfonium salts actively initiate cationic polymerization in the

presence of UV light, they are remarkably latent in the absence of light. In fact, fully formulated solutions of some salts in epoxide monomers have shelf lives of several years.[12]

The wavelength at which the diaryliodonium and triarylsulfonium salts exhibit their maximum UV absorbance depends somewhat upon substituents attached to the ring, but typically falls between 225 and 275 nm[9,33] (some sulfonium salts absorb near 300 nm[9]). Diaryliodonium salts of hexafluoroantimonate produce the fastest rates of reaction of the onium salts due to the size and acidity of the anion. However, since absorption is governed by the aromatic portion of the molecule, their absorption maximum is usually lower than other onium salts, near 250 nm.

Although the initiators absorb strongly at wavelengths near 250 nm, their absorption diminishes at longer wavelengths.[9,32] This fact could limit the efficiency of the initiators for photopolymerizations driven by mercury lamps which provide most of their emission at wavelengths above 300 nm.[9,33] However, the spectral region over which the initiators are effective may be expanded by the addition of a variety of photosensitizers, including hydrocarbons, ketones and heterocyclic compounds.[9] These compounds actively sensitize the iodonium and sulfonium initiators by an electron transfer process, rendering them effective in the long UV and visible wavelengths of light.[9,32,33] Andersen *et al.*[34] showed that the radical polymerization of styrene could be initiated by photoexcitation of anthracene added to the styrene monomer. The anthracene initially absorbs the light, which rapidly populates its metastable excited triplet state. This excited anthracene then can interact with a stryene molecule to produce anthracene and styrene radicals which lead to styrene polymerization.

Anthracene and its derivatives can be used to photosensitize cationic polymerization reactions. In these reactions, the anthracene absorbs light and transfers that energy to the diaryliodonium salt which then fragments and initiates the cationic polymerization. In this way cationic photopolymerizations can be initiated using near-UV or even visible wavelengths. However, little is known about the kinetics and mechanism of the photosensitation for these cationic reactions.

I.4. Need for Research on Cationic Photopolymerizations

UV-initiated cationic photopolymerizations have considerable potential for the development of improved coatings and inks. These reactions may be used to rapidly form highly crosslinked polymer films exhibiting excellent adhesion, abrasion resistance, and chemical resistance. Furthermore, these 100% solid systems emit no volatile organic components and cure with a fraction of the energy requirements of thermal systems. Unlike free radical photopolymerizations, the cationic reactions are not inhibited by atmospheric oxygen, and may be used to polymerize epoxides and vinyl ethers. These monomers exhibit many desirable properties, including low volatility, good rheological characteristics and negligible toxicity.[7,33] Fully formulated systems containing monomer, pigment and initiator exhibit shelf lives of more than a year,[12] and initiators may be chosen to be effective for wavelengths at which the pigments have low extinction coefficients. Finally, the UV irradiation will not significantly degrade the substrate (unlike electron beam curing) and the cationic polymerization can withstand moderate amounts of water without a significant decrease in reaction rate.[13,33]

Despite the promise of UV-initiated cationic photopolymerizations, these reactions have received only limited attention. This fact may be attributed primarily to the lack of suitable initiators until recent years. In fact, most of the work on cationic photopolymerizations reported in the literature focuses on the initiation step of the reaction (for reviews, see references 8-12,30-33,35). The development of thermally stable UV-sensitive cationic photoinitiators has lead to increased interest in the cationic photopolymerizations of epoxides and vinyl ethers in the last ten years; [31-33,35-39] however, the field is significantly less developed than that of free-radical photopolymerizations. For example, the reaction kinetics of free radical photopolymerizations of multifunctional acrylates and methacrylates have been extensively investigated,[6,15-29] revealing anomalous kinetic behavior, including immediate onset of autoacceleration, the formation of heterogeneous networks, and the attainment of a maximum conversion significantly less than unity. However, similar experiments have not been reported for cationic photopolymerizations.

The reaction kinetics of cationic photopolymerizations of diepoxides and bisvinyl ethers typically have been characterized only macroscopically in terms of the tack-free time of the polymer film. Similarly, the resulting highly crosslinked polymer networks have typically received only a cursory characterization by the pencil hardness test and solvent rub tests. In addition, the cationic photopolymerizations reported in the literature are usually initiated using mercury lamps. There have been few studies as to the effect of the wavelength of the light source on the polymerization rate (especially for wavelengths below 300 nm). Fundamental investigations of the reaction and the resulting polymer networks are needed if the variables that effect the properties of the polymer films are to

be fully understood. A thorough characterization of the reaction kinetics would allow the optimum curing procedure to be established, and would reveal whether phenomena such as limiting conversions, and trapped active centers are important in these systems. Characterization of the resulting networks would allow the homogeneity of the network to be determined, and could resulting in the establishment of important structure-property relations.

I.5. List of References

1. E.L. Graminski, *Fundamental Chemical and Engineering Issues in Paper Currency Production*, National Science Foundation, Washington D.C., 1, 1991.

2. P.E. Sundell, S. Jonsson, A. Hult, "High-Energy-Radiation-Induced Cationic Polymerization of Vinyl Ethers in the Presence of Onium Salt Initiators," *Radiation Curing of Polymeric Materials*, C.E. Hoyle and J.F. Kinstle Eds., ACS Symposium Series 417, ACS, Washington D.C., 459, (1989).

3. H.C. Kim, A.M. El-Naggar, G.L. Wilkes, Y. Yoo, J.E. McGrath, "Structure-Property Behavior of Caprolactone-Ally Glycidyl Ether Copolymers Cross-Linked by Electron-Beam Irradiation," *Radiation Curing of Polymeric Materials*, C.E. Hoyle and J.F. Kinstle Eds., ACS Symposium Series 417, ACS, Washington D.C., 474 (1989).

4. V. Stannett and A. Deffieux, "Cationic Polymerization and Grafting of Initiated by High Energy Radiation," *Cationic Polymerization and Related Processes*, E.J. Goethals, Eds., IUPAC, Oxford, UK, 307, 1984.

5. J. Pacansky and R.J. Waltman, "Electron-Beam Exposure of Organic Materials," *Radiation Curing of Polymeric Materials*, C.E. Hoyle and J.F. Kinstle Eds., ACS Symposium Series 417, ACS, Washington D.C., 498 (1989).

6. J.G. Kloosterboer, "Network Formation by Chain Crosslinking Photopolymerization and its Applications in Electronics," *Adv. Polym. Sci.*, **84**, 1 (1988).

7. C.G. Roffey, *Photopolymerization of Surface Coatings*, Wiley, New York, 1981.

8. S.P. Pappas, *UV Curing: Science and Technology, Vol. 2*, Technology Marketing Corporation, Norwalk, CT, 1985.

9. J.V. Crivello, "Cationic Polymerization-Iodonium and Sulfonium Salt Photoinitiators," *Adv. Polym. Sci.*, **62,** 1, (1984).

10. J.V. Crivello and J.L. Lee, "Alkoxy-Substituted Diaryliodonium Salt Cationic Photoinitiators," *J. Polym. Sci., Polym. Chem.*, **27**, 3951, (1989).

11. A. Ledwith, S. Al-Kass, A. Hulme-Lowe, "Mechanisms for Photoinitiation of Cationic Polymerization," *Cationic Polymerization and Related Processes*, E.J. Goethals, Ed., IUPAC, Oxford, UK, 275, 1984.

12. J.V. Crivello, "Recent Progress in the Design of New Photoinitiators for Cationic Polymerization," *Cationic Polymerization and Related Processes*, E.J. Goethals, Ed., IUPAC, Oxford, UK, 289, 1984.

13. A. Reiser, *Photoreactive Polymers*, Wiley, New York, NY, 1989.

14. S.P.Lapin, "Radition-Induced Cationic Curing of Vinyl-Ether-Functionalized Urethane Oligomers," *Radiation Curing of Polymeric Materials*, C.E. Hoyle and J.F. Kinstle, Eds., ACS Symposium Series 417, ACS, Washington D.C., 363, (1989).

15. P.E.M. Allen, G.P. Simon, D.R.G. Williams and E.H. Williams, "Dynamic-Mechanical Properties and Cross-Polarized, Proton-Enhanced, Magic Angle Spinning ^{13}C NMR Time Constants of Poly[oligo(ethylene glycol) dimethacrylates]," *Macromolecules*, **22**, 809, (1989).

16. K. Miyazaki and T. Horibe, *J. Biomedical Mater. Res.*, **22**, 1011, (1988).

17. G.H. Hubca, C.R. Oprescu, G.H. Dragan, and M. Dimonie, "Synthesis and Polymerization of Polyethylene Glycol Dimethacrylates. IV, Study of the Polymerization Process of Polyethylene Glycol Dimethacrylates," *Rev. Roum. Chem.*, **27**, 435, (1982).

18. J.G. Kloosterboer and C.F.C.M. Litjen, "Chain Cross-linking Photopolymerization of Tetraethyleneglycol Diacrylate," *Cross-linked Polymer Chemistry*, R. Dickie, S. Labana and R. Bauer,Eds., ACS Symposium Series 367, ACS, Washington D.C., 409, (1988).

19. H.M.J. Boots, J.G. Kloosterboer, and G. van de Hei, "Inhomogeneity During Bulk Polymerization of Divinyl Compounds," *Brit. Polym. J.*, **17**, 219, (1985).

20. H. Galina, B. Kolarz, P. Wieczorek, and M. Wojczynska, " Homogeneity of Gel and Microsyneresis in Porous Styrene-Divinylbenzene Copolymers," *Brit. Polym. J.*, **17**, 215, (1985).

21. W. Funke, "Reactive Microgels-Polymers Intermediate in Size Between Single Molecules and Particles," *Brit. Polym. J.*, **21**, 107, (1989).

22. J. Bastide, and L. Leibler, *Macromolecules*, **21**, 2649, (1988).

23. A. Matsumoto, H. Matsuo, H. Ando and M. Oiwa, "Solvent Effects in the Copolymerization of Methyl Methacrylate with Oligoglycol Dimethacrylate," *Eur. Polym. J.*, **25**, 237, (1989).

24. J. Baselga, M. Llorente, I. Hernandez-Ruentes, and I. Pierola, "Network Defects in Polymacrylamide Gels," *Eur. Polym. J*, **25**, 471, (1989).

25. D. Turner, Z. Haque, S. Kalachandra and T. Wilson, "Structure and Properties of Polydimethacrylates: Dental Applications," *Polym. Mater. Sci. Eng. Proceed.* **56**, 769, (1987).

26. G.P. Simon, P.E.M. Allen, D.J. Bennett, D.R.G. Williams and E.H. Williams, "Nature of Residual Unsaturation During Cure of Dimethacrylates Examined by CPPEMAS ^{13}C NMR and Simulation Using a Kinetic Gelation Model," *Macromolecules*, **22**, 3555, (1989).

27. J.G. Kloosterboer, G.F.C.M. Lijten and C.P.G. Zegers, "Formation of Densely Crosslinked Polymer Glasses by Photopolymerization," *Polym. Mater. Sci. Eng. Proceed.*, **60**, 122, (1989).

28. P.E.M. Allen, D.J. Bennett, S. Hagias, A. Hounslow, G. Ross, G.P. Simon, D.G.R. Williams and E.H. Williams, "The Radical Polymerization of Dimethacrylate Monomers - The Use of NMR Spectrometry to Follow the Development of Network Structure," *Eur. Polym. J.*, **25**, 785, (1989).

30. J.V. Crivello and J.H.W. Lam, "The Photoinitiated Cationic Polymerization of Epoxy Resins," *Epoxy Resin Chemistry*, R.S. Bauer, Ed., ACS Symposium Series, 114, ACS, Washington D.C., 1, (1979).

31. S.P. Pappas, "Photoinitiation of Cationic and Concurrent Radical-Cationic Polymerization. Part V.," *Prog. Org. Coat*, **13**, 35, (1985).

32. J.V. Crivello, "Photoinitiated Cationic Polymerization of Coatings," *Organic Coatings, Science and Technology, Vol. 5*, G.D. Parfitt and A.V. Patsis, Eds., Marcel Dekker, Inc., New York, NY, 35, 1983.

33. W.R. Watt, "Photosensitized Epoxides as a Basis for Light-Curable Coatings," *Epoxy Resin Chemistry*, R.S. Bauer, Ed., ACS Symposium Series 114, ACS, Washington D.C., 17, (1979).

34. V.S. Anderson and R.G.W. Norrish, "The Polymerization of Styrene Sensitized by Molecules in the Triplet State," Proc. Roy. Soc. (London), **251**, 1, (1959).

35. F. Loshe and H. Zweifel, "Photocrosslinking of Epoxy Resins", *Adv. Polym. Sci.*, **78**, 61, (1986).

36. J.V. Crivello and D.A. Conlon, "Aromatic Bisvinyl Ethers: A New Class of Highly Reactive Thermosetting Monomers," *J. Polym. Sci., Polym. Chem.*, **21,** 1785, (1983).

38. G. Manivannan, J.P. Fouassier, "Primary Processes in the Photosensitized Polymerization of Cationic Monomers," *J. of Polym. Sci. Polym. Chem.*, **29**, 1113, (1991).

39. P. Sundell, S. Jonsson, A. Hult, "Photo-Redox Induced Cationic Polymerization of Divinyl Ethers," *J. Polym. Sci., Polym Chem.*, **29**, 1525, (1985).

CHAPTER II. BACKGROUND

II.1. Cationic Polymerizations

II.1.1. Properties of Cationic Polymerizations

Cationic polymerizations are chain reactions in which a propagating cationic center successively reacts with many monomer units to form long polymer chains. Classes of monomers which will undergo cationic polymerizations include α-olefins, 1,3-dienes, vinyl ethers, and epoxides. Cationic polymerizations are not as well characterized as radical polymerizations partially because they proceed at very rapid rates, and may be sensitive to small concentrations of impurities.[1] Cationic initiators are typically protonic or Lewis acids, and the resulting reactive cations are sufficiently stable to have a reasonable lifetime for chain growth by propagation. The polymer chain growth may be terminated by chain transfer of the reactive center, or occasionally by counterion combination. Compounds such as water, alcohols, and esters are particularly effective chain transfer agents. Although chain transfer results in a decrease in the average primary polymer chain length, it should not affect the polymerization rate because the resulting cation will continue to propagate.[1] The decrease in the average primary polymer chain length will not effect the properties of the polymer due to the high level of crosslinking.

The average molecular weight will not be effected greatly, also due to the highly cross-linked network formed in the reaction.

Kinetic data for cationic polymerizations are difficult to interpret for several reasons.[1-3] First of all, the reactions often proceed so rapidly that the steady-state assumption is not valid for the reactive centers.[1] The analysis is further complicated by the fact that the nature of the propagating center and the counterion are often unclear.[1-3] For kinetic modeling of these reactions, it is common to assume several types of propagating centers ranging from completely free (unpaired) ions to covalent species. The unpaired species typically exhibit much higher kinetic constants for propagation than pair species. Cationic polymerization rates are often higher than those for free radical polymerizations for a variety of reasons. For cationic polymerizations of unsaturated monomers, the kinetic constants for propagation are usually higher than those for free radical reactions, while the rate constants for termination are lower. Both of these trends contribute to higher reaction rates for the cationic reactions. Furthermore, the concentration of propagating species is usually two orders of magnitude higher for cationic polymerizations than for free radical polymerizations.

While cationic polymerizations are not used extensively for the commercial synthesis of long polymer chains, they show considerable promise for photopolymerizations of highly crosslinked polymer films. Due to the predominance of transfer processes during the course of the reaction, linear cationic polymerizations tend to yield polymers of moderate molecular weight and relatively broad distributions. These facts tend to limit the usefulness of the reactions for the synthesis of linear high polymers. However, for photopolymerizations of multifunctional monomers, a high linear primary

chain length is not necessary because the resulting highly crosslinked polymers derive their excellent properties from the network structure, not from long linear chains. For these systems the insensitivity to oxygen and high reaction rates exhibited by cationic polymerizations represent significant advantages.

Fundamental investigations of the reaction and the resulting polymer networks are needed if the variables that effect the properties of the polymer films are to be fully understood. A thorough characterization of the reaction kinetics would allow the optimum curing procedure to be established, and would reveal whether phenomena such as limiting conversions, and trapped active centers are important in these systems. Characterization of the resulting networks would allow the homogeneity of the network to be determined, and could result in the establishment of important structure-property relations. Finally, the effect of the wavelength and light source on the kinetics and the reaction/structure of the polymer films should be thoroughly investigated.

II.1.2. Cationic Photopolymerizations of Epoxides and Vinyl Ethers

The development of thermally stable cationic photoinitiators in the late 1970s has lead to increased interest in cationic photopolymerizations. Most of the work reported in the literature has focused on the synthesis and development of appropriate monomers and initiators for cationic photopolymerizations of high performance polymer films.[4-23] Several classes of monomers exhibiting desirable properties and rapid polymerization rates have been reported, including epoxides,[4,10-14] novel silicon-containing epoxy resins[17,18,23] and a variety of urethane and bisvinyl ethers.[4,15,16] The selection of appropriate

monomers and initiators is now reasonably broad; however, the characteristics of the cationic photopolymerization reactions have received only limited attention. There is a need for fundamental studies of the kinetics of the reactions, as well as the structure and physical properties of the resulting highly crosslinked polymer networks. Such studies would allow the optimum formulations and curing procedures to be established.

Experimental studies of the cationic photopolymerizations of epoxides and vinyl ethers have provided information about the salient features of the reactions. The observed polymerization rate depends upon several variables including the type and concentration of the initiator, the intensity and wavelength of the UV light source, temperature, and the structure of the monomer. When diaryliodonium and triaryl-sulfonium salts are used as the photoinitiators, the optimum initiator concentrations are typically 2-3 wt%.[10,13] Until now, most investigators have used mercury lamps for the UV light source.[9,10,13] Many monomers exhibit a substantial increase in cure rate as temperature is increased.[9,11,20,21] This fact presents potential complications for kinetic studies of extremely rapid cationic photopolymerizations. Polymerization reaction of epoxides and vinyl ethers are highly exothermic and can liberate significant amounts of heat in a very short period of time. Therefore, it is important to monitor the temperature of the film during the polymerization process.

The cure rate of cationic photopolymerizations is typically characterized by the tack-free time of the polymer film. Cycloaliphatic epoxides generally exhibit shorter tack-free times than bisphenol-A epoxy resins due to enhanced epoxy ring strain.[11] Vinyl ethers and silicon-containing epoxides exhibit reaction rates that are an order of magnitude higher than these epoxides.[9,18] Reported tack-free times range from less than

one second to several minutes;[9-14] however, the meaning of the tack-free time in terms of the degree of cure is unclear. Differential scanning calorimetry experiments[9] indicate that the reaction proceeds long after the tack-free time. In fact, films with tack-free times of a few seconds often exhibit exothermic polymerization reactions for several minutes. The studies also indicate that UV cured epoxides typically exhibited a cure rate which passed through a maximum, then rapidly decreased to smaller values. This behavior was attributed to diffusion limited propagation upon vitrification in the highly crosslinked films.[20,21] This interpretation is supported by the fact that tack free time may be decreased by the addition of chain transfer agents[20,21] which delay vitrification. Unfortunately the chain transfer agents cause a reduction in crosslink density, undermining the mechanical properties and the chemical resistance of the cured film.[9]

II.1.3. Photosensitization of Cationic Polymerizations

Although there have been relatively few systematic studies as to the effect of the wavelength of the light source on the characteristics of cationic polymerizations, several experimental observations suggest that wavelength could be an important operating variable. For example, the cure rate of a given monomer depends upon which initiator is used for the photopolymerization. When medium pressure mercury lamps are used as the light source (these lamps provide most of their emission in the 300-340 nm region of the spectrum[4]), the cure rate is highest for diazonium salts, followed by triarylsulfonium, and diaryliodonium salts.[13] This trend can be attributed to more efficient use of the mercury arc radiation by the diazonium salt since this initiator exhibits a maximum absorbance at

a wavelength of approximately 320 nm,[13] while the triarylsulfonium and diaryliodonium salts exhibit their maxima at lower wavelengths of around 260 and 235 nm, respectively. A similar effect is observed when photosensitizers are added to a reaction mixture.[4,20,21] The photosensitizers lead to an increased cure rate due to more efficient use of the mercury arc radiation. These results illustrate the importance of the initiation step in the determination of the cure rate and results suggest that the effect of light sources operating in shorter wavelengths should be investigated. One method of overcoming short wavelength absorption of onium salts is to use photosensitizers to expand the spectral region over which onium salts are effective. Photosensitizers make it possible to initiate polymerization in the near UV or visible wavelengths of light as a result of a direct interaction between an excited state of a photosensitizer and the initiator. Heterocyclic and fused ring aromatic compounds often show activity as photosensitizers. Anthracene has been used to photosensitize both free radical[24] and cationic[25,26] polymerizations. Anthracene absorbs strongly at wavelengths between 320-390 nm, and therefore expands the initiating window to the near visible region of the spectrum (overlapping with mercury lamps emission in the 300-340 nm region of the spectrum[4]).

II.2. Fluorescence Cure Monitoring

To date, most of the work on cationic photopolymerizations reported in the literature focuses on the initiation step of the reaction, and the polymerizations themselves are not well characterized. It is clear that cationic photopolymerizations of vinyl ethers proceed very rapidly; however, few detailed kinetic studies have been

performed for these reactions. For example, the kinetics of these photopolymerizations have been characterized in a very cursory manner in terms of the tack-free time of a curing polymer film, but detailed profiles of conversion versus time are not available.

A major reason for the lack of kinetic studies is the extremely rapid reaction rates exhibited by cationic photopolymerizations of divinyl ethers. Because these reactions proceed to completion in a matter of seconds, there are few experimental techniques with sufficient time resolution to characterize these polymerizations. Differential scanning calorimetry (DSC) has been used extensively to study free radical photopolymerizations of acrylates[27] as well as cationic photopolymerizations of epoxides,[18,28] however the technique's relatively slow response-time limits its applicability for vinyl ether photopolymerizations. Since the DSC response time is approximately 2-3 seconds, [29,30] the technique is only applicable for vinyl ether photopolymerizations that are initiated with relatively low intensity light[16] when the cure time is relatively long (tens of seconds). Real-time infrared spectroscopy has recently been used to monitor high-speed, laser-induced radical photopolymerizations. [29-31] This technique has a response time of 0.02 seconds and therefore could be useful for characterizing cationic photopolymerizations. The advantages and limitations of this technique have recently been addressed. [29] Furthermore, polymerizations of multi-functional monomers are complicated by the fact that highly crosslinked structures are formed, which makes it difficult to measure the primary kinetic chain length. For this reason, the photopolymerizations of monoepoxides have received more detailed analysis than that of diepoxides.[10,14] Information obtained from linear polymerizations is of limited value for highly crosslinked polymerizations of multi-functional monomers. New techniques such as fluorescence spectroscopy need to

be developed as a time-resolved, *in situ* technique for monitoring the extent of cure in these high speed polymerizations.

Fluorescence methods are well suited to these experiments because they provide a highly sensitive and selective means of non-invasive, real-time measurement of reactant concentration.[32,33] Fluorescence spectroscopy is particularly attractive as an *in situ,* time-resolved technique for monitoring these high speed polymerizations because it has an extremely short intrinsic timescale (typically 10^{-9} seconds). The response time for the monitoring technique is invariably determined by the speed of the detection system. In recent years, several authors[34-37] have reported the use of fluorescence techniques for monitoring polymerizations. Most of these fluorescence techniques monitor polymerization indirectly through the corresponding increase in viscosity. For example, several fluorescence monitoring schemes are based upon fluorescence probes which exhibit enhanced fluorescence intensity with increasing viscosity due to decreased radiationless energy transfer. Wang *et al.*[34,37] have used a similar technique to monitor viscosity and chemical changes during polymerization of epoxy and methyl methacrylate systems. They determined that for certain probe molecules, the fluorescence intensity increases as the system viscosity increases due to the reduced ability of the probe to relax through vibrational and rotational modes.[34] Their reaction system also included a probe molecule which has constant fluorescence intensity with viscosity changes as an internal standard[35] This technique was not very useful for monitoring the degree to cure above the gel point and was subject to uncertainty due to variations in background fluorescence. Alternatively, Stroeks *et al.*[36] and Wang *et al.*[35] investigated the use of viscosity-sensitive excimer formation to monitor the cure of epoxy resins. However, Stroeks *et al.*

concluded that the apparent intensity changes in the excimer peak were actually dominated by changes in the intensity of the overlapping monomer peak (which was enhanced due to reduced radiationless transfer). Finally, Scarlata and Ors[38] have monitored the cure of an epoxy resin by measuring an increase in fluorescence polarization which they attributed to a viscosity-induced decrease in the rotational mobility of the probe molecule.

One drawback of the viscosity-sensitive techniques for monitoring crosslinking polymerizations is their limited utility for conversions above the gel point where there is relatively little change in the local viscosity with time. A novel fluorescence monitoring method not based upon viscosity, was recently reported by Sung *et al.*[39,40] Their scheme, which is applicable to amine/epoxy systems, is based upon a reactive chromophore which mimics the reactivity of the amine curing agent. The fluorescence quantum yield of the chromophore increases as the primary amine is converted to a tertiary amine, thereby allowing the reactive state of the amine to be monitored. In more recent work,[41,42] Sung and collaborators have used intrinsic fluorescence and phosphorescence to characterize cure in epoxy composites. Bathochromic shifts in emission spectra were observed as a function of cure time giving a sensitive method for evaluating extent of cure.

The kinetics of cationic photopolymerizations of vinyl ethers can be investigated using *in situ* laser-induced fluorescence spectroscopy. The fluorescence intensity of the photosensitizer can be monitored during the reaction to obtain a direct measure of the rate of initiation, and provide indirect information on the rate of propagation. The response time for the monitoring technique is determined by the speed of the detection system. In our studies, a high-speed diode array detection system was employed, and fluorescence

spectra were collected in intervals as short as 2 milliseconds. Therefore, this fluorescence monitoring method has a considerably faster response time than DSC and real-time IR methods, and provides ample time-resolution to characterize the cationic photopolymerizations. In addition, since the fluorescence method allows a relatively wide window of wavelengths to be monitored (as opposed to a single wavelength), spectral changes arising from more than one functionality can be monitored simultaneously.

The fluorescence monitoring scheme reported here is considerably different than the viscosity-sensitive methods reported in the literature. First, because cationic photopolymerizations proceed to completion in a matter of seconds, our studies require considerably faster sampling methods than the aforementioned epoxy resin studies. A more fundamental difference between our fluorescence monitoring scheme and the viscosity-sensitive probe approach arises from the fact that we are monitoring the fluorescence of one of the reactants (the photosensitizer), and not that of an inert probe. This technique provides a more direct measurement of the reaction itself, and does not lose sensitivity at the gel point. Laser induced fluorescence spectroscopy can be used to monitor divinyl ether photosensitization reactions because the intensity of many of the aromatic hydrocarbons used as the photosensitizers changes as the reaction proceeds. Therefore, laser induced fluorescence was chosen to monitor the photosensitization rate of cationic polymerization of divinyl ethers photosensitized with varying concentrations of anthracene and its derivatives.

II.3. Photosensitization Mechanism

In order to expand the spectral region over which cationic initiators are effective, a variety of photosensitizers may be added to the system. In general, photosensitization results from a direct interaction between an excited photosensitizer molecule (the first excited singlet state or the lowest energy triplet state) and the initiator. Photosensitization is often attributed to an energy transfer mechanism in which the excited-state photosensitizer interacts with a ground state initiator molecule to form an exciplex. In the exciplex, the excited-state energy is transferred to the initiator, which fragments to create active centers. According to this mechanism, the photosensitizer functions essentially as a catalyst and is regenerated in its ground-state while the initiator is promoted to an excited state, and fragments to create active centers. For energy transfer to be thermodynamically feasible, the excited-state energy of the photosensitizer must be greater than that of the acceptor.[4] The energy transfer mechanism is not feasible for photosensitization of onium salts by anthracene derivatives due to the relatively low excited state energy of the anthracene derivatives. Pappas and Gatechair[44] reported that this energy transfer process may occur for onium salts with photosensitizers such as acetophenone and benzophenone which have relatively high triplet energies (> 290 kJ/mol) and high oxidation potentials, but the energy transfer results in a triplet state initiator molecule which is unreactive to bond cleavage.[44] In more recent work, Dektar and Hacker demonstrated that triplet energy transfer photolysis does take place for diaryliodonium salts sensitized by xanthone and benzophenone. However, the triplet

energy transfer mechanism is not thermodynamically feasible for photosensitization of iodonium salts by anthracene due to the relatively low excited state energy of the anthracene.[45]

It has been generally accepted that the photosensitization of diaryliodonium initiators most often proceeds by the electron transfer mechanism.[4,11,25] Electron transfer from the excited state of the photosensitizer to the initiator within an exciplex results in a photoredox reaction in which the photosensitizer is oxidized to form a radical-cation and the initiator is reduced to a radical species.[43] The thermodynamic feasibility of this reaction is governed by the oxidation potential of the excited state photosensitizer and the reduction potential of the initiator. Although there is general agreement that photosensitization of diaryliodonium salts by anthracene occurs by electron transfer, there is disagreement on the identity of the anthracene excited state (singlet or triplet) from which the electron transfer occurs. In early work Andersen *et al.*[24] demonstrated that the radical polymerization of styrene could be photosensitized by anthracene. Based upon lifetime considerations, the authors concluded that it was triplet state anthracene that interacted with styrene to produce anthracene and styrene radicals which lead to polymerization. Crivello[4] reported that the photosensitization of iodonium salts by aryl ketones, condensed ring aromatic hydrocarbons and dyes takes place by an electron transfer mechanism from the lowest energy triplet state. Based upon anthracene emission quenching studies, Pappas and collaborators[11,44] concluded that the electron transfer occurs from the first excited singlet state of anthracene. Similarly, Schnabel *et. al.*[47,48] have concluded from flash photolysis studies, that anthracene reacts with N-ethoxy-2-methyl-pyridinium ions from the excited singlet state. However, none of these authors

demonstrated their proposed mechanisms with definite experiments. Finally, based on CINDP (Chemically Induced Dynamic Nuclear Polarization) studies, DeVoe *et. al*[46] concluded the electron transfer to the iodonium salts occurs from the anthracene excited singlet state.

A series of studies will be performed to establish the photosensitization mechanism for cationic photopolymerizations of vinyl ethers photosensitized by anthracene derivatives. Results obtained using several different anthracene derivatives as the photosensitizer will provide considerable insight into the photosensitization mechanism. Furthermore, a series of studies will be performed to determine which anthracene excited state (singlet or triplet) is involved in photosensitization of diaryl-iodonium salts. Anthracene phosphorescence and fluorescence lifetime studies were performed to determine the effect of the initiator on the lifetimes of the triplet and singlet. The phosphorescence measurements will be used to examine the triplet lifetime of the anthracene when used as a photosensitizer. The role of the triplet state will be investigated further using studies performed using an anthracene triplet quencher and from computer simulations of the photophysical-state populations. Other photo-induced reactions of anthracene which could interfere with the photosensitization will also be investigated. Dimerization and oxidation will be examined as competing reactions, in order to eliminate the possibility of the reduction in anthracene fluorescence being attributed to these side reactions.

Both the reactivity and relative population of the singlet and triplet state need to be investigated to determine the relative number of active centers generated from each state. The relative population of the triplet and singlet state depends primarily on the

intersystem crossing rate constant. The reaction pathway for photosensitization can be represented by a series of coupled differential equations. The differential equations are first or second order and depend strongly on the rate constants for the reaction. Solving these differential equations by numerical methods using rate constants from experiments or literature can provide a model of the photosensitization process. The Rosenbrock method for stiff systems with variable step size will be used to solve the set of equations, using developed or commercially prepared programs. The predictions from the models will be matched with experimental data to aid in determining the relative number of active centers formed from the singlet and triplet states.

II.4. Infrared and Raman Cure Monitoring

II.4.1. Introduction to Infrared and Raman Spectroscopy

Due to technological advances, infrared (IR) and Raman spectroscopy are becoming increasingly important tools for the investigation of polymers. With the development of Fourier transform infrared (FTIR) spectroscopy, spurred by the discovery of the fast Fourier transform (FFT) algorithm by Cooley and Tukey in 1965,[49] the usefulness of IR spectroscopy was greatly expanded. Even today as sampling techniques, lasers, detection systems, computers and software become more sophisticated previous limitations continue to be overcome. For example, it is now possible, and desirable in many cases, to examine polymer systems *in situ*.[50] High speed FTIR instruments are now capable of collecting an entire spectrum in times as short as 5 ns.[51] Until recently, IR

techniques have been used far more extensively than Raman techniques. However, in the late 1960's as laser technology started to come of age, Raman spectroscopy developed as a complementary procedure.[52] Once regarded solely as a laboratory technique, Raman spectroscopy can now be used for on-line process analysis, and environmental monitoring. For example, there are now commercially available, portable, on-line Raman systems containing various novel lasers, fiberoptic sampling probes, CCD detectors and complete computer analysis systems.[53]

IR and Raman are practical techniques for hydrogels, since the infrared absorption spectra for polymers are surprisingly simple considering the large number of atoms involved.[54] The simplicity results from the fact that many normal vibrations have almost the same frequency and appear as one band. Furthermore, the strict IR and Raman selection rules prevent many of the vibrations from producing absorptions,[54] therefore simplifying the spectrum.

The usefulness of IR and Raman spectroscopy ultimately lies in the variety of qualitative and quantitative information they can provide about the nature of the polymer under investigation. Information that can be obtained using these techniques includes: the chemical nature (structural units, branching, end groups, additives, and impurities), steric order (isomerism and stereoregularity), conformational order (physical arrangement of the chain), state of aggregation (crystalline, mesomorphous, amorphous phases, number of chains per unit cell, etc.), and orientation of the polymer chain and side groups.[52]

IR and Raman spectra provide complementary rather than duplicate information. For example, IR spectroscopy is generally better suited for the identification of polar

groups, while Raman is valuable for the investigation of the homonuclear polymer backbone.[52] Raman spectroscopy is well suited for the study of low concentration aqueous systems such as hydrogels, since water is an ideal solvent due to its poor Raman scattering. This is a distinct advantage over IR techniques since water absorbs strongly in the IR region and overwhelms the spectrum.[55] Another advantage of Raman spectroscopy arise from the fact that Raman scattering from molecular vibrations can be measured in the visible region of the spectrum. In the this region, optics can be made of relativity inexpensive and robust materials such as glass or quartz, and sensitive detectors with high signal-to-noise ratios are readily available.[56] Since Raman spectroscopy is a visible light technique, remote sampling with fiberoptic probes gives excellent signal throughput and precise positioning of the sampling beam. Intrinsic limitations of Raman spectroscopy arise from the requirement of an intense monochromatic (preferably columnated) light source, and the possible interference from highly colored or fluorescence materials.[56]

As discussed in detail later in this chapter, IR and Raman spectroscopy are based upon distinct physical processes. Fundamentally, Raman is a scattering technique while IR spectroscopy is based upon light absorption, therefore the sampling techniques of the two methods are significantly different. In transmission IR spectroscopy the light is required to pass through the sample to reach the detector, therefore severe constraints are imposed on the sample thickness (typically the thickness must be less than about 40 μm). Methods such as attenuated total reflectance (ATR) may be used with thick samples, but present thier own problems and limitations associated with the contact to the ATR crystal, and the limited depth of penetration. In contrast, since Raman spectroscopy is based upon light scattered by the sample thick samples are not a problem since

backscattered light may be collected and analyzed. Therefore Raman spectroscopy generally requires very little, if any, sample preparation.

The most significant limitations of Raman spectroscopy arise from interference from samples that are highly fluorescent or colored. This limitation ultimately arises from the relatively low intensity of the scattered Raman light, which necessitates intense light sources. In colored samples, the incident light may lead to significant heating of the sample. If the incident light induces fluorescence, the Raman signal must be resolved from the fluoresced light (fluorescene is typically several orders of magnitude more intense than Raman scattering). Both techniques are good for analysis of microscale sample sizes. Although, IR spectroscopy has the advantage of better resolutions with resolutions down to approximately 0.05 cm^{-1}, while Raman instruments are limited to about 0.25 cm^{-1}.[56] In addition, both techniques are fairly easily adapted for high and low temperature work.[56]

There are two general types of infrared spectrometers. The older of the two types is referred to as a dispersive spectrometer. This type of spectrometer uses a monochromator and slits to separate the infrared radiation into individual frequencies.[57] The more recently developed type of instrument is known as a Fourier transform infrared spectrometer (FTIR). These instruments are based on the Michelson interferometer and require no monochromators or slits.[57] The areas of continuing improvement in FTIR instrumentation include increased scan speed and resolution, improved signal-to-noise ratios, expansion of the range of wavelengths over which the instrument operates, data handling software, and automation. Examples of these improvements include FTIR instruments which are capable of resolutions down to 1 cm^{-1} and signal-to-noise ratios of

2,000:1 with high speeds able of obtaining spectra in intervals as short as 5 nanoseconds.[51]

The most significant area of improvement in Raman spectroscopy has been the development of relatively low cost, high power lasers. Some of the more recent improvements include enhanced detection systems, such as charge coupled devices (CCD), and the use of fiber-optics for remote process analysis.[51] Other improvements in IR and Raman instrumentation make use of the increased power of personal computers and computer software. It is now possible to collect, analyze, annotate, and even "cut and paste" selected spectrographs into reports and presentations all within the same computer. In addition, computerized libraries of known IR and Raman spectra continue to grow, allowing for more extensive computer matches of characteristic group frequencies.[51]

There are many applications of IR and Raman spectroscopy to the investigation of hydrogels. Specific applications include investigations of controlled drug release delivery systems, and contact lens materials; identification of biocompatible polymers; and characterization of synthesis products.

II.4.2. Physical Basis and Background for IR Spectroscopy

A brief introduction to the basic principles of infrared spectroscopy is presented in this section. The infrared (IR) region of the spectrum consists of light with wavenumbers between 10,000 cm^{-1} and 10 cm^{-1} (wavelengths between 1.0 μm and 1,000 μm), with the range from 10,000 to 4,000 cm^{-1} (1,000 - 2.5 μm) referred to as the near infrared; 4,000 to 400 cm^{-1} (2.5 - 25 μm) the mid-infrared; and 400 to 10 cm^{-1} (25 - 1,000 μm) the far infrared regions.[56] The basic premise behind IR spectroscopy is that when infrared light

is passed through a sample, certain frequencies are absorbed while others are transmitted, resulting in an absorption spectrum that is dependent on the molecular vibrational frequencies.

In polymers, molecular bonds have different vibrational frequencies which correspond to characteristic IR absorption bands. Therefore an IR spectrum may be used for identification of the types of bonds and functional groups present in a specific polymer sample.[58] IR absorption bands due to rotational transitions may be observed for gases;[52] however, the rotation of the molecule is highly restricted in solids, and rotational transitions are not observed. For the study of polymer systems we are only concerned with molecular vibrations posessing characteristic absorption bands throughout the IR spectrum.

In an infrared spectrometer, the sample under investigation is exposed to the light which spans the entire IR region (either simultaneously as in an FTIR or one wavelength at a time as in a dispersive IR). Both the classical and quantum mechanical viewpoints are useful in describing what fundamentally occurs on the molecular level. The sample absorbs the light only at the specific frequencies that match the natural vibrational frequencies of its constituent molecules.[59] In order for a molecular vibration to absorb in the IR region it must cause a change in the magnitude of the dipole moment.[52,60,62] The intensity of this absorption is dependent on how effective the molecule transfers the infrared photon energy to molecular vibrational energy. This is dependent on the change induced in the dipole moment.[59] It has been shown that the intensity of an IR absorption band is proportional to the square of the change in its dipole moment.[59,60,62] If a molecule

has a center of symmetry in its equilibrium configuration, then any vibrations for which this symmetry is retained will be infrared inactive.[59]

The frequency of a photon, v_p, is determined by its energy, E_p, according to Equation 1.[59]

$$E_p = hv_p \qquad \text{Eq. (1)}$$

Quantum mechanical considerations dictate that molecular energy assumes only specific discrete values. The values of the vibrational energy levels, E_{vib}, are given by,[59]

$$E_{vib} = (n+ {}^1/_2)hv \qquad \text{Eq. (2)}$$

Where h is Planck's constant, v is the classical vibrational frequency of the oscillator and n is a quantum number. If this equation is applied to the infrared absorption of a photon where the vibrational energy of the molecule is E_m, and the frequency of the induced vibration is v_m, then by substitution,

$$E_m = (n+ {}^1/_2)hv_m \qquad \text{Eq. (3)}$$

The only variable in this equation is the quantum number, which can only have integer values. If the quantum number changes by +1 or -1, then the molecule gains or loses energy, respectively. For an unsymmetrical diatomic molecule this amount of energy is ΔE_m, which is equal to the difference between the energy of the n quantum level the energy of the n+1 level. This gives the result,[59]

$$\Delta E_m = hv_m \qquad \text{Eq. (4)}$$

Since the change in energy, ΔE_m, is due to the transfer of energy from the photon to the molecule, $\Delta E_m = E_p$, and subsequently $v_p = v_m$. This states that the frequency, v_p, of a photon which has the proper energy to cause the vibrational quantum number to jump up one level is equal to the classical vibrational frequency of the molecule, v_m.[59] For

harmonic vibration the vibrational quantum number may only change by ±1, all other transitions are forbidden. This selection rule corresponds to conditions where the electric field of the photon causes the molecule to vibrate at the field's frequency, and induces a molecular dipole moment. For an anharmonic quantum mechanical oscillator the selection rule allows for integer changes in the quantum number of ±1, ±2, ±3, etc. In this case, the excited molecule vibrates at the corresponding integer multiple of the molecular frequency.[59] At room temperatures most molecules are in the ground vibrational state, therefore, the allowed transition that dominates infrared spectroscopy and is of most interest is from $n = 0$ to $n = 1$. This is referred to as the fundamental transition. The relative intensities of other allowed transitions are low since the populations of the higher energy levels are low compared to the ground state at room temperatures.[59] Although additional bands, known as overtones and combination bands, may result from anharmonic terms in the potential energy of the molecule.[61] Since anharmonic oscillator energy levels are not equally spaced, the frequency is no longer completely independent of amplitude.[59] The additive effect of the harmonic and anharmonic terms results in the appearance of absorption bands that are shifted from their characteristic absorption wavelength.

II.4.3. Instrumentation for Infrared Spectroscopy

The original type of infrared technique is known as a dispersive IR. A dispersive IR instrument consists of prisms or gratings that separate or disperse the IR radiation into its component wavelengths.[61] Generally modern dispersive infrared spectrometers are

made using gratings rather than prisms with a series of diffraction gratings used to separate the entire IR region.[59] The diffracted light is then reflected with an off-axis paraboloid through an exit slit into a detector. A movable mirror allows a progressive scanning of the individual wavelengths. As a whole, this setup acts as a monochromator thus focusing one wavelength at a time onto the detector. Before reaching the monochromator, the IR radiation is first passed through the sample. In a double beam instrument the IR radiation is split into two beams, one of which is passed through the sample; the other is passed through a reference cell. A rotating sector mirror, called a chopper, alternately reflects or transmits each beam to the monochromator.[58] By comparing the two intensities, the absorption of the sample can be determined.

In contrast to the traditional dispersive instruments, the modern Fourier transform infrared (FTIR) spectrometers do not require a system of slits or a monochromator. Instead, light containing all IR frequencies is passed through the sample simultaneously and those not absorbed reach the detector. The advantage is an improved signal-to-noise ratio and a higher throughput compared to the dispersive IR method.[52,59,63] The key component of the FTIR instrument is the Michelson interferometer, which was first developed around the turn of the century, but was not applied to infrared spectroscopy until the development of digital computers that could quickly and accurately derive the IR spectra from the interferograms by taking the inverse Laplace transform.[52]

In the Michelson interferometer, a beamsplitter is used to transmit half of the source radiation to a movable mirror and to reflect the other half to a fixed mirror. The two beams are then reflected back to the beamsplitter and recombined either constructively or destructively depending on the position of the movable mirror.[59] In an

FTIR spectrometer, this recombined beam is then passed through the sample to a detector,[52] where the interferogram is obtained. In the simplest case of a monochromatic radiation source the intensity (amplitude) of the detector signal is merely the cosine function of the mirror position.[52,59] For polychromatic radiation, however, the interferogram is a summation of all of the constructive and destructive interferences resulting from the interactions between all of the wavelengths.[59] The cosine Fourier transform provides the mathematical relationship between the detected interferogram intensity, *I(x)*, which is a function the mirror position, and the infrared absorption intensity, *I(v)*, as a funciton of frequency,[59,63]

$$I(x) = \int_{-\infty}^{\infty} I(v)\cos(2\pi xv)dv \qquad \text{Eq. (5)}$$

In order to obtain the infrared spectrum from this interferogram quickly, a computer is required to calculate the following inverse transform,[59,63]

$$I(v) = \int_{-\infty}^{\infty} I(x)\cos(2\pi xv)dx \qquad \text{Eq. (6)}$$

The optical path difference, x, is a function of the position of the moveable mirror and is very accurately determined through the use of an internal standard typically a helium-neon laser.[63]

Ideally, the light source for infrared spectroscopy should be continuously tunable over the entire infrared region at power levels above the microwatt range.[59,64] One source that provides an ideal continuous high energy output is a blackbody slit cavity; however, this source is impractical since it requires high temperatures.[59] There are several common types of infrared light sources that come close to matching the ideal characteristics of the

blackbody radiator in the infrared region. These include the Nersnst Glower and the Globar.[59] The Nernst Glower consists primarily of rare earth oxides such as zirconium, yttrium, and thorium oxide which are fashioned into rods about 20 mm long and 1 mm in diameter. They are normally operated at 1900 °C since they are nonconducting at room temperature and must be heated to reach a conducting state.[59] The Globar is a silicon carbide rod, 50.8 mm long and 4.8 mm in diameter that operates at about 1200 °C.[59] The disadvantage of the Globar is that it requires a water-cooled jacket to protect the silvered electrical contacts. In comparison, the Globar has similar radiator properties as the Nernst Glower, although the Nernst Glower gives better preformance in the region below 15 μm.[59] Unless high performance in this region is specifically needed, the Globar is recommended due to its advantage of being more rugged.

A recently developed source of infrared light is a laser pumped nonlinear optical parametric device, such as an optical parametric oscillator (OPO).[64] Optical parametric devices were identified some time ago as promising sources of tunable infrared radiation. However, until recently they proved to be less than ideal due to difficulties such as low optical damage thresholds, spectral bandwidth limitations, and complicated wavelength control methods.[64] Lately, significant improvements in the production of nonlinear optical materials and the availability of stable injection-seeded single-mode or ultrashort-pulse high-peak-power solid-state laser pump sources has resulted in new developments in optical parametric devices.[64] These devices require a coherent diffraction-limited pump source, such as an injection-seeded Nd:YAG laser, to deliver the necessary beam quality, peak power, and pulse energy, as well as high pulse-repetition rate, and narrow bandwidths. The Nd:YAG lasers operate in the nanosecond and picosecond regimes. For

ultrafast spectroscopic applications, femtosecond-pulse lasers such as Ti:Al_2O_3 /dye lasers have proven useful.[64] Parametric devices using these pump sources and newly developed nonlinear optical materials such as $AgGaS_2$ and $AgGaSe_2$ can now generate infrared radiation throughout the mid-IR (fingerprint) region.[64] Previously identified materials such as $LiNbO_3$ and $LiIO_3$ have transmission characteristics that limit them to wavelengths shorter than 4 μm and 5 μm, respectively. Now, essentially any wavelength from the UV to the mid-IR can be produced by selecting different crystals (nonlinear optical materials) and pump sources.[64] Use of this type of light source is currently limited to high end systems because of its relatively high cost compared to the Glower or Globar sources.

Infrared detectors consist of two general types, thermal and photon detectors. Thermal detectors measure a change in a physical property of a material as it is heated; whereas, photon detectors use changes in the electrical properties of a semiconductor caused by incoming photons, to detect IR radiation.[65] Thermal detectors tend to be nonselective detectors, in that they have a response directly proportional to the incident energy and largely independent of the wavelength.[59] Photon detectors, on the other hand, are much more selective detectors since they have a response curve that is strongly dependent on the wavelength of the incident radiation. Traditionally nonselective thermal detectors have been the better choice for spectroscopy, because of their relative wavelength independence[59] and versatility.[65] However, these types of detectors tend to have slow response times and low relative sensitivity.[65] With improvements in semiconductor technology and the increasing need for fast response times and better sensitivity, photon detectors are gaining favor. Thermal detectors include thermocouples,

thermopiles, thermistors, bolometers, and pyroelectric detectors. Some examples of photon detectors include photoconductive, and photovoltaic cells.[65]

Thermocouples and bolometers are two commonly used detectors. Bolometers have the advantages over thermocouples of faster response times and greater sensitivities. A bolometer uses the temperature dependence of a material's electrical resistance to meaure the intensity of incident radiation. Bolometer's are often constructed of semiconductors. Although, superconducting materials have been used for improved sensitivities and faster response times.[59]

The fast response requirements of the rapid-scanning interferometers in FTIR instruments, and the convience of room temperature operation is often meet by the use of a pyroelectric detector.[52] This detector's response is based on the temperature sensitivity of the residual electrical polarization that can be induced in pyroelectric crystals, such as triglycine sulfate.[59] When this type of material is polarized by an electrical field a residual polarization is retained by the material after the field is removed. The voltage across this crystal is then temperature dependent and is measured by electrodes placed on the crystal faces. This device is essentially independent of wavelength from the near infrared through the far infrared.[59]

Photoconductive and photovoltaic detectors have the advantages of rapid response times and high sensitivity compared to thermal detectors. They have the disadvantage of being limited in their detection range, providing poor preformance in the far-IR region.[65] In addition, they often require liquid nitrogen or helium cooling. Both of these detectors depend on the quantum interaction between photons from the incident light and the semiconductor material in the detector.[65]

Overall for the slower dispersive IR instruments, the cheaper thermal detectors are generally the best choice. For high speed applications and especially rapid FTIR work, a photon detector is essential.[65] More detailed information on the various types of detectors available for IR spectroscopy is presented by Colthup *et. al* in reference[59] and Cuirczak in reference.[65]

II.4.4. Sampling Techniques for Infrared Spectroscopy

The physical state (*i.e.* solid, optically dense) of most polymers makes careful sample preparation imperative since it is generally necessary for the IR beam to be transmitted through the sample. Therefore, at least some sample preparation is necessary before a spectrum can be obtained. In addition, the quality of the spectrum is often dependent on the care taken in preparing the sample. Poorly prepared samples that are too thick, nonuniform; or contain impurities, can result in poor or misinterpreted data. There are a number of methods for polymer sample preparation available depending on the physical state of the sample. For solid polymers, IR samples may be prepared by dissolution, dispersion into KBr pellets or mulls, thin film casting, microtoming, microsampling, and attenuated total reflectance (ATR).[52,58,66] For liquid polymer samples, liquid films can be examined by placing several drops between two salt plates.[58]

The method of dissolution requires the identification of a solvent that dissolves the polymer under investigation but does not absorb in the IR region of interest. For this reason this method is seldom used despite the advantage of excellent reproducibility.[52] A

number of authors, such as D. O. Hummel and J. E. Stanfield have summarized the IR absorption spectra of commonly used solvents.

For dispersive IR systems, the spectrum of the solvent is removed from the polymer spectrum by placing the solvent in the reference beam. It is generally advantageous to prepare solutions with as high a concentration as possible. For polymer systems, this method is often most valuable for cases where only a narrow spectral region is of interest for which a suitable solvent exists.[52] With FTIR systems there is no problem removing the solvent absorption bands, unless water is the solvent. The strength and breadth of the IR absorption spectrum of water in aqueous systems, such as hydrogels, can easily surpass the dynamic range limitation of the instrument. In order to subtract the water spectrum, the FTIR spectrum must be examined so that the dynamic range of the detector is not exceeded by the presence of excessive amounts of water.[52]

One of the more commonly used sample preparation techniques for the investigation of polymer systems is to make film samples. This method has the advantage of providing a means for studying polymers in their solid state. The dimensional requirements of the film are such that it is large enough to cover the entire cross section of the light beam, thick enough to provide sufficiently intense bands for groups that are present in low concentrations, but thin enough to allow beam penetration. The film thickness may also need to be reduced to prevent saturation of the detector in IR regions that absorb more strongly than others. Typical dimensions are on the order of 15 mm x 5 mm with thicknesses in the range of 0.001 to 1 mm.[52] Some of the techniques for forming polymer films include solvent casting, melt casting, and hot pressing. Solvent casting is useful for polymers that can be readily dissolved in a volatile solvent. While

melt casting can be used for thermoplastics, some samples require hot pressing in which a hydraulic press is used to provide thinner sample films.[52]

Another IR sample preparation method often used for polymers is the pressed disk technique. This technique involves grinding the polymer sample into a fine powder, and then mixing a small amount with an IR transparent matrix, such as powdered potassium bromide. This mixture is then molded at high pressures in a special die. Often the die is evacuated[59] and pressures range up to 1,000 N/mm^2.[52] A disadvantage of this technique is that many of the matrix materials (salts) absorb water and exhibit water absorbance peaks near 3450 cm^{-1} and 1635 cm^{-1}.[52] A similar technique which is more useful for water-sensitive samples, is the mull method. In this method the polymer is ground into a powder and dispersed into a liquid phase, commonly mineral oil (Nujol),[59] hexachlorobutadiene, or perfluorocarbon.[52] This paste is squeezed between two IR transparent plates. The major disadvantage of this method is the limitation of spectral regions that can be observed due to absorbance bands of the dispersion material.[52] A table of transmission ranges and refractive indices for a number of common matrix materials is presented by Siesler in reference.[52]

Two final sample preparation methods are microtoming and microsampling. Microtoming involves the use of a sharp glass or diamond knife to cut extremely thin samples with thicknesses down to the nanometer scale. The technique is rather tedious and requires considerable practice to master, but may be useful for highly crosslinked polymers for which a solvent can't be found. In order be microtomed, a sample it must be suitably hard so as not to deform greatly under the knife pressure. Softer samples often must be microtomed under cyrogenic conditions. Microsampling is a technique that

is used to obtain IR spectra from very small specimens, such as a microtomed sample.[52] This technique requires the attachment of an optical device that reduces the image of the monochromator slit at the sample position.[52] This type of system can introduce several sources of error that need to be considered. As an example, diffraction phenomena or imperfections in the optical system can cause false radiation that will result in smaller intensities of the absorption bands.[52]

Finally, for polymer samples for which satisfactory transmission spectra can not be obtained by any of the above techniques, it may be possible to use attenuated total refection (ATR) to acquire an IR spectra.[67,68] ATR is based on the phenomenon of total internal reflectance between two materials of different refractive indices. Experimentally, the sample under investigation with a refractive index of n_2 is placed in direct contact with the reflecting surface of a prism. The prism has a refractive index of n_1 that is larger than n_2. Total internal reflectance occurs at an angle above the critical angle of incidence, α_c, of the light beam. This angle is defined by the relation,[52,59]

$$\sin \alpha_c = n_2/n_1 \qquad (n_1 > n_2) \qquad \text{Eq. (7)}$$

The penetration depth of the light beam into the sample is generally on the order of several micrometers. This provides the absorption path without requiring transmission of the radiation through the entire thickness of the sample. The spectrum obtained is very similar to the transmission spectrum. The only difference is that the absorption bands observed with ATR at longer wavelengths have higher intensities compared to transmission spectra.[52]

A second type of reflection spectroscopy is reflection-absorption (RA) spectroscopy. This technique makes use of external reflections. A thin film of the

sample is placed on a reflecting metal surface and irradiated with a light beam having an angle of incidence usually between 70° and 89°. This technique has been used for the detection of thin polymer films on metal surfaces, and investigations of the adhesion between polymers and metals.[69]

II.4.5. IR Application to Polymers

Infrared spectroscopy, especially FTIR, is very useful in both the qualitative and quantitative characterization of the functional groups present in polymers. Additionally, infrared spectroscopy can be used for the detection and identification of additives, the study of oxidation and degradation reactions, and the investigation of molecular interactions, configurations, and hydrogen bonding.[52] Hydrogen bonding is of particular importance for hydrogels such as poly(vinyl alcohol) (PVA) and poly(2-hydroxyethyl methacrylate) (PHEMA) which contain hydroxyl groups. In general, the presence of hydrogen bonding results in a frequency shift and intensity increase in the IR peak corresponding to the proton donating group.[52] IR spectra have also found use in the study of polymer deformation, stress relaxation, fracture, and fatigue.[63] Finally, IR techniques can be used to investigate kinetics,[70] network formation and identification,[71] and diffusion.[50,52]

One of the major reasons for the continuing interest in hydrogels is their potential application as biocompatible materials in medical implants. Such applications include membranes, structural materials, and matrices for the immobilization or diffusion controlled release of bioactive agents.[72] FTIR is useful for studying the interactions

between polymers and blood due to the development of digitized spectra which allow manipulations (such as spectral subtraction) to be readily performed. This feature is of great importance in the study of many biological and hydrogel systems since the large water absorption bands, which can obscure the spectra of interest may be subtracted out.[52,70,73] For example, Gendreau *et. al* have used FTIR/ATR to study the adsorption of blood plasma proteins onto various surfaces. The sensitivity and absorbance subtraction ability of FTIR spectroscopy was crucial in allowing them to construct a time-resolved picture of the proteins' rapid adsorbance including changes that occurred in a small percentage of the proteins. These investigators further used their FTIR/ATR technique in kinetic studies to determine total as well as relative protein adsorbance by plotting individual IR band intensities versus time.[70]

Infrared spectroscopy has been successfully used in the analysis of the polymerization process. With the use of high speed FTIR spectrometers, kinetic studies can often be performed *in situ* to determine reaction order and activation energy. IR spectra can also be used to identify the structural changes and the extent of cross-linking that occur in a polymerization reaction.[61] The extent of cross-linking can often be followed from the decrease in the double bond stretching mode at 1640 cm^{-1} if a suitable internal intensity standard can be found.[63] Hasirci used IR spectra to identify the major source of cross-links in hydrogels synthesized from 2-vinylpyridine and divinyl-benzene/ethylbenzene monomers initiated with gamma radiation. He found that the major source of cross-links was the bifunctional divinylbenzene monomer.[71] Earhart *et. al* used FTIR spectroscopy in their investigation of the effect of poly(vinyl alcohol) on the mechanism and kinetics of the copolymerization of vinyl acetate and butyl acrylate.

These investigators used the FTIR spectra to monitor the increase in the concentration of acetate moieties on the polymer chains resulting from the grafting of vinyl acetate onto poly(vinyl alcohol).[74] Finally, Gulari *et. al* used FTIR spectroscopy to follow, in real time, the conversion of the bulk polymerization of both styrene and methyl methacrylate. By monitoring the integrated peak area for the IR absorbance of the carbon-carbon double bond (1643 cm^{-1}), they were able measure conversion with less error than methods involving the ring breathing mode of the aromatic ring at 1000 cm^{-1} as an internal reference.[75]

IR spectra often play an important role in the synthesis of hydrogels by providing a convenient means of characterizing the final products. For example, Allcock and Kwon used IR spectroscopy to help characterize the structures of hydrogels formed from glyceryl phosphazenes. They were specifically interested in the cross-linking and binding ability of the hydroxyl units present on the glyceryl side groups. IR spectroscopy was used to help verify the synthesis of isopropylideneglyycerol, and to aid in the identification of the hydrolytic degradation products of glyceryl polyphosphazenes by measuring the IR absorbance of the O-H (3500 - 3200 cm^{-1}) and P=N (1250 cm^{-1}) groups.[72] Edwards *et. al* used IR and Raman spectroscopy to characterize copolymers of methyl methacrylate with butadiene. They compiled a complete table of the wavenumbers and vibrational assignments for the 50:50 methyl methacrylate-1,3-butadiene copolymer.[76,77]

Hydrogen bonding can play a significant role in both the reactivity of the monomer and the structure of the resulting polymer. Several investigators have looked at the effect of hydrogen bonding between different solvents and acrylic and methacrylic

acids.[78-81] For example, Saini *et al* reported that they were able to use IR spectra of copolymers of methacrylamide and methyl methacrylate polymerized in different solvents to show that the copolymer composition was solvent dependent.[78] Other researchers found similar effects for the polymerizaton of acrylic,[79-81] methacrylic,[80,81] and itaconic[81] acids. Bajoras and Makuška used infrared spectra to suggest that hydrogen bonding between a mixed dimethyl sulphoxide (DMSO) - water solvent and acrylic acid resulted in a marked decrease in the polymerization activity of the acid. They concluded that this decrease was the result of a decreased probability for the formation of π-complexes caused by an increase in the activity of the acid molecules in the hydogen bond complexes when in the presence of water.[81]

Furthermore, the effect of hydrogen bonding on the molecular structure of poly (vinylpyrrolidone) (PVP) and PHEMA, which are hydrogels commonly used for soft contact lens, was studied using both FTIR and Raman spectroscopy by Monti and Simoni.[82] The investigators used these two techniques to determine how the adsorbed water interacted with the hydrogels by comparing the spectra of dried and hydrated soft contact lenses. They found that the water interacts with the hydrophilic groups of the hydrogel, such as carbonyl groups, by hydrogen bonding. Furthermore, they determined that the strength of this interaction is dependent on which hydrophilic group is involved, and that for PVP lenses the water alters the conformation of the hydrophobic groups.[82]

Changes in the structure of the crystalline regions of poly (tetramethylene terephthalate) due to an applied stress were studied by Ward and Wilding using FTIR.[83] They found that differences in the spectra between the stressed and unstressed state could be attributed to changes in the *trans/gauche* isomerism of the polymer chains. Under

stress the conformation changed from a *gauche-trans-gauche* form (identified by C-H rocking bands at 917 cm^{-1} and 752 cm^{-1}) to an all *trans* conformation (identified by C-H rocking bands at 962 cm^{-1} and 840 cm^{-1}).[83] An additional use has been made of infrared spectroscopy in the study of the stereoregulatity of poly(methyl methacrylate) (PMMA).[84,85,86] Dybal *et al* used the infrared spectra of PMMA to find that in a stereocomplex of isotactic and syndiotactic PMMA the extended chain form of the syndiotactic PMMA is preferred.[85]

II.4.6. Physical Basis and Background for Raman Spectroscopy

As discussed earlier, infrared spectroscopy involves vibrational transitions due to adsorption of photons between the actual energy levels in the infrared region of the electro-magnetic spectrum. In contrast, Raman spectroscopy involves the inelastic scattering of photons rather than their direct absorption or emission. When radiation is incident on a molecule several possible interactions may take place and the incident radiation may be absorbed, transmitted, refracted, diffracted, or reflected. A fraction of the light is elastically scattered and, therefore, unchanged in energy (Rayleigh scattering).[56] A smaller fraction of the radiation will be scattered inelastically giving rise to the Raman effect. Both the Rayleigh and Raman scattering are very weak with intensities of roughly $I_{Rayleigh} \approx 10^{-4} I_{source}$, and $I_{Raman} \approx 10^{-8} I_{source}$,[61] resulting in the need for high power, monochromatic laser sources. The intensity of the molecular scattering is dependent on the frequency of the excitation source to the forth power, as well as the polarizability of the scattering molecules as shown in Equation 8.[49]

$$I_{mn} = \frac{2^7 \pi^5}{3^2 c^2} I_0 (\nu_0 + \nu_{mn})^4 \sum_{\rho\sigma} \left| (\alpha_{\rho\sigma})_{mn} \right|^2 \qquad \text{Eq. (8)}$$

Here the subscripts m and n represent a transition from the m vibrational level to the n level. Alpha, α, is the $\rho\sigma$ component of the polarizability tensor, where $\rho\sigma$ assumes nine possible designations (i.e. xx, xy, xz, yz, etc.). The net result is a strong dependence of the Raman intensity on the excitation frequency with higher frequency excitation leading to a larger Raman scattering cross-section and higher intensity Raman signals.

The inelastic scattering of radiation results in two possible processes. Molecules in the ground state give Raman scattering with energy $h(\nu_0 - \nu_1)$. These transitions result in a reduction of the energy and is known as Stokes scattering. The second possibility results when vibrationally excited state molecules inelastically scatter back to the ground state, giving an energy $h(\nu_0 + \nu_1)$. These transitions result in an increase in energy and are known as anti-Stokes scattering. The change in energy of the molecule in both Stokes and anti-Stokes scattering corresponds to the vibrational energy levels of the molecule. This gives rise to the Raman spectrum.

The ratio of the Stokes and anti-Stokes intensity is governed by the sample temperature. The ratio can be determined from the Boltzman distribution,

$$\frac{\text{anti - Stokes intensity}}{\text{Stokes intensity}} = \frac{(\nu + \nu_m)^4}{(\nu - \nu_m)^4} e^{-(h\nu_m / kT)} \qquad \text{Eq. (9)}$$

when the system is at thermal equilibrium.[59] At ordinary temperatures most of the molecules exist in the ground state and therefore Stokes lines have greater intensities than anti-Stokes lines. It is possible to use the ratio of Stokes and anti-Stokes to determine the temperature of a sample.

While infrared and Raman spectra both involve vibrational and rotational energy levels, they provide complementary information. This is because the intensity of the spectral band depends on how effectively the photon energy is transferred to the molecule. Furthermore, the mechanism for the photon/energy transfer differs in the two techniques.[59] In order for a molecular vibration to be Raman active, the vibration must be accompanied by a change in the polarizability of the molecule. In Raman spectroscopy, an electromagnetic wave of frequency ν interacts with the polarizable electron cloud, causing it to oscillate. The oscillating electron cloud coupled to the molecular vibrations gives inelastic scattering in all directions. The vibrational analysis of molecules through the use of group theory, allows the calculation of the number and activity of the Raman bands expected in the spectrum of the molecule.

In general, the Raman scattered light from an unpolarized random sample will be polarized to some extent.[61] For a specific scattering geometry, the polarization is dependent upon the symmetry of the molecular vibration giving rise to the line. In solid samples the polarization is more complicated. However, the directionality in the crystal can be used to obtain Raman data. Polarization measurements in conjunction with dichroic measurements from IR spectroscopy can be a powerful tool for the structural determination of polymers.[61]

Near IR Fourier transform (FT) Raman spectroscopy is designed to eliminate the fluorescence problem encountered in conventional Raman spectroscopy.[87] If a Raman sample is even slightly fluorescent, the fluorescence will normally be much more intense and obscure the Raman signal. The use of an excitation frequency below the threshold for the fluorescence process, such as 1064 nm, will remove many problems associated

with fluorescence interference. The Raman scattering from 1064 nm will occur in the near-IR region. Conventional FTIR instrumentation with added filters for rejection of the Rayleigh line can be used with little modification. FT Raman spectroscopy holds a significant promise for bulk chemical characterization of biomaterials and drug delivery systems.[88] Conventional Raman spectroscopy is not widely used due to problems associated with background fluorescence and photodegradation of molecules sensitive to visible light. Further advantages of FT Raman spectroscopy include the requirement for little sample preparation and the rapid analysis time for most materials.[88]

The advantages of FT Raman are counterbalanced by the difficulties in the distinction between inherently weak Raman and strong Rayleigh scattering. In the Fourier transform process, the noise in the intense Rayleigh line is redistributed across the entire spectrum.[87] Therefore, FT Raman spectroscopy must have an extremely effective means of removing stray light at the laser wavelength. Furthermore, since lower frequency IR radiation is used as the excitation source, the Raman scattering cross-section is reduced, and the IR radiation can cause excessive local heating of the sample.

When the laser wavelength used to excite the Raman effect lies under an intense electronic absorption band of a chromophore, a considerable resonance enhancement of the Raman signal by a factor of 10^3 to 10^6 may occur.[87] The enhanced vibrational modes are generally totally symmetric and are associated only with the electronic chromophore being excited. Accordingly, the enhancement can increase the Raman signal in certain cases. However, nonlinear variations in intensities that depend in a complex way on the proximity of the laser excitation wavelength to the electronic maximum of the sample can

be seen in certain samples.[89] Therefore care must be exercised in quantitative analysis to account for this nonlinearity in peak intensity.

II.4.7. Hardware Requirements for Raman Spectroscopy

The monochromatic and intense light provided by lasers offers clear advantages for Raman Spectroscopy. Therefore with the advent of lasers in 1960, lasers quickly replaced all other sources becoming the standard.[59] Today there are many different types of lasers available which range greatly in frequency and power output. Not only can high power Ar^+ and Kr^+ lasers be used directly, but they can also be used for pumping dye lasers and tunable solid state lasers in order to increase the range of the exciting frequency. Frequency doubling of Nd:YAG lasers at high conversion rates and intense diode lasers have also increased the availability of Raman sources. This ability to change excitation wavelength can help to eliminate the problems caused by fluorescence of samples and low detector sensitivity in regions of the spectrum.

Gratings used in early monochromators for Raman spectroscopy were mechanically ruled. Modern holographically ruled gratings are now commonly available providing dramatic improvements in signal-to-noise ratios. Furthermore, the introduction of concave holographic gratings in place of the conventional plane gratings, has aided in increasing the throughput since concave gratings require no additional optical elements. Since stray light rejection and throughput are of critical importance, improvements in double and triple monochromator design have also increased the signal-to-noise ratios.

Finally, higher quality materials and improvements in the manufacture of optical components have increased the light collection of Raman spectrometers.

The recent advances in detector technology have again changed the future of many Raman techniques. Photomultiplier tubes and photodiode arrays are now being replaced in Raman spectrometers by charge couple devices (CCD). CCD detectors are a class of extremely low noise devices that often consist of millions of pixels.[90] CCD detectors can be cooled to liquid nitrogen temperatures giving remarkably low dark current levels, thereby allowing for long exposure time experiments. Although CCD technology has had more than 20 years to mature, advances are continually being made in CCD manufacturing technology and design techniques.[90] New CCD devices can provide nearly photo-counting performance in each pixel and simultaneously achieve dynamic ranges between 10^4 to 1 counts and 10^6 to 1 counts.[90] CCD detectors also offer the possibility of 2-dimensional imaging which may be used to determine the homogeneity of samples. CCD detectors can be coated to have high sensitivity in the UV, VIS, x-ray and IR regions. The high sensitivity of CCDs in the 700-1,000 nm region has reduced the problems caused by intense visible fluorescence of some samples.

Fiber-based devices for Raman spectroscopy are becoming more important in a variety of applications.[91] Fiber optic technology allows the excitation and emitted light to be routed to the point of interest using a small sampling probe, thereby offering the advantages of flexibility and remote sampling. Small portable, fiber optic Raman systems can now be purchased commercially from several sources.

The last major component of a Raman system is the data acquisition system. The improvements in speed and power of compact computers allows complete analysis

systems to run on microcomputers. Collection of large numbers of data points, data manipulation, background removal, spectrum plotting and analysis can now be accomplished with smaller and faster computers. For analysis of complex multicomponent data, new computer systems also include spectral identification programs based on growing spectral libraries.

Technological advances, such as those described above, allow high quality Raman data to be obtained for systems and samples that would have been impossible to investigate only 15 years ago. Limitations of old techniques have been removed and new applications are being continually developed. Furthermore, as technology increases, Raman spectroscopy systems are becoming less expensive, thereby opening a wider variety of potential applications.

II.4.8. Sampling Techniques for Raman Spectroscopy

As previously mentioned, sampling techniques for Raman require little preparation in many cases. This is an advantage over IR techniques which require careful sample preparation. In solution sampling for Raman spectroscopy, the polymer solution may simply be contained in a glass or quartz capillary tube and the scattered light viewed at a right angle to the excitation radiation. The laser beam excitation source is narrow, collimated, and unidirectional, so it can be manipulated in a variety of ways to access many sample configurations.[61] As mentioned earlier, water has an extremely weak Raman spectrum and is an excellent solvent for Raman spectroscopy. Thus, solution studies on water soluble or swellable polymers are increasing in importance.[52,92]

Solid sampling techniques for Raman spectroscopy depend on the nature of the sample. Highly scattering and turbid samples are most often studied in a front surface geometry, while for clear samples right-angle scattering can be used. Powdered samples can be packed into glass tubes or cavities for a front surface or a transverse sampling geometry. Fiber samples can be examined by lumination of the fiber at 90^{o} to the fiber axis and the radiation is collected at 90^{o} to both the fiber axis and the excitation source. Deformation caused by high temperatures or swelling processes in solid polymeric materials can be studied using Raman polarization measurements and varying the sample orientation.

Microsampling in Raman can easily be obtained because the coherent visible light source can be tightly focused. In micro-Raman, microscopes are coupled to the Raman spectrometer allowing samples from 2 to 10 μm in size to be examined.[56] The ability to examine small spot sizes allows micro-Raman to determine heterogeneities in solid polymer samples. Micro-Raman can also be used to study small volume gas and liquid samples down to the nanoliter range.[56]

Surface-enhanced Raman scattering (SERS) spectroscopy has been established as a powerful method for elucidation of the structure of molecules adsorbed on specially prepared metal surfaces.[93] The enhancement effect can increase Raman scattering by a factor of 10^{3} - 10^{6}.[94] Furthermore, adsorption of molecules on the SERS active metal surface causes fluorescence quenching in some highly fluorescent compounds, thereby reducing the fluorescence interference. However for this sampling technique, the overall theoretical approach to successfully explain these phenomena is not yet clear.[56]

II.4.9. Application to Polymers

Raman spectroscopy is extremely valuable in many different areas of polymer characterization.[56] In addition to the identification of the specific type of polymer, it can be used to determine functional groups, end-groups, structure, conformation, kinetics of polymerization and crosslinking, orientation of chains; and to follow changes in structural parameters as the polymers are exposed to environmental or mechanical stresses.

Raman spectroscopy can be used for quantitative work as well as qualitative studies. Both added internal standard and reference bands are used for quantitative work. Ratioing techniques have been used to determine the concentration of unreacted monomer in polymer systems. Additionally, the band ratio technique has been successfully employed to determine the composition of copolymers.[56] The intensity ratios of the characteristic bands of two homopolymers, which have structural units in the chain similar to those expected in the copolymer, were used to determine the composition of each monomer in the copolymer.[76,77]

Quantitative micro-Raman spectroscopy has been used to determine impurities in polymer systems. The ability to study small samples will allow the analysis of impurities which are contaminating polymer materials.[76] *In situ* solid state analysis of excipents or additive molecules within a polymeric biomaterial have been performed with Raman spectroscopy.[88] Davies *et. al* have studied the role of additive-polymer interaction with drugs by monitoring shifts in Raman bands indicative of chemical changes at the

molecular level.[88] A major feature of this study was the ability to detect quantitatively the molecular structures of a drug and polymer by Raman spectroscopy.

Micro-Raman and FT Raman have both been used to monitor the appearance or disappearance of specific functional groups within a polymer after exposure to degradation processes such as hydrolysis or irradiation.[88] In biomedical polymers, a significant degree of interest has been focused on the analysis of polymer degradation for drug release. Raman spectroscopy allows the degradation process in aqueous biological systems to be studied *in situ.*[88] The use of micro-Raman coupled with fiber optics may allow Raman spectroscopy to be used for *in vivo* analysis and diagnostics.[88]

Raman spectroscopy of thin films less than 5 μm thick is extremely difficult owing to the small scattering volume of the sample.[95] A technique know as waveguide Raman spectroscopy (WSR) has been developed to overcome this limitation. The radiation is coupled into the polymer sample using a prism and propagates by total internal reflection. This technique has been used to study organic films, laminates, and orientation studies of isotactic poly(methyl methacrylate).[76] Furthermore, the partial orientation of small guest molecules in poly(vinyl alcohol) matrices have been analyzed by the WSR technique.[96]

Recently, near-infrared FT Raman spectroscopy applications of waveguide Raman spectroscopy (WRS) have been demonstrated.[97] In the study, waveguide Raman spectroscopy measurements using near-infrared excitation and a Michelson interferometer were combined with fiber optics for examination of submicron cellulose acetate and poly(vinyl alcohol) films. FT Raman spectra of films containing small molecule

chromophores imbedded in polymer matrices were obtained. This technique seems to have potential for advancement in many areas.

Solution studies of polymers relate the conformation of the polymer chain to other solution properties. The structure of the polymer chain changes upon dissolution or swelling and undergoes transformation with changes in the pH, ionic strength, or salt content of the solution.[98] All of these properties can have large effects on hydrogels, and since water is an excellent Raman solvent, Raman spectroscopy is attractive for studying changes in polymer chain structure. For example, Koenig *et. al* have investigated the conformation of syndiotactic polymethacrylic acid (PMAA) at various degrees of neutralization in aqueous solutions.[99] They determined progressive changes in C-COOH motions in a neutralization range from 0.1 to 0.4 fractions.

Studies of polymers in the solid state can yield information on the structure and conformation of polymer backbones. For polymers such as polymethacrylic acid (PMAA) in aqueous solutions, the local conformation does not seem to change drastically from solid state to solution.[98] Koenig *et. al* have shown that the Raman spectra of PMAA in the solid state and in aqueous solution are strikingly similar.[99] The only frequency shifts seen were attributed to the difference in the state of hydrogen bonding in the solid and aqueous solution. The similarity in Raman spectra suggest that little, if any, detectable conformational changes in the PMAA structure occurs with dissolution. Koenig has also studied poly(ethylene glycols) (PEG) in aqueous solutions.[100] The Raman spectra suggest that the PEG molecules in aqueous solution have changed from a helical structure to a new, less ordered but not completely disordered structure.

Raman scattering from the solid state can be used to obtain information about the distribution of molecular orientations in a solid polymer.[101] The molecular orientations in solid polymers have been shown to be capable of providing quantitative information about the second and fourth moments of the orientation distribution functions in non-crystalline polymers.[101] Raman spectroscopy also offers the possibility of obtaining information about non-crystalline regions of crystalline polymers. The orientation of non-crystalline regions of polymers may improve the understanding of properties such as elastic modulus and shrinkage.

Raman spectra can be used to obtain information on the stereoregularity of polymers from both the solution and solid state, while preserving the sample integrity. The stereoregularity of a polymer greatly effects the morphological and physical properties of the polymer.[102] Tudor *et. al* have shown that polymer morphology is a crucial factor in the hydrolysis rate of polymers used for drug release. In this work, FT Raman spectroscopy was used to indicate the morphology of poly(anhydride) samples for use in drug release polymers.[55] Furthermore, the ordered structure of poly(methyl methacrylate) has been extensively studied by Raman techniques in order to determine the stereoregularity.[84-104] These studies show the promise of Raman techniques for non-destructive orientation and stereoregularity studies of polymers in solution and solid state.

Raman spectroscopy can be used to follow the polymerization process and provide information on the extent of polymerization and structural information on the end-product.[76] The intensity of the C = C stretching vibration of the monomer decreases as the polymerization proceeds. Ratioing of peak intensities to initial intensities can give direct information on conversion as a function of time. Gulari *et. al* have used Raman

spectroscopy to monitor the polymerization rate of bulk methyl methacrylate (MMA)[75] By following the reduction in the scattering intensity of the carbon double bond, the percent conversion of MMA as a function of time was monitored with Raman spectroscopy. Perhaps the most interesting finding in this research was the detection of a new peak at 1545 cm^{-1} present only during rapid polymerization period. It was concluded that the peak is due to a free radical intermediate formed by the addition of AIBN (azobis-(isobutyronitrile)) to MMA. This free radical is probably stabilized through conjugation with either the cyan group or the ester group. The fact that a strong signal was obtained from a reaction intermediate which is in low concentration and short lived suggests that there is significant enhancement of the Raman band by resonance.[75]

The recent advances in Raman techniques have made it possible to explore the kinetic behavior of faster polymerizations.[76] The polymerization reaction can be followed to completion with Raman techniques. Many techniques lose their sensitivity after the gel point and are therefore limited in following high conversion reactions. Raman has been shown to work well for bulk polymerization of fast reacting monomers.

Large scale process monitoring seems to be possible using Raman techniques to measure a change in a reactant or the concentration of a product. To overcome the problems of sample geometry, non-invasive fiber optic systems have been built to carry out remote sensing.[105,106] The near-infrared Fourier transform Raman technique can be significantly enhanced by use of fiber optic assemblies.[107] As mentioned previously, near-infrared FT Raman is limited by sample alignment problems and the generation of excessive temperatures. However, both problems can be reduced with the easier positioning of the fiber probe and the lower laser power densities required for meaningful

signal to noise ratios.[107] Due to this lower power requirement near-infrared FT Raman spectra of systems which contain highly absorbing or fluorescing molecules can now be easily obtained without large temperature increases.

II.4.10. Raman Cure Monitoring

Raman spectroscopy is attractive for monitoring the curing of polymeric systems because it can provide real-time measurement of the vibrational structure of the sample. The consumption of double bonds during polymerization affords the possibility of monitoring the vinyl stretching frequency using raman scattering as a means of tracking the polymerization reaction kinetics.

Raman spectroscopy was used to monitor the cure *in situ* during the cationic photopolymerization of a divinyl ether photosensitized with anthracene. Since Raman spectroscopy arises from molecular vibrations, the consumption of double bonds can be directly measured during polymerization reactions. By monitoring the double bond concentration, Raman spectroscopy gives a direct method of obtaining the propagation rate during the reaction. Furthermore, the short intrinsic time scale makes Raman spectroscopy attractive as a time-resolved technique to monitor cure in these high speed reactions.

A series of Raman experiments were performed on cationic photopolymerizations of a divinyl ether initiated with a diaryliodonium salt of hexafluoroantimonate photosensitized by anthracene. The photosensitizer allowed the initiating wavelength to be shifted from the deep UV region of the spectrum to the near UV region around 350

nm.[109] Isothermal Raman experiments were performed for a series of reaction temperatures, and used to determine the overall activation energy of the polymerization reaction. Since the Raman profiles give a direct measure of conversion versus time, the rate of reaction was determined during the photopolymerizations. Finally, the Raman profiles were used in conjunction with previously determined photosensitization rate constants[109] to determine the kinetic constant for the propagation reaction. The resulting profiles for the propagation rate constants as functions of conversion provide important insight into the nature of cationic photopolymerizations.

As mentioned earlier, the fluorescence monitoring technique developed to follow cure gave a direct measure of the photosensitization reaction rate and the production of active cationic centers.[109] The combination of the fluorescence and Raman techniques allows both the photosensitization rate and the propagation rate to be determined *in situ* for these high speed cationic polymerizations. The Raman technique was compared with the earlier fluorescence method in order to verify both reaction monitoring techniques.

II.5. Cure Monitoring Using Photo-Differential Scanning Calrimetery

In general carbocationic polymerization kinetics are complex and vary from system to system. Therefore a simple, coherent, kinetic expression of general validity is not available for cationic polymerizations.[118] There are several difficulties that contribute to this deficiency. First, the reactivity of the carbocationic center depends strongly on the proximity of the counterion and a number of propagating species may be identified, including ion pairs, solvated ions, or aggregates. The reactivities of the separated or

solvated cations are greatly increased over ion pairs and have different chemical characteristics.[118] Second, the pseudo steady-state active center concentration assumption is invalid for cationic polymerizations. In contrast to free radical polymerizations, combination of active centers does not occur and termination is generally suppressed in cationic polymerizations. Therefore, in most cases the rates of initiation and termination are not equal, and non-steady state calculations are required.[118] In addition, transfer reactions are typically important in cationic polymerizations and the polymerization rate constants are affected by the nature of the counter-ion and solvent. Kinetic analysis of cationic polymerizations is not impossible, but requires careful individual consideration for each system under investigation.

Photo-differential scanning calorimetry (PDSC) offers a simple method to characterize the kinetics of photopolymerization reactions. Since the polymerizations are highly exothermic, the reaction rate may be measured by monitoring the rate at which heat is released from the polymerizing sample. Therefore the profiles of reaction heat versus time provided by PDSC may be used to characterize the reaction kinetics and evaluate polymerization rate constants.[119] Several authors have used PDSC to characterize free radical photopolymerizations;[27,119-122] however, application of the technique to cationic photopolymerizations of divinyl ethers is more problematic. First, the polymerizations of divinyl ethers proceed very rapidly, and care must be taken to ensure that the reaction rate does not exceed the time resolution of the instrument. Since the DSC response time is on the order of 2-3 seconds,[29,123] relatively low light intensities must be used to increase the reaction time for the divinyl ether photopolymerizations.[16] Second, photopolymerizations of divinyl ethers are highly exothermic, and to maintain

isothermal conditions during the reactions, very small sample sizes must be used (0.5 - 1.5 mg). If larger samples sizes are used, the heat evolved during the reaction generally cannot be removed on the time scale of the reaction.

In this this research, PDSC was used to study the photosensitized cationic homopolymerization of a model divinyl ether monomer. Divinyl ethers have received increased attention in recent years because they generally exhibit very low vapor pressures, relatively low viscosities and low toxicity,[124] but polymerize very rapidly to form films that exhibit excellent clarity, adhesion, and solvent resistance. There are now a number of commercially available divinyl ether monomers, however relatively few detailed kinetic studies have been reported. Understanding the kinetics of these cationic photopolymerizations is important due to the increasing number of applications for rapid, solvent-free curing of polymer films. This recent surge in applications of UV-initiated photopolymerizations has been motivated by at least two factors: environmental concerns about the production of volatile organic emissions, and the need for high-speed reactions to enhance production rates (see refs 4,27,124,125).

A series of PDSC experiments were performed on cationic photopolymerizations of a divinyl ether initiated with a diaryliodonium salt of hexafluoroantimonate photosensitized by anthracene. The photosensitizer allowed the initiating wavelength to be shifted from the deep UV region of the spectrum to the near UV region around 350 nm.[126] Isothermal PDSC experiments were performed for a series of reaction temperatures and light intensities. The profiles were used in conjunction with previously determined photosensitization rate constants[126] to determine the kinetic constant for propagation. The kinetic constant for termination was determined from a series of

unsteady-state "dark-cure" reactions at different temperatures and light exposure times. The resulting profiles for the propagation and termination rate constants as functions of conversion provide important insight into the nature of the cationic photopolymerizations.

II.6. Luminescence Temperature Monitoring

II.6.1. Need for Temperature Monitoring

Most of the early work on cationic photopolymerizations focused on the identification and synthesis of appropriate monomers and initiators, (for reviews see references 4 and 5) and only recently have detailed studies of the reactions been reported.[108,109] For example,[109] a novel *in situ* laser-induced fluorescence technique for monitoring the initiation reaction in these high-speed polymerizations was reported. Due to its extremely short intrinsic time scale, the fluorescence technique provided a means to characterize the kinetics of these polymerizations which proceed too rapidly to be monitored by traditional methods such as differential scanning calorimetry (DSC). These studies indicate that although the reactions are extremely rapid (the systems typically react to completion in a few seconds), most of the conversion occurs in the last 100 milliseconds due to a dramatic increase in the reaction rate. This characteristic reaction profile was attributed to thermal runaway resulting from the large amount of heat released by the rapidly polymerizing system.

Luminescence techniques was developed to monitor the sample's internal temperature in real-time during polymerization. The temperature measurement may be

accomplished in a straightforward manner by monitoring emission energy, lifetime, or intensity. The most simplistic method is to monitor the emission intensity from a fluorophore, which is typically a strong function of the local temperature. The temperature sensitive lanthanide probes can be purchased commercially or produced in a one step synthesis. Several lanthanide candidates hace been evaluated, most having the general form of $Eu(btfa)_3$ and $Eu(hfa)_3$. Successful completion of these experiments will provide a detailed kinetic picture of the polymerization reaction, including the effect of temperature.

Initial temperature profiles have been obtained using thin wire thermocouples embedded into films (Figure II.1.). An Omega (WB-FAI B8 IBM 8-Channel) High Speed data acquisition card installed in an IBM PC was used to acquire temperature data as function of time. The Omega system is capable of recording up to 2500 temperature measurements per second. Fully formulated systems (monomer and initiator) were coated on glass substrates at an average of 0.067 mm thickness. A thermocouple wire (0.02 mm diameter) was placed in the film before the exposure to the UV lamp. The lamp and temperature acquisition are started at the same time, recording the temperature rise during the course of the reaction. The Omega system was used to obtain initial temperature profiles to establish the parameters for the temperature measurement.

The importance of thermal runaway will be determined by monitoring the temperature *in situ* during cationic photopolymerizations of DVE-3. Since these studies are complicated by the rapid rate at which the reaction takes place as well as the thin-film geometry and the need for an optically-transparent, noninvasive probe, traditional

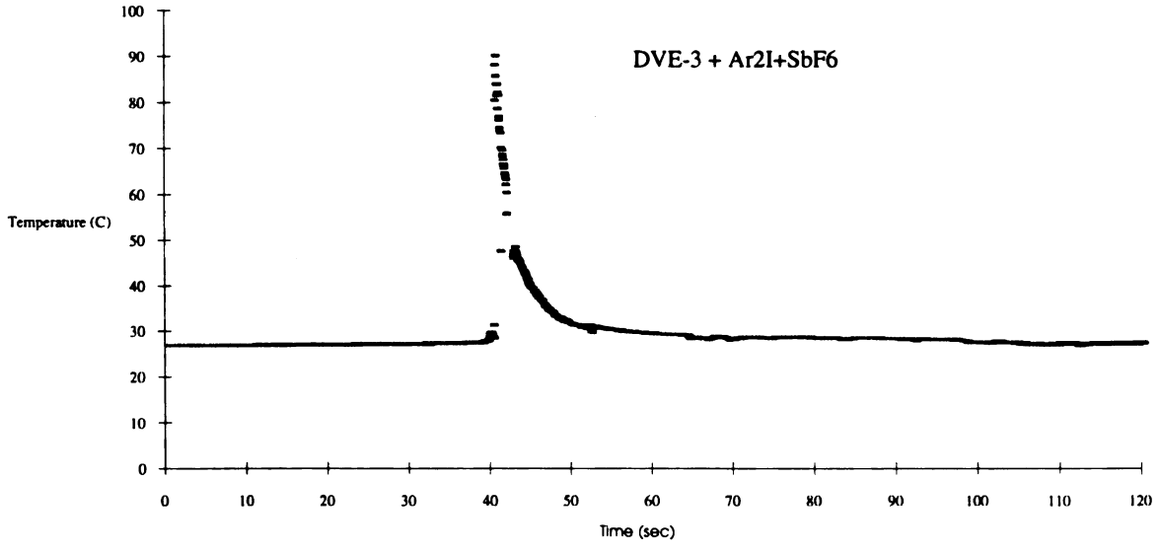

Figure II.1. *Temperature profile for a thin film reaction of DVE-3 on a glass substrate.*

methods of temperature monitoring are inadequate. For example, thermocouples are invasive, opaque, and even in their smallest form, have a size-scale comparable to the film thickness. Raman spectroscopy could theoretically be used to determine temperature by comparison of the magnitudes of the Stokes and the anti-Stokes lines. However, Raman is characterized by an inherent signal weakness and is often obscured by sample fluorescence. Luminescence techniques for temperature monitoring have also been reported in the literature.[110] For example, temperature-sensitive excimer formation,[111] and a second technique based upon temperature-induced spectral shifts[110] have been used to characterize temperature in fuel sprays, and organic solvents. These techniques are not applicable to polymerizing systems because they are sensitive to changes in viscosity.

In this research, a luminescence scheme for *in situ* monitoring of temperature during cationic photopolymerizations of DVE-3 photosensitized by anthracene was developed. Due to its short intrinsic time scale, luminescence techniques are attractive for monitoring the local temperature of these reactions which may proceed to completion in a few seconds. Furthermore, luminescence techniques provide a non-intrusive method for monitoring the temperature since trace amounts of the luminescence probe may be readily incorporated into the reaction mixture. Tris(β-diketone) chelates of europium fulfill the requirements of a temperature-dependent luminescence probe for our studies. These probes exhibit a linear response for a wide temperature range, and are insensitive to changes in viscosity. In addition, the excitation wavelength of these probes is ideally suited for our studies.

II.6.2. Probe Requirements

In addition to exhibiting a temperature-dependent response, the luminescence temperature probe for our studies must meet specific spectral requirements. Anthracene, which absorbs between 320 and 390 nm, was used as a photosensitizer to expand the initiating window to the near-visible region of the spectrum. The anthracene photosensitizer makes it possible to initiate polymerization in the near-UV or visible wavelengths as a result of a direct interaction between an excited state of a photosensitizer and the initiator.[109] In our experiment, 351 nm or 364 nm ultraviolet (UV) light was used to initiate the photopolymerization. Therefore, these wavelengths are the most convenient for excitation of the temperature probe, since they would eliminate the need for two laser beams. In addition, the emission wavelengths of the temperature probe must not overlap with the fluorescence of the anthracene photosensitizer in the 425 nm region.

A class of compounds which satisfies both spectral requirements is the lanthanide substituted tris(β-diketone) chelates, which absorb from 280 to 380 nm[112] and emit in the 620 nm range.[113] These compounds exhibit an interesting "antenna" effect which is responsible for the temperature dependence of the luminescence. The light absorption by the lanthanide itself is very weak; however, the ligand plays the role of an antenna by absorbing light and efficiently transferring the excitation energy to the metal ion.[114] This non-radiative intramolecular transfer from the excited state of the ligand to the highly luminescent europium metal center results in a number of interesting luminescent

properties. A number of authors[111,113-117] have characterized the chemical and photophysical properties of these chelates. These authors found that the luminescence efficiency varies greatly with the identity of the ligand, degree of coordination, temperature, and solvent.[112,114] Sager *et. al* reported that the underlying photophysical process proceeds by the following four-step mechanism: (1) ground singlet absorption to the excited singlet state; (2) radiationless intersystem crossing from the excited singlet to the lowest lying triplet state; (3) transfer of energy to the chelated ion; and (4) characteristic ionic fluorescent emission.[112]

II.7. Modeling of the Formation of Highly Crosslinked Polymers

Very few models for the formation of highly crosslinked polymer networks by cationic photopolymerizations have been reported in the literature. However, free-radical crosslinking reactions have received considerable attention, and many of the approaches used for free-radical reactions could also be appropriate for cationic polymerizations. Models which have been developed to describe free radical crosslinking reactions may be divided into three classes[127] 1) statistical models, 2) kinetic descriptions, and 3) kinetic gelation models based upon computer simulated random walks. The statistical models consider an ensemble of polymer structures built from monomer units according to probabilistic rules for bond formation. The recursive nature of the polymer structure is exploited to obtain expressions for statistical averages of the ensemble. While this approach is useful for lightly-crosslinked polymer networks formed in reactions containing small concentrations of a multifunctional crosslinking agent, it is of limited

value for highly crosslinked homopolymerizations of multifunctional monomers. Reaction nonidealities such as extensive intramolecular cyclization, heterogeneity, and topological constraints are difficult to treat using this approach.

The kinetic approach based upon the solution of a set of differential equations describing the disappearance of reactants is also of limited value for describing highly crosslinked cationic photopolymerizations. Even the basic step of identifying the reactive species to consider in the kinetic model is a nontrivial task for cationic polymerizations because the reactivity of a propagating cationic center depends upon the identity and the location of its counter ion. For kinetic modeling purposes it is common to assume several types of propagating centers ranging from completely free (unpaired) ions to covalent species; however, the choice of the number of such species to include is somewhat arbitrary. The analysis is further complicated by the difficulty in evaluating the kinetic constants, and the fact that the quasi-steady-state assumption is not valid for the reactive centers.[118] The largest shortcoming of the kinetic approach is the inability to provide structural information about the crosslinked polymer network.[128]

The final type of model for free radical copolymerization/crosslinking reactions are kinetic gelation models based upon random walk on cubic lattices. The first kinetic gelation model was reported by Manneville and de Seze.[129] These authors distributed bifunctional and tetrafunctional monomer units randomly on a cubic lattice, then started the simulation by allowing a fraction of the sites to simultaneously become active centers. At each step during the simulation, an active center was chosen at random and allowed to "choose" one of its first or second nearest neighbors. If the chosen site had an unreacted functionality, a bond was formed and the active center was transferred, while if the

chosen site had an active center, the centers annihilated one another and termination was achieved. Manneville and de Seze recognized that their model incorporated two drastic simplifications:[129] constraining the system to a cubic lattice, and ignoring the possibility of molecular motion.

The kinetic gelation approach has been refined and modified by several authors. In a series of papers,[130-133] Herrmann and collaborators attempted to include inert solvents, and monomer mobility. Mobility was included by allowing monomer units and neighboring solvent molecules to periodically exchange positions. Even with monomer mobility included in this manner, the authors found that an unreasonably large fraction of the radicals became trapped by becoming surrounded by inert species. This trapping resulted in a maximum attainable conversion which was typically less that 60%. Boots and collaborators[134-136] relaxed the assumptions of instantaneous and simultaneous initiation by running simulations in which initiation occurred at a much slower rate than termination. Finally, Simon et al[137] allowed an exponentially decaying rate of initiation.

Although kinetic gelation models can account for reaction heterogeneity, and to some extent topological constraints, they are currently unable to accurately describe free radical reactions. While many of the simulations predict correct trends such as increasing gel point conversion with decreasing crosslinker concentration, they are presently unable to account for many of the molecular phenomena which can significantly affect the reaction characteristics. As recognized by Manneville and de Seze in their original paper,[129] most of the limitations of the models arise from the choice of a lattice, and the inability to properly account for molecular motions. For example, constraining the system to a cubic lattice limits the number of units an active center may react with to six,

and significantly distorts the bond angles in the polymer backbone chain. The backbone bond angle is important because the polymer conformation will determine the probabilities of cyclization and of trapping. The inability to account for monomer and polymer mobility precludes the possibility of accurately including diffusion-controlled reactions. Furthermore, Boots and Dotson[138] illustrated that failure to account for polymer mobility results in an overestimation of the heterogeneity in the reaction.

II.8. List of References

1. G. Odian, *Principles of Polymerization*, 2nd Ed., Wiley, New York, NY, 1981. 22.

2. P.H. Plesch, "Propagation Rate Constants in the Cationic Polymerization of Alkenes," *Cationic Polymerization and Related Processes*, E.J. Goethals ed., IUPAC, Oxford, UK, 1 (1984).

3. D.J. Dunn, *Developments in Polymerization*, R.N. Haward, Ed., Applied Science Publishers, London, **1**, 45 (1979).

4. J.V. Crivello, "Cationic Polymerization-Iodonium and Sulfonium Salt Photoinitiators," *Adv. Polym. Sci.*, **62**, 1, (1984).

5. J.V. Crivello and J.L. Lee, "Alkoxy-Substituted Diaryliodonium Salt Cationic Photoinitiators," *J. Polym. Sci., Polym. Chem.*, **27**, 3951 (1989).

6. A. Ledwith, S. Al-Kass, A. Hulme-Lowe, "Mechanisms for Photoinitiation of Cationic Polymerization," *Cationic Polymerization and Related Processes*, E.J. Goethals, Ed., IUPAC, Oxford, UK, 275, 1984.

7. J.V. Crivello, "Recent Progress in the Design of New Photoinitiators for Cationic Polymerization," *Cationic Polymerization and Related Processes*, E.J. Goethals, Ed., IUPAC, Oxford, UK, 289, 1984.

8. A. Reiser, *Photoreactive Polymers*, Wiley, New York, NY, 1989.

9. S.P.Lapin, "Radition-Induced Cationic Curing of Vinyl-Ether-Functionalized Urethane Oligomers," *Radiation Curing of Polymeric Materials*, C.E. Hoyle and J.F. Kinstle, Eds., ACS Symposium Series 417, ACS, Washington D.C., 363 (1989).

10. J.V. Crivello and J.H.W. Lam, The Photoinitiated Cationic Polymerization of Epoxy Resins," *Epoxy Resin Chemistry*, R.S. Bauer, Ed., ACS Symposium Series, 114, ACS, Washington D.C., 1 (1979).

11. S.P. Pappas, "Photoinitiation of Cationic and Concurrent Radical-Cationic Polymerization. Part V.," *Prog. Org. Coat,* **13**, 35 (1985).

12. J.V. Crivello, "Photoinitiated Cationic Polymerization of Coatings," *Organic Coatings, Science and Technology, Vol. 5,* G.D. Parfitt and A.V. Patsis, Eds., Marcel Dekker, Inc., New York, NY, 35, 1983.

13. W.R. Watt, "Photosensitized Epoxies as Basis for Light-Curable Coatings," *Epoxy Resin Chemistry*, R.S. Bauer, Ed., ACS Symposium Series 114, ACS, Washington D.C. , 17, 1979.

14. F. Loshe and H. Zweifel, "Photocrosslinking of Epoxy Resins," *Adv. Polym. Sci.*, **78**, 61 (1986).

15. J.V. Crivello and D.A. Conlon, "Aromatic Bisvinyl Ethers: A New Class of Highly Reactive Thermosetting Monomers," *J. Polym. Sci., Polym. Chem.*, **21**, 1785 (1983).

16. J.V. Crivello, J.L. Lee, D.A. Conlon, "Photoinitiated Cationic Polymerization with Multifunctional Vinyl Ether Monomers," *J. Rad. Cur.*, **10**, 6 (1983).

17. J.V. Crivello and J.L. Lee, "UV Cure of Epoxy-Silicone Monomers," *Radiation Curing of Polymeric Materials*, C.E. Hoyle and J.F. Kinstle, Eds., ACS Symposium Series 417, ACS, Washington D.C., 398 (1989).

18. J.V. Crivello and J.L Lee, "The Synthesis, Charaterization, and Photoinitiated Cationic Polymerization of Silicon-Containing Epoxy Resins," *J. Polym. Sci., Polym. Chem.*, **28**, 479 (1990).

19. J. Pelgrims, "Cationic UV Polymerization of Cyracure Cycloaliphatic Epoxies," *Pigm. Resin Technol.*, **16**, 4 (1987).

20. J.V. Crivello , D.A. Conlon, D.R. Olson, and K.K. Webb, "The Effects of Polyols as Chain Transfer Agents and Flexibilizers in Photoinitiated Cationic Polymerization," *J. Rad. Cur.*, **13**, 3 (1986).

21. J.V. Crvello, D.A. Conlon, D.R. Olson, and K.K. Webb, "Accelerators in UV Caioinc Polymerization," *Polym. Paint Colour J.*, **178**, 696 (1988).

22. A. Ledwith, , *Macromol. Chem. Suppl.*, **3**, 348 (1979).

23. R.P. Eckberg and K.D. Riding, "UV Cure of Epoxysiloxanes and Epoxysilicones," *Radiation Curing of Polymeric Materials*, C.E. Hoyle and J.F. Kinstle, Eds., ACS Symposium Series 417, ACS, Washington D.C., 382 (1989).

24. V.S. Anderson, R.G.W. Norrish, "The Polymerization of Styrene Sensitized by Molecules in the Triplet State," *Proc. Roy. Soc. (London)*, **251**, 1, (1959).

25. G. Manivannan, J.P. Fouassier, "Primary Processes in the Photosensitized Polymerization of Cationic Monomers," *J. Polym. Sci., Polym. Chem.*, **29**, 1113 (1991).

26. E.W. Nelson, T.P. Carter, A.B. Scranton, "Photosensitization of Cationic Photopolymerizations by Anthracene and its Derivatives," *Proc. of ACS, Poly. Mat. Sci. Eng.*, ACS Fall Meeting, Chicago, **69**, 363, (1993).

27. J.G. Kloosterboer, "Network Formation by Chain Crosslinking Photopolymerization and its Applications in Electronics," *Adv. Polym. Sci.*, **84**, 1 (1988).

28. Crivello, J.V. "The Synthesis and Cationic Polymerization of Novel Epoxide Monomers," *Polymer Eng. and Sci.* , **32**, 1462 (1992).

29. Decker, C.; Moussa, K. "Real-Time Monitoring at Ultrafast Curing By UV-Radiation and Laser Beams," *J. Coatings Tech.*, **62**, 55 (1990).

30. J.G. Kloosterboer and G.F.C.M. Lijten, "Chain Cross-linking Photopolymerization of Tetraethyleneglycol Diacrylate," *Crosslinked Polymers*, R.A. Dickie, S.S. Labana, and R.S. Bauer, Eds., ACS Symposium Series 367, ACS, Washington D.C., 409 (1988).

31. C. Decker, K. Moussa, "Real-Time Kinetic Study of Laser-Induced Polymerization," *Macromolecules*, **22**, 4455 (1989).

32. C. E. Hoyle, J. M. Torkleson, *Photophysics of Polymers*, ACS Symposium Series 358, ACS, Washington D.C., (1987), and references therein.

33. H. Moravrety, *Photophysical and Photochemical Tools in Polymer Science*, M. A. Winnick, ed., Reidel, Dordrecht, 1 (1986), and references therein.

34. F.W. Wang, W.J. Pummer, B.M. Fanconi, and En-Shinn Wu, "Fluorescence Monitoring of Viscosity and Chemical Changes During Polymerization," in Photophysics of Polymers, ACS Symposium Series, Vol. 417, American Chemical Society, Washington D.C., (1987).

35. F.W. Wang, R.E. Lowry, and W.H. Grant, "Novel Excimer Fluorescence Method for Monitoring Polymerization: 1. Polymerization of Methyl Methacrylate," *Polymer*, **25**, 690 (1984).

36. A. Stroeks, M. Shorhun, A.M. Jamieson, and R. Shimha, *Polymer*, **29**, 467 (1988).

37. F.W. Wang, R.E. Lowry, B.M. Fanconi, "Novel Fluorescence Method for Cure Monitoring of Epoxy Resins," *Polymer*, **27**, 1529 (1986).

38. S.F. Scarlata and J.A. Ors, "Fluorescence Polarization: A Method to Monitor Polymer Cure," *Polymer Comm.*, **27**, 41 (1986).

39. C.S.P. Sung, I-J. Chin, W-C.Yu, "A Novel Fluorescence Technique for Monitoring Cure Reactions in Epoxy Networks," *Macromolecules* , **18**, 1512 (1985).

40. C.S.P. Sung, E. Pyun, H-L. Sun, "Characterization of EpoxyCure by UV-Visible and Fluorescence Spectroscopy: Azochromophoric Labeling Approach," *Macromolecules*, **19**, 2922 (1986).

41. J.C. Song, C.S.P. Sung, "Intrinsic Phosphorescence of Curing Agent for Cure Characterization of Epoxy Composites," *ACS PMSE Proceedings*, **67**, 497, (1992).

42. J.C. Song, C.S.P. Sung, *ACS Polymer Preprints*, **32-3**, 362 (1991).

43. P. Sundell, S. Jonsson, A. Hult, "Photo-Redox Induced Cationic Polymerization of Divinyl Ethers," *J. Polym. Sci., Polym Chem.*, **29**, 1525 (1985).

44. L. R. Gatechair and S.P. Pappas, "Cationic Photoinitiation Efficiency," *Proc. Org. Ctg. and App. Polym. Sci. Division*, **46**, 707, (1982).

45. J. L. Dektar, N. P. Hacker, "Photochemistry of Diaryliodonium," *J. Org. Chem.*, **55**, 639 (1990).

46. R. J. DeVoe, M. R. V. Sahyun, E. Schmidt, N. Serpone, D. K. Sharma, *Can. J. Chem.*, **66**, 319 (1988).

47. Y. Yagci, I. Lukac, W. Schnabel, "Photosensitized Cationic Polymerization Using N-ethoxy-2-methylpyridinium hexafluorophosphate," *Polymer*, **34**, 1130 (1993).

48. N. Johnen, W. Schanbel, S. Kobayashi, J.-P. Fouassier, *J. Chem. Soc. Faraday Trans.*, **88**, 1385 (1992).

49. P.C. Painter, M.M. Coleman, J.L. Koenig, *The Theory of Vibrational Spectroscopy and its Applications to Polymeric Materials*, John Wiley & Sons: New York, NY, 1982.

50. H. Ishida, (Ed.); *Fourier Transform Infrared Characterization of Polymers*, Polymer Science and Technology; Plenum Press: New York, NY,Vol. 36, 1987.

51. "Instrumentation '94," *Chemical and Engineering News*, **72:11**, 32, (1994).

52. H.W. Siesler, K.Holland-Moritz, *Infrared and Raman Spectroscopy of Polymers*, Practical Spectroscopy Series, Marcel Dekker, Inc.: New York, NY, Vol. 4, 1980.

53. "PittCon showcases real-world Raman spectroscopy, NEWSBREAKS," *Laser Focus World*, **30:4**, 9 (1994).

54. F. W. Billmeyer, *Textbook of Polymer Science*, 3rd ed., John Wiley & Sons, Inc.: New York, NY, 1984.

55. A.M. Tudor, C.D. Melia, M.C. Davies, P.J. Hendra, S. Church, A.J.Domb, R. Langer, "The Application of Fourier Transform Raman Spectroscopy to the Analysis of Poly(anhydride) Homo- and Co-polymers," *Spectrochim. Acta.*, **47A**, 1335-1343 (1991).

56. J. G. Grasselli, M. K.Snavely, B. J. Bulkin, *Chemical Applications of Raman Spectroscopy*, John Wiley & Sons, Inc.; New York, NY, 1981.

57. L.H. Sperling, *Introduction to Physical Polymer Science*, 2nd ed., John Wiley & Sons, Inc.: New York, NY, 1992.

58. J.F. Rabek, *Experimental Methods in Polymer Chemistry, Phyical Principles and Applications*, John Wiley & Sons, Inc.: New York, NY, 1980.

59. N.B. Colthup, L.H. Daly, S.E. Wiberley, *Introduction to Infrared and Raman Spectroscopy*, 2nd ed., Academic Press: New York, NY, 1975.

60. P. J. Hendra, "Raman Spectroscopy," In *Polymer Spectroscopy*; D.O. Hummel, Ed., Verlag Chemie GmbH: Weinheim/Bergstr., 112-185, 1974.

61. J. L. Koenig, *Spectroscopy of Polymers*; ACS Professional Reference Book; ACS: Washington, D.C., 1992.

62. J. D. Ingle, S. R. Crouch, *Spectrochemical Analysis*, Prentice Hall: Englewood Cliffs, New Jersey, 1988.

63 B.M. Fanconi, "Fourier Transform Infrared Spectroscopy of Polymers - Theory and Application," *J. of Test. Eval.*, **12**, 33-39 (1984).

64. U. Simon, F. K. Tittel, "Optical Parametric Device Serve as Sources for IR Spectroscopy," *Laser Focus World*, **30:5**, 99 (1994).

65. E. W. Ciurczak, "Detectors in Infrared Spectroscopy," *Spectroscopy*, **8:8**, 12 (1993).

66. S. C. Brown, A. B. Harvey, "Polymers," In *Infrared and Raman Spectroscopy, Part C*; E. G. Brame, and J. G. Grasselli, Eds., Practical Spectroscopy Series; Marcel Dekker, Inc.: New York, NY, Vol 1, 873-932, 1977.

67. S. E. Polchlopek, "Attenuated Total Reflectance," In *Applied Infrared Spectroscopy*; D. N. Kendall, Eds.; Reinhold, New York, NY, 462, 1966.

68. R. L. Harris, G. R. Svoboda, "Determination of Alkyd and Monomer-Modified Alkyd Resins by Attenuated Total Reflectance Infrared Spectrometry," *Anal. Chem.*, **34:12**, 1655-1657 (1962).

69. H. G. Tompkins, "Infrared Reflection - Absorption Spectroscopy," In *Methods of Surface Analysis*; A. W. Czanderna, Eds., Elsevier, Amsterdam 447, 1974.

70. R.M. Gendreau, S. Winters, R.I. Leininger, D. Fink, C.R. Hassler, R.J. Jakobsen, "Fourier Transform Infrared Spectroscopy of Protein Adsorption from Whole Blood: *Ex Vivo* Dog Studies," *Appl. Spectrosc.*, **35**, 353-357 (1981).

71. V.N. Hasirci, "PVNO-DVB Hydrogels: Synthesis and Characterization," *J. Appl. Polym. Sci.*, **27**, 33-41 (1982).

72. H.R. Allcock, S. Kwon, "Glyceryl Polyphosphazenes: Synthesis, Properties and Hydrolysis," *Macromolecules*, **21**, 1980-1985 (1988).

73. R.M. Gendreau, R.J. Jakobsen, "Fourier Transform Infrared Techniques for Studying Complex Biological Systems," *Appl. Spectrosc.*, **32**, 326-328 (1978).

74. N.J. Earhart, V.L. Dimonie, M.S. El-Aasser, J.W. Vanderhoff, "Infrared Studies on the Grafting Reactions of Poly(vinyl alcohol)," In *Polymer Characterization: Physical Property Spectroscopic and Chromatographic Methods*; C.D. Craver, T. Provder, Eds., American Chemical Society, Vol. 227, 333-341 (1990).

75. E. Gulari, K. McKeigue, K.Y.S. Ng, "Raman and FTIR Spectroscopy of Polymerization: Bulk Polymerization of Methyl Methacrylate and Styrene," *Macromolecules*, **17**, 1822-1825 (1984).

76. H.G.M. Edwards, A.F. Johnson, I.R. Lewis, "Applications of Raman Spectroscopy to the Study of Polymers and Polymerization Processes," *J. Raman Spectrosc.*, **24**, 475-483 (1993).

77. Edwards, H. G. M.; Johnson, A. F.; Lewis I. R.; Wheelwright, S. J.; "Raman and FTIR Spectroscopic Sudies of Copolymers of Methylmethacrylate with Butadiene," *Spectrochimica Acta*, **1993**, *49A*, 457- 464.

78. G. Sain, A. Leoni, F. Simone, "Solvent Effects in Radical Copolymerization III. Methacrylamide," *Die Makromolekulare Chemie*, **147**, 213-218 (1971).

79. A.Chapiro, J. Dulieu, "Influence of Solvents on the Molecular Associations and on the Radication Initiated Polymerization of Acryalic Acid," *European Polymer Journal*, **13**, 563-577 (1977).

80. R. Y. Makushka, G. I. Bayoras, Y. K.Shulskus, A. B. Bolotin, Z. A. Roganova, A. L. Smolyanskii, "Effect of Complex Formation on Reactivity of Acrylic and Methacrylic Acids in Radical Polymerizations," *Polymer Science U.S.S.R.*, **27:3,** 634-641 (1985).

81. G. Bajoras, R.Makuška, "Peculiarities of Radical Homo- and Copolymerizations of Acrylic, Methacrylic, and Itaconic Acids in Complexing Solutions," *Polymer Journal*, **18:12**, 955-965 (1986).

82. P. Monti, R. Simoni, "The Role of Water in the Molecular Structure and Properties of Soft Contact Lenses and Surface Interactions," *Journal of Molecular Structure*, **269**, 243-255 (1992).

83. I.M. Ward, M.A.Wilding, "Infra-red and Raman Spectra of Poly (*m*-Methylene Terephthalate) Polymers," *Polymer*, **18**, 327-335 (1977).

84. J. Dybal, J. Spevácek, B. Schneider, "Ordered Structures of Syndiotactic Poly(methyl Methacrylates) Studied by a Combination of Infrared, Raman, and NMR Spectroscopy," *J. Polym. Sci.: Part B: Polym. Phys.*, **24**, 657-674 (1986).

85. J. Dybal, J.Stokr, B. Schneider, "Vibrational Spectra and Structure of Stereoregular Poly(Methyl Methacrylates) and of the Stereocomplex," *Polymer*, **24**, 971-980 (1983).

86. J. Dybal, S. Krimm, "Normal-Mode Analysis of Infrard and Raman Spectra of Crystalline Isotactic Poly(Methyl Methacrylate)," *Macromolecules*, **23**, 1301-1308 (1990).

87. T.Hirschfeld, B. Chase, "FT-Raman Spectroscopy: Development and Justification," *Appl. Spectrosc.*, **40**, 133 (1986).

88. M. C. Davies, J. S. Binns, C. D. Mellia, D. Bourgois, "Fourier Transform Raman Spectroscopy of Polymeric Biomaterials and Drug Delivery Systems," *Spectrochimica Acta*, **46A**, 277-283 (1990).

89. S. A. Asher, C. R. Johnson, "Raman Spectroscopy of Coal Liquid shows that Fluorescence Interference is Minimized with Ultraviolet Excitation," *Science*, **225**, 311 (1984).

90. P. P. Suni, "Custom Photodetector arrays Meet Design Challenges," *Laser Focus World*, **30:4**, 131 (1994).

91. E. D. Jungbluth, "Fiber based Devices Light Up CLEO," *Laser Focus World*, **30:5**, 88 (1994).

92. W. L. Peticolas, "Applications of Raman Spectroscopy to Macromolecules" *Biochimie*, **57**, 417 (1975).

93. J.S. Suh, K.H. Michaelian, "Surface-Enhanced Raman Spectroscopy of Acrylamide and Polyacrylamide Adsorbed on Silver Colloid Surfaces: Polymerization of Acrylamide on Silver," *J. of Raman Spectrosc.*, **18**, 409-414 (1987).

94. *Surface Enhanced Raman Scattering*, R. Chang, F. Furtak, Eds., Plenum Press: New York, NY, 1982.

95. M. L. Howe, K. L. Watters, R. G Greenler, "Investigation of Thin Surface Films and Adsorbed Molesules Using Laser Raman Spectroscopy," *J. Phys. Chem.*, **80**, 382 (1976).

96. N. E. Schlotter, J. F. Rabolt, "Measurments of Optical Anisotropy of Trapped Molecules in Oriented Polymer Films by Waveguide Raman Spectroscopy (WRS)," *Applied Spectroscopy*, **38:2**, 208 (1984).

97. C. G. Zimba, V. M. Hallmark, S. Turrell, J. D.Swalen, J. F. Rabolt, "Applications of Fourier Transform Raman Spectroscopy to Studies of Thin Polymer Films," *J. Phys. Chem.*, **94**, 939-943 (1990).

98. J. L. Koenig, "Raman Scattering of Synthetic Polymer - A Review," *Applied Spectroscopy Reviews*, **4:2**, 233-306 (1971).

99. J. L. Koenig, A. C. Angood, J. Semen, J. B. Lando, "Laser-Excited Raman Studies of the Conformational Transition of Syndiotactic Polymethacrylic Acid in Water," *J. Am. Chem. Soc.*, **91**, 7250 (1969).

100. J.L. Koenig, A.C. Angood, "Raman Specta of Poly (Ethylene Glycols) in Solution," *J. Polym. Sci.*, **8**, 1787-1796 (1970).

101. D.I. Bower, "Polarised Fluorescence and Raman Spectroscopy," *Structure and Properties of Oriented Polymers*, Polymers Applied Sciences: London, 1975.

102. G. Odian, *Principles of Polymerization*; John Wiley & Sons, Inc.: New York, NY, 619, 1991.

103. A. Neppel, I. S. Bulter, "Raman Spectra of Fully Deuteriated Syndiotactic and Isotactic Poly(methyl methacrylate)," *J. Raman Spect.*, **15:4**, 257-263 (1984).

104. J. Purvis, D. I. Bower, "A Study of Molecular Orientation in Poly(Methyl Methacrylate) by means of Laser-Raman Spectroscopy," *Polymer*, **I**, 645-654 (1974).

105. K. P. J. Williams, "Remote Sampling Using a Fiber-Optic Probe in Fourier Transform Raman Spectroscopy," *J. Raman Spectrosc.*, **21**, 147 (1990).

106. P. J. Hendra, G. Ellis, D. J. Cutler; "Use of Optical Fibers in Raman Spectroscopy," J. Raman Spectrosc., **19**, 413 (1988).

107. E. N. Lewis, V. F. Kalasinsky, I. W. Levin, "Near-Infrared Fourier Transform Raman Spectroscopy Using Fiber-Optic Assemblies," *Anal. Chem.*, 60, 2658-2661 (1988).

108. C. Decker, D. Decker, *RadTech 94 North American Proceedings*, RadTech International North America, 602, 1994.

109. E. W. Nelson, T. P. Carter, A. B. Scranton, "Fluorescence Monitoring of Cationic Photopolymerizations of Divinyl Ethers Photosensitized by Anthracene Derivatives," *Macromolecules*, **27**, 1013-1019 (1994).

110. K. F. Schrum, A. M. Williams, S. A. Haerther, D. Ben-Amotz, "Molecular Fluorescence Thermometry," *Anal. Chem.*, **66**, 2788-2790 (1994).

111. A. M. Murray, L. A. Melton, *Appl. Opt.*, **24**, 2783-2787 (1985).

112. W. F. Sager, N. Filipescu, F. A. Serafin, "Substituent Effects on Intramolecular Energy Transfer. I. Absorption and Phosphorescence Spectra o Rare Earth β-Diketone Chelates," *J. of Phys. Chem*, **69 (4)**, 1092-1100 (1965).

113. F. Halverson, J. S. Brinen, and J. R. Leto, "Luminescence of Europium Hexafluoro-acetylactetonate," *J. of Chem. Phys.*, **40 (10)**, 2790-2792 (1964).

114. B. Alpha, R. Ballardini, V. Balzani, J-M. Lehn, S. Perathoner, N. Sabbatini, "Antenna Effect in Luminescent Lanthanide Cryptates: A Photophysical Study," *Photochemistry and Photobiology*, **52 (2)**, 299-306 (1990).

115. M. F. Richardson, W. F. Wagner, D. E. Sands, "Rare-Earth Trishexafluoroacetyl-acetonates and Related Compounds,"*J. Inorg. Nucl. Chem.*, **30**, 1275-1289 (1968).

116. S. Sato, M. Wada, "Relations between Intromolecular Energy Transfer Efficiencies and Triplet State Engergies in Rare Earth β-Diketone Chelates," *Bulletin of the Chemical Society of Japan*, **43**, 1955-62 (1970).

117. E. J. Schimitschek, J. A. Trias, "IR and Raman Spectra of Europium(III) β-Diketoneates," *J. Inorgan. Nucl. Chem.*, **32**, 811-831 (1970).

118. J. P. Kennedy, and E. Marechal, *Carbocationic Polymerization*, John Wiley & Son, New York, 1982.

119. T. Doornkamp, and Y. Y. Tan, *Polymer Commun.*, **31**, 362 (1990).

120. J. G. Kloosterboer, and G.F.C.M. Lijten, *Polymer*, **28**, 1149 (1987).

121. K. S. Anseth, C. M. Wang, and C. N. Bowman, "Kinetic Evidence of Reaction Diffusion during the Polymerization of Multi(meth)acrylate Monomer," *Macromolecules*, **27**, 650 (1994).

122. K. S. Anseth, C. M. Wang, and C. N. Bowman, "Reaction Behavior and Kinetic Constants for Photopolymerizations of Multi(meth)acrylates," *Polymer*, **35**, 3243 (1994).

123. J. G. Kloosterboer, G. F. C. M. Lijten, in *Cross-Linked Polymers*, R.A. Dickie, S .S. Labana, and R. S. Bauer, Eds., ACS Symposium Series 367; ACS: Washington DC, 1987.

124. C. G. Roffey, *Photopolymerization of Surface Coatings*, Wiley, New York, 1981.

125. S. P. Pappas, *UV Curing, Science and Technology*, Vol. 2, Technology Marketing Corporation, Norwalk, CT, 1985.

126. E. W. Nelson, T. P. Carter, A. B. Scranton, "The Role of the Triplet State in the Photosensitization of Cationic Polymerizations by Anthracene," *J. of Poly. Sci., Poly. Chem.*, **33**, 247-256 (1995).

127. A.B. Scranton and N.A. Peppas, "A Statistical Model of Free-Radical Copolymerization/Crosslinking Reactions," *J. Polym. Sci. Polym. Chem*, **28**, 39 (1990).

128. K. Dusek, "Formation-structure Relationships in Polymer Networks," *Brit. Polym. J.*, **17**, 185 (1985).

129. P. Manneville and L. de Sez, in "Numerical Methods in the Study of Critical Phenomena," edited by I. della Dora, J. Demongeot and B. Lacolle, Springer, Berlin (1981).

130. H.J. Herrmann, D.P. Landau and D. Stauffer, "New Universality Class for Kinetic Gelation," *Phys. Rev. Lett.*,**49**, 412 (1982).

131. H.J. Herrmann, D. Stauffer and D.P. Landau, "Computer Simulation of a Model Irreversible Gelation," *J. Phys. Math. Gen.*, **16**, 1221 (1983).

132. D. Matthews-Morgan, D.P. Landau and H.J. Herrmann, "Effects of Solvent in a Kinetic Gelation Model," *Phys. Rev.*,**B11**, 6328 (1984).

133. R. Bansil, H.J. Herrmann and D. Stauffer, "Computer Simulation of Kinetics of Gelation by Addition Polymerization in a Solvent," *Macromolecules*, **17**, 998 (1984).

134. J.G. Kloosterboer, G.M.M. van de Hei and H.M.J. Boots, "Inhomogeneity During the Photopolymerization of Diacrylates: DSC Experiments and Percolation Theory," *Polym. Commun.*, **25**, 354 (1984).

135. H.M.J. Boots and R.B. Pandey, "Kinetic Gelation Model, Qualitative Percolation Study of Free Radical Crosslinking Polymerizations," *Polym. Bull.*, **11**, 415 (1984).

136. H.M.J. Boots, J.G. Kloosterboer and G.M.M. van de Hei, "Inhomogeneity During Bulk Polymerization of Divinyl Compounds," *Brit. Polym. J.*,**17**, 219 (1985).

137. G.P. Simon, P.E.M. Allen, D.J. Bennett, D.R.G. Williams, E.H. Williams, "Nature of Residual Unsaturation During Cure of Dimethacrylates Examined by CPPEMAS ^{13}C NMR and Simulation Using a Kinetic Gelation Model," *Macromolecules*, **22**, 3555 (1989).

138. H.M.J. Boots and N.A. Dotson, "The Simulation of Free-radical Crosslinking Polymerization: The Effect of Diffusion," *Polym. Comm.*, **29**, 346 (1988).

CHAPTER III. OBJECTIVES

Based upon the introduction and background chapters, it is clear that UV-initiated cationic photopolymerizations of bisvinyl ethers exhibit considerable potential for the development of high-speed, low-cost, pollution-free coatings and inks. However, because appropriate monomers and initiators have been developed only recently, the characteristics of these reactions including the structure and properties of the resulting highly crosslinked polymer films have received very limited attention. Fundamental characterization of the photopolymerization reactions and the resulting polymer structures is imperative if the potential of these reactions is to be realized, and optimum formulations and curing procedures are to be established.

The broad objective of this research effort is to provide fundamental experimental and theoretical investigations of UV-initiated cationic photopolymerizations of bisvinyl ethers. In order to characterize these high speed reactions, new novel techniques for cure and temperature monitoring will be developed and used to determine reaction rate profiles and temperature profiles during the cationic photopolymerization. These new methods and techniques should be general in their ability to monitor cure and temperature and will be widely applicable in high speed polymerization reactions. Furthermore the photosensitization reaction between anthracene and diaryliodonium salts will be investigated to provide further understanding of this process. These studies will

complement the more macroscopic studies currently in the literature, and will provide answers to lingering questions about the nature of these reactions.

Specific objectives of this project are:

i. to obtain complete, time-resolved profiles of the monomer conversion as a function of time under a variety of reaction conditions;

ii. to obtain detailed, time-resolved profiles of the temperature of the system as a function of time during the course of the reactions;

iii. to investigate the effect of the wavelength and intensity of the incident UV-light on the characteristics of the reactions;

iv. to provide further understanding of the mechanism of photosensitization of the cationic photopolymerization by anthracene and similar compounds;

v. to provide new methods and techniques for monitoring cure in high speed reactions, and for obtaining *in-situ* temperature profiles during reaction.

CHAPTER IV. *IN SITU* FLUORESCENCE SPECTROSCOPY: CURE MONITORING TECHNIQUE

IV.1. Introduction

Cationic photopolymerizations of vinyl ethers were investigated using *in situ*, time resolved fluorescence spectroscopy. Due to its short intrinsic timescale, fluorescence spectroscopy provides a means to characterize these polymerizations which are too rapid to be monitored by traditional methods. The fluorescence intensity of the photosensitizer (anthracene or its derivatives) was monitored as a function of time with spectra collected in intervals as short as 2 milliseconds. An observed reduction in fluorescence intensity was attributed to consumption of the photosensitizer, providing a means to monitor the production of active cationic centers. The reaction rate was found to increased as the initiator or photosensitizer concentrations were increased. Also, reactions photosensitized by anthracene and 9,10-dimethylanthracene produced the fastest rates, followed by 9-vinylanthracene, while the polymerization rate for 9,10-diphenyl-anthracene was considerably slower due to steric hindrance or resonance effects. These results illustrate the tremendous potential of in situ, time-resolved fluorescence spectroscopy for monitoring polymerizations.

In this chapter, the kinetics of cationic photopolymerizations of vinyl ethers were investigated using *in situ* laser-induced fluorescence spectroscopy. The fluorescence intensity of the photosensitizer was monitored during the reaction to obtain a direct measure of the rate of initiation, and to provide indirect information on the rate of propagation. Fluorescence spectroscopy is particularly attractive as an *in situ,* time-resolved technique for monitoring these high speed polymerizations because it has an extremely short intrinsic timescale (typically 10^{-9} seconds). The response time for the monitoring technique is determined by the speed of the detection system. In these studies, a high-speed diode array detection system was employed, and fluorescence spectra were collected in intervals as short as 2 milliseconds. Therefore, the fluorescence monitoring method has a considerably faster response time than DSC and real-time IR methods, and provides ample time-resolution to characterize the cationic photopolymerizations. In addition, since the fluorescence method allows a relatively wide window of wavelengths to be monitored (as opposed to a single wavelength), spectral changes arising from more than one functionality can be monitored simultaneously.

The fluorescence monitoring scheme reported here is considerably different than the viscosity-sensitive methods reported in the literature. First, because cationic photopolymerizations proceed to completion in a matter of seconds, these studies require considerably faster sampling methods than the epoxy resin studies discussed in the background chapter. However, a more fundamental difference between our fluorescence monitoring scheme and the viscosity-sensitive probe approach is that the fluorescence of one of the reactants (the photosensitizer), and not that of an inert probe is monitored. Therefore, this technique provides a more direct measurement of the reaction itself, and

does not lose sensitivity at the gel point. In the following chapter, a description of the fluorescence monitoring technique will be given, along with a discussion of its benefits and limitations.

IV.2. Experimental

IV.2.1. Materials

In these studies, 3,6,9,12-tetraoxatetradeca-1,13-diene (DVE-3) (GAF Chemicals Corp.) was used as the monomer. The initiator (UV9310C - GE Silicones) had a composition of 5-10 wt % linear alkylate dodecylbenzene, ~50 wt % 2-ethyl-1,3-hexanediol, and ~50 wt % bis(4-dodecylphenyl)iodoniumhexafluoroantimonate. Initiator concentrations specified in the remainder of this chapter correspond to the total UV9310C concentration. The anthracene, 9-vinylanthracene, 9,10-diphenylanthracene and 9,10-dimethylanthracene photosensitizers were all purchased from Aldrich Chemical Company and were used as received.

IV.2.2. Absorption and Fluorescence Measurements

Absorption spectra of monomer, initiator and photosensitizers were obtained using a Hewlett Packard UV-VIS 8452A diode array spectrophotometer. The laser-induced fluorescence studies were performed in the *LASER* Laboratory at Michigan State University. The fluorescence and photosensitization were both excited with a Coherent Innova 200 Argon ion laser operating at 363.8 nm. A Newport 845HP-01 Digital Shutter

system was opened with an electric pulse from the detector controller, ensuring that the initiation and fluorescence acquisition were started simultaneously. Fifteen milliwatts of unfocused laser radiation (measured with a Scientech 362 Power/Energy meter) in a ~3 mm dia. beam was directed to the quartz capillary tube containing the sample, whose longitudinal axis was perpendicular to the laser beam direction. The quartz capillary was approximately 1 inch in length with an inner diameter of 1 mm and an outer diameter of 2 mm. A typical reaction system contained ~1 wt % initiator (UV9310C) and ~10^{-2} wt % of photosensitizer in monomer (DVE-3). The fluorescent light was collected at an angle of 90° from the incident beam and 90° from the long axis of the quartz tube (see Figure IV.1.). The fluorescence signal was collected using a Spex 1877 Triplemate spectrometer with a subtractive dispersion filter stage and a spectrograph stage. An EG&G Princeton Applied Research Model 1421 intensified diode array, cooled to -20 °C to minimize dark charge levels, was used to detect the signal. The data was analyzed with an EG&G Princeton Applied Research Model OMA III detector controller. To simulate typical process conditions for coating, ink, adhesive and electronic applications, all reactions were initiated at room temperature and were performed without external heating or cooling.

A fluorescence spectrum spanning 300 nm centered around 450 nm was collected with 150 groove/mm gratings in both the filter and spectrograph stages. The OMA III detection system has the capability of collecting this entire spectrum in 16.67 ms. However, if smaller regions of the spectrum are collected, less time is required per

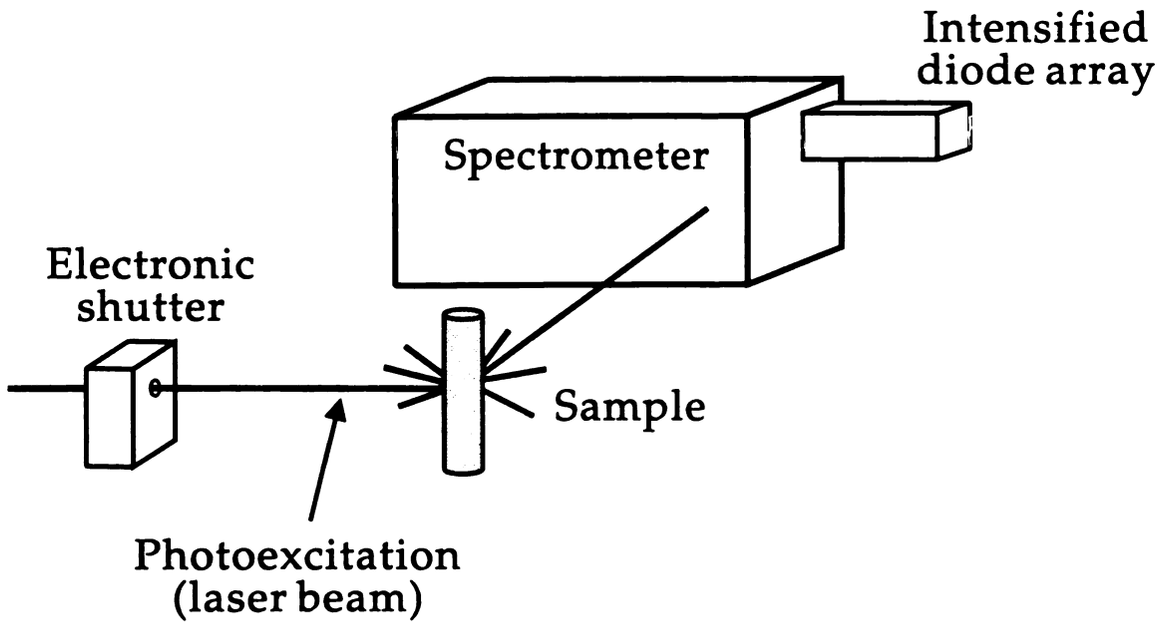

Figure IV.1. *Experimental Setup for Fluorescence Cure Monitoring.*

acquisition. Spectral regions from 50 to 100 nm were collected in intervals as short as 2 milliseconds per spectrum.

IV.3.1. Results and Discussion

IV.3.1. Absorption Experiments

Absorption spectra for the monomer, initiator and photosensitizer are shown in Figure IV.2. The figure illustrates that the initiator exhibits a maximum at 210 nm, a second local maximum at 240 nm and rapidly decreasing absorption up to 290 nm. The monomer (DVE-3) absorption lies completely below 240 nm, leaving a clean spectral region above 300 nm. Anthracene and its derivatives exhibit strong absorption in the 300-400 nm region. Due to this strong absorption, the initiating wavelength for the photopolymerization may be shifted to this region by including anthracene or its derivatives as photosensitizers.

IV.3.2. Fluorescence Experiments

Figure IV.3. contains a representative series of fluorescence spectra obtained during the cationic photopolymerization of DVE-3. In this figure, each spectrum represents the total fluorescence intensity collected during a 17 ms exposure time; other experiments were performed with intervals as short as 2 ms per scan. This time

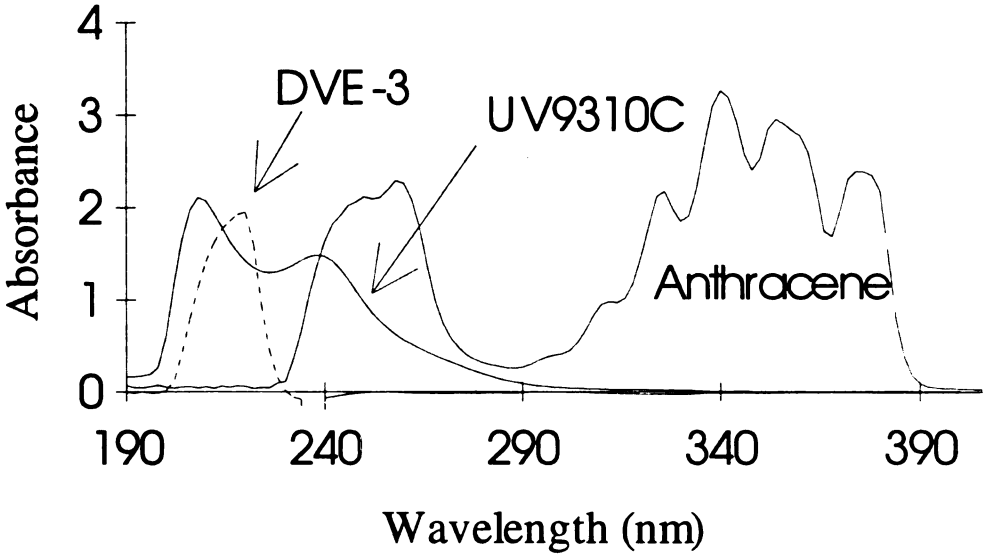

Figure IV.2. *Absorption Spectrum of Monomer (DVE-3), Initiator (UV9310C) and Photosensitizer (Anthracene).*

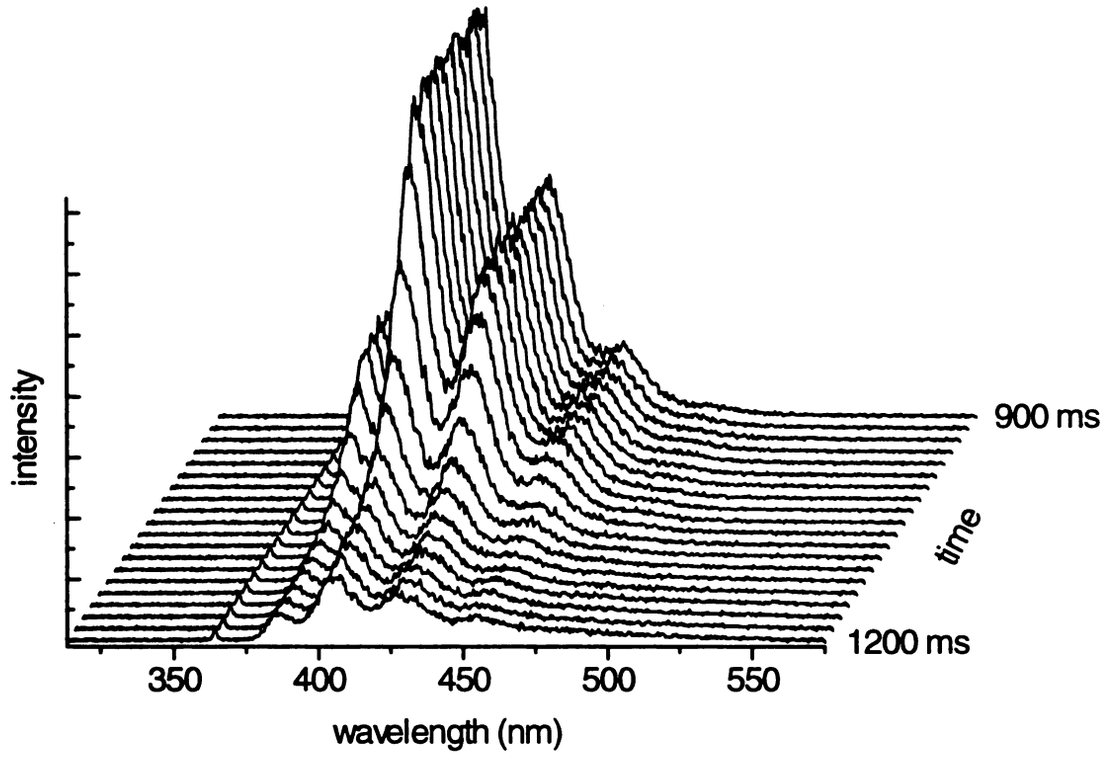

Figure IV.3. *Polymerization of DVE-3 monomer (0.5 wt % initiator) produced by exciting anthracene (2.8 x10^{-2} wt %), at 363.8 nm, and monitored by measuring the intensity of the anthracene fluorescence at time intervals of 17 ms.*

dependent plot (with time as the depth axis) consists of twenty spectra for the anthracene fluorescence excited at 363.8 nm (15 mW laser power). As illustrated in Figure IV.3., under the experimental conditions shown, the anthracene fluorescence was found to decrease slowly for the first second, and then drop dramatically over the next 100 ms. Finally, after about 1.5 seconds, the fluorescence intensity levels off and maintains a relatively low steady-state value. Under other experimental conditions, the time required to attain the final (relatively low) steady-state fluorescence intensity was as short as 0.4 seconds.

The decrease in anthracene fluorescence intensity illustrated in Figure IV.3. may be attributed to the consumption of anthracene during the photosensitization reaction. The photosensitization likely proceeds by an electron-transfer mechanism illustrated in Figure IV.4.[1] The mechanism in Figure IV.4. illustrates the important photochemical and electron transfer steps in the reaction. Some possible proton and hydride transfer steps which may occur after the cation-radical is formed are of no consequence for the monitoring scheme, and are omitted from the figure. A more detailed reaction mechanism is reported in reference 2. According to this mechanism, when the anthracene is exposed to 363.8 nm light, it absorbs photons and populates the first excited singlet state. From the first excited singlet state, a fraction of the anthracene undergoes inter-system crossing to populate the lowest triplet state (which may be represented as having unpaired electrons in the 9 and 10 positions). As shown in step 1 of Figure IV.4., the triplet state anthracene may then form an excited state complex with the initiator. In the exciplex, the anthracene may undergo electron transfer to the

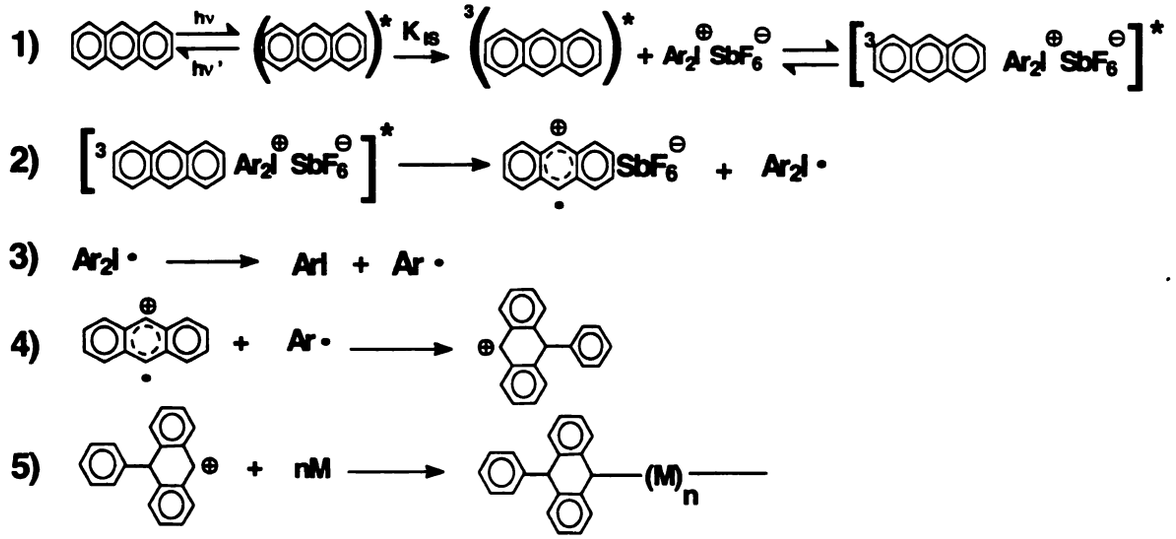

Figure IV.4. *Photosensitization mechanism based on electron transfer from triplet state anthracene to initiator.*

initiator forming a radical-cation which is capable of initiating cationic polymerization (step 2 of Figure IV.4.). As a result of this set of reactions, the anthracene becomes attached to the polymer as a chain end, and loses the aromatic nature of the center ring[1] (steps 4 and 5 of Figure IV.4.). This mechanism (including the role of the triplet state) was recently corroborated by pulsed laser lifetime studies of the singlet and triplet states.[2]

The above mechanism for photosensitization suggests that the reduction in the fluorescence intensity illustrated in Figure IV.3. arises from the loss of the aromaticity of the center anthracene ring during the photosensitization reaction. Therefore, as long as no other anthracene-consuming reactions are taking place, the anthracene fluorescence provides an indication of the number of cationic active centers formed in the reaction system. Each time an anthracene molecule is consumed in the photosensitization reaction, one active cationic center is formed, therefore the magnitude of the fluorescence decrease at a given time (the difference between the initial steady-state fluorescence and the value at the time of interest) provides a measurement of the number of propagating active centers in the reaction system. In this manner, real-time monitoring of the anthracene fluorescence provides valuable kinetic information. The reduction in fluorescence intensity provides a direct measure of the rate in the initiation step of the reaction as well as an indication of the number of propagating active centers.

A series of experiments were performed to ensure that the fluorescence decrease could be attributed entirely to the photosensitization reaction, and that no other anthracene-consuming side reactions were present. Anthracene may participate in a few photo-induced side reactions such as dimerization and oxidation, therefore studies were performed to determine the extent to which these reactions contributed to the

fluorescence decrease. Experiments were performed for two distinct systems: one containing only monomer and photosensitizer, and another containing monomer, photosensitizer, and initiator. The system containing no initiator showed very little decrease in fluorescence intensity even after a few minutes of irradiation. In contrast, the system containing all three components exhibited a rapid decrease in fluorescence intensity in a few seconds (much like that shown in Figure IV.3.). These results indicate that, at least for the polymerization time-scale, the photo-dimerization and oxidation reactions do not lead to a decrease in fluorescence intensity and our observed fluorescence decrease may be attributed entirely to the photosensitization reaction.

IV.3.3. Initiation and Polymerization Kinetics

Based upon the above discussion, it was concluded that fluorescence spectroscopy could be used for kinetic studies of cationic photopolymerizations by monitoring the fluorescence intensity of the photosensitizer (anthracene or its derivatives). A series of fluorescence spectra such as the ones shown in Figure IV.3. were analyzed by measuring the fluorescence intensity at a selected wavelength (typically 425 nm) as a function of reaction time. Figures IV.5. - IV.9. contain plots of data collected in this manner. A series of experiments were performed to investigate the effects of a variety of variables on the polymerization kinetics, including the effect of the initiator concentration, the photosensitizer concentration, and the functionalization of anthracene.

Figure IV.5. contains plots of the fluorescence intensity versus time for reaction systems containing anthracene (~10^{-2} wt %) and initiator (0.5 wt % or 1 wt %) in DVE-3

monomer. The general shape of the curves in Figure IV.5. seems to be characteristic of these cationic photopolymerizations. Immediately after the shutter is opened, the fluorescence intensity increases until it attains a relatively constant, quasi-steady-state value. Subsequently, the fluorescence intensity slowly decreases as the anthracene is consumed and active centers are formed. At some threshold value of time (~ 750 ms for the 1 wt % initiator case, and ~ 1250 ms for the 0.5 wt % initiator case) the fluorescence intensity falls dramatically (losing ~70% of its value) in less than 100 milliseconds. This seems to indicate that the rate of the photosensitization reaction increases dramatically at this point, possibly due to elevated temperatures arising from the heat of polymerization. A calculation of the adiabatic polymerization temperature illustrates that this temperature increase may be substantial. Based upon estimates of the heat capacity of the monomer (Cp_m ~ 400 J/mol K by the empirical method of Sternling and Brown[3]) and the heat of polymerization for vinyl ethers (ΔH_p ~ 60 kJ/mol[4]) the adiabatic temperature rise was calculated to be ~150 °C.

If the observed sudden decrease in fluorescence intensity arises from thermal run-away of the initiation and/or propagation reactions, then the rate constants must increase substantially in the adiabatic temperature range. Therefore, a consideration of the activation energies of the photosensitization and propagation reactions is important. The quenching of photo-excited molecules is diffusion controlled with an activation energy of ~15 kJ/mol[5] for small molecules in organic solutions, while the activation energy of propagation for vinyl ethers is approximately 30 kJ/mol.[6] Using an Arrhenius equation for a 125 degree temperature rise (a conservative estimate of the temperature increase), the rate constants of initiation and propagation are found to increase by factors of 6.0 and

35, respectively. The overall rate of polymerization, which depends upon both initiation and propagation, is characterized by an activation energy $E_R = E_I + E_P$, where E_R, E_I and E_P are the activation energies for overall polymerization, initiation, and propagation, respectively. Based upon this equation, the activation energy for polymerization is 45 kJ/mol, and the polymerization rate increases by a factor of approximately 210 for a 125 °C temperature change.

In the above discussion of the activation energy for overall polymerization, termination was assumed to be negligible. In a cationic polymerization active centers do not terminate with one another, and chain transfer normally leads to an active center which is capable of propagation. Therefore, the only possible termination arises from combination with the counter ion or reaction with contaminants which give unreactive cations. The possibility of combination with the hexafluoroantimonate ion is low because of the size of the anion, justifying the assumption of zero termination. The inclusion of termination would decrease the value of E_R since the activation energy for termination would be subtracted.

Based upon the above discussion of the reaction energetics, the sudden decrease in fluorescence intensity exhibited in Figure IV.5. is attributed to a large increase in temperature which causes a large increase in reaction rate. To investigate whether the intensity decrease arises in part from temperature-dependent fluorescence, a series of studies were performed in a thermostated cell. In the adiabatic temperature range, the fluorescence intensity of the photosensitizer was found to remain essentially constant or increase slightly. Therefore the fluorescence decrease exhibited in Figure IV.5. cannot arise from temperature-dependent fluorescence of the photosensitizer, and is attributed to

consumption of the anthracene during photosensitization. Therefore, based upon these fluorescence studies, the number of active centers, and therefore the rate of polymerization, may be characterized both by the overall rate of fluorescence decrease, and by the time for the onset of the rapid drop in fluorescence intensity. In order to verify the actual temperature rise, *in situ* monitoring of temperature during these cationic photopolymerizations is currently under investigation by laser-induced fluorescence.

IV.3.4. Effect of Initiator Concentration

Figure IV.5. illustrates just how rapidly the reaction occurs when the sample is irradiated with laser light. A cursory observation would suggest that in both cases, the liquid monomer sample becomes a solid polymer almost immediately after the shutter is opened. The detailed time-resolution provided by the laser experiment illustrates that, as expected by simple kinetic considerations, the polymerization rate is noticeably higher for the sample containing the higher concentration of initiator (as indicated by the time for the rapid decrease in fluorescence). In either case, the reaction is very rapid with most of the fluorescence decrease occurring in less than 1.25 seconds.

IV.3.5. Effect of Photosensitizer Concentration

Figure IV.6. contains plots of fluorescence intensity versus time for systems containing 1 wt % initiator, and various concentrations of anthracene in monomer. The

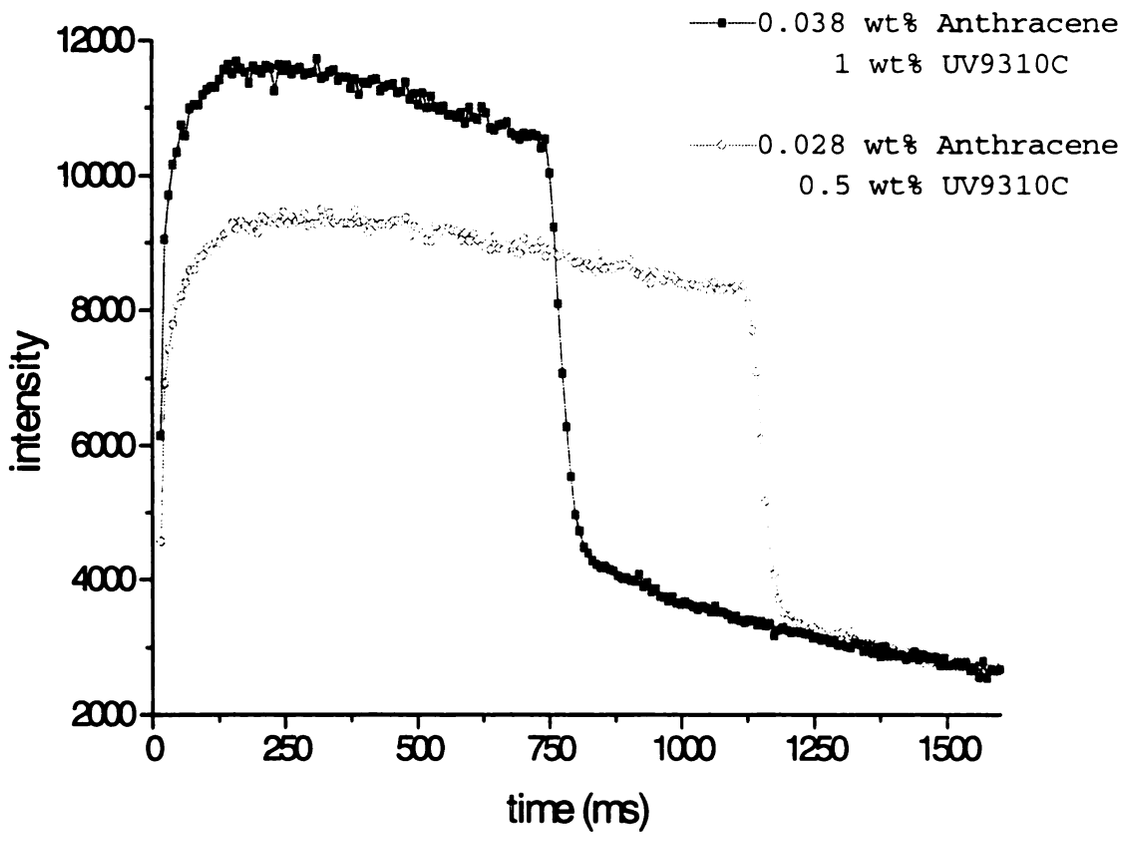

Figure IV.5. *Fluorescence intensity at 425 nm for polymerization of DVE-3 monomer with varying concentrations of initiator (UV9310C) and 10^{-2} wt % of anthracene as the photosensitizer.*

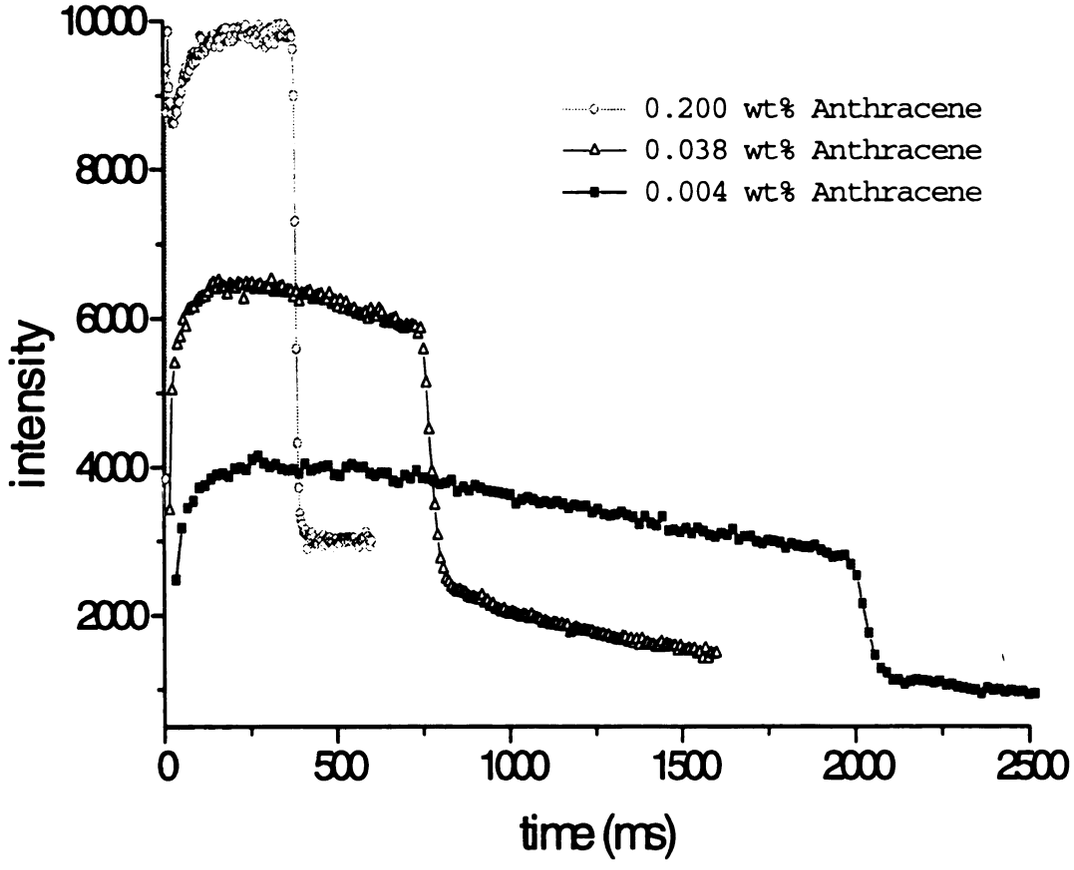

Figure IV.6. *Fluorescence intensity for polymerization of DVE-3 monomer with varying concentrations of anthracene photosensitizer and 1 wt % initiator (UV9310C).*

figure illustrates that as the anthracene concentration is increased from 0.004 wt % to 0.038 wt %, the time for the onset of the rapid fluorescence decrease changes nearly threefold from ~2000 msec to ~750 msec. Therefore, the reaction rate is very sensitive to the anthracene concentration, and increases significantly as the anthracene concentration is increased an order of magnitude from 0.004 wt % to 0.038 wt %. If the photosensitizer concentration is increased another order of magnitude (to ~0.2 wt %) the time required for the rapid drop in fluorescence decreases further (~400 msec), but at a smaller incremental rate (by less than a factor of two). Therefore, the reaction rate becomes less sensitive to the photosensitizer as the anthracene concentration is increased. This trend may be explained by the fact that the high anthracene concentrations lead to a high optical density (O.D. ~2 for 100 μm sample thickness in the 0.2 wt % anthracene case) which limits the penetration of the light into the sample. Therefore, many of the anthracene molecules near the back of the sample are not excited, and cannot produce active cationic centers. This hypothesis is supported by the fact that in the first few seconds of the experiment, the polymerization was limited to approximately the front half of the sample.

IV.3.6. Effect of Anthracene Functionalization

Experiments were performed using a variety of anthracene derivatives as photosensitizers. The purpose of these experiments was to determine the effect of anthracene functionalization on the rate of the cationic photopolymerizations. In Figure IV.7., the fluorescence intensity for reaction systems containing 0.004 wt %

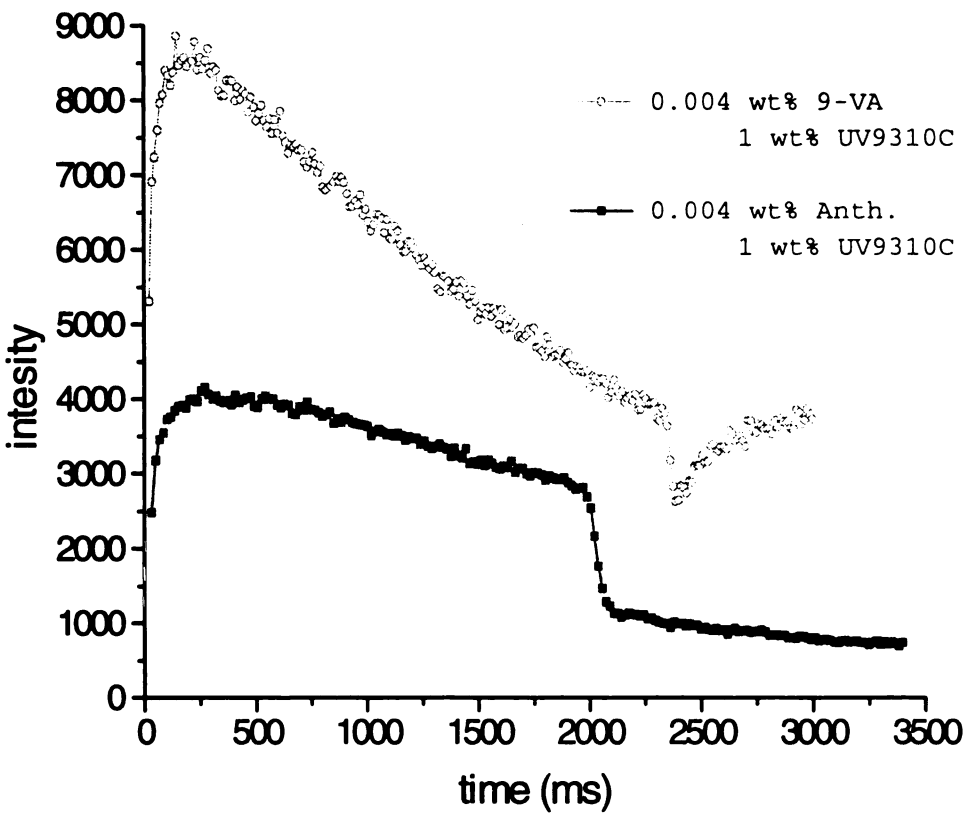

Figure IV.7. *Fluorescence intensity for polymerization of DVE-3 monomer with UV9310C and 10^{-3} wt % of 9-vinylanthracene and anthracene as the photosensitizers.*

anthracene or 9-vinylanthracene as the photosensitizer is plotted versus time. The figure illustrates that the reaction is somewhat more rapid for anthracene than for 9-vinylanthracene since the rapid decrease in fluorescence occurs in about 2 seconds for anthracene, and in about 2.3 seconds for 9-vinylanthracene. It is interesting to note that the curve for 9-vinylanthracene exhibits a steeper slope and a larger fluorescence decrease in the early stages of polymerization. This may arise from its ability to participate in the propagation of the active center through its vinyl functionality.

Fluorescence studies were also performed using two other anthracene derivatives as photosensitizers: 9,10-diphenylanthracene and 9,10-dimethylanthracene. The fluorescence intensity of 9,10-diphenylanthracene has been shown to be relatively insensitive to changes in viscosity,[7] therefore these studies were performed in part to investigate the possibility that the decrease in fluorescence intensity observed in Figures IV.5. and IV.7. are due to viscosity effects. In Figure IV.8., the fluorescence intensity for systems containing 10^{-2} wt % 9,10-diphenylanthracene or 9,10-dimethylanthracene as photosensitizers are plotted versus time. The figure illustrates that, as in the previous experiments with anthracene, the fluorescence intensity of these probes initially exhibits a gradual decrease with time, then shows a dramatic drop as the reaction proceeds. The fact that the general shapes of the fluorescence profiles are the same as those for anthracene and 9-vinylanthracene indicate that viscosity effects are not responsible for the decrease in fluorescence.

Comparison for Figures IV.5. and IV.8. illustrate that for the 9,10-diphenylanthracene system, the decay time was 2.5 times longer than that of the 10^{-2} wt %

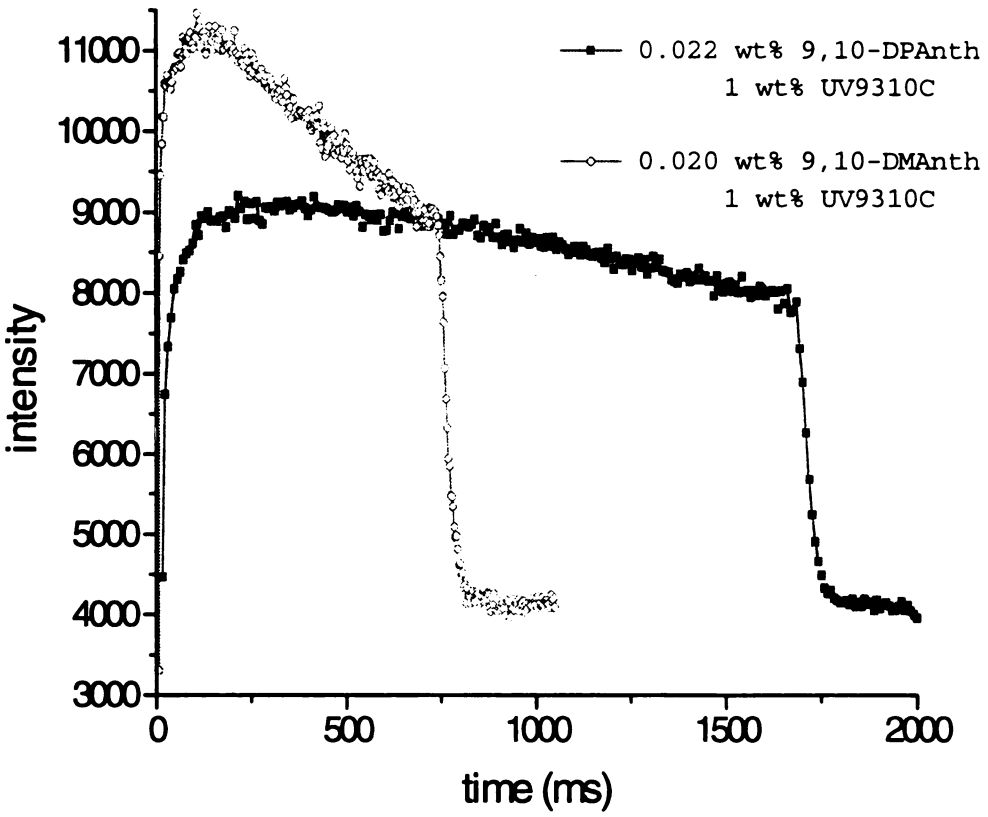

Figure IV.8. *Polymerization of DVE-3 monomer with UV9310C and 10^{-2} wt % of 9,10-diphenylanthracene and 9,10-dimethylanthracene as the photosensitizers, monitored by photosensitizer fluorescence intensity.*

anthracene system and nearly 2 times longer than that of the 9-vinylanthracene system. In contrast, the 9,10-dimethylanthracene decay time was the same as the decay time for anthracene. These results indicate that the 9,10-diphenylanthracene photosensitizer reaction is hindered due to steric effects of the phenyl rings or formation of a stable cation-radical due to electronic stabilization. The methyl groups of 9,10-dimethyl-anthracene seem to have little effect on the reaction when used as the photosensitizer. These results are consistent with the electron transfer mechanism for photosensitization shown in Figure IV.4.

IV.3.7. Fluorescence Experiments Without Monomer

The photosensitizer fluorescence intensity was also monitored for a system containing photosensitizer and initiator but no monomer. The reaction system without the divinyl ether monomer will not include any temperature effects arising from the heat of polymerization. Since these polymerizations are highly exothermic and very rapid, the reaction may take place under nearly adiabatic conditions with a significant increase in temperature. This increase in temperature could in turn increase the reaction rate further. Figure IV.9. contains a plot of anthracene fluorescence intensity versus time for 0.02 wt % photosensitizer and 1.2 wt % of initiator in methanol. Comparison of Figure IV.9. with Figures IV.5.- IV.8. reveals a dramatically different fluorescence profile for the system without monomer. The system containing only photosensitizer and initiator exhibits a fluorescence intensity which decays exponentially over a time period of twelve

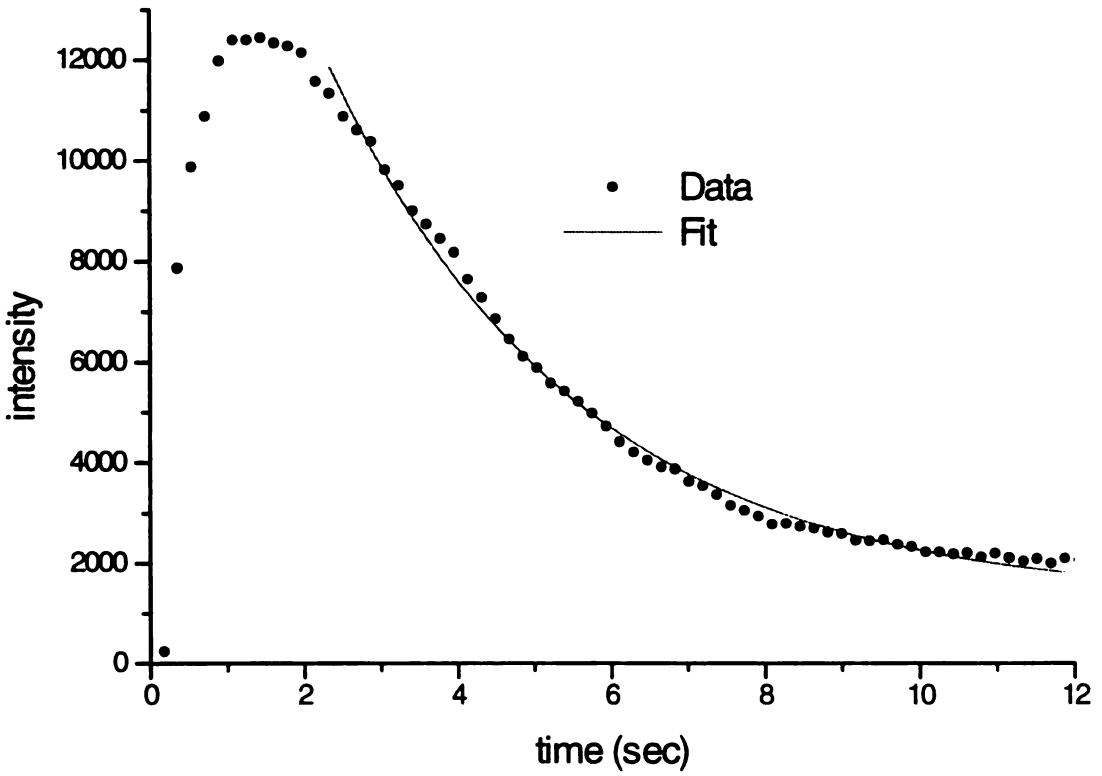

Figure IV.9. *Fluorescence intensity at 425 nm for photosensitization reaction of 2.2 x 10^{-2} wt % of anthracene as the photosensitizer and 1.2 wt % of diaryliodonium hexafluoroantimonate (UV9310C) in methanol.*

seconds, with no sharp decrease at an intermediate time as was observed for the systems which also contained DVE-3. This suggests that the rapid decrease in fluorescence seen in Figures IV.5. - IV.8. is due to a temperature increase arising from the heat of polymerization. This hypothesis is supported by the fact that the time scale of the photosensitization reaction in methanol is seconds as compared to milliseconds for the divinyl ether reaction systems. The time constant for the best-fit exponential decay was found to be 4.7 seconds for the curve in Figure IV.9.

IV.3.8. Initial Increase in Fluorescence Intensity

During the initial stage of the fluorescence monitoring experiments, an increase in the signal was observed for all reactions. However, the photosensitization reaction mechanism should lead to a monotonic decrease in the anthracene concentration as active centers are generated. Therefore, a set of experiments were performed to determine the cause of this initial increase in the fluorescence intensity.

Figure IV.10. shows a typical fluorescence monitoring curve for a cationic photopolymerization of DVE-3. As can be seen in the figure, the signal initially increases dramatically during the first 500 ms. The figure also shows a fluorescence profile where the sample in moved to new unreacted section of the sample. If the build-up was an inherent aspect of the photosensitization reaction, the increase should repeat for the new location. However, the new location does not show a similar increase, indicating that the increase in not caused by the photosensitization reaction. Since the new location started to

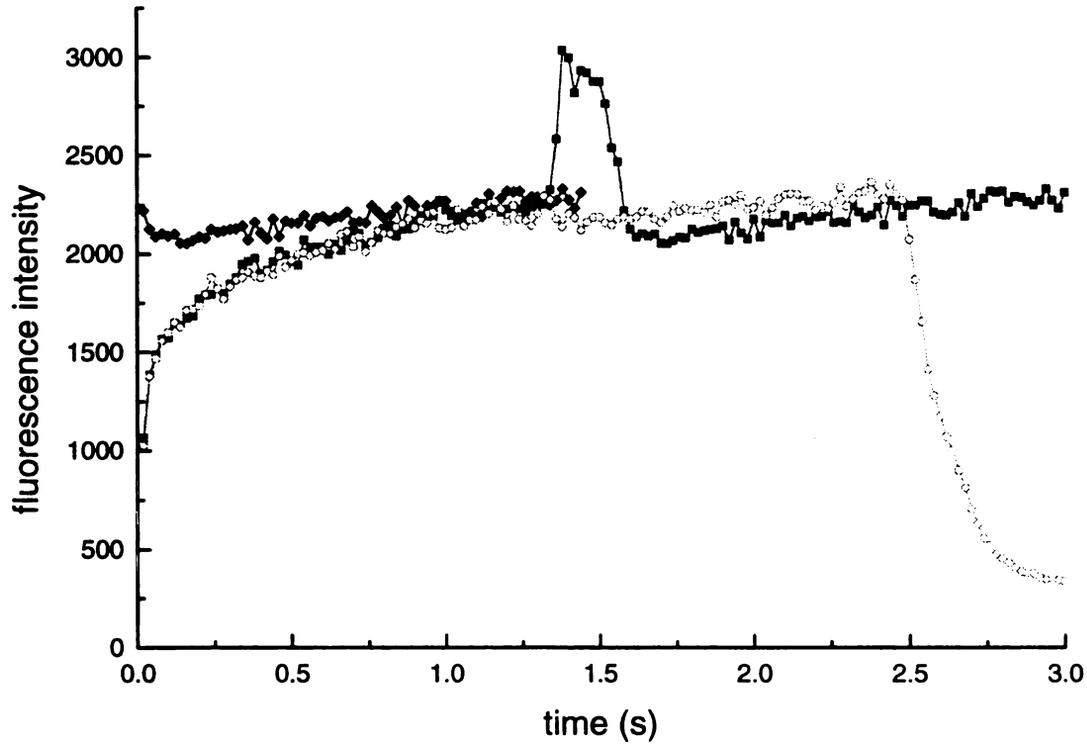

Figure IV.10. *Fluorescence monitoring of DVE-3 with 2.4 x 10^{-2} wt % anthracene and 1 wt % initiator. The sample was moved during the reaction to a new unreacted section.*

react only after the sample was moved, the third curve in Figure IV.10. is a repositioning of the new location profile to time zero. The repositioned curve and the typical curve illustrate very well the difference in the build-up at the start of the two runs.

Further evidence that the build-up is not an inherent feature of the reaction is shown in Figure IV.11. In this experiment, the photosensitization reaction was started, but the fluorescence emission was block between the sample and the detector. If the initial build-up was caused by the reaction, the increase should be reduced since the reaction had been underway for approximately 250 ms when the detector was started. However, the figure shows that the increase was unchanged even through the reaction was started well before the detector was started. This indicates that the increase is related to the detector and not the reaction system.

Figure IV.12. shows three different curves in which the initiation shutter and the detector were started at different times relative to each other. First the initiation shutter was delayed 1 second relative to the start of the detector acquisition. If the detector was causing the build-up, starting the detector before the reaction may allow the detector to "warm-up" and therefore no build-up would be seen at the start of the reaction. However, Figure IV.12. show that the build-up is still seen for this curve. This indicates that a "warm-up" period is not required by the detector. Second, the initiation reaction was started and the fluorescence emission was allowed to reach the detector. However, the detector acquisition was not started for one second after the initiation. In this case, no initial build-up is seen, indicating that the build-up in the detector is a light related phenomena. The third curve in Figure IV.12. is typical experiment where the initiation shutter was opened simultaneously with the start of the detector acquisition.

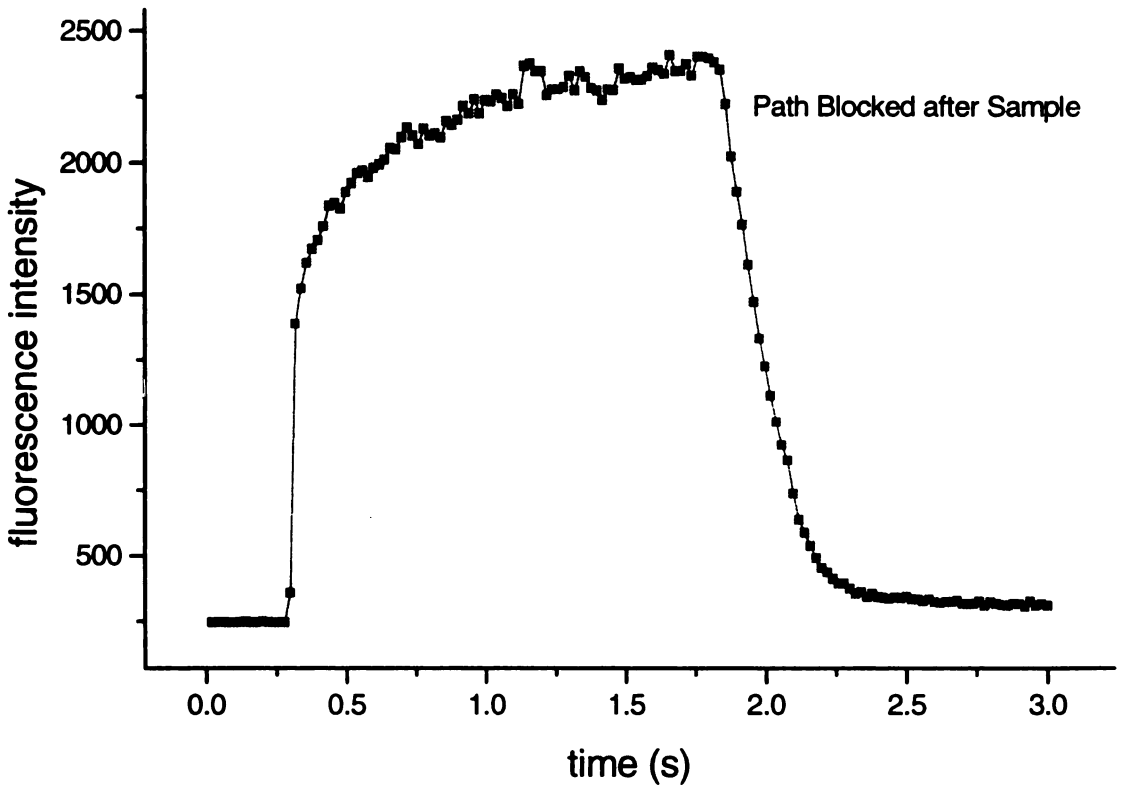

Figure IV.11. *Initiation Started at time equal zero, but the fluorescence emission was not allowed to reach the detector for the first 250 ms of the reaction.*

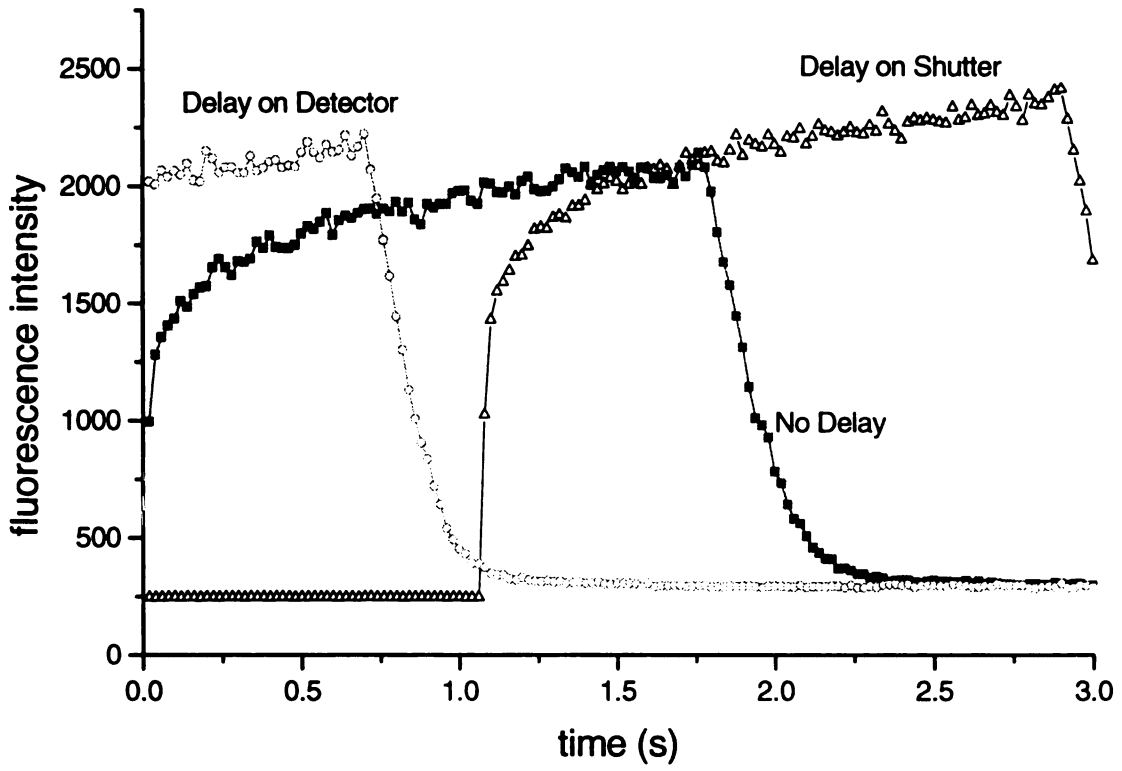

Figure IV.12. *Different time delays of the initiation shutter and the detector to determine the cause of the initial build-up.*

As detailed in the section above, this build-up in the anthracene fluorescence intensity was determined to be an instrument artifact and not inherent to the photosensitization reaction. The initial detector response seems to be related to the light reaching the detector surface. One possible explanation for this build-up is an increase in the intensifier efficiency during the start of the reaction. The intensifier operates in a similar fashion to a photomultiplier tube. When a photon strikes the intensifier surface a number of the photons are released which then cascades toward the detector surface. This process requires light to initiate and may take a finite length of time to reach its full value of the enhancement. However, the important information determined using this technique is not affected by the initial increase. Finally, this build-up was not seen with the new CCD detector that was purchased and implemented.

IV.4. Conclusions

This chapter demonstrates the utility of *in-situ* laser-induced fluorescence spectroscopy for monitoring cationic photopolymerizations of vinyl ethers photosensitized by anthracene and its derivatives. Due to its extremely short intrinsic timescale, fluorescence spectroscopy provides a means to characterize the kinetics of these polymerizations which are too rapid to be monitored by traditional methods such as DSC. In these studies, the fluorescence intensity of the photosensitizer was monitored as a function of time with spectra collected in intervals as short as 2 milliseconds. The profile of the fluorescence intensity versus reaction time invariably exhibited the same general shape with an initial increase to a quasi-steady-state value, followed by a gradual

decrease over several hundred milliseconds, followed in turn by a dramatic reduction in a period of less than 100 milliseconds to a final, relatively constant value.

The observed reduction in fluorescence intensity is attributed to the consumption of the anthracene in the photosensitization process, with the associated production of active cationic centers. Experiments were performed to demonstrate that anthracene-consuming side reactions such as photo-induced dimerization did not contribute to the reduction in fluorescence. Therefore, it was concluded that the magnitude of the fluorescence decrease provides a direct measure of the rate of the initiation step, as well as an indication of the number of propagating active centers. The sharp decrease in fluorescence was attributed to large temperature increases arising from the heat of polymerization in these nearly adiabatic reactions (experiments were performed without external heating or cooling to simulate typical process conditions in coating, adhesive, and electronic applications). This conclusion was corroborated by experiments performed with initiator and photosensitizer but in the absence of monomer. In these experiments, which would have no effects from the heat of polymerization, the fluorescence intensity exhibited no sharp reduction in intensity, but rather decreased exponentially over a period of twelve seconds.

The rate of the cationic photopolymerizations were characterized in terms of the overall rate of the fluorescence decrease, and the time for the onset of the rapid reduction in fluorescence intensity. Experiments were performed to determine the effects of the initiator concentration, the photosensitizer concentration, and anthracene functional-ization on the polymerization rate. As expected, the reaction rate was found to increase as the initiator concentration or the photosensitizer concentration was increased. A

practical concentration limit for the photosensitizer of approximately 0.2 wt % for 500 μm films was established due to high optical densities which limit the penetration of light into the sample. Reactions photosensitized by anthracene and 9,10-dimethylanthracene produced the fastest rates, while the slowest rates were observed for 9,10-diphenyl-anthracene, perhaps due to steric hindrance or electronic interference caused by the phenyl rings. The 9,10-diphenylanthracene studies also illustrated that the fluorescence intensity decrease was insensitive of viscosity changes.

The fluorescence monitoring technique described here offers a non-intrusive, time resolved method for monitoring cationic photopolymerizations. Based upon this technique, our studies have provided previously inaccessible information about the rate of the cationic photopolymerizations and the effects of various reaction conditions. However, the technique has limitations. For example, although these studies based upon the magnitude of the photosensitizer fluorescence provide direct information about the rate of generation of active centers, they provide little information about the rate at which the active centers propagate once they are formed. Also, although the response time is considerably faster than the current alternatives, it is limited by the speed of the detection system (2 ms in our case). Finally, although the studies reported here illustrate the tremendous potential of *in situ*, laser-induced fluorescence spectroscopy for monitoring polymerizations, they provide only one example of a much more general technique. Many other fluorescence monitoring schemes which provide complementary information could be developed. For example, the use of laser-induced fluorescence for the *in situ* monitoring of temperature during these cationic photopolymerizations will be used to investigate this polymerization reactions, and strategies for using reactive probes to

monitor the propagation reaction are under development. Clearly, there is considerable potential for novel applications of time-resolved fluorescence spectroscopy for monitoring polymerizations.

IV.5. List of References

1. E.W. Nelson, T.P. Carter, and A.B. Scranton, "Photosensitization of Cationic Photopolymerizations by Anthracene and its Derivatives," *Proceedings of American Chemical Society, Poly. Mat. Sci. Eng.*, ACS Fall Meeting, Chicago, **69**, 363 (1993).

2. E.W. Nelson, T.P. Carter, A.B. Scranton, " The Role of the Triplet State in the Photosensitization of Cationic Polymerization by Anthracene," *J. of Polym. Sci. Part A: Polym. Chem.* **33**, 247-256 (1995).

3. A. Bondi, "Estimation of The Heat Capacity of Liquids," *I & E C Fundamentals*, **5**, 442 (1966).

4. S. Jonsson, P-E. Sundell, A. Hult, "Photoredox Induced Cationic Polymerization of Divinyl Ethers," *Radtech 90-North America, Radiation Curing Conference and Exposition Proceedings*, **417** (March 25-29,1990).

5. P.E.M. Allen, C.R. Patrick, *Kinetics and Mechanisms of Polymerization Reactions*, John Wiley and Sons, New York, 79, 1974.

6. *Encyclopedia of Polymer Science and Engineering, Second Edition*, J.I. Kroschwitz, Ed., **17**, 453, 1989.

7. F.W. Wang, W.J. Pummer, B.M. Fanconi, En-Shinn Wu, *Photophysics of Polymers*, C.E. Hoyle, J.M. Torkelson, Eds., American Chemical Society, Washington D.C., (1987).

CHAPTER V. PHOTOSENSITIZATION MECHANISM: EXPERIMENTS AND MODELS

V.1. Introduction

In this chapter, the photosensitization mechanism for cationic polymerizations initiated by diaryliodonium salts photosensitized by anthracene were investigated using fluorescence and phosphorescence spectroscopy. *In situ* photosensitizer fluorescence measurements confirmed that the photosensitization reaction proceeds by an electron transfer process. Transient phosphorescence studies demonstrated that electron transfer occurred from the triplet excited state of anthracene to the initiator, with an intrinsic kinetic rate constant of $2 \times 10^8 l / mol \cdot s$. Further evidence for the role of the triplet state was provided by an observed 7-fold decrease in the polymerization rate upon addition of a triplet state quencher. Finally, numerical solution of the photophysical kinetic equations indicated that the triplet state concentration was approximately three orders of magnitude higher than that of the singlet state, and that 94-96 % of the active cationic centers are produced by reaction of the initiator with the triplet state. These results indicate that the electron transfer occurs primarily from the triplet state of anthracene, with the singlet state providing only a minor contribution to the photosensitization reaction.

In this chapter, a series of studies were performed to determine which anthracene excited state (singlet or triplet) is involved in photosensitization of diaryliodonium salts. Anthracene phosphorescence and fluorescence lifetime studies were performed to determine the effect of the initiator on the lifetimes of the triplet and singlet. The role of the triplet state was investigated further from studies performed using an anthracene triplet quencher and from computer simulations of the photophysical-state populations.

V.2. Experimental

V.2.1. Materials

Anthracene, 9,10-dihydroanthracene, 9,10-diphenylanthracene and 9-phenyl-anthracene were purchased from Aldrich Chemical Company and were used as received The initiator (UV9310C; GE Silicones) had a composition of 5-10 wt % linear alkylate dodecylbenzene, ~50 wt % 2-ethyl-1,3-hexanediol, and ~50 wt % bis(4-dodecyl-phenyl)iodoniumhexafluoroantimonate. In this initiator, various dodecyl isomers have been attached to the phenyl rings of the diphenyliodonium salt in order to impart solubility in the monomer. These alkane substituents have little effect on the photo-sensitization reaction with anthracene.[1] Initiator concentrations specified in the remainder of this chapter correspond to the total UV9310C concentration.

V.2.2. Laser Fluorescence Measurements

The laser-induced fluorescence studies were performed in the *LASER* Laboratory at Michigan State University. The fluorescence and photosensitization were both excited with a Coherent Innova 200 argon ion laser operating at 363.8 nm. A Newport 845HP-01 digital shutter system was opened with an electronic pulse from the detector controller, ensuring that the illumination and fluorescence acquisition were started simultaneously. Fifteen milliwatts of unfocused laser radiation (measured with a Scientech 362 power/energy meter) in a ~3-mm-diameter beam was directed upon the quartz capillary tube (1 mm inner diameter, 2 mm outer diameter) placed perpendicular to the beam direction. The fluorescence was collected at an angle of 90° from the incident beam and 90° from the longitudinal axis of the quartz tube. The fluorescence signal was analyzed using a Spex 1877 Triplemate spectrometer with a subtractive dispersion filter stage and a spectrograph stage. An EG&G Princeton Applied Research Model 1421 intensified diode array, cooled to -20 °C to minimize dark charge levels, was used to detect the signal, and was interfaced to an EG&G Princeton Applied Research Model 1463 OMA III detector controller.

V.2.3. Phosphorescence Lifetime Measurements

Phosphorescence lifetime studies were performed using a nanosecond pulsed Nd:YAG laser (Quanta-Ray DCR-1) for the excitation source. The fundamental output

of the Nd:YAG was frequency tripled giving the third harmonic (355 nm) with a pulse width of 8 ns and a 10 Hz pulse rate. Eight mW (Scientech 365 power/energy meter) of laser light was directed through a photodiode trigger (Motorola MRD-500) and into a quartz cuvette containing the sample. The phosphorescence was dispersed with a Spex 1680A monochromator, detected by a Hamamatsu R928 photomultiplier, and the signal was analyzed with a Tektronix DSA602A storage oscilloscope. The phosphorescence was monitored at 670 nm with a 600 nm long pass filter placed at the monochromator entrance slit. In order to remove oxygen, the methanol/anthracene samples were subjected to freeze-pump-thaw cycles until the residual pressure when frozen was below 5.0×10^{-5} torr.

V.2.4. Fluorescence Lifetime Measurements

The picosecond-lifetimes were obtained using a single-photon timing (SPT) instrument constructed in-house. SPT (also known as time-correlated single-photon counting) measures ultra-fast luminescence lifetimes from the time-delay between the arrival of a laser excitation pulse at the sample and the detection of the first collected emission photon. This sub-nanosecond timing is accomplished using a time-to-amplitude converter (TAC; Tennelec Model TC 862) which outputs a voltage proportional to the measured delay time. The TAC timing is started and stopped by pulses from a pair of constant-fraction discriminators (CFDs; Tennelec Model TC 455). The CFDs produce output pulses at the same relative height of the input trigger pulse, even if the input pulse height is fluctuating shot-to-shot (which can be a problem for laser pulses and single-

photon pulses). The "start timing" input is ordinarily generated from the laser pulse and the "stop timing" input generated by the first detected emission photon; however, the instrument may also be run in "reverse-timing" mode where these assignments are reversed. The luminescence from the sample is collected, collimated and focused into a SPEX 1681 monochromator. The detector is a thermoelectrically cooled Hamamatsu Model R1564 microchannel plate, which provides an electrical pulse for each detected single-photon event. The TAC output voltage for each Δt is converted to a digital value by a multi-channel analyzer (Nucleus, Model 8000AT) and placed into the appropriate "bin" of a histogram of number of events vs. delay time. This histogram looks precisely like a classically produced luminescence decay curve, and provides the same lifetime information about the sample. The laser system is comprised of a Coherent Antares mode-locked Nd:YAG laser which is frequency doubled, and the 2^{nd} harmonic used to pump a sync-pumped, cavity-dumped Coherent 702 dye laser running rhodamine 6G dye. This laser was operated at 610 nm and subsequently frequency-doubled to 305 nm and used as the excitation source for the anthracene. The (uncorrected) autocorrelation width of the laser pulses is ~ 6 ps. The total SPT instrument response time is less than 50 ps.

V.2.5. Absorption and Fluorescence Measurements

Absorption spectra of initiator and photosensitizers were obtained using a Hewlett Packard UV-VIS 8452A diode array spectrophotometer. An Aminco-Bowman Series 2 Luminescence Spectrometer was used to measure the fluorescence of the various compounds. The temperature of the fluorescence samples was controlled by a

Polyscience 9100 refrigerated constant temperature circulator connected to a jacketed cuvette holder in the spectrometer.

V.3. Results and Discussion

V.3.1. Photosensitization Mechanism

These results indicate that photosensitization of diaryliodonium salts by anthracene proceeds by electron transfer primarily form the anthracene triplet excited state. The important photochemical steps of the proposed mechanism are shown in Figure V.1. In the first step of this mechanism, the photosensitizer absorbs light and populates the first excited singlet state. From the excited singlet state, the anthracene may return to the ground state by fluorescence or radiationless deactivation, or undergo intersystem crossing to the triplet state. In the second step of the mechanism, an exciplex is formed from the association of a triplet state anthracene and a ground state initiator molecule. This exciplex formation is the only diffusion controlled step in the mechanism and therefore is the rate limiting step in the reaction. In the exciplex, an electron may be transferred from the anthracene to the initiator (step 3 of the mechanism), resulting in the formation of a radical-cation in the 9 and 10 positions of the anthracene (this location is favored due to resonance stabilization). This radical-cation may undergo several possible reactions, however the important result for our purposes is the production of cationic

1. Photoexcitation

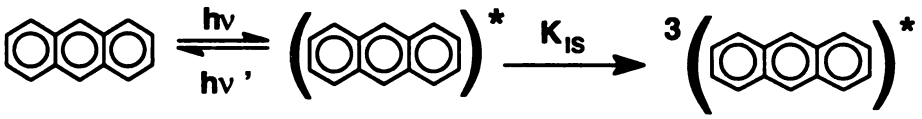

2. Exciplex Formation

3. Electron Transfer

Figure V.1. *Proposed photosensitization mechanism based on electron transfer from triplet state anthracene to initiator.*

active centers capable of initiating polymerization. The possible photolysis products of the photosensitized diaryliodonium salts have been examined in considerable detail by Dektar and Hacker.[2]

Not shown in Figure V.1. is the possibility of the excited singlet state anthracene forming an exciplex with a ground-state initiator molecule. Once formed, the singlet-state exciplex could undergo a redox reaction to produce cationic active centers in a manner analogous to steps 2 and 3 of Figure V.1. As discussed later in this chapter, a series of studies to determine the relative importance of reaction from the singlet state to reaction from the triplet state were performed, and the fraction of active centers produced by each path were evaluated. Previous fluorescence studies[3] corroborate the proposed photosensitization mechanism shown in Figure V.1. First, the observed decrease in fluorescence is consistent with the electron-transfer scheme since anthracene is consumed when the central ring loses an electron. In contrast, during the energy transfer mechanism the anthracene would be regenerated and not consumed. The order of reactivity of the anthracene derivatives is also consistent with the electron transfer scheme.

Our results illustrated that anthracene and 9,10-dimethylanthracene resulted in the most rapid reactions, followed by 9-vinylanthracene and 9,10-diphenylanthracene, respectively.[3] The relatively low reactivity of 9,10-diphenylanthracene may be attributed to steric effects associated with the bulky aromatic substituents in the 9 and 10 positions, and to the enhanced resonance stabilization afforded the radical-cation by these substituents. Similarly, the vinyl substituents of 9-vinylanthracene produces some steric hindrance and resonance stabilization of a 9,10 radical-cation compared with anthracene or 9,10-dimethylanthracene.

Further evidence for the electron transfer mechanism for photosensitization may be obtained from thermochemical considerations.[4] The electron transfer scheme is thermodynamically feasible if the excited state energy of the photosensitizer (E^*) is greater than the difference between the energy (E_{sens}^{ox}) required to oxidize the photosensitizer and the energy (E_{init}^{red}) released by reduction of the initiator.[5] Therefore, the magnitude of the free energy (ΔG) of photosensitization should be negative. As illustrated for clarity in Figure V.2., the free energy change of photosensitization (ΔG) can be readily determined using the Rehm-Weller Equation:[6]

$$\Delta G = (E_{sens}^{ox} - E_{init}^{red}) - E^* \qquad \text{Eq. 1}$$

Figure V.2. illustrates the division of the photosensitization process into two hypothetical steps. During the process energy is released in the transition from excited state to ground state (ΔG_1 is negative) however energy is consumed in the redox reaction (ΔG_2 is positive). Some authors have mistakenly used the excitation energy in place of the donor excited state energy when calculating ΔG.[1,4]

The energy required to oxidize anthracene has been reported to be 106 kJ/mol.[7] Similarly, the reduction energy for the diaryliodonium initiator (E_{init}^{red}) has been determined to fall in the range of -19 to -48 kJ/mol.[5,8] The excited-state energy of the photosensitizer may be calculated from the frequency of the 0-0 fluorescence (singlet state) or phosphorescence (triplet state) transition. As shown in Figure V.3., the values of E* are 315 and 176 kJ/mol for the singlet and triplet states, respectively.[9] Based upon these values, ΔG for electron transfer from the singlet and triplet states of anthracene to the diaryliodonium salt were determined to be -175 kJ/mol and -36 kJ/mol respectively.

Free Energy of Photosensitization Reaction

$$A^* + I \xrightarrow{\Delta G} A_{ox} + I_{red}$$

$$A^* + I \xrightarrow{\Delta G_1} A + I \xrightarrow{\Delta G_2} A_{ox} + I_{red}$$

$$\Delta G_1 = -E^* \qquad \Delta G_2 = E^{ox}_{sens} - E^{red}_{init}$$

A* - Excited State Anthracene (singlet or triplet)

A - Ground State Anthracene

A_{ox} - Oxidized Anthracene

I - Initiator

I_{red} - Reduced Initiator

Transition Energy Released from Excited State to Ground State (E*)

$$S_1 \longrightarrow S_0 + h\nu \qquad h\nu = 315 \text{ kJ/mol}$$

$$T_1 \longrightarrow S_0 + h\nu \qquad h\nu = 176 \text{ kJ/mol}$$

Figure V.2. *Hypothetical pathway and energetics of the photosensitization reaction.*

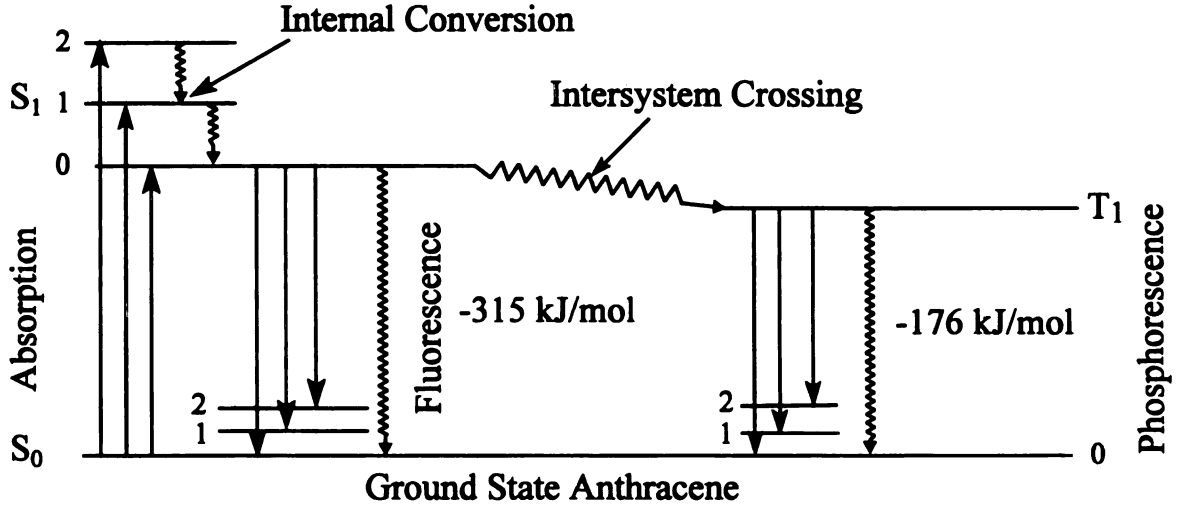

Figure V.3. *Electronic energy level diagram for anthracene fluorescence and phosphorescence.*

The 0-0 transition of the fluorescence and phosphorescence were used in the calculation since they represent the transition to the ground state of the photosensitizer. The 0-0 transition is the highest energy transition (Figure V.3.) and gives the most negative value for ΔG. However the wavelength which gives $\Delta G = 0$ can be calculated to be 855 nm, which is well past both fluorescence and phosphorescence of anthracene. Therefore, both fluorescence and phosphorescence of anthracene have favorable free energy values making the electron transfer reaction thermochemically feasible.

The above analysis illustrates that photosensitization is thermodynamically feasible from both the singlet and triplet state of anthracene. However, in order to determine the relative amounts of reaction from each state the kinetics of the photo-sensitization must be considered. Figure V.3. shows the relative energy levels for the singlet and triplet states of anthracene. The distinction can be important because the two states have considerably different lifetimes, and may interact differently with molecules that may be present in the reaction system. For example, some compounds may act as triplet state quenchers, but may have little or no effect on the singlet excited state.

Lifetime considerations would seem to favor electron transfer from the triplet state rather than the singlet state. The triplet state lifetime is three orders of magnitude longer than that of the singlet state, therefore it is much more likely that a triplet state molecule will encounter an initiator molecule during its lifetime. Also, the triplet state contains two unpaired electrons and can be represented as a diradical in the 9 and 10 positions. This facilitates donation of an electron from the triplet state anthracene. For example, Andersen *et al.*[10] demonstrated that the radical polymerization of styrene could be photosensitized by anthracene and concluded based upon lifetime considerations that it

was triplet-state anthracene that interacted with styrene. Furthermore, it has been demonstrated that standard radical initiators may serve as photosensitizers for onium salts through a similar electron transfer process.[11] However, both the reactivity and relative populations of the singlet and triplet states need to be investigated to determine the relative number of active centers generated from each state.

V.3.2. Fluorescence and Phosphorescence Lifetime Studies

Transient fluorescence and phosphorescence studies were performed to determine the anthracene singlet and triplet state lifetimes both in the presence and the absence of the initiator. Oxygen is a known triplet quencher, and was removed using several freeze-pump-thaw cycles to increase the signal to noise ratio. Transient phosphorescence profiles for anthracene in methanol and anthracene plus initiator in methanol are shown in Figure V.4. In this experiment, the phosphorescence was collected at 670 nm with a 600 nm long pass filter located at the monochromator inlet. The figure illustrates that the phosphorescence decay rate increased nearly 26-fold when 2.0 wt % initiator was included in the sample. This dramatic reduction in the triplet lifetime upon the addition of the initiator provides direct evidence that electron transfer occurs from the triplet state of anthracene during the photosensitization process. The phosphorescence decay profiles in Figure V.4. were fit with single exponential decay functions yielding a time constant of 9.55×10^{-6} s in the absence of initiator, and 3.85×10^{-7} s in the presence of 2.0 wt % initiator. Since the initiator is present in great excess its concentration may be assumed to

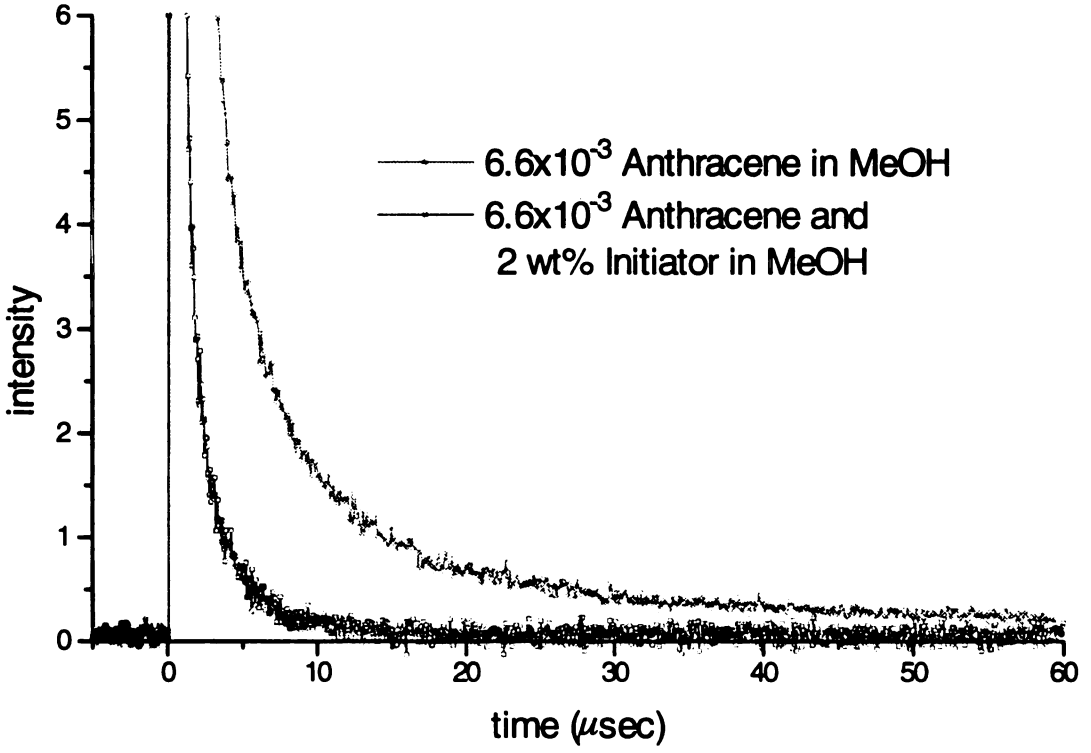

Figure V.4. *Transient phosphorescence profiles of 6.6 × 10^{-3} wt % anthracene in methanol with and without 2.0 wt % initiator.*

remain constant during the reaction. Therefore, an apparent rate constant for photosensitization can be calculated assuming that the relaxation of the triplet state is first order, as shown in Equations 2 and 3. The solution to these rate expressions are the exponential decay function shown in Equation 4 and 5.

$$\frac{d[^3A]}{dt} = -(k_{phos} + k_{nonrad})[^3A_0] \qquad \text{Eq. 2}$$

$$\frac{d[^3A]}{dt} = -(k_{phos} + k_{nonrad} + k^*_{senphos})[^3A_0] \qquad \text{Eq. 3}$$

$$\frac{[^3A]}{[^3A_0]} = e^{-(k_{phos}+k_{nonrad})t} \qquad \text{Eq. 4}$$

$$\frac{[^3A]}{[^3A_0]} = e^{-(k_{phos}+k_{nonrad}+k^*_{senphos})t} \qquad \text{Eq. 5}$$

Where $[^3A]$ represents the triplet state anthracene concentration at time t, $[^3A_0]$ represents the initial triplet concentration, k_{phos} is the rate constant for phosphorescence, k_{nonrad} is the rate constant for all non-radiative processes, and $k^*_{senphos}$ is the pseudo rate constant for photosensitization. The rate constants may be evaluated based upon the exponential time constants as shown below:

$$(k_{phos} + k_{nonrad}) = \frac{1}{9.55 \times 10^{-6}\ \text{sec}} \qquad \text{Eq. 6}$$

$$(k_{phos} + k_{nonradit} + k^*_{senphos}) = \frac{1}{3.85 \times 10^{-7}\ \text{sec}} \qquad \text{Eq. 7}$$

Combination of Eq. 6 with Eq. 7 yields a value of $2.50 \times 10^6\ s^{-1}$ for the pseudo kinetic rate constant, $k^*_{senphos}$, ($k^*_{senphos} = k_{senphos}[I]$). Substitution of the diaryliodonium concentration into this expression ($[I] \sim 0.014 \pm 0.004$ *mol/l*) yields a value of 2×10^8

l/mol·s for the intrinsic kinetic constant for photosensitization from the triplet state, $k_{senphos}$.

Transient fluorescence studies were also performed to determine the effect of the initiator on the singlet-state lifetime. As shown in Figure V.5., a small reduction in the fluorescent lifetime from 4.2 ns to 3.2 ns was observed. These values are consistent with literature values for the fluorescent lifetime of anthracene which range from 5.03 ns to 2.64 ns.[12,13]

Reaction rate constants from fluorescence lifetime experiments were calculated assuming all reduction in lifetime results in production of active centers. The transient fluorescence profiles in Figure V.5. were fit with single exponential decay functions. The time constant for anthracene excited at 305 nm and monitored at 425 nm was found to be 4.2×10^{-9} s in the absence of initiator, and 3.2×10^{-9} s in the presence of initiator. Since the initiator is in great excess, it was again assumed to remain constant during the reaction. In an analysis analogous to that outlined earlier for the triplet state, a value of 5.7×10^{9} *l/mol·s* was found for the intrinsic kinetic constant for initiation from the singlet state, $k_{senfluor}$.

Comparison of the rate constants for photosensitization reveals that the singlet state rate constant is over an order of magnitude higher than the triplet state rate constant. However, to determine the relative importance of the singlet and triplet states for the production of cationic active centers, the relative populations of the states must be considered. Since the triplet state has a much longer lifetime, its population may exceed

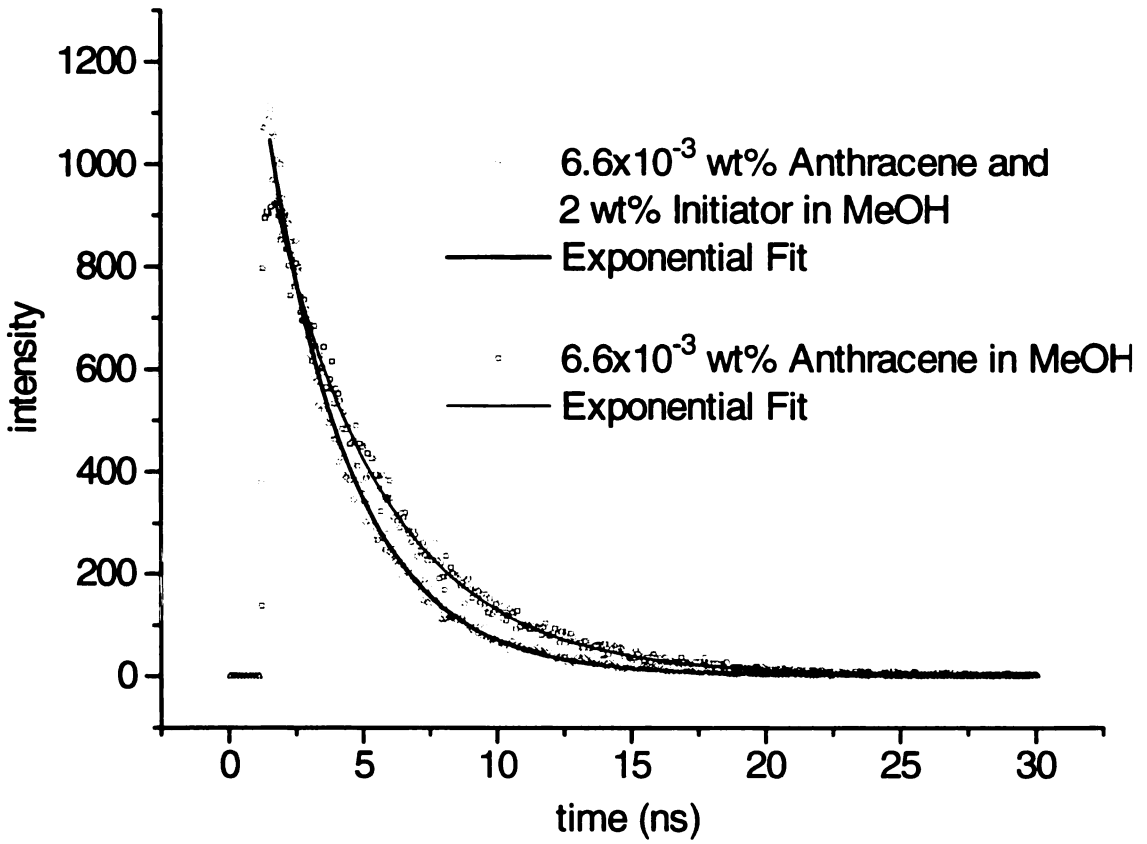

Figure V.5. *Transient fluorescence profiles for 6.6 × 10^{-3} wt % anthracene in methanol with and without 2 wt % initiator.*

the population of the singlet state by orders of magnitude. The relative population of the triplet and singlet state depends primarily on the intersystem crossing rate constant (k_{isc}). Experimental measurement of this constant is difficult and literature values range from 7.38×10^7 to 1.12×10^8 s^{-1} for anthracene in solution.[5,9]

The underlying photophysics of the sensitization reaction can be described by equations 8-15. These equations represent the anthracene electronic state transitions as well as the reaction of excited-state anthracene with initiator. Other possible photochemical reactions of anthracene have been excluded due to their relative unimportance.

$$h\nu + A \xleftarrow{k_{abs}} {}^1A \qquad \text{Eq. 8}$$

$${}^1A \xrightarrow{k_{fluor}} A + h\nu \qquad \text{Eq. 9}$$

$${}^1A \xrightarrow{k_{nonrad}} A \qquad \text{Eq. 10}$$

$${}^1A \xrightarrow{k_{isc}} {}^3A \qquad \text{Eq. 11}$$

$${}^3A \xrightarrow{k_{phos}} A + h\nu_p \qquad \text{Eq. 12}$$

$${}^3A \xrightarrow{k_{nonrad}} A \qquad \text{Eq. 13}$$

$${}^3A + I \xrightarrow{k_{senphos}} Rt \qquad \text{Eq. 14}$$

$${}^1A + I \xrightarrow{k_{senfluor}} Rs \qquad \text{Eq. 15}$$

Here *I* represents the diaryliodonium salt and *A* represents ground state anthracene, while ${}^1A$ and ${}^3A$ represent anthracene singlet and triplet excited states, respectively. In addition, k_{abs} is the rate constant for photon absorption, and k_{fluor} is the rate constant for fluorescence. Finally, *Rs* represents active centers created by reaction of the initiator with singlet-state anthracene while *Rt* represents active centers created from reaction with the

triplet state. The remaining symbols used in the equations have been defined earlier in this chapter.

Based upon the above reaction pathway for photosensitization, balances on the various reaction species yield the following set of coupled, first and second order kinetic equations.

$$\frac{d[A]}{dt} = k_{abs}([^1A] - [A]) + (k_{fluor} + k_{nonrad})[^1A] + (k_{phos} + k_{nonrad})[^3A] \quad \text{Eq. 16}$$

$$\frac{d[^1A]}{dt} = k_{abs}([A] - [^1A]) - (k_{fluor} + k_{nonrad})[^1A] - k_{isc}[^1A] - k_{senfluor}[^1A][I] \quad \text{Eq. 17}$$

$$\frac{d[^3A]}{dt} = k_{isc}[^1A] - (k_{phos} + k_{nonrad})[^3A] - k_{senphos}[^3A][I] \quad \text{Eq. 18}$$

$$\frac{d[I]}{dt} = -k_{senfluor}[^1A][I] - k_{senphos}[^3A][I] \quad \text{Eq. 19}$$

$$\frac{d[Rs]}{dt} = k_{senfluor}[^1A][I] \quad \text{Eq. 20}$$

$$\frac{d[Rt]}{dt} = k_{senphos}[^3A][I] \quad \text{Eq. 21}$$

Solution of this set of equations requires the evaluation of the various kinetic constants. The sum of the rate constants k_{fluor} and k_{nonrad} were determined from the fluorescence lifetime measurements described previously, yielding $(k_{fluor} + k_{nonrad}) = 1.38 \times 10^8\ s^{-1}$. Based upon the known values of the laser power, the beam cross-sectional area, and the photon flux, the value of k_{abs} was calculated to be $2.79\ s^{-1}$ for our experiments. Finally, as discussed above, the value for the intersystem crossing constant (k_{isc}) has been reported to range from 7.38×10^7 to $1.12 \times 10^8\ s^{-1}$ for anthracene solutions.[5,9] Based upon these values of the kinetic constants, the set of differential equations were solved numerically using the Rosenbrock method for stiff systems.[14]

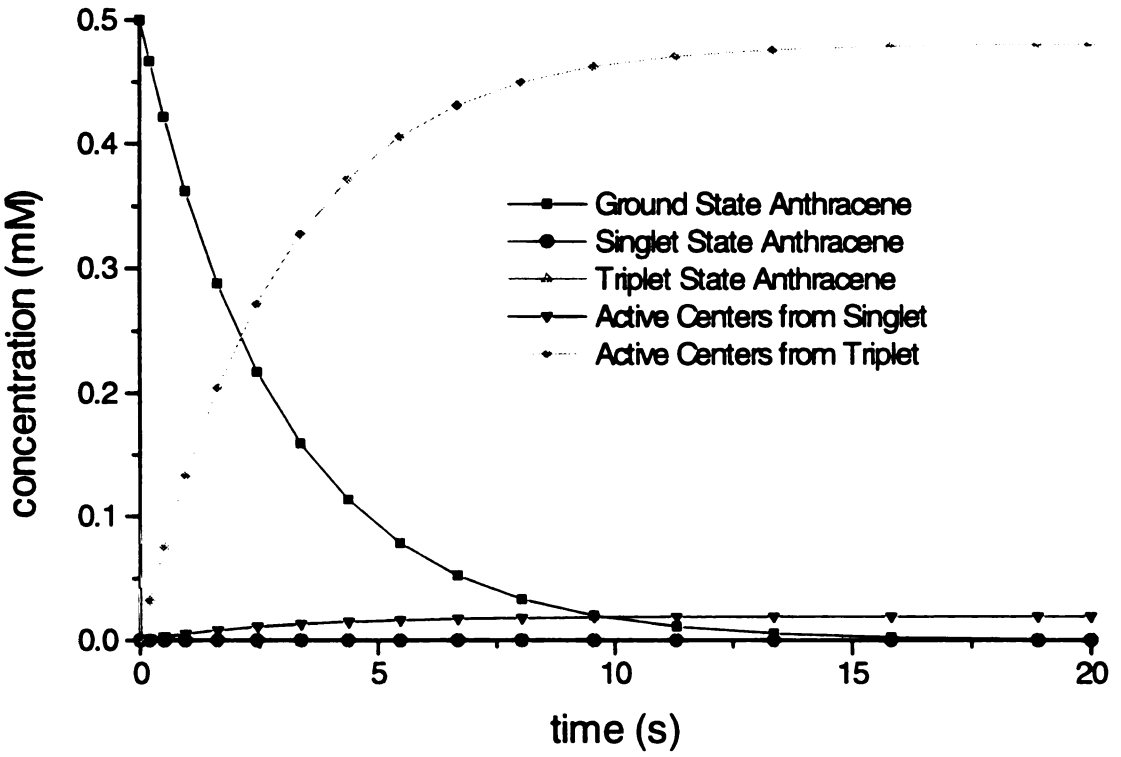

Figure V.6. *Simulation results for the concentration profiles of the reaction species. The initial [A] was taken to be 0.5 mM with [I] = 14.5 mM.*

Figure V.6. contains simulation results for the concentration profiles of various species in the reaction system. For the range of k_{isc} used (7.38×10^7 to 1.12×10^8 s^{-1}), the fraction of active centers produced from the triplet state was found to range from 94 to 96 %. Therefore, assuming that all of the reaction with the singlet state results in the formation of active centers, only 4-6% of the active centers arise from the singlet state. As shown in Figure V.6., the simulation results indicate that the anthracene concentration decays exponentially with time, while the number of active centers produced increases monotonically. The singlet and triplet state concentrations each pass through a maximum then decay towards zero. Except for reaction times less than a few milliseconds, the triplet state concentration is always approximately three orders of magnitude greater than that of the singlet state. Finally, based upon the simulation results, the time constant for the exponential decay of the anthracene concentration ranges from 3.0 to 3.7 seconds.

In a final experiment, the steady state anthracene fluorescence intensity was monitored as a function of time for reaction systems containing photosensitizer and initiator in methanol. For a reaction system containing 1.0×10^{-2} wt % anthracene and 1 wt % initiator, the photosensitizer fluorescence intensity was found to decay exponentially with a time constant of 4.7 seconds.[3] This fluorescence decrease was attributed to consumption of the anthracene by electron transfer during the photosensitization reaction. In Figure V.7. the experimental photosensitizer fluorescence intensity profile is plotted along with the simulation results for the anthracene concentration as a function of time. The simulation results are based upon the independently measured rate constants ($k_{fluor} + k_{nonrad}$, $k_{phos} + k_{nonrad}$, $k_{senfluor}$, $k_{senphos}$) and the

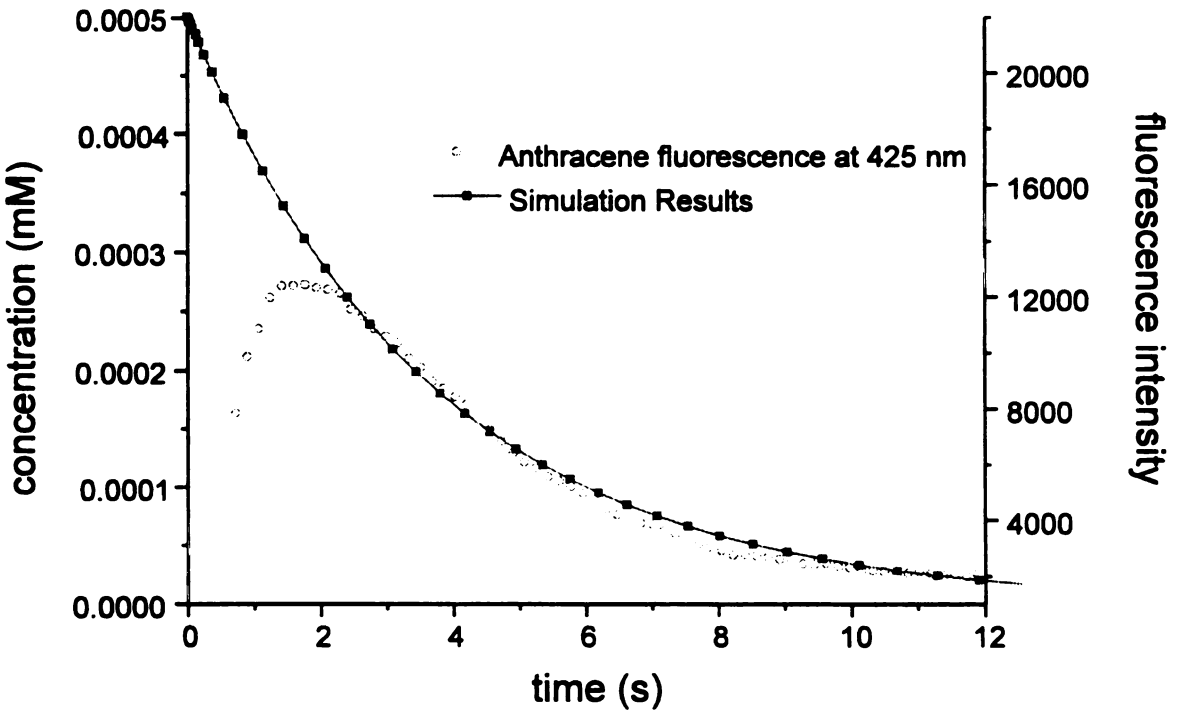

Figure V.7. *Comparison of computer simulation and experimental photosensitizer fluorescence intensity for reaction of anthracene (0.5mM - 1.0 × 10^{-2} wt %) and diaryliodonium hexafluoroantimonate (14.5 mM - 1 wt %) in methanol.*

literature value of k_{isc}, with no adjustable due to an instrumental artifact, the fluorescence intensity and simulation results show good agreement.

V.3.3. Triplet Quencher Studies

If the photosensitization reaction takes place primarily from the triplet state of the photosensitizer, the introduction of a phosphorescence quencher should dramatically lower the rate of active center production. For example, dihydroanthracene (DHA) will react with triplet anthracene[15] by transferring a hydrogen atom to the triplet state anthracene yielding two monohydro-anthracyl radicals which subsequently dimerize.[16] The resulting anthracene dimer does not photosensitize the diaryliodonium salt. Therefore, DHA effectively decreases the triplet anthracene concentration but has essentially no effect on the singlet state anthracene concentration. Transient fluorescence and phosphorescence studies were performed to determines the effect of DHA on the lifetimes of the singlet and triplet states of anthracene. Systems containing 5×10^{-3} wt % anthracene in methanol exhibited a two-fold reduction in the triplet state lifetime but essentially no change in the singlet state lifetime upon addition of 5×10^{-2} wt % DHA. Based upon these results, the rate constant for reaction of DHA with triplet state anthracene was calculated to be 1.8×10^{7} l/mol·s. These studies verify that the triplet state was quenched without significantly effecting the singlet-state lifetime. The DHA will therefore act as a retarder or inhibitor towards triplet-state photosensitization by effectively competing with the initiator for the triplet anthracene.

The above discussion illustrates that DHA reacts only with the triplet state of anthracene without directly effecting the singlet state concentration. Therefore DHA provides a means of distinguishing the anthracene excited state (singlet or triplet) from which the photosensitization occurs. If the electron transfer to the diaryliodonium salt occurs primarily from the triplet state of anthracene, the addition of DHA to a cationic photopolymerization should reduce the polymerization rate by inhibiting the production of active centers. If, however, the photosensitization occurs primarily form the singlet state, the addition of DHA to the reaction system should have relatively little effect on the production of active centers. To determine the effect of DHA on the cationic photopolymerization of a divinyl ether (3,6,9,12,-tetraoxatetradeca-1,13-diene) the polymerization was monitored using a previously described fluorescence technique.[3] A reaction system containing 2.6×10^{-2} wt % anthracene and 2 wt % initiator exhibited a 7-fold reduction in polymerization rate upon addition of 0.21 wt % of DHA. As shown, Figure V.8. exhibits the sudden decrease at 5.5 seconds indicating more than a 7-fold reduction in the rate of photosensitization upon addition of DHA, compared to reactions with similar anthracene and initiator concentrations. This considerable reduction in polymerization rate upon addition of DHA provides further evidence that the photosensitization reaction occurs predominantly from the triplet state of anthracene.

V.3.4. Competing Reactions

Other photo-induced reactions of anthracene which could interfere or compete with photosensitization were also investigated. Dimerization and oxidation are two

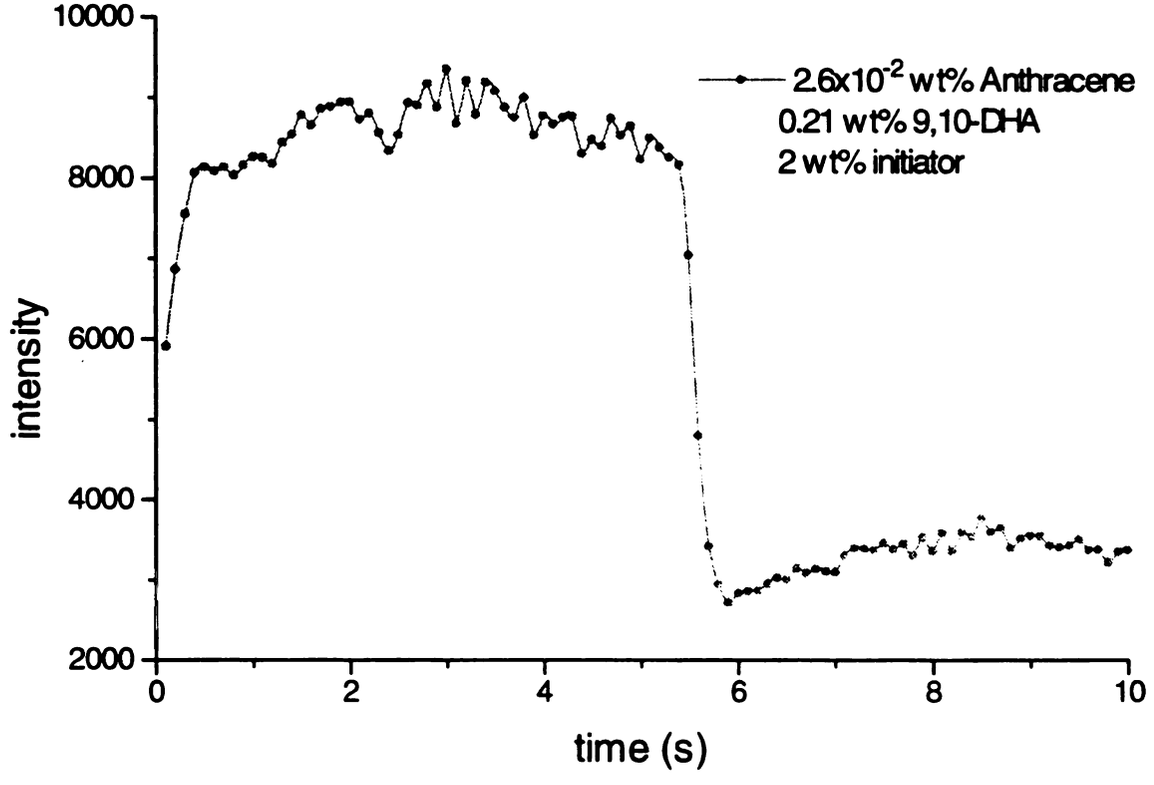

Figure V.8. *Polymerization of DVE-3 monomer with 2.1 wt % initiator and 10^{-2} wt % anthracene as the photosensitizer in the presence of 0.21 wt % of the triplet quencher 9,10-dihydroanthracene.*

possible reactions which remove anthracene and form non-reactive compounds. For example, a stable photodimer is formed when anthracene is excited with 350 nm light by the following reaction:

$$A + {}^1A \rightarrow A_2 \qquad \text{Eq. 22}$$

Once formed the dimer is not capable of photosensitizing the reaction. Experiments were performed to determine the rate of dimer formation. The dimer reaction can be monitored by measuring its UV-VIS absorption spectrum at 280 nm. The half-life for the dimer reaction was found to be ~ 3 hours, therefore it was determined that the dimerization reaction is not largely interfering with photosensitization.

The second possible interfering reaction is the oxidation of anthracene. Oxygen is known to react with anthracene by the following paths:

$$O_2 + {}^1A \rightarrow O_2\,{}^3A \qquad \text{Eq. 23}$$

$$O_2 + {}^3A \rightarrow O_2\,{}^3A \qquad \text{Eq. 24}$$

$$O_2\,{}^3A \rightarrow O_2 + A \qquad \text{Eq. 25}$$

$$A + O_2\,{}^3A \rightarrow AO_2 + A \qquad \text{Eq. 26}$$

In these reactions no effort has been made to remove or lower the oxygen concentration, and the photosensitization reaction reaches completion in under 2 seconds for all cases. The oxygen may be acting as a competing reaction of photosensitization, but the oxygen is at a much lower concentration than the initiator. Oxygen concentration calculated from comparison of similar organic solvents[18] was found to be ~1 x 10^{-8} M. At this concentration the oxygen is not appreciably interfering with the photosensitization reaction.

V.3.5. Fluorescence of the Products from Photosensitizing Diaryliodonium Salts with Anthracene

Anthracene has been shown to photosensitize diaryliodonium salt photoinitiators by electron transfer leading to the production of cationic active centers.[1-3,17,20] In this process, an excited state anthracene molecule transfers an electron to the iodonium salt, which results in the decomposition of the diaryliodonium salt. The photochemistry of diaryliodonium salts including photosensitization by several compounds has been examined to great extent.[2,17] However, there has been some question of the anthracene photophysical state that is transferring the electron.[3,17] Furthermore, there are some remaining questions as to the finial result of the anthracene after the photosensitization reaction.

In the photosensitization reaction, an anthracene cation radical is produced when an electron is transferred to the diaryliodonium salts. Dektar and Hacker have reported the production of phenylanthracenes by reaction of anthracene cation radicals with aryl radicals formed by fragmentation of diaryliodonium salts, followed by proton loss.[2] However, they could only account for ~30 % of the anthracene consumed by the photosensitization reaction. In this research, anthracene fluorescence intensity has been used to monitor the photosensitization reaction *in situ*.[3] The anthracene fluorescence intensity decreases during the reaction as the anthracene is consumed. However, if phenylanthracene is produced from this reaction, phenylanthracene fluorescence should be seen to grow in as the reaction proceeds. Since no phenylanthracene fluorescence is

seen in the experiments, we assume that the anthracene was converted to a non-fluorescent species. If anthracene losses the aromatic nature of its central ring by reaction with an aryl radical followed by a second reaction to neutralize the positive charge, its fluorescence will be greatly reduced.

In order to determine if phenylanthracene is a major product produced during the photosensitization reaction, experiments were conducted using UV-VIS absorption and fluorescence measurements. Phenylanthracene and 9,10-diphenylanthracene were compared to anthracene and solutions of anthracene and diaryliodonium that were photochemically reacted. The absorption and fluorescence of 9,10-dihydroanthracene was also compared as a model for anthracene products which have lost the aromatic nature of the center ring.

Absorption of all the anthracene derivatives were measured in methanol solutions at similar molar concentrations. Methanol was used as the solvent since it has excellent optical properties and also contains an extractable proton. However, the experiments were also done in the divinyl ether monomer. Figure V.9. shows the relative absorption of the anthracene compounds in the 300 to 450 nm region. At 365 nm, the molar absorptivity of anthracene was determined to be ~3000 l/mol·cm, while the absorptivity of 9-phenylanthracene and 9,10-diphenylanthracene were found to be ~6000 and ~4500 l/mol·cm respectively. Therefore, if either of the compounds are produced, they would absorb more strongly at 365 nm than anthracene. In constant, the absorption of 9,10-dihydroanthracene is essentially zero at 365 nm.

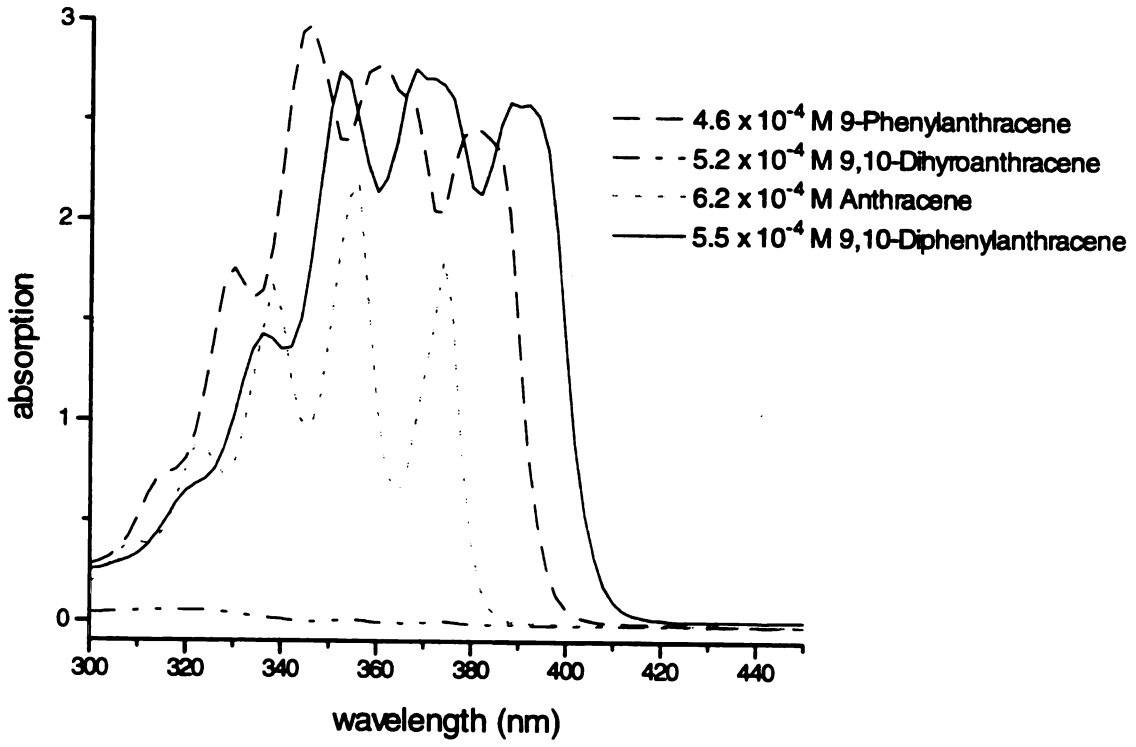

Figure V.9. *Relative absorption of anthracene and its derivatives.*

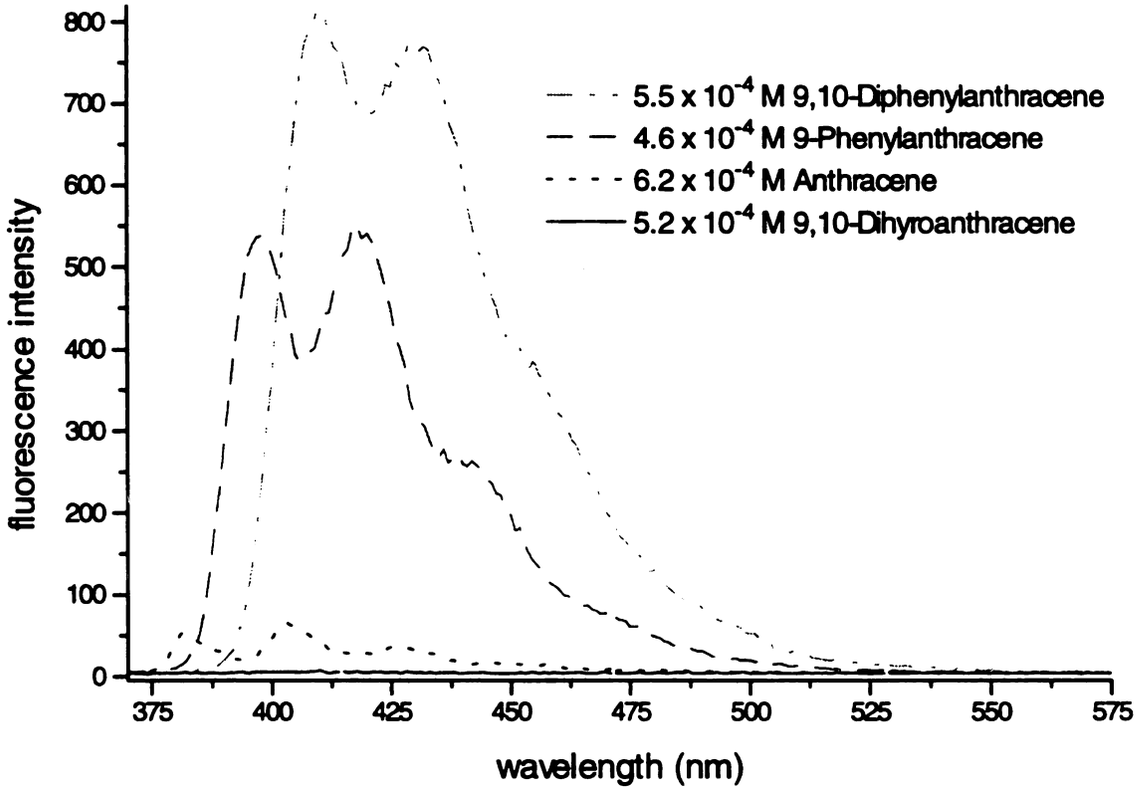

Figure V.10. *Relative fluorescence intensity of anthracene and its derivatives.*

The fluorescence of the same solutions was measured with excitation at 365 nm. The fluorescence emission was measured from 370 to 600 nm. Figure V.10. show the relative intensity and spectral shape of the anthracene derivatives. As expected, 9,10-dihydroanthracene shows no fluorescence when excited with 365 nm light. The relative fluorescence intensity increases from anthracene, 9-phenylanthracene to 9,10-diphenyl-anthracene. The 9-phenylanthracene intensity is 8 time that of the anthracene fluorescence, and 9,10-diphenylanthracene is 12 time more intense. These studies were performed to highlight the intensity of fluorescence and differences in spectral shape of the anthracene compounds.

As shown in previous work[3], when anthracene fluorescence intensity is followed during photosensitization of diaryliodonium salts in methanol, no change in the position or shape of the peaks is seen. As shown above, if 9-phenylanthracene or 9,10-diphenylanthracene is being produced in appreciable amounts, changes in the fluorescence spectra should be observed. Figure V.11. show the fluorescence of an anthracene and diaryliodonium solution before and after photosensitization. The anthracene fluorescence has decreased considerably, however the spectral shape has changed only slightly. The small change in the spectrum can be seen when the relative intensity of the first and third peaks of the anthracene are compared. In the reacted solution the third peak has grown in intensity slightly compared to the first peak. This increase occurs around 425 nm where 9-phenylanthracene does have a spectral peak. However, the amount of change is small compared to the overall reduction in the fluorescence intensity.

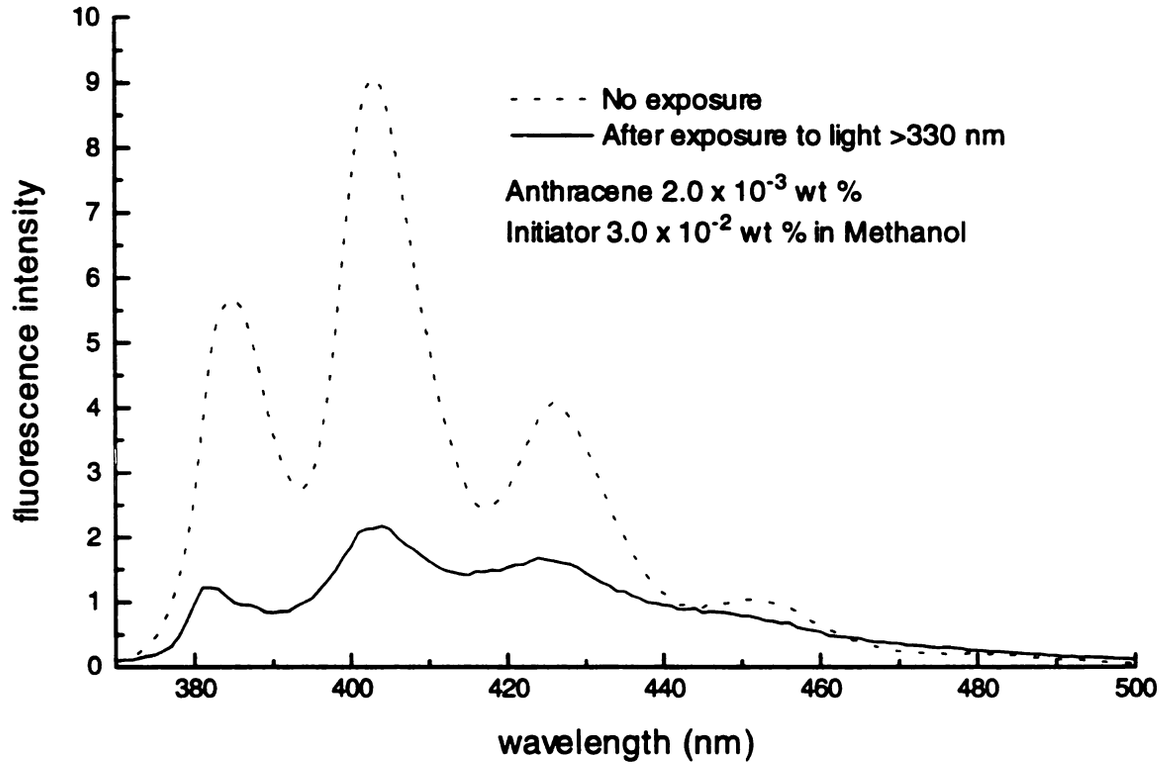

Figure V.11. *Fluorescence intensity of anthracene before and after photosensitization of diaryliodonium salts.*

The mechanism for the formation of phenylanthracenes by reaction of aryl radicals with the anthracene cation radical proposed by Dektar and Hacker[2] involves proton loss from the anthracene cation radical to remain aromatic in nature. However, we have shown that diaryliodonium salts can also be photosensitized by 9,10-dimethylanthracene and 9,10-diphenylanthracene[3], which do not contain available hydrogen atoms at the 9-10 positions. The 9,10-dimethylanthracene was shown to have a similar rate to anthracene, however 9,10-diphenylanthracene photosensitization rate was determined to be much slower, indicating an inference caused by the phenyl substituents.[3]

9-Phenylanthracene has also been found to photosensitize diaryliodonium salts. The fluorescence intensity was followed both in methanol and during a cationic polymerization of DVE-3. Figure V.12. shows the fluorescence profile for photo-sensitization of diaryliodonium by 9-phenylanthracene. The fluorescence profile was obtained by methods that have been described elsewhere.[3] The fluorescence profile decreases as the reaction proceeds again with no shift in the position of the peaks and no new fluorescence peaks from reaction products.

In this research, the exact products from the anthracene photosensitization reaction have not been determined. However, the final product produced in these reactions is non-fluorescent in the 400 - 500 nm region when excited at 365 nm. Our fluorescence studies indicate that large amounts of 9-phenylanthracene are not produced by the photosensitization of diaryliodonium salts by anthracene. The important processes in the reaction are the production of cationic active centers and the loss of anthracene fluorescence as the photosensitization reaction occurs.

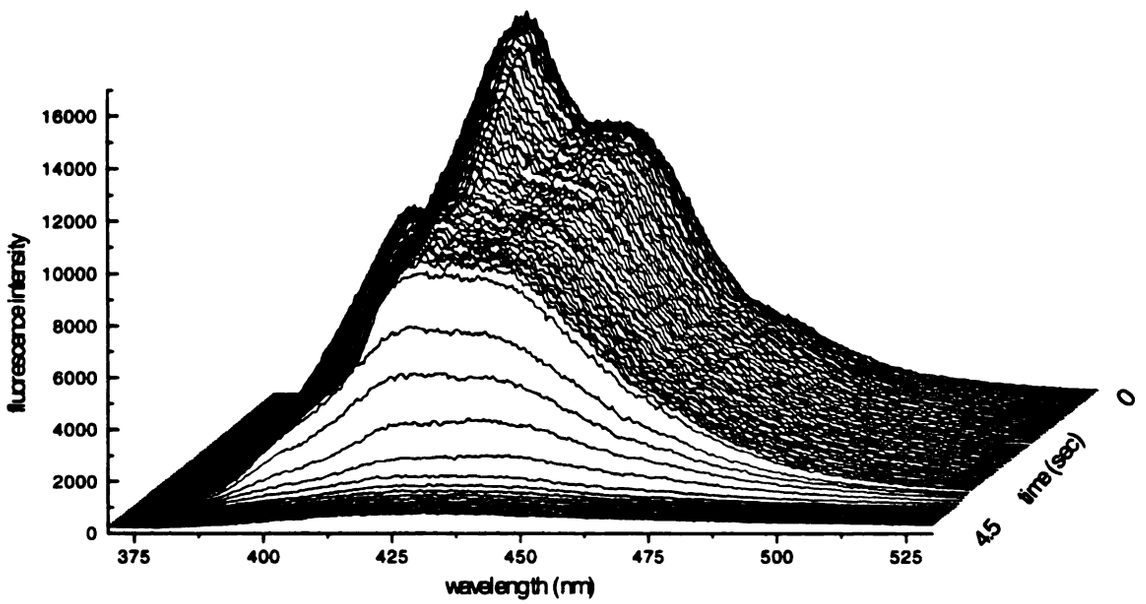

Figure V.12. *Fluorescence profile during polymerization of DVE-3 monomer (1 wt % initiator) produced by exciting 9-phenylanthracene (1.1×10^{-2} wt %), at 363.8 nm, and monitoring the fluorescence intensity at time intervals of 70 ms.*

V.4. Conclusions

In conclusion, our studies indicate that photosensitization of diaryliodonium salts by anthracene occurs by electron transfer primarily from the excited triplet state of the photosensitizer to the initiator (see Figure V.1.). The observed 26-fold increase in the rate of anthracene phosphorescence decay upon addition of initiator (see Figure V.4.) provides direct evidence for reaction from the triplet state. Based upon these studies, the intrinsic rate constant for photosensitization from the triplet state was found to be $k_{senphos} = 2 \times 10^8 \; l / mol \cdot s$. Further evidence for the importance of the triplet state is provided by the 7-fold decrease in the polymerization rate for a reaction system containing an anthracene triplet-state quencher (DHA) compared to corresponding system with no quencher. Finally, numerical solution of the photophysical kinetic equations indicate that the triplet state concentration is approximately three orders of magnitude higher than that of the singlet state, and that 94-96 % of the active cationic centers are produced by reaction of the initiator with the triplet state.

V.5. List of References

1. J. V. Crivello, "Cationic Polymerization-Iodonium and Sulfonium Salt Photoinitiators", *Adv. Polym. Sci.*, **62**, 1 (1984).

2. J. L. Dektar, N. P. Hacker, "Photochemistry of Diaryliodonium", *J. Org. Chem.*, **55**, 639 (1990).

3. E. W. Nelson, T. P. Carter, A. B. Scranton, "Fluorescence Monitoring of Cationic Photopolymerizations: Divinyl Ether Polymerizations Photosensitized by Anthracene Derivatives," *Macromolecules*, **27**,1013 (1994).

4. S. P. Pappas, J. H. Jilek, *Photogr. Sci. and Eng.*, **23**, 141 (1979).

5. G. J. Kavarnos, *Photoinduced Electron Transfer*, M. J. S. Dewar, J. D. Dunitz, K. Hafner, S. Ito, J.-M. Lehn, K. Niedenzu, K. N. Raymond, C. W. Rees, F. Vogtle, Ed., Topics in Current Chemistry 156, Springer-Verlag, New York, 27, 1990.

6. D. Rehm, A. Weller, *Isr. J. Chem.*, **8**, 259 (1970).

7. P. Sundell, S. Jonsson, A. Hult, "Photo-Redox Induced Cationic Polymerization of Divinyl Ethers," *J. Polym. Sci., Part A: Polym Chem.*, **29**, 1525 (1991).

8. Y. Yagci, I. Lukac, W. Schnabel, "Photosensitized Cationic Polymerization Using N-ethoxy-2-methylpyridinium hexafluorophosphate", *Polymer*, **34**, 1130 (1993).

9. N. J. Turro, *Molecular Photochemistry*, W. A. Benjamin, New York, 86, 1965.

10. V. S. Andersen, R .G. W. Norrish, " The Polymerization of Styrene Sensitized by Molecules in the Triplet State", *Proc. Roy. Soc. (London)*, **251**, 1 (1959).

11. S. Jonsson, P.-E. Sundell, A. Hult, *Radtech 90-North America*, Radiation Curing Conference and Exposition Proceeding, March 25-29, 417, 1990.

12. R. F. O'Dowd, A. O'Hare, J. Cooke, J.K. Taaffe, "Laser System and Data Analysis Techniques for Absorbing and Non-Absorbing Excited Transients," *J. Phys. E: Sci. Instrum.*, 15, 736 (1982).

13. I. B. Berlman, *Handbook of Fluorescence of Aromatic Molecules*, 2nd ed., Academic Press, New York, 356, 1971.

14. R. L. Borrelli, C. S. Coleman, *Differential Equations - A Modeling Approach*, Prentice - Hall Inc., 1987.

15. F. C. Bevington, *Photochemistry and Reaction Kinetics, Polymer Chemistry*, P. G. Ashmore, F. S. Dainton, T. M. Sugden, Ed., University Press: Cambridge, 202, 1967.

16. R. G. W. Norrish, J. P. Simons, "The Polymerization of Styrene Sensitized by Molecules in the Triplet State," *Proc. Roy. Soc. (London)*, **251**, 4 (1959).

17. R. J. DeVoe, M. R. V. Sahyun, E. Schmidt, N. Serpone, D. K. Sharma, "Electron Transfer Sensitized Photolysis of 'Onium Salts," *Can. J. Chem.*, **66**, 319 (1988).

18. Guerry, D. Jr. *Vanderbilt University Ph.D. Thesis*, 1944.

19. E. W. Nelson, T. P. Carter, A. B. Scranton, "The Role of the Triplet State in the Photosensitization of Cationic Polymerizations by Anthracene," *J. Polym. Sci., Part A Polym. Chem.*,**33**, 247, (1995).

20. S. P. Pappas, "Photoinitiation of Cationic and Concurrent Radical-Cationic Polymerization. Part V," *Prog. Org. Coat.*, **13**, 35 (1985).

21. J. V. Crivello, *Organic Coatings, Science and Technology*, G. D. Parfitt, A. V. Patsis, Ed., Marcel Dekker, Inc., New York, Vol. 5, 35, 1983.

CHAPTER VI. *IN SITU* RAMAN SPECTROSCOPY: CURE MONITORING AND KINETICS

VI.1. Introduction

In this chapter, Raman spectroscopy was used to monitor the cure *in situ* during the cationic photopolymerization of a divinyl ether photosensitized with anthracene. Since Raman spectroscopy arises from molecular vibrations, the consumption of double bonds can be directly measured during polymerization reactions. By monitoring the double bond concentration, Raman spectroscopy gives a direct method of obtaining the propagation rate during the reaction. Furthermore, the short intrinsic time scale makes Raman spectroscopy attractive as a time-resolved technique to monitor cure in these high speed reactions.

A series of Raman experiments were performed on cationic photopolymerizations of a divinyl ether initiated with a diaryliodonium salt of hexafluoroantimonate photosensitized by anthracene. The photosensitizer allowed the initiating wavelength to be shifted from the deep UV region of the spectrum to the near UV region around 350 nm.[1] Isothermal Raman experiments were performed for a series of reaction temperatures, and used to determine the overall activation energy of the polymerization reaction. Since the Raman profiles give a direct measure of conversion versus time, the

rate of reaction was determined during the photopolymerizations. Finally, the Raman profiles were used in conjunction with previously determined photosensitization rate constants[1] to determine the kinetic constant for the propagation reaction. The resulting profiles for the propagation rate constants as functions of conversion provide important insight into the nature of the cationic photopolymerizations.

VI.2. Experimental

VI.2.1. Materials

In these studies, 3,6,9,12-tetraoxatetradeca-1,13-diene (DVE-3) (GAF Chemicals Corp.) was used as the monomer. The monomer was dried over molecular sieves to remove any traces of water. The initiator (UV9310C - GE Silicones) had a composition of 5-10 wt % linear alkylate dodecylbenzene, ~50 wt % 2-ethyl-1,3-hexanediol, and ~50 wt % bis(4-dodecylphenyl)iodoniumhexafluoroantimonate. Initiator concentrations specified in the remainder of this chapter correspond to the total UV9310C concentration. The anthracene photosensitizer (Aldrich Chemical Company) was used as purchased. The spectral region over which cationic initiators are effective may be expanded by the addition of a variety of photosensitizers.[2] These compounds make it possible to initiate the photopolymerization using near-UV or even visible wavelengths of light.[2-4] Therefore, a typical reaction system would contain ~1 wt % initiator (UV9310C) and ~10^{-2} wt % of photosensitizer in monomer (DVE-3).

VI.2.2. Raman Experiments

The photopolymerization kinetics were investigated by monitoring the Raman spectrum as a function of time. The Raman samples were excited with 250 mW of 496.5 nm light from a Coherent Innova 200 Argon ion laser. The photosensitization reaction was initiated with 363.8 nm light from a Coherent Innova 70 Argon ion laser. The initiation laser output of fifteen milliwatts (measured with a Scientech 362 Power/Energy meter) was attenuated with different optical density filters. Since the reaction is highly sensitive to the initiation intensity, the optical density filters were used to control the rate of the polymerization reaction. If the initiation power is two high, the reaction will thermally runaway causing the polymer to char and lose optical clarity. When the laser power is set too low, the reaction rate is much slower than typical industrial process conditions.

A Newport 845HP-01 Digital Shutter system was opened with an electric pulse from the detector controller, ensuring that the initiation beam and the acquisition were started simultaneously. Shuttering only the initiation beam allowed the Raman spectra to be collected before and after initiation of the polymerization reaction. This permitted dark cure rates to be obtained by terminating the initiation beam and following the reaction with the second (non-initiating) beam.

Both laser beams were focused on a quartz capillary tube placed perpendicular to the beam direction. Since the beams were focused to a small spot size, the alignment of the two beams was imperative to insure that both beams were sampling the same reaction

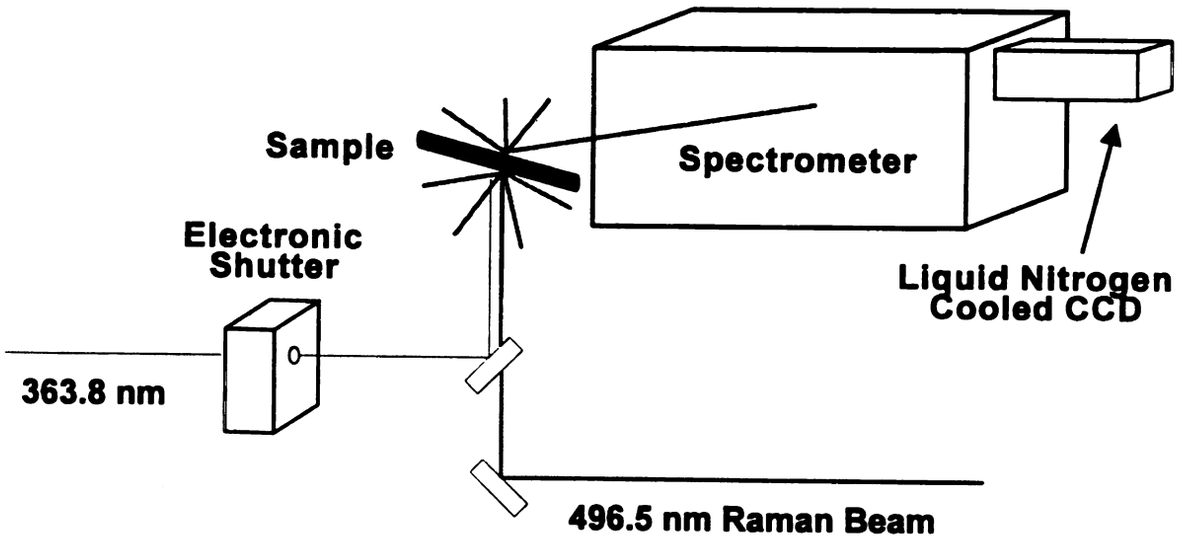

Figure VI.1. Experimental setup for Raman cure monitoring.

volume. The quartz capillary was approximately 1 inch in length with an inner diameter of 1 mm and an outer diameter of 2 mm. The Raman scatter was collected at an angle of 90° from the incident beam and 90° from the long axis of the quartz tube (see Figure VI.1.). The sample holder was jacketed with cooling water and the temperature was controlled with a circulating water bath.

The Raman signal was collected using a Spex 1877 Triplemate monochromator with a subtractive dispersion filter stage and a second spectrograph stage. The scattered light was passed though a depolarizer, placed before the monochromator, to remove any polarization effects on the signal intensity. A gated EG&G Princeton Applied Research Model 1530 C/CUV CCD, cooled to -120°C, to minimize dark current levels, was used to detect the signal. The data was analyzed with a OMA 4000 detector controller and software. A 1000 cm^{-1} wide Raman spectrum, centered at 535 nm, was collected with 600 gr/mm gratings in the filter stage and 1200 gr/mm in the spectrograph stage.

VI.3. Results and Discussion

VI.3.1. Raman Cure Monitoring

As mentioned in the background chapter, the major problem associated with Raman spectroscopy is the interference from molecule fluorescence. For our system, which contains a highly fluorescent probe (anthracene), the Raman spectrum must be outside the range of the anthracene photosensitizer fluorescence. Anthracene fluorescence is centered at ~ 425 nm and is essentially zero by 500 nm. In addition, the

Raman cross-section is related to the 4th power of the incident light energy.[5] Therefore, the lowest wavelength (highest energy) outside the anthracene fluorescence (496.5 nm) was chosen as the scattering beam. Furthermore, our instrumental setup (gratings and detector) is most sensitive for wavelengths in the 500 nm range.

To monitor the reaction kinetics, the peaks in the Raman spectrum which correspond to the reactive double bonds were identified. In addition, a peak whose intensity is independent of cure was selected as an internal standard. The three major peaks in Figure VI.2. were identified by comparison with known compounds of similar composition.[6,7] The sharp peak at 1322 cm^{-1} corresponds to the C-H bending of the hydrogens attached to a vinyl carbon. The two peaks at 1458 cm^{-1} and 1469 cm^{-1} represent the wagging and bending of the ethyl-ether hydrogens (O-C**H$_2$**-C**H$_2$**-O), respectively. Both of these peaks should remain relatively unchanged during the polymerization reaction, since they represent unreactive sections of the monomer molecule. Finally, the doublet at 1622 cm^{-1} and 1636 cm^{-1} represents the C=C stretching of the vinyl ether bonds. The 1622 cm^{-1} peak results from the trans configuration of the vinyl ether bond as shown in Figure VI.3. The 1636 cm^{-1} peak represents the cis isomer of the vinyl ether bond. The cis isomer has slightly more steric hindrance than the trans conformation, resulting in the lower Raman intensity.

When the initiation beam is blocked and a Raman spectrum is collected no reaction is seen. However, if the sample is exposed to the initiation beam the reaction proceeds to completion in a few seconds depending upon the reaction conditions. This indicates that no thermal initiation is occurring. If the power of the Raman scattering beam is increased to 500 mW, thermal initiation will occur when the laser beam is

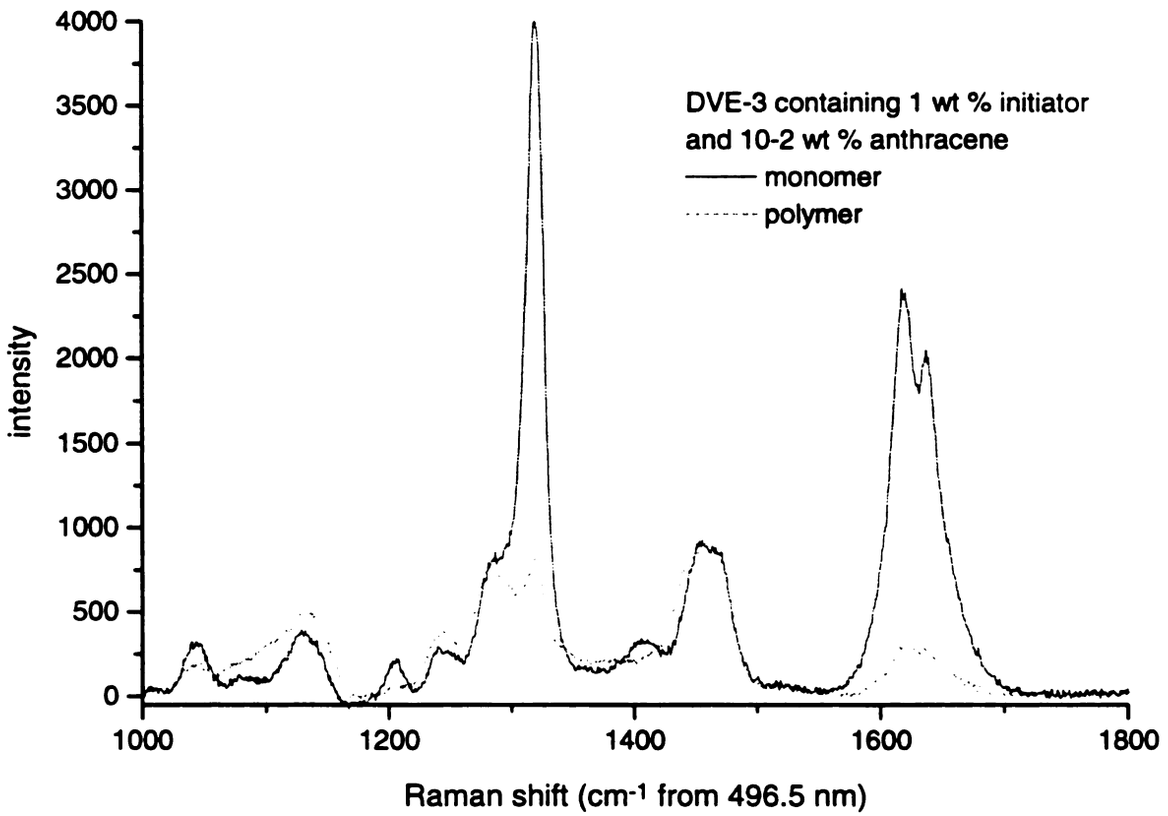

Figure VI.2. *Raman spectra of DVE-3 before and after cationic photopolymerization.*

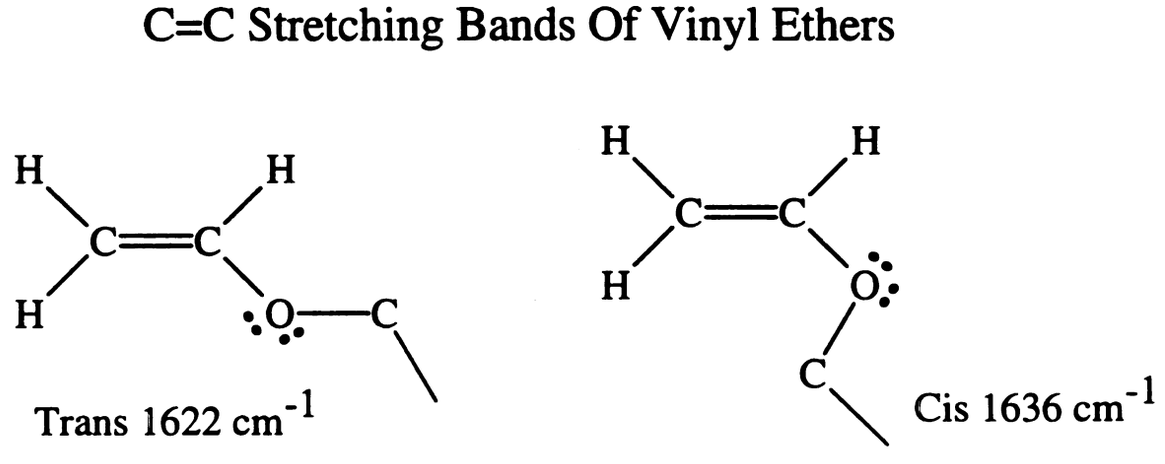

Figure VI.3. *Cis and Trans isomers which result in the ~1630 cm^{-1} doublet in the monomer Raman spectrum.*

allowed to illuminate the sample for approximately 2-3 minutes. Figure VI.2. compares the DVE-3 Raman spectra of monomer and polymer, after isothermal cationic photopolymerization at 25°C. The relative intensities of the 1630 cm^{-1} doublet versus the 1458 cm^{-1} peak indicates the conversion of double bonds. Furthermore, increases in the peaks at 1133 cm^{-1} and 1282 cm^{-1} correspond to the production of polymer. Since the Raman intensity is proportional to the double bond concentration, monitoring either the 1322 or 1622 cm^{-1} peaks versus the 1458 cm^{-1} peak provides a direct measure of conversion.

Figure VI.4. shows 60 Raman spectra collected at intervals of 0.792 seconds for a duration of 50 seconds *in situ* during the cationic photopolymerization of DVE-3 with 1 wt % initiator and 10^{-2} wt % anthracene photosensitizer. The temperature of the reaction was controlled at 20°C using the jacketed sample holder. As expected, the ~1630 cm^{-1} doublet and the 1322 cm^{-1} peak decrease as the reaction proceeds. Moreover, the 1458 cm^{-1} band remains relatively unchanged during the reaction, further indicating the conversion of monomer to polymer. As demonstrated in Figure VI.4., the Raman monitoring technique allows a complete spectrum (1000 cm^{-1}) to be monitored *in situ*. This provided a much more detailed reaction profile than can be achieved by monitoring a single wavelength during the reaction.

Using the initial 1322 cm^{-1} peak intensity, the double bond conversion can be calculated for each spectra as the reaction proceeds. Figure VI.5. is a plot of double bond conversion versus time for the same polymerization reaction shown in Figure VI.4. In this experiment, Figure VI.5. indicates that the conversion starts initially slow and increases as the reaction proceeds, reaching a maximum conversion of ~ 70 percent. The

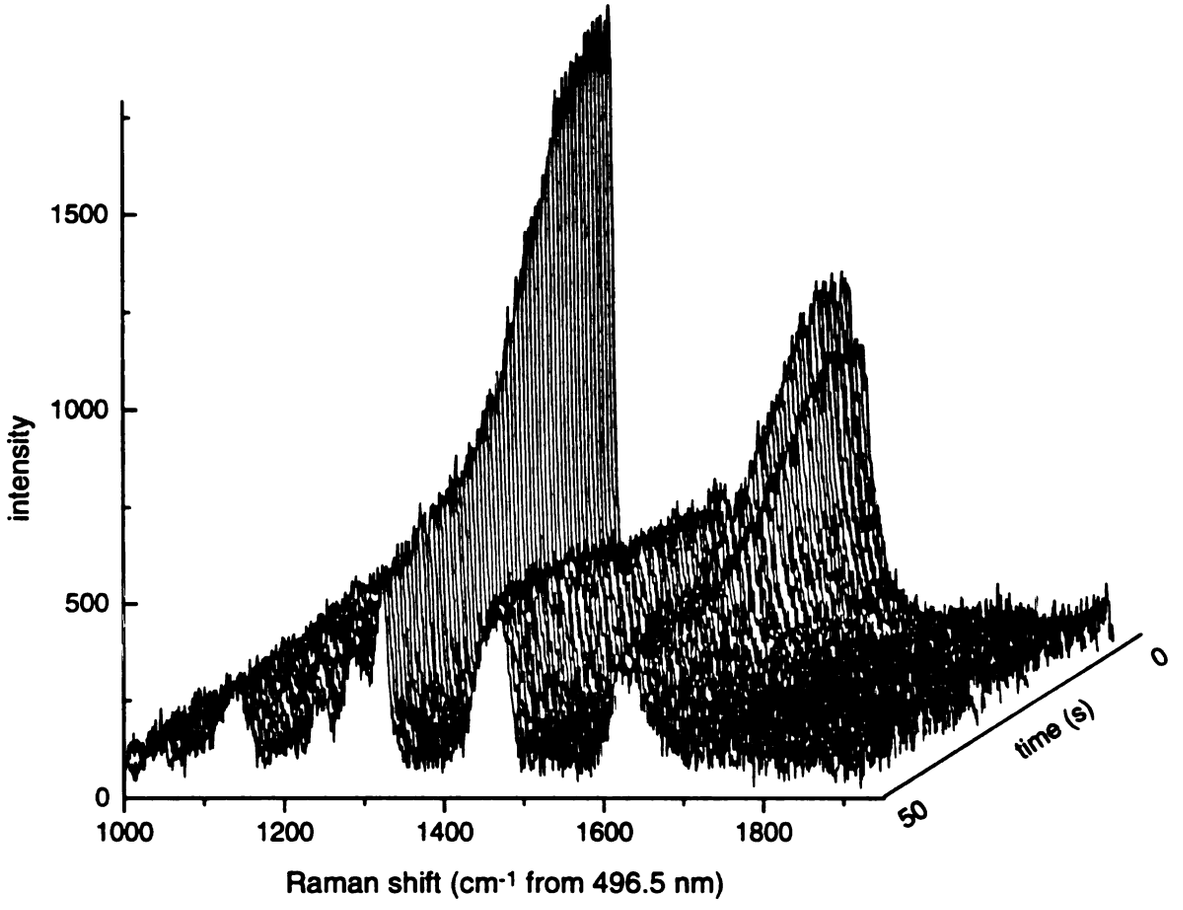

Figure VI.4. *Raman spectra during a cationic photopolymerization of DVE-3 with 1 wt % initiator and 10^{-2} wt % anthracene.*

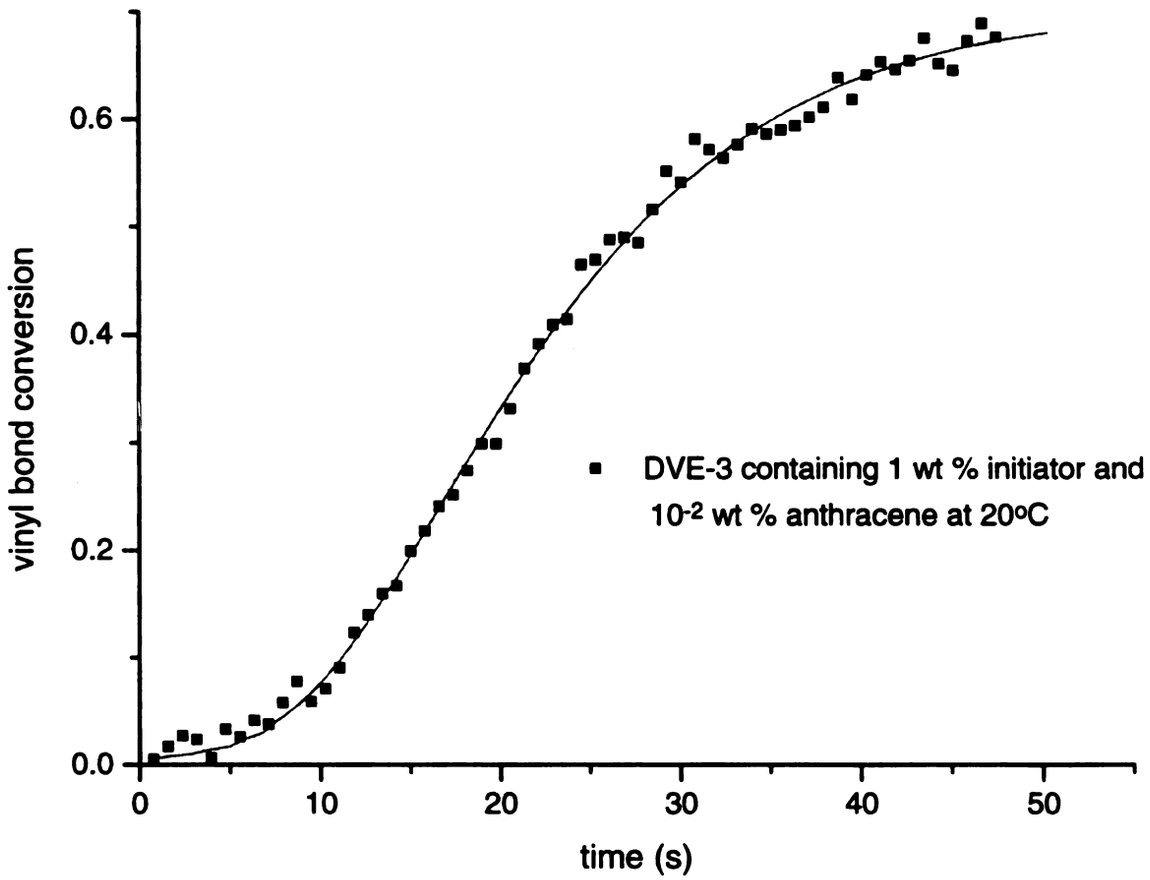

Figure VI.5. *Double bond conversion during a cationic photopolymerization of DVE-3 calculated from the 1322 cm^{-1} Raman band.*

Raman monitoring studies indicated that the final conversion value for the cationic photopolymerization of DVE-3 is dependent on the rate of the reaction. The final conversions were found to range from 60 to 85 percent when the temperature of the reaction is varied from 20 to 50 °C.

As described in Chapter IV., a fluorescence monitoring technique was developed that followed the anthracene photosensitizer fluorescence as the reaction proceeds.[1] Since the fluorescence technique monitors the production of active centers directly and the polymerization reaction indirectly, the Raman technique should verify the ability of the fluorescence technique to monitor cure profiles. Figure VI.6. shows the relationship between the fluorescence and Raman monitoring techniques. The two curves represent the same sample mixture run at the same experiment conditions (initiation intensity, temperature, integration time, sample rate, etc.). The decrease in photosensitizer fluorescence intensity corresponds to the production of active centers and therefore an increase in the rate of the polymerization reaction.

The Raman curve shown in Figure VI.6. follows the intensity of the 1322 cm^{-1} peak during the photopolymerization reaction. As can be seen from Figure VI.6. , the two techniques show good agreement in the rate of reaction as indicated by the decrease in signals at the same reaction time. This comparison helps to validated the fluorescence monitoring method for determining cure profiles. Moreover by using both of the techniques, the rate of propagation and initiation can be measured directly during these high speed reactions and used to determine the rate constants for the reaction.

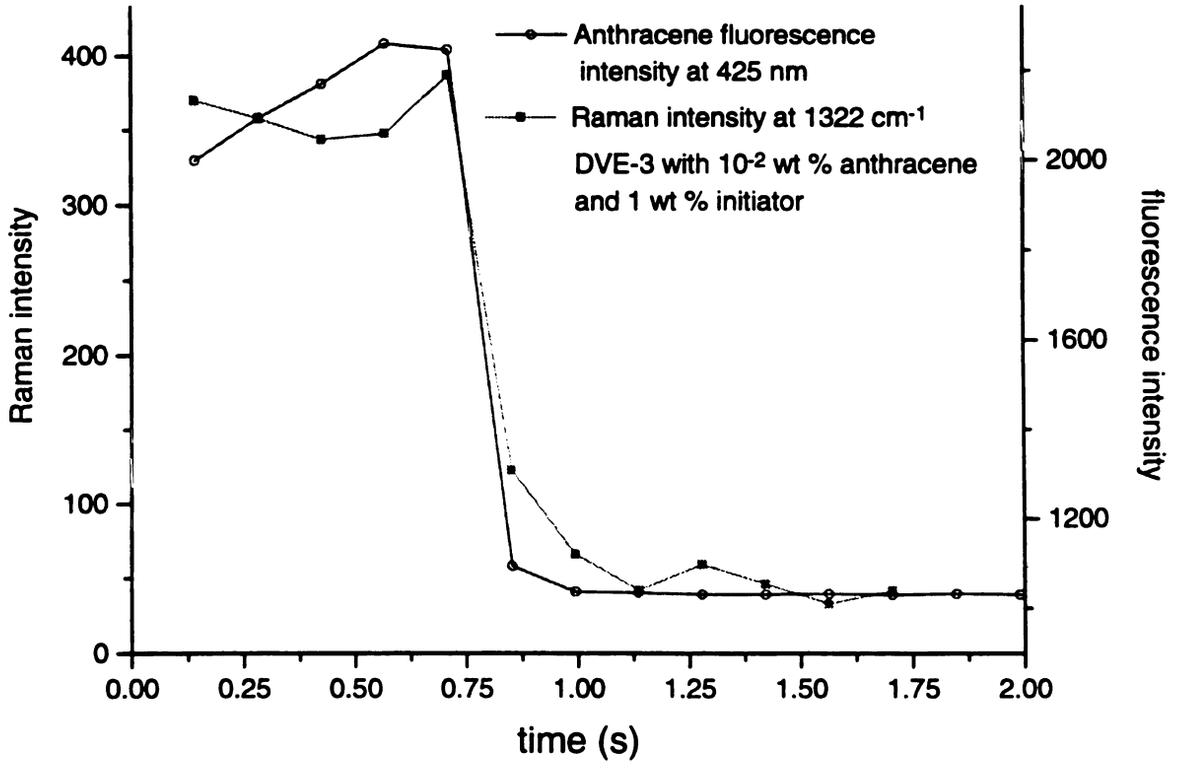

Figure VI.6. *Comparison of fluorescence and Raman monitoring techniques.*

VI.3.2. Effect of Light Intensity

As mentioned, the Raman monitoring studies have indicated that the final conversion value for the cationic photopolymerization of DVE-3 is dependent on the rate of the reaction. Experiments were run at many different excitation intensities to determine the effect of light intensity on the reaction profile. In order to increase the stability of the laser output, the 363.8 nm laser beam was attenuated with a neutral density filter instead of adjusting the laser power. The excitation intensity was measured with the power meter directly before the lens used to focus the beam in to the sample. A range of optical densities form 0.1 to 3.0 were used to adjust the light intensity.

The light intensity studies indicated that the rate of reaction for the cationic photo-polymerization of DVE-3 photosensitized by anthracene is extremely sensitive to the excitation intensity. Reactions performed at different intensities ranged from under 1 sec to several minutes to reach the final conversion. Optical densities under 0.5 displayed reaction rates that resulted in extreme temperatures and degradation of the polymer. In this case, the polymer loses optical clarity and the Raman spectra changes drastically. The final conversion can not be determined since all the Raman peaks are lost including the internal standard. If optical densities greater than 3.0 were used to attenuate the laser beam, the reaction rate was too slow to compare with reaction rates needed for most applications. Therefore, neutral density filters between 1.0 and 3.0 were used to produce reaction rates which were able to be maintained isothermal and easily monitored by the Raman system.

VI.3.3. Effect of Temperature

Isothermal reactions were performed at a series of temperatures between 20 and 50 °C to determine an overall activation energy for the polymerization reaction. A maximum temperature of 50 °C was used to ensure that no thermal initiation occurred during the photopolymerization. An average initial reaction rate was determined for each temperature by measuring the time required to reach a specific conversion. A conversions of 20 percent were chosen, and the activation energy was determined from an Arrhenius fit to the data.

Figure VI.7. shows Raman conversion profiles for the cationic polymerization of DVE-3 photosensitized with 1.0 x 10^{-2} wt % anthracene and 1 wt % initiator controlled at temperatures form 20 to 50°C. As expected the reaction rate and the total conversion increased with increasing temperature. Based upon an Arrhenius fit, the overall activation energy (E_R) for the cationic polymerization was determined to be 25.1 ± 6.1 kJ/mol at 20 percent conversion. Since the Raman method measures the overall reaction rate, these values represent an overall activation energy which includes initiation, propagation, and termination.

$$E_R = E_P + E_I - E_T \qquad \text{Eq. 1.}$$

For equation 1 to be valid, the active center production must continue throughout the reaction. Based upon previous measurements of the kinetic constants for photosensitization,[8] the photosensitizer is only approximately 40 percent consumed at 20 percent conversion for each temperature. Therefore, active centers should be produced

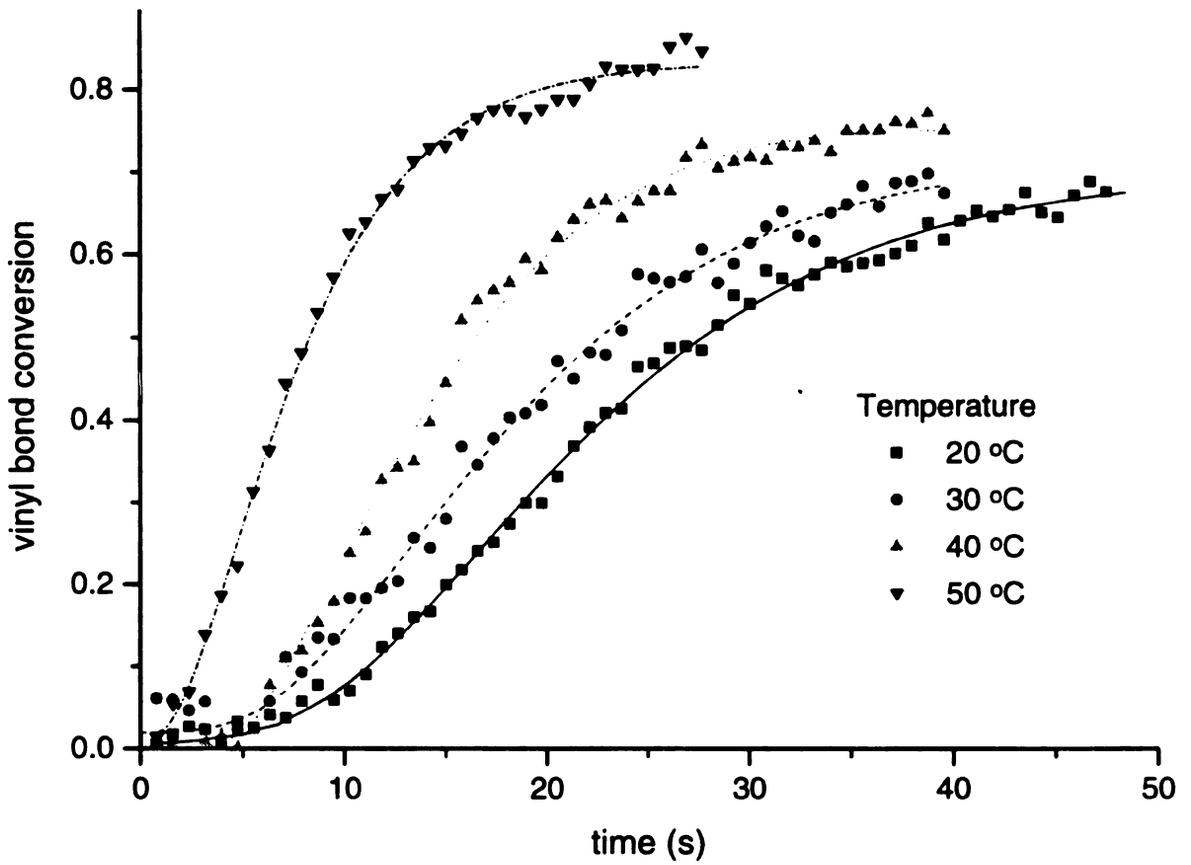

Figure VI.7. *Raman conversion profiles for isothermal reactions ranging from 20 to 50 °C.*

throughout the photopolymerization reaction for all temperatures. The activation energy determined from Raman spectroscopy also agreed well with the activation energy determined from Photo-Differential Scanning Calorimetry (PDSC) studies (E_R = 26.5 ± 3.2kJ/mol).[9]

VI.3.4 Initiation Rate Constant

In these photopolymerizations, active cationic centers are produced through a photosensitization reaction in which an electron is transferred from an excited state anthracene molecule to the initiator.[8] Although the reaction proceeds by a multi-step photochemical mechanism,[8] the rate of generation of active centers may be described by the following simple expression:

$$\text{Rate of active center generation} = k_i[A][I] \qquad \text{Eq. 2.}$$

where $[A]$ is the anthracene concentration, $[I]$ is the initiator concentration, and k_i is an initiation rate constant which accounts for a number of photophysical steps including excitation, intersystem crossing, exciplex formation, and electron transfer.[8] According to this convention, k_i is dependent on the incident light intensity, and must be adjusted for each initiation intensity. In our reactions, the initiator (diaryliodonium salt) concentration greatly exceeds the anthracene concentration and can be assumed to be constant during the reaction.[8] Therefore a pseudo-first-order kinetic constant, $k_i^* = k_i[I]$, may be used to describe the rate of generation of active centers. The above analysis is based upon the assumptions that one active center is produced per anthracene and initiator molecules[10,11]

and that all reactive centers are capable of propagating the reaction, as indicated by previous fluorescence measurements.[1]

The overall rate of change of the active center concentration may be derived by combining the rate of generation by photosensitization with the rate of consumption by termination:

$$\frac{d[M^+]}{dt} = k_i^*[A] - k_t[M^+] \qquad \text{Eq. 3.}$$

This equation may be integrated (with the initial condition $[M_0^+] = 0$ and the exponentially decreasing anthracene concentration) to yield the following equation:

$$[M^+] = [A_0]\frac{k_i^*}{k_t - k_i^*}(e^{-k_i^* t} - e^{-k_t t}) \qquad \text{Eq. 4.}$$

In this equation, the termination rate constant, k_t was determined in earlier work.[9] The initiation rate constant, k_i was determined from solving the photophysical rate expressions, using the initiation intensity and the anthracene absorption coefficient as described elsewhere.[8] For the Raman experiments, the incident light intensity used in this calculation was determined by measuring the power of the initiation laser beam (363.8 nm). Using the incident light intensity value and the cross sectional area of the laser beam, k_i^* was determined to be 6.21 x 10^{-2} s^{-1} at 25 C by solving the corresponding set of rate expressions.[8]

The activation energy for the photosensitization reaction was determined from fluorescence measurements of the photosensitization reaction between anthracene and the diaryliodonium salt. As previously described, the rate constant, k_i^*, was determined for several different temperatures and fit to an Arrhenius equation to yield an average

activation energy, E_I, of 28.5 ± 1.6 kJ/mol. Using this activation energy, the temperature-dependence of k_i^* was described. Based upon the values of k_t, k_i^*, E_I, and A_0, equation 4 was used to obtain profiles of the active center ($[M^+]$) concentration as a function of time for each of the Raman reactions.

VI.3.5 Propagation Rate Constant

As previously mentioned, the instantaneous conversion can be determined with the Raman technique, since the vinyl bond conversion as a function of time is measured directly. The conversion profile was obtained by setting the initial Raman spectra equal to zero conversion and calculating conversion for each of the following time slices. The rate of polymerization (R_p) can be determined from the derivative of the conversion profile. As shown in Figure VI.7., the conversion data was fit with a triple exponential expression. Since noise in the actual data can cause large variations in the derivative, the exponential fit of the conversion profile was used to calculate the rate of polymerization.

According to kinetic analysis, the rate of propagation is given by a propagation rate constant multiplied by the active center concentration and the monomer concentration as shown below:

$$R_p = \frac{d[M]}{dt} = k_p[M][M^+] = [A_0]\frac{k_p k_i^*}{k_t - k_i^*}(e^{-k_i^* t} - e^{-k_t t})[M] \qquad \text{Eq. 5.}$$

If a number of propagation centers with different reactivities exists, this equation may be used to fit the polymerization data to yield an apparent propagation constant that comprises all types of propagating centers (e.g. ion pairs, separated ions, etc.).[9] In this

chapter, this approach will be used to interpret changes in the value of the apparent propagation constant, k_p.

The instantaneous vinyl bond concentration ([M]) can be calculated from the Raman conversion profile and the initial vinyl bond concentration using the following equation:

$$[M] = [M_0] \times (1 - \text{fractional conversion}) \qquad \text{Eq. 6.}$$

Equation 6 gives the vinyl bond concentration in mol/l of vinyl bond, since [M] represents mols of double bonds per liter. Figure VI.8. verifies the importance of temperature during the cationic photopolymerization of DVE-3, as characterized by the increase in conversion and rate of the reaction with temperature.

Profiles of the rate of polymerization (propagation) plotted versus vinyl bond conversion obtained by using equations 6 are shown in Figure VI.9. The figure illustrates that as the temperature is increased the maximum value of R_p increase accordingly. As the reaction takes place, the value of R_p increases to a maximum and then decreases with further vinyl bond conversion. Figure VI.9. also demonstrated that as the rate of reaction increases with increasing temperature, the limiting conversion for the cationic photopolymerization also increases. This indicates that the final conversion of the reaction is a function of the rate of the reaction. Finally, the values for R_p determined from Raman spectroscopy agrees very well the values determined by the PDSC technique.[9]

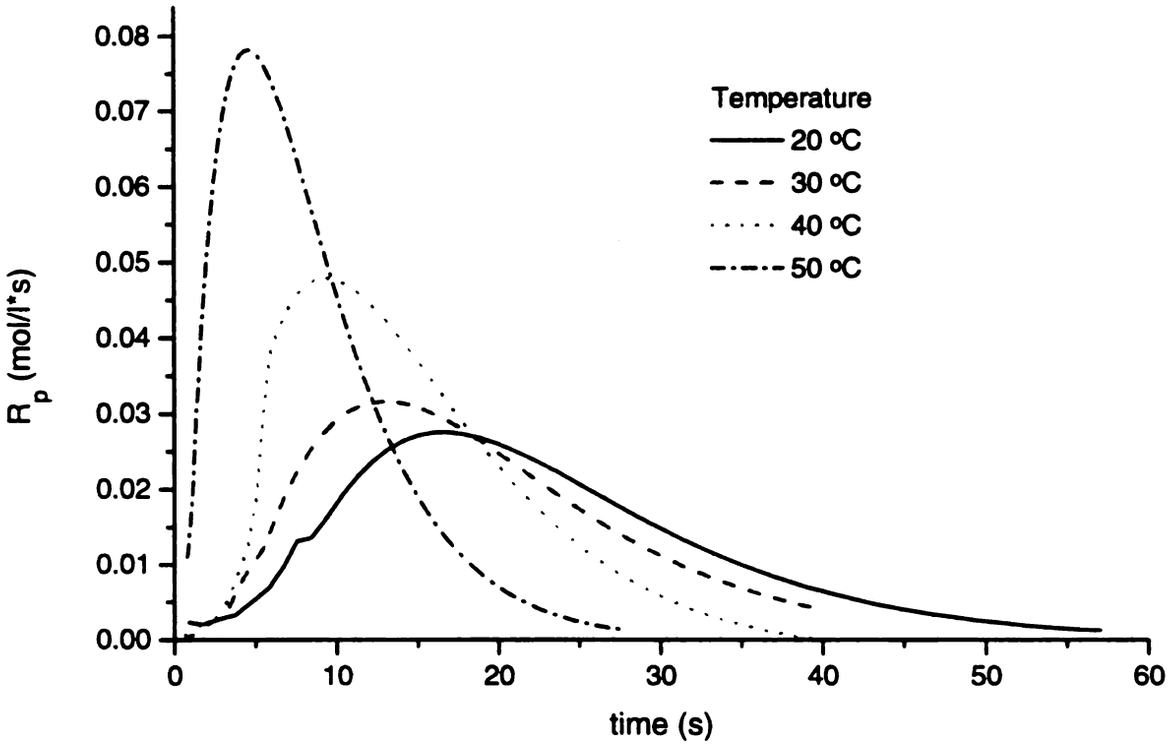

Figure VI.8. *Rate of reaction for several different temperatures versus time for a cationic photopolymerization of DVE-3 with 1 wt % initiator and 10^{-2} wt % anthracene.*

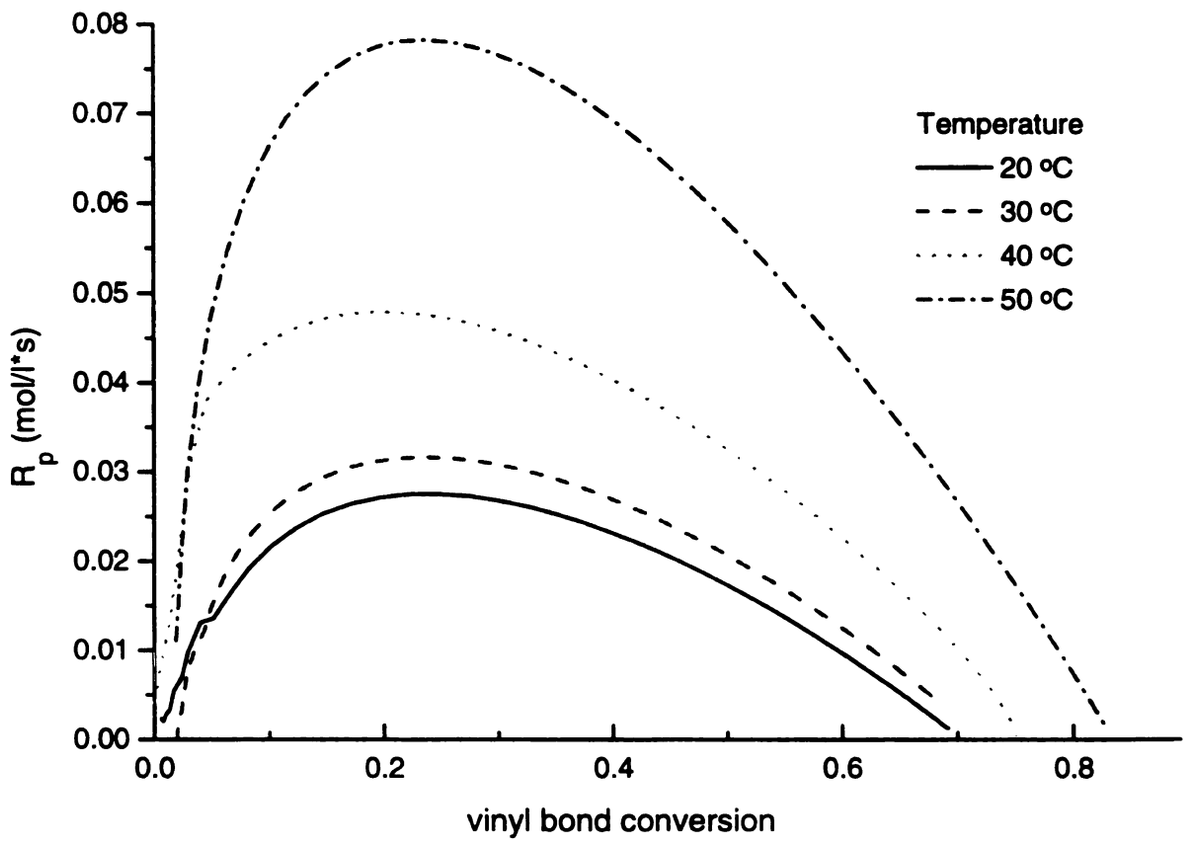

Figure VI.9. *Overall rate of propagation versus conversion for DVE-3 photosensitized with 10^{-2} wt % anthracene and 1 wt % initiator.*

For each Raman experiment, a profile of the quantity $k_p[M^+]$ may be obtained using the empirical profiles of R_p and $[M]$. Based only of the Raman data, this product may be determined using the following version of equation 5.

$$k_p[M^+] = \frac{R_p}{[M]} \qquad \text{Eq. 7.}$$

Profiles of $k_p[M^+]$ obtained in this manner are shown in Figure VI.10. As shown in the figure, $k_p[M^+]$ initially increases sharply, and then levels off at a plateau value between 0.001 and 0.01 s^{-1} depending upon the reaction temperature (as temperature is increased a higher value of $k_p[M^+]$ is observed). Finally, the value of $k_p[M^+]$ decreases as a limiting conversion is reached. The shape of the profiles in Figure VI.10. indicates that the apparent propagation rate constant k_p changes as the reaction proceeds. If k_p remained constant throughout the reaction, the change in $k_p[M^+]$would be governed by the active center concentration. Therefore, the $k_p[M^+]$ value would increase monotonically until it reached a maximum when all of the photosensitizer is consumed.

More information about the behavior of k_p may be obtained by coupling the Raman data with the k_i^* and k_t values discussed previously. Profiles of the apparent propagation rate constant, k_p were obtained by substituting the values of $[A_0]$, k_i^*, and k_t along with the empirically determined profiles of $[M]$ and R_p into equation 5. Figure VI.11. shows k_p as a function of reaction conversion. The curves exhibit a similar characteristic shape to the $k_p[M^+]$ profiles of Figure VI.10., although the plateau value is much higher due to the small active center concentration. The similarity in shape indicates that relative changes in k_p are much larger than those for $[M^+]$. The final

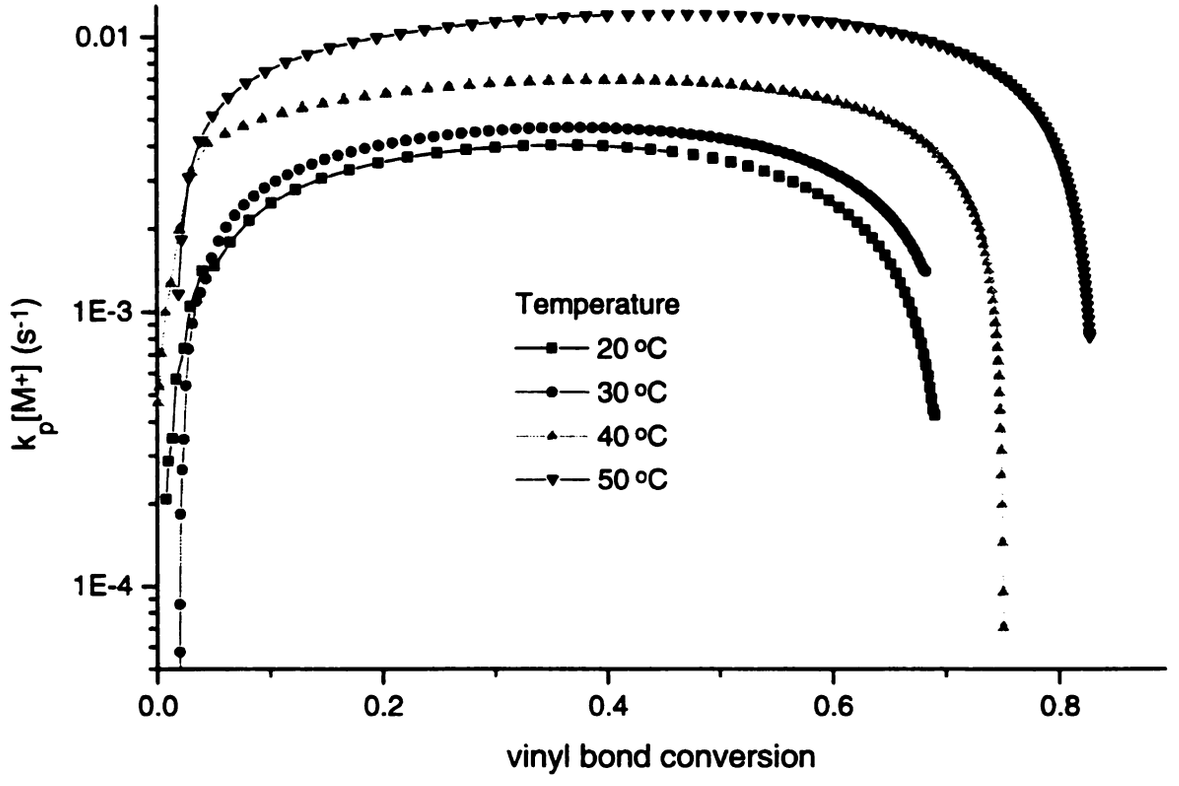

Figure VI.10. *$k_p[M^+]$ versus conversion for the cationic photopolymerization of DVE-3 at temperatures ranging from 20 to 50 °C.*

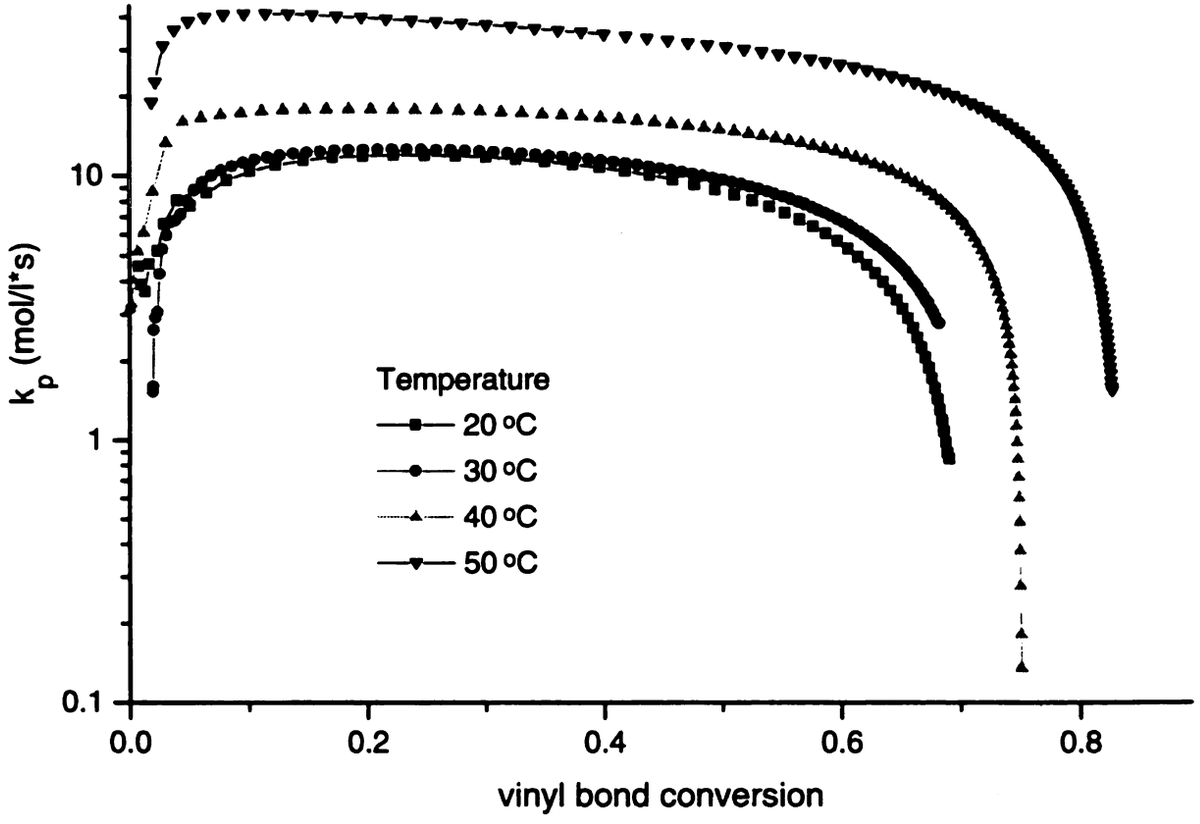

Figure VI.11. *k_p versus conversion of the photopolymerization of DVE-3 at various temperatures.*

magnitude obtained for k_p values were between 10 and 40 l/mol*s, which also compare very satisfactorily with values from the PDSC data (5-30 l/mol*s).[9]

As described in a previous contribution,[9] a possible explanation for the initial large increase in the apparent rate constant for propagation is a change in the reactivity of the carbocation species due to the proximity of the counterion. In this stage of the reaction, polymerization leads to a large local increase in viscosity which reduces diffusional mobility. However, the active carbocation retains considerable mobility by propagating with double bonds of different monomer units. This type of mobility of the active center has been termed "reaction diffusion." In contrast, since the counterion cannot undergo similar diffusion, the large hexafluoroantimonate counterion experiences a decrease in mobility as the viscosity increases. During this process, the counterion and carbocation may become separated and since separated ions are orders of magnitude more reactive than ion pairs,[12] the apparent value of k_p increases dramatically during the early stages of the reaction. This type of "reaction diffusion" is well known for free radical systems[13,14] and may aid in explaining the shape of the curves in Figures VI.10. and VI.11. The final decrease in k_p arises from active center trapping during these highly crosslinked polymerizations. A limiting conversion at which the reaction ceases is observed despite the presence of active centers. Similar profiles were obtained with the PDSC technique giving an independent verification of the two techniques. As previously mentioned, the above analysis is based upon the assumptions that one active center is produced per anthracene and initiator molecules[10,11] and that all reactive centers are capable of propagating the reaction.[1]

VI.4. Conclusions

In this contribution Raman spectroscopy was used to monitor cationic photo-polymerizations of a divinyl ether. Using the Raman technique a complete spectra of approximately 1000 cm^{-1} can be monitoring *in situ* during the cationic photo-polymerization. Since molecular vibrations associated with the vinyl bonds are measured, the Raman technique offers a direct method for monitoring vinyl bond conversion during a polymerization reaction. The conversion profiles provided by the Raman technique were used to characterize the reaction kinetics and evaluate polymerization rate constants.

The Raman experiments were used to determine kinetic constants for a series of unsteady-state divinyl ether polymerizations at different temperatures and light exposure intensities. The kinetic constant for propagation was obtained from the Raman experiments in conjunction with previously determined photosensitization rate constants. As expected, an increase in the initiating light intensity or an increase in the reaction temperature resulted in an increased reaction rate. This increase in reaction rate was found to result in higher final conversions for the cationic photopolymerization.

An apparent propagation rate constant that comprises all types of propagating centers (e.g. ion pairs, separated ions, etc.) with different reactivities was determined from the Raman reaction profiles. The apparent propagation constant, k_p, initially increases sharply, and then levels off at a plateau value (as temperature is increased a higher value of k_p is observed). Finally, the value of k_p decreases as a limiting conversion

is reached. This profile shape indicates that the apparent propagation rate constant k_p changes greatly as the reaction proceeds. The initial large increase in the apparent rate constant for propagation may be explained by a change in the reactivity of the carbocation species due to the proximity of the counterion. During the polymerization, the counterion and active carbocation become separated due to a decrease in mobility of the large hexafluoroantimonate counterion as the system viscosity increases. Since separated ions are orders of magnitude more reactive than ion pairs,[1] the apparent value of k_p increases dramatically during the early stages of the reaction. The final decrease in k_p arises from active center trapping during these highly crosslinked polymerizations. Therefore a limiting conversion at which the reaction ceases is observed despite the presence of active centers.

The Raman conversion profiles for propagation were compared with Photo-Differential Scanning Calorimetry profiles from earlier experiments. The two techniques displayed good agreement for the overall activation energy and the propagation rate constant, k_p, verifying the data obtained by each techniques. The profiles of propagation as functions of conversion provide important insight into the nature of these high-speed cationic photopolymerizations. Understanding the kinetics of these cationic photo-polymerizations is important due to the increasing number of applications for rapid, solvent-free curing of polymer films.

VI.5. List of References

1. E. W. Nelson, T. P. Carter, A. B. Scranton, "Fluorescence Monitoring of Cationic Photopolymerizations: Divinyl Ethers Photosensitized by Anthracene Derivatives," *Macromolecules*, **27**,1013 (1994).

2. J.V. Crivello, "Cationic Polymerization -- Iodonium and Sulfonium Salt Photoinitiators," *Adv. Polym. Sci.*, **62**, 1 (1984).

3. W.R. Watt, "Photosensitized Epoxides as a Basis for Light-Curable Coatings," *Epoxy Resin Chemistry*, R.S. Bauer, Ed., ACS Symposium Series, Vol. 114, American Chemical Society, Washington D.C., 17, (1979).

4. J.V. Crivello *Organic Coatings, Science and Technology*, G.D. Parfitt and A.V. Patsis, Ed., Dekker, New York, **5**, 35, (1983).

5. P.C. Painter, M.M. Coleman, and J.L. Koeing, *The Theory of Vibrational Spectroscopy and its Applications to Polymeric Materials*, John Wiley & Sons, New York, 1982.

6. H.W. Siesler, K. Holland-Moritz, *Infrared and Raman Spectroscopy of Polymers*, Practical Spectroscopy Series, Marcel Dekker, Inc.: New York, NY, Vol. 4, 1980.

7. R.M. Silverstein, G.C. Bassler, and T.C. Morrill, *Spectrometric Identification of Organic Compounds*, 5^{TH} ed., John Wiley & Sons Inc., NY, 113, 1991.

8. E.W. Nelson, T.P. Carter and A.B. Scranton, "The Role of the Triplet State in the Photosensitization of Cationic Polymerizations by Anthracene," *J. Polym. Sci; Part A: Polym. Chem.*, **33**, 247-256 (1995).

9. E.W. Nelson, J.L. Jacobs, A.B. Scranton, K.S. Anseth, and C.N. Bowman, "Photo-differential Scanning Calorimetry Studies of Cationic Polymerizations of Divinyl Ethers," *Polymer*, in press.

10. J. L. Dektar, and N.P. Hacker, "Photochemistry of Diaryliodonium," *J. Org. Chem.*, **55**, 639-647, (1990).

11. R. J. DeVoe, M. R. Sahyun, E. Schmidt, N. Serpone, and D. K. Sharma, "Electron Transfer Sensitized Photolysis of 'onium Salts," *Can. J. Chem.* **66**, 319 (1988).

12. J. P. Kennedy and E. Marechal *Carbocationic Polymerization*, John Wiley & Son, New York, 1982.

13. K. S. Anseth, C. M. Wang and C. N. Bowman, "Kinetic Evidence of Reaction Diffusion during the Polymerization of Multi(meth)acrylate Monomers," *Macromolecules*, **27**, 650 (1994).

14. K. S. Anseth and C. N. Bowman, "Reaction Diffusion Enhanced Termination in Polymerizations of Multifunctional Monomers," *Polymer Reaction Engineering*, **1(4)**, 499-520, (1992-93).

CHAPTER VII. *IN SITU* PHOTO-DIFFERENTIAL SCANNING CALORIMETRY: CURE MONITORING AND KINETICS

VII.1. Introduction

Photo-differential scanning calorimetry (PDSC) experiments were used to determine effective kinetic constants for propagation and termination for a series of unsteady-state divinyl ether polymerizations at different temperatures and light intensities. For these cationic photopolymerizations the reaction rate and limiting conversion were both found to increase as the reaction temperature was increased. At all temperatures the profile for the propagation rate constant, k_p, exhibited a dramatic increase at the start of the reaction, plateaued at a value between 5 and 30 l/mol*s (depending upon temperature), and then decreased as the reaction reached a limiting conversion due to trapping of the active centers. The effective termination rate constant, k_t, was very low, with active center lifetimes approaching twenty minutes. Finally, the overall activation energy for polymerization was found to be 26.5 ± 3.2 kJ/mol.

Photo-differential scanning calorimetry (PDSC) offers a simple method to characterize the kinetics of photopolymerization reactions. Because the polymerizations are highly exothermic, the reaction rate may be measured by monitoring the rate at which heat is released from the polymerizing sample. Therefore, the profiles of reaction heat

versus time provided by PDSC may be used to characterize the reaction kinetics and evaluate polymerization rate constants.[1] Several authors have used PDSC to characterize free radical photopolymerizations[1-5] however application of the technique to cationic photopolymerizations of divinyl ethers is more problematic. First, the polymerizations of divinyl ethers proceed very rapidly, and care must be taken to ensure that the reaction rate does not exceed the time resolution of the instrument. Since the DSC response time is on the order of 2-3 seconds,[6,7] relatively low light intensities must be used to increase the reaction time for the divinyl ether photopolymerizations.[8] Second, photopolymerizations of divinyl ethers are highly exothermic, therefore to maintain isothermal conditions during the reactions very small sample sizes must be used (0.5 - 1.5 mg). If larger sample sizes are used, the heat evolved during the reaction generally cannot be removed on the time scale of the reaction.

A series of PDSC experiments were performed on cationic photopolymerizations of a divinyl ether initiated with a diaryliodonium hexafluoroantimonate salt photosensitized by anthracene. Isothermal PDSC experiments were performed for a series of reaction temperatures and light intensities. The profiles were used in conjunction with previously determined photosensitization rate constants[9] to determine the kinetic constant for propagation. The kinetic constant for termination was determined from a series of unsteady-state "dark-cure" reactions at different temperatures and light exposure times. The resulting profiles for the propagation and termination rate constants as functions of conversion provide important insight into the nature of the cationic photopolymerizations.

VII.2. Experimental

VII.2.1. Materials

In these studies, 3,6,9,12-tetraoxatetradeca-1,13-diene (DVE-3) (ISP) was used as the monomer. The monomer was dried over molecular sieves to remove any traces of water. As in previous spectroscopic studies,[9,10] a commercially available initiator (UV9310C - GE Silicones) was used. The initiator formulation includes 5-10 wt % linear alkylate dodecylbenzene, ~50 wt % 2-ethyl-1,3-hexanediol, and ~50 wt % bis-(4-dodecylphenyl) iodoniumhexafluoroantimonate. Initiator concentrations specified in the remainder of this chapter correspond to the total UV9310C concentration. The photosensitizer, anthracene, was purchased from Aldrich Chemical Company and was used as received. A representative reaction sample contained 10^{-2} wt % anthracene and 1 wt % initiator in DVE-3.

VII.2.2. PDSC Experiments

The PDSC experiments were conducted using a differential scanning calorimeter equipped with a photocalorimetric accessory (Perkin Elmer, DSC-DPA 7). The photocalorimeter accessory included transfer optics to produce full beam ultraviolet light of varying intensity and a monochromator to produce light of a given wavelength. The initiation light source was a 100 watt mercury arc lamp used in conjunction with neutral

density filters (Melles Griot) to control the intensity of the incident light. The strong mercury line at 365 nm was used to excite the anthracene photosensitizer. The polymerization reactions were run isothermally by means of a refrigerated recirculating chiller (NESLAB, CFT-25) maintained at 5 °C. Small sample sizes (0.5 - 1.5 mg) were required in order to limit the total heat released during the polymerization reaction so that isothermal conditions could be maintained. The samples were placed in uncovered aluminum DSC pans and cured with UV light intensities varying from 0.4-1.6 mW/cm^2 at various reaction temperatures.

VII.3. Results and Discussion

VII.3.1. Effect of Light Intensity

Experiments were performed at several different excitation intensities in order to determine the effect of light intensity on the reaction profiles. The light intensity at 365 nm was adjusted by placing a neutral density filter after the excitation monochromator. A range of optical densities from 0.5 to 2.0 were required to adjust the light intensity. At optical densities less than 0.5, the reaction proceeded very rapidly which prevented isothermal conditions. Optical densities greater than 2.0 resulted in very slow reactions limiting the number of reactions that could be completed in a reasonable time.

Figure VII.1. shows the relationship of reaction rate and light intensity. As expected, an increase in the initiating light intensity resulted in an increased reaction rate

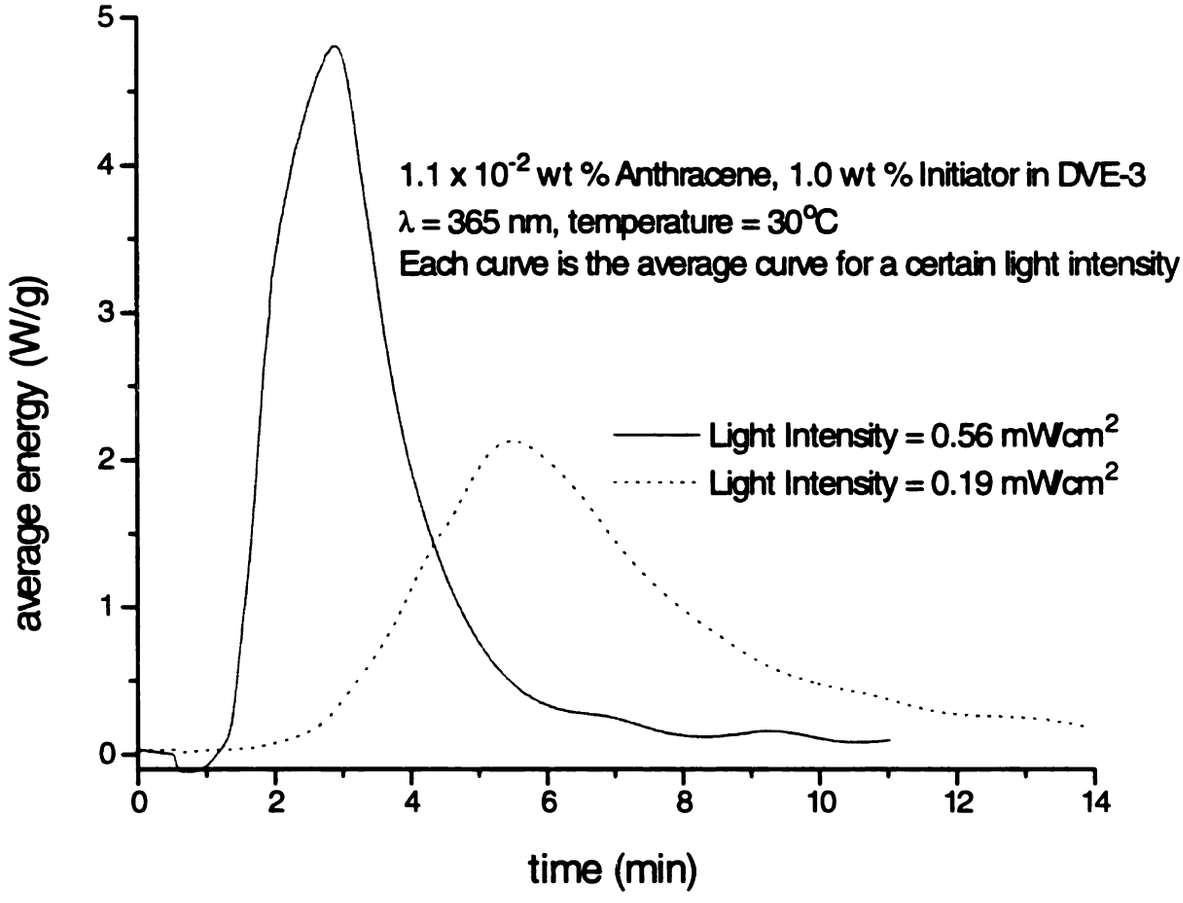

Figure VII.1. *PDSC exotherms for the cationic polymerization of DVE-3 at different light intensity values.*

as indicated by the exotherm reaching its maximum more rapidly. For example, at 0.56 mW/cm^2 the heat flux reached the maximum at 2.5 ± 0.7 minutes with an average peak area of 660 ± 59 J/g, while for initiating intensities of 0.19 mW/cm^2 the maximum was reached at 5.4 ± 0.7 minutes and had an average area of 553 ± 14 J/g. Each of the curves in Figure VII.1. is an average of several profiles obtained at each light intensity, therefore the average curves are slightly shorter and wider than the original data. However, the average curves represent the general shape and provide the correct average time at the peak maximum and the average area.

VII.3.2. Effect of Temperature

Reactions were performed at a series of temperatures between 20 and 50 °C in order to determine an overall activation energy for the polymerization reaction. A maximum temperature of 50 °C was used to ensure that no thermal initiation occurred. An average initial reaction rate was determined for each temperature by measuring the time required to reach 20 % conversion. This conversion was chosen since it represents the maximum conversion for the lowest temperature experiment. The activation energy was determined from an Arrhenius fit to the data.

Figure VII.2. shows PDSC exotherms for the cationic polymerization of DVE-3 photosensitized with 1.0 x 10^{-2} wt % anthracene and 1 wt % initiator controlled at temperatures from 20 to 50 °C. As expected, the reaction rate and total conversion increased with increasing temperature as illustrated by the fact that the exotherms reach

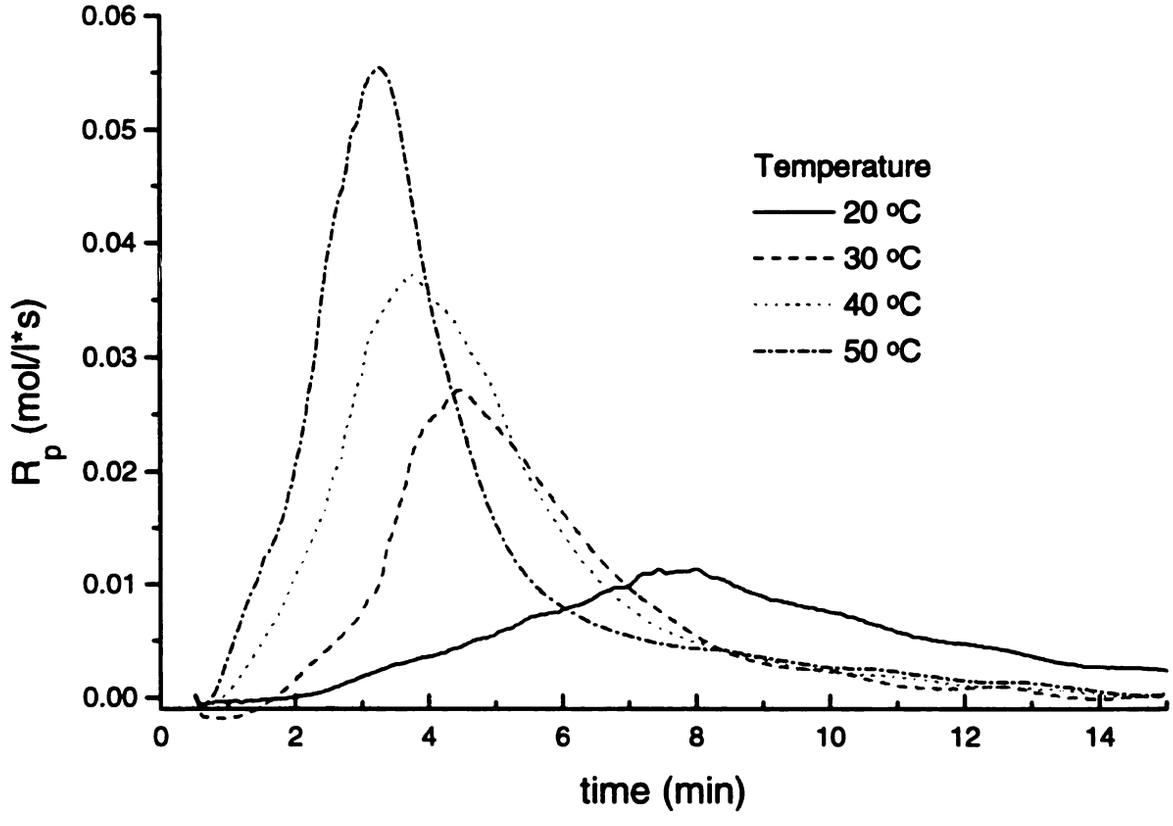

Figure VII.2. *PDSC exotherms for the cationic polymerization of DVE-3 at temperatures ranging from 20 to 50 °C.*

the maximum in a shorter time and exhibit larger integrated heat as the temperature is increased. Based upon an Arrhenius fit, the overall activation energy for the cationic polymerization was determined to be 26.5 ± 3.2 kJ/mol. Since the PDSC measures the total heat of reaction, this value represents an overall activation energy including initiation, propagation, and termination.

$$E_R = E_P + E_I - E_T \qquad \text{Eq. 1.}$$

For equation 1 to be valid, the active center production must continue throughout the reaction. Based upon previous measurements of the kinetic constants for photosensitization,[9] the photosensitizer is not completely consumed until well after the time for the peak maximum, therefore the active center concentration continues to increase at the peak maximum (the point where the reaction rate was measured). Therefore, equation 1 can be used to represent the overall activation energy for the photopolymerization reaction.

VII.3.3. Termination Rate Constant

To determine the termination rate constant, k_t, for the polymerization of DVE-3, dark cure experiments were performed. In these studies the polymerization samples were exposed to the initiating light for a short period of time, after which the light source was removed. The remaining cure was monitored with no exposure to the light source, and the reaction rate was found to decay exponentially. Samples that were exposed for 2 minutes or less had total double bond conversions of less than 5 percent. Since the change in the vinyl bond concentration during the dark cure was small, it was assumed

that the reduction in the polymerization rate was caused by the decline in the number of active centers due to termination and not due to depletion of monomer.

The PDSC exotherms were fit with an exponential decay curve from the point at which the excitation source was removed with an average exponential time constant of 17.3 ± 0.4 minutes. Therefore, the termination rate constant, k_t, was calculated to be 0.0010 ± 0.0002 s^{-1}. These results illustrate that the cationic centers exhibit a relatively long lifetime and relatively small termination rate constants compared to free radical systems. This arises from the fact that, in contrast to free radicals, cationic centers do not terminate with one another. Termination in cationic systems typically occurs due to combination with the counterion or other nucleophilic species. As will be shown later, the termination rate constant for the polymerization reaction was determined to be approximately 5 times lower than the initiation rate constant.

VII.3.4. Initiation Rate Constants

In these photopolymerizations active cationic centers are produced through a photosensitization reaction in which an electron is transferred from an excited state anthracene molecule to the initiator.[9] Although the reaction proceeds by a multi-step photochemical mechanism,[9] the rate of generation of active centers may be described by the following simple expression:

$$\text{Rate of active center generation} = k_i[A][I] \qquad \text{Eq. 2}$$

where $[A]$ is the anthracene concentration, $[I]$ is the initiator concentration, and k_i is an initiation rate constant which accounts for a number of photophysical steps including

excitation, intersystem crossing, exciplex formation, and electron transfer.[9] According to this convention, k_i is dependent on the incident light intensity. In these reactions the initiator (diaryliodonium salt) concentration greatly exceeds the anthracene concentration and can be assumed to be constant.[9] Therefore a pseudo-first-order kinetic constant, $k_i^* = k_i[I]$, may be used to describe the rate of generation of active centers. The above analysis is based upon the assumptions that one active center is produced per photosensitizer and initiator molecules and that all reactive centers are capable of propagating, as indicated by previous fluorescence measurements.[10]

The overall rate of change of the active center concentration, [M$^+$], may be derived by combining the rate of generation by photosensitization with the rate of consumption by termination:

$$\frac{d[M^+]}{dt} = k_i^*[A] - k_t[M^+] \qquad \text{Eq. 3.}$$

This equation may be integrated (with the initial condition $[M_0^+] = 0$ and the exponentially decreasing anthracene concentration) to yield the following equation:

$$[M^+] = [A_0]\frac{k_i^*}{k_t - k_i^*}(e^{-k_i^* t} - e^{-k_t t}) \qquad \text{Eq. 4.}$$

In this equation, the termination rate constant, k_t was evaluated above while the initiation rate constant, k_i may be determined from solving the photophysical rate expressions as described in earlier work.[9] For the PDSC experiments the incident light intensity used in this calculation was determined by measuring the energy absorbed by graphite discs placed in the sample and reference cells. Using the incident light intensity value, k_i^* was

determined to be 4.03×10^{-3} s^{-1} at 25 °C by solving the corresponding set of rate expressions.[9]

The activation energy for the photosensitization reaction was determined from fluorescence measurements of the photosensitization reaction between anthracene and the diaryliodonium salt. The rate constant, k_i, was determined for several different temperatures and fit to an Arrhenius equation to yield an activation energy, E_i, of 28.5 ±1.6 kJ/mol. Using this activation energy, the temperature-dependence of k_i^* was described. Based upon the values of k_t, k_i^*, E_i, and A_o, equation 4 was used to obtain profiles of the active center ($[M^*]$) concentration as a function of time for each of the PDSC reactions.

VII.3.5. Propagation Rate Constant

As previously mentioned, the rate of polymerization (R_p) is directly proportional to the rate at which heat is released from the polymerizing sample and is therefore proportional to the height of the DSC exotherm measured in W/g. For a polymerization rate in units of mol(double bonds)/(L sec), the proportionality constant is the density (ρ - the density of the reaction mixture) divided by the heat of polymerization, ΔH_p, and the instantaneous rate of polymerization may be calculated from the following relationship:

$$R_p = \frac{d[M]}{dt} = \frac{\text{height of exotherm (W / g)} * \rho}{\Delta H_p} \qquad \text{Eq. 5.}$$

According to kinetic analysis, the rate of propagation is given by a propagation rate constant multiplied by the active center concentration, $[M^*]$, and the vinyl bond concentration, $[M]$, as shown below:

$$R_p = \frac{d[M]}{dt} = k_p[M][M^+] = [A_0]\frac{k_p k_i^*}{k_t - k_i^*}(e^{-k_i^* t} - e^{-k_t t})[M] \qquad \text{Eq. 6.}$$

If a number of propagating centers with different reactivities exist, this equation may be used to fit the polymerization data to yield an apparent propagation constant that comprises all types of propagating centers (e.g. ion pairs, separated ions, etc.). In this paper we will use this approach to interpret changes in the value of the apparent propagation constant, k_p.

The vinyl bond concentration ($[M]$) and the conversion may be calculated from the integral of the reaction rate profile (equation 5). Therefore, the instantaneous double bond concentration may be calculated form the PDSC profile using the following equations:

$$[M] = [M_0] - \left(\frac{\text{exotherm area (J / g)} * \rho}{\Delta H_p}\right) \qquad \text{Eq. 7.}$$

$$\text{Conversion} = \left(\frac{\text{exotherm area (J / g)} * \rho}{\Delta H_p [M_0]}\right) \qquad \text{Eq. 8.}$$

Equation 7 gives the vinyl bond concentration in mol/l when ρ is the density of the reaction mixture. The heat of reaction for the vinyl bond was determined to be 75 kJ/mol by reacting a monovinyl ether to high conversion. A complete profile of the double bond concentration or conversion may be obtained by determining the area under the DSC curve as a function of time and applying equation 7 or 8.

For each PDSC exotherm, a profile of the quantity $k_p[M^*]$ may be obtained using the empirical profiles of R_p and [M]. Based only on the PDSC data, this product may be determined using the following version of equation 6.

$$k_p[M^*] = \frac{R_p}{[M]} \qquad \text{Eq. 9.}$$

Profiles of the rate of polymerization (propagation) obtained by applying equations 5 and 8 to a set of PDSC exotherms are shown in Figure VII.3. The figure illustrates that as the temperature is increased the maximum value of R_p increases accordingly. Furthermore, the conversion at the peak maximum is shifted to higher values as the temperature increases. Therefore Figure VII.3. verifies the importance of temperature during the cationic photopolymerization of DVE-3, as characterized by the increase in conversion and rate of the reaction with temperature.

Profiles of $k_p[M^*]$ obtained in this manner are shown in Figure VII.4. As shown in the figure, $k_p[M^*]$ initially increases sharply and then levels off at a plateau value between 0.001 and 0.01 s^{-1} depending upon the reaction temperature (as temperature is increased a higher value of $k_p[M^*]$ is observed). Finally, the value of $k_p[M^*]$ decreases as a limiting conversion is reached. The shape of the profiles in Figure VII.4. indicates that the apparent propagation rate constant k_p changes as the reaction proceeds. If k_p remained constant throughout the reaction, this change in $k_p[M^*]$ would be governed by the active center concentration. Therefore, the $k_p[M^*]$ value would increase monotonically until it reached a maximum when all of the photosensitizer is consumed.

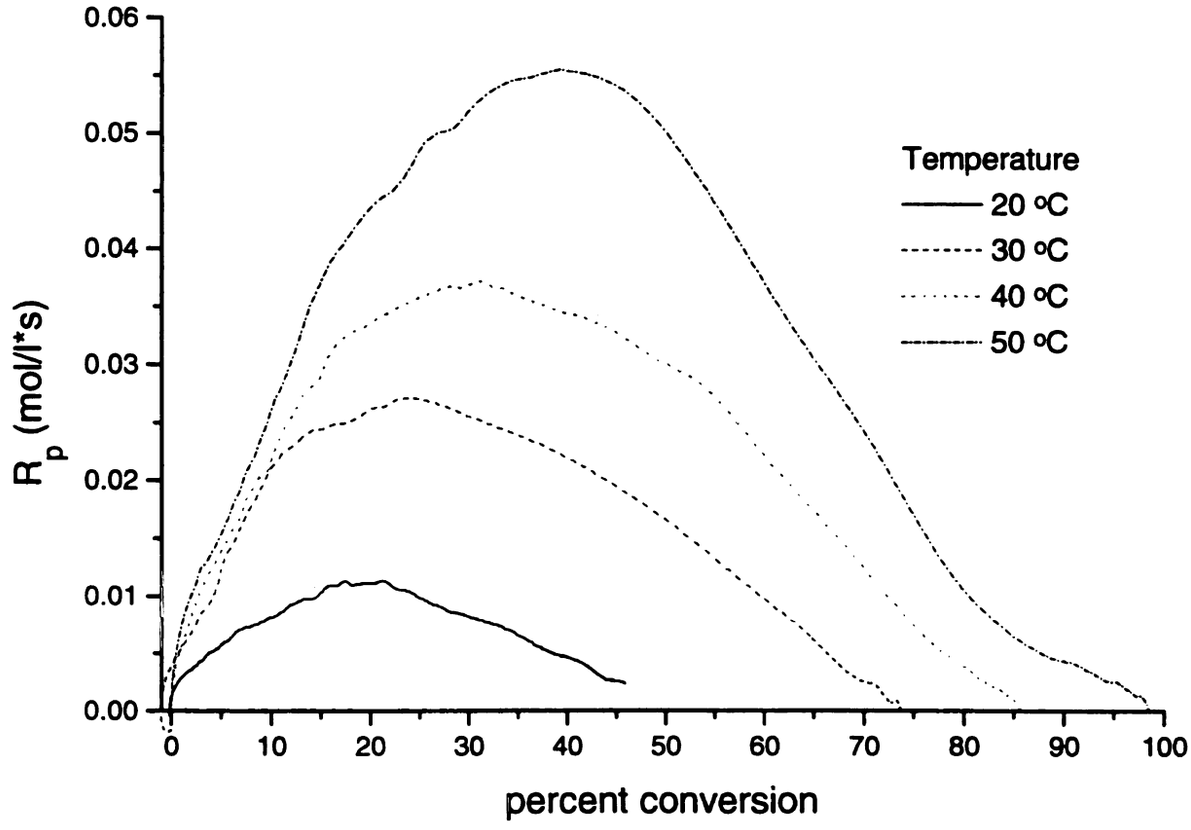

Figure VII.3. *Overall rate of propagation versus conversion for DVE-3 photosensitized with 1.0 x 10^{-2} wt % anthracene and 1 wt % initiator.*

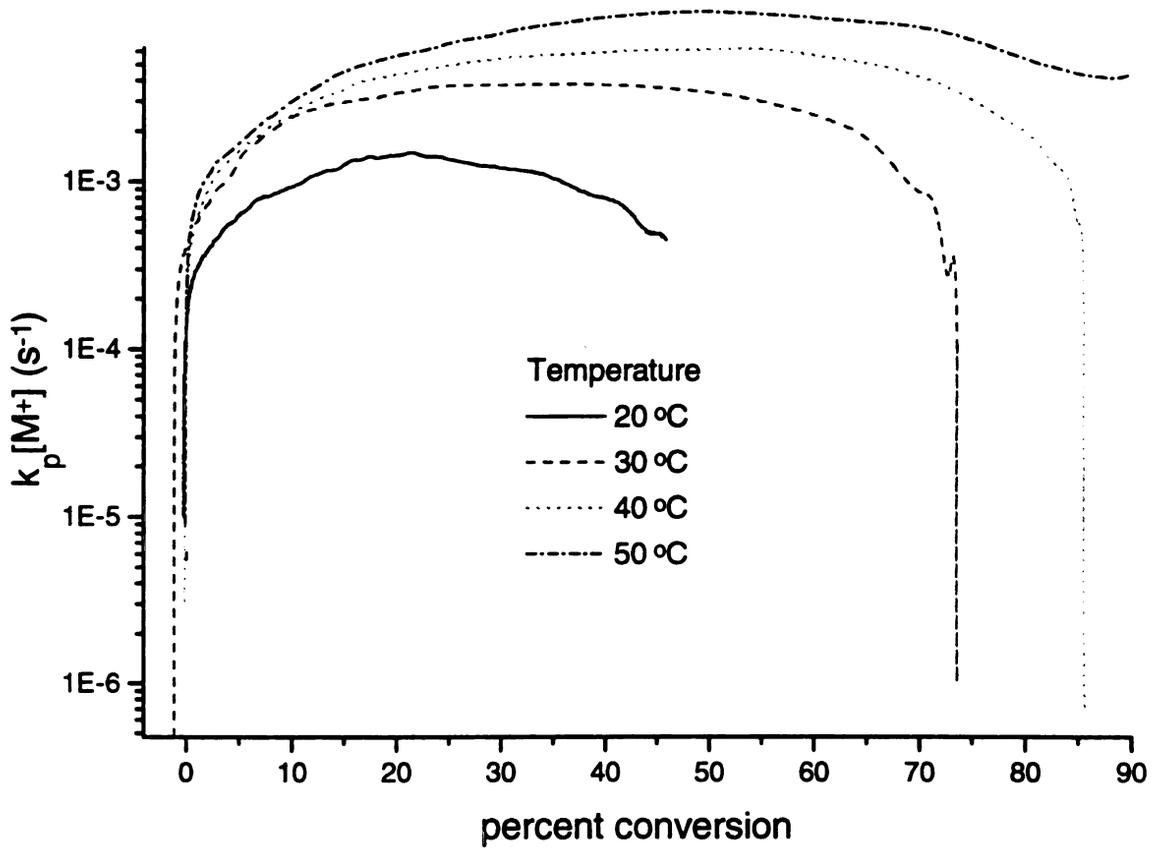

Figure VII.4. *k_p [M^+] versus conversion for the cationic photopolymerization of DVE-3 at temperatures ranging from 20 to 50 °C.*

More information about the behavior of k_p may be obtained by coupling the PDSC data with the k_i^* and k_t values discussed previously. Profiles of the apparent propagation rate constant, k_p were obtained by substituting the values of $[A_0]$, k_i^*, and k_t along with the empirically determined profiles of $[M]$ and R_p into equation 6. Figure VII.5. shows k_p as a function of vinyl bond conversion. The curves exhibit a similar characteristic shape as the $k_p[M^*]$ profiles of Figure VII.4., although the plateau value is much higher due to the small active center concentration. The similarity in shape indicates that relative changes in k_p are much larger than those for $[M^*]$. The final magnitude obtained for k_p values were between 5 and 30 l/mol*s, which compare satisfactorily with values from the literature.[11]

One possible explanation for the initial large increase in the apparent rate constant for propagation is a change in the reactivity of the carbocation species due to the proximity of the counterion. In the early stage of the reaction, polymerization leads to a large local increase in viscosity which reduces diffusional mobility. The active carbocation retains considerable mobility through propagation since the cation effectively moves through the reaction mixture by reacting with new monomers. This type of mobility has been termed "reaction diffusion" and may become the dominant mechanism for mobility of the active center in highly crosslinked polymerizations.[4,12] However, the large hexafluoroantimonate counterion experiences a decrease in mobility as the viscosity increases since it cannot diffuse through the reaction mixture in a similar manor. During this process, the counterion and carbocation become separated, and since separated ions are orders of magnitude more reactive than ion pairs,[13] this would lead to a large increase in the apparent propagation rate constant, k_p. This type of "reaction diffusion" is well

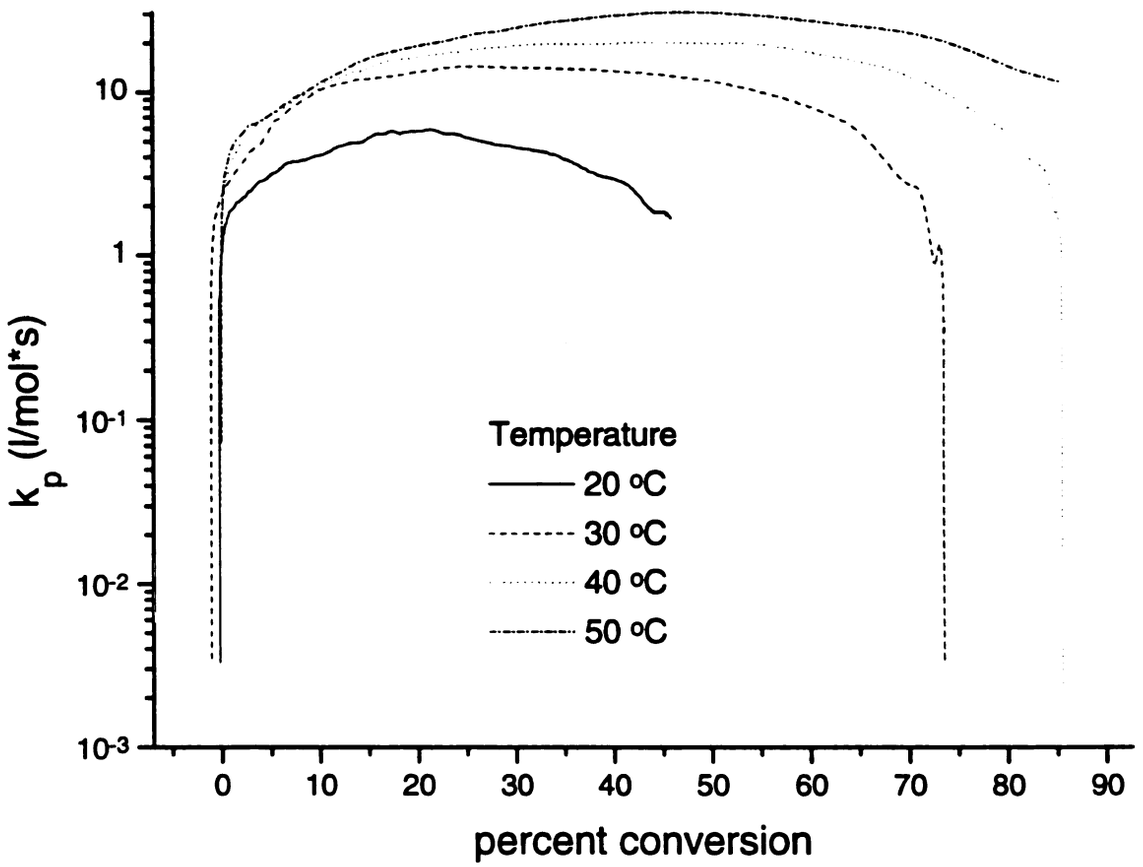

Figure VII.5. *k_p versus conversion for the photopolymerization of DVE-3 at various temperatures.*

known for highly crosslinked free radical systems[4,12] and may aid in explaining the shape of the curves in Figures VII.4. and VII.5. The final decrease in k_p arises from active center trapping during these highly crosslinked polymerizations. Therefore a limiting conversion at which the reaction ceases is observed despite the presence of active centers. As previously mentioned, the above analysis is based upon the assumptions that one active center is produced for each photosensitizer molecule consumed and that all reactive centers are capable of propagating.[10]

VII.4. Conclusions

In this contribution photo-differential scanning calorimetry (PDSC) was used to monitor cationic photopolymerizations of a divinyl ether. The PDSC method offers a direct method for evaluating the heat generated during a polymerization reaction. The heat of reaction profiles provided by PDSC were used to characterize the reaction kinetics and evaluate polymerization rate constants. However, the reaction system was extremely rapid and highly exothermic, making DSC measurements particularly challenging. To maintain isothermal reaction conditions, low light intensities and very small sample sizes (0.5 - 1.5 mg) were used to increase the reaction time for the divinyl ether photopolymerizations.

The PDSC experiments were used to determine kinetic constants for a series of unsteady-state divinyl ether polymerizations at different temperatures and light exposure times. Kinetic constants for propagation and termination were obtained from the PDSC experiments in conjunction with previously determined photosensitization rate constants.

As expected, an increase in the initiating light intensity or an increase in the reaction temperature resulted in an increased reaction rate. This increase in reaction rate was found to result in higher final conversions as determined from the total heat of reaction.

To determine the termination rate constant, k_t, PDSC dark cure exotherms were fit with an exponential decay from the point at which the excitation source was removed (the exponential time constant was 17.3 ± 0.4 minutes). These results illustrate that the cationic centers exhibit a relatively long lifetime and relatively small termination rate constants compared to free radical systems, arising from the fact that cationic centers do not terminate by combination with themselves.

An apparent propagation rate constant that comprises all types of propagating centers (e.g. ion pairs, separated ions, etc.) with different reactivities was determined from the PDSC reaction profiles. The apparent propagation constant, k_p, initially increases sharply and then levels off at a plateau value (as temperature is increased a higher value of k_p is observed). Finally, the value of k_p decreases as a limiting conversion is reached. This profile shape indicates that the apparent propagation rate constant k_p changes greatly as the reaction proceeds. The initial large increase in the apparent rate constant for propagation may be explained by a change in the reactivity of the carbocation species due to the proximity of the counterion. During the polymerization, the counterion experiences a decrease in the mobility of the large hexafluoroantimonate counterion as the viscosity of the system increases. However, the active carbocation retains diffusional mobility by reacting with vinyl bonds and may lead to separation of the two species. Since separated ions are orders of magnitude more reactive than ion pairs,[13] the apparent value of k_p increases dramatically during the early stages of the

reaction. The final decrease in k_p arises from active center trapping during these highly crosslinked polymerizations. Therefore, a limiting conversion at which the reaction ceases is observed despite the presence of active centers.

The PDSC profiles for the propagation and termination rate constants as functions of conversion provide important insight into the nature of these high-speed cationic photopolymerizations. Understanding the kinetics of these cationic photopolymerizations is important due to the increasing number of applications for rapid, solvent-free curing of polymer films.

VII.5. List of References

1. T. Doornkamp and Y. Y. Tan *Polymer Commun.*, **31**, 362 (1990).
2. J. G. Kloosterboer "Network Formation by Chain Crosslinking Photopolymerizations and Its Application in Electronics," *Adv. Polym. Sci.* , **84**, 1 (1988).
3. J. G. Kloosterboer and G.F.C.M. Lijten *Polymer*, **28**, 1149 (1987).
4. K. S. Anseth, C. M. Wang and C. N. Bowman "Kinetic Evidence of Reaction Diffusion during the Polymerization of Multi(meth)acrylate Monomers," *Macromolecules*, **27**, 650 (1994).
5. K. S. Anseth, C. M. Wang and C. N. Bowman, "Reaction Behavior and Kinetic Constants for Photopolymerizations of Multi(meth)acrylate Monomers," *Polymer*, **35**, 3243 (1994).
6. C. Decker and K. J. Moussa "Real-Time Monitoring at Ultrafast Curing By UV-Radiation and Laser Beams," *Coatings Tech.* , **62**, 55 (1990).
7. J. G. Kloosterboer, G. F. C. M. Lijten, in *Cross-Linked Polymers*, R. A. Dickie, S. S. Labana, and R. S. Bauer, Eds., ACS Symposium Series 367; ACS: Washington DC, (1987).
8. J. V. Crivello, J. L. Lee and D. Conlon "Photoinitiated Cationic Polymerization with Multifunctional Vinyl Ethers," *J. Rad. Curing* **10**, 6 (1983).

9. E. W. Nelson, T. P. Carter, A. B. Scranton "The Role of the Triplet State in the Photosensitization of Cationic Polymerizations by Anthracene," *J. of Poly. Sci., Poly. Chem.*, **33**, 247 (1995).

10. E. W. Nelson, T. P. Carter, A. B. Scranton "Fluorescence Monitoring of Cationic Photopolymerizations: Divinyl Ethers Photosensitized by Anthracene Derivatives," *Macromolecules*, **27**,1013 (1994).

11. G. Odian, *Principles of Polymerization*, 2nd Ed., Wiley, NY, 22, 1981.

12. K. S. Anseth and C. N. Bowman "Reaction Diffusion Enhanced Termination in Polymerizations of Multifunctional Monomers," *Polymer Reaction Engineering*, **1(4)**, 499-520 (1992-93).

13. J. P. Kennedy, and E. Marechal *Carbocationic Polymerization*, John Wiley & Son, New York, 1982.

CHAPTER VIII. *IN SITU* LUMINESCENCE TEMPERATURE PROFILES

VIII.1. Introduction

In this chapter, the temperature-dependent luminescence of tris(β-diketone) chelates of europium was used for *in situ* temperature measurements during cationic photopolymerizations of vinyl ethers. These molecular-level luminescent probes provided a real-time, noninvasive method for monitoring temperature during these high-speed polymerizations. Two specific probes, tris(benzoyl-1,1,1-trifluoroacetone) europium and tris(1,1,1,5,5,5-hexafluoroacetylacetone) europium met several stringent spectral and performance requirements for application in our system. The luminescence from these probes exhibits a reproducible temperature dependence over a wide temperature range and is not sensitive to changes in viscosity. *In situ* temperature profiles obtained using this novel technique verified the importance of thermal effects during these highly exothermic photopolymerizations. These studies have demonstrated the utility of the of the tris(β-diketone) europium chelates for characterizing the temperature during high-speed photopolymerizations that cannot be monitored using conventional techniques.

Most of the early work on cationic photopolymerizations focused on the identification and synthesis of appropriate monomers and initiators (for reviews see

references 1 and 2). Not until recently have the detailed studies of the reaction been reported.[3,4] For example, in a previous contribution[4] Nelson *et al.* reported a novel *in situ* laser-induced fluorescence technique for monitoring the initiation reaction in these high-speed polymerizations. Due to its extremely short intrinsic time scale, the fluorescence technique provided a means to characterize the kinetics of these polymerizations which proceed too rapidly to be monitored by traditional methods such as differential scanning calorimetry (DSC). These studies indicate that although the reactions are extremely rapid (the systems typically react to completion in a few seconds), most of the conversion occurs in the last 100 milliseconds due to a dramatic increase in the reaction rate. Nelson *et al.* attributed this characteristic reaction profile to thermal runaway resulting from the large amount of heat released by the rapidly polymerizing system.

Due to its short intrinsic time scale, luminescence techniques are attractive for monitoring the local temperature of these reactions which may proceed to completion in a few seconds. Furthermore, luminescence techniques provide a non-intrusive method for monitoring the temperature since trace amounts of the luminescence probe may be readily incorporated into the reaction mixture. Tris(β-diketone) chelates of europium fulfill the requirements of a temperature-dependent luminescence probe for our studies. As described in the remainder of this chapter, these probes exhibit a linear response for a wide temperature range, and are insensitive to changes in viscosity. In addition, the excitation wavelength of these probes is ideally suited for our studies.

VIII.2. Probe Requirements

In addition to exhibiting a temperature-dependent response, the luminescence temperature probe for these studies must meet specific spectral requirements. Anthracene, which absorbs between 320 and 390 nm, was used as a photosensitizer to expand the initiating window to the near-visible region of the spectrum. The anthracene photosensitizer makes it possible to initiate polymerization in the near-UV or visible wavelengths as a result of a direct interaction between an excited state of a photosensitizer and the initiator.[4] In this experiment, 351 nm or 364 nm ultraviolet (UV) light was used to initiate the photopolymerization. Therefore, these wavelengths are the most convenient for excitation of the temperature probe, since they would eliminate the need for two laser beams. In addition, the emission wavelengths of the temperature probe must not overlap with the fluorescence of the anthracene photosensitizer in the 425 nm region.

A class of compounds which satisfies both spectral requirements is the lanthanide substituted tris(β-diketone) chelates, which absorb from 280 to 380 nm[5] and emit in the 620 nm range.[6] These compounds exhibit an interesting "antenna" effect which is responsible for the temperature dependence of the luminescence. The light absorption by the lanthanide itself is very weak, however the ligand plays the role of an antenna by absorbing light and efficiently transferring the excitation energy to the metal ion.[7] This non-radiative intramolecular transfer from the excited state of the ligand to the highly luminescent europium metal center results in a number of interesting luminescent

properties. A number of authors[6-11] have characterized the chemical and photophysical properties of these chelates. These authors found that the luminescence efficiency varies greatly with the identity of the ligand, degree of coordination, temperature, and solvent.[5,7] Sager *et. al* reported that the underlying photophysical process proceeds by the following four-step mechanism: (1) ground singlet absorption to the excited singlet state; (2) radiationless intersystem crossing from the excited singlet to the lowest lying triplet state; (3) transfer of energy to the chelated ion; and (4) characteristic ionic fluorescent emission.[5]

VIII.3. Experimental

VIII.3.1. Materials

The monomer, 3,6,9,12-tetraoxatetradeca-1,13-diene (DVE-3) and the photosensitizer, anthracene, were purchased from Aldrich Chemical Co. The monomer was dried over molecular sieves to remove any traces of water and the photosensitizer was used as received. The cationic initiator (UV9310C-GE Silicones) had a composition of 5-10 wt % linear alkylate dodecylbenzene, ~50 wt % 2-ethyl-1,3-hexanediol, and ~50 wt % bis(4-dodecylphenyl)iodonium hexafluoroantimonate. The initiator concentrations specified in the remainder of this chapter correspond to the total UV9310C concentration.

A free radical polymerization system was used to identify any viscosity dependencies of the temperature probes. The monomer, 2-hydroxethyl acrylate (HEA), was purchased from Aldrich Chemical Co. This system was polymerized in solution with

N,N-Dimethyl-formamide (DMF) in order to maintain optical clarity. The initiator for this polymerization was 2,2-azobisisobutyronitrile (AIBN), purchased from Polyscience Inc.

VIII.3.2. Synthesis of Temperature Probes

The temperature probes under primary investigation were tris(benzoyl-1,1,1-trifluoroacetone) europium ($Eu(btfa)_3$), and tris(1,1,1,5,5,5-hexafluoroacetylacetone) europium ($Eu(hfa)_3$). Both of these probes were synthesized as described below. The ligands 1,1,1,5,5,5-hexafluoroacetylacetone (hfa) and benzoyl-1,1,1-trifluoroacetone (btfa) were purchased from Lancaster Synthesis Inc., and the europium (III) chloride hexahydrate was purchased from Aldrich Chemical. The europium compound was added to approximately 50 ml of distilled water. The pH was increased to 8.5 by the addition of ammonium hydroxide. As the europium solution was stirred, a stoichiometric amount of the ligand was added. After allowing the solution to react over night with stirring, the precipitate was filtered and dried for 24 hours at 70°C. This procedure was based on modifications of those reported in references 5,6,9-11.

VIII.3.3. Absorption and Luminescence Measurements

Absorption spectra of monomers, initiators, photosensitizers, and luminescent temperature probes were obtained using a Hewlett Packard UV-vis 8452A diode-array spectrophotometer. For the temperature studies, the luminescence was monitored using

an Aminco-Bowman Series 2 Luminescence Spectrometer. The excitation frequencies were varied from 340 to 364 nm. Based upon the absorption spectrum of each lanthanide chelate, the optimum concentration for measuring the luminescence was determined. A concentration that absorbed too strongly would result in an artificially low luminescence reading, due to a shorter path length resulting from the low penetration depth into the sample. The temperature was controlled with a Polyscience 9100 refrigerated constant-temperature circulator connected to a jacketed cuvette holder inside the luminescence spectrometer. A mixture of ethylene glycol and water was used as the heating fluid.

The luminescence monitoring of the temperature probes *in situ* during the cationic photopolymerization was performed in the MSU *LASER* laboratory. The luminescent temperature probe and cationic photopolymerization reaction were both excited with a Coherent Innova 200 Argon ion laser tuned at either 363.8 or 351.1 nm. A Newport 845HP-01 digital shutter system was opened with an electric pulse from the multichannel analyzer, ensuring that the illumination and the acquisition were started simultaneously. Fifteen milliwatts of unfocused laser radiation (measured with a Scientech 362 Power/Energy meter) in an ~3 mm dia. beam was directed on to the quartz capillary tube containing the sample. The sample geometry and instrument set-up have been described in further detail in an earlier publication.[4] The quartz capillary was approximately 2.5 cm in length with an inner diameter of 1 mm and an outer diameter of 2 mm. The fluorescent light was collected at an angle of 90° from the incident beam and 90° from the longitudinal axis of the quartz tube. The temperature of the sample was controlled by a jacketed tube holder coupled to a thermostated water bath.

The luminescence signal was collected using a Spex 1877 Triplemate spectrometer with a subtractive dispersion filter stage and a spectrograph stage. An EG&G Princeton Applied Research Model 1530-C/CUV CCD detector, cooled to -120 ^{o}C to minimize dark charge levels, was used to detect the signal. The data was analyzed with an EG&G Princeton Applied Research Model OMA IV detector controller. Luminescence spectra spanning 50 to 100 nm centered at 620 nm were collected with 150 groove/mm gratings in both the filter and spectrograph stages. These spectra were typically collected in intervals of 50 ms.

VIII.4. Results and Discussion

VIII.4.1. Probe Selection

The two most promising temperature sensitive luminescence probes, $Eu(hfa)_3$ and $Eu(btfa)_3$, were selected based on their ability to meet the system requirements. The structures of these lanthanide β-diketone chelates are shown in Figure VIII.0. In these chelates six of the nine coordination sites are occupied by organic ligands and the remaining three sites are occupied by water molecules. The choice of the organic ligand is important since it determines the absorption wavelength and helps to impart solubility in the monomer. These two chelates meet the solubility and spectral requirements for these studies.

The absorbance spectra of $Eu(btfa)_3$ and $Eu(hfa)_3$ are shown in Figure VIII.2. The figure illustrates that the extinction coefficient of $Eu(btfa)_3$ is an order of magnitude

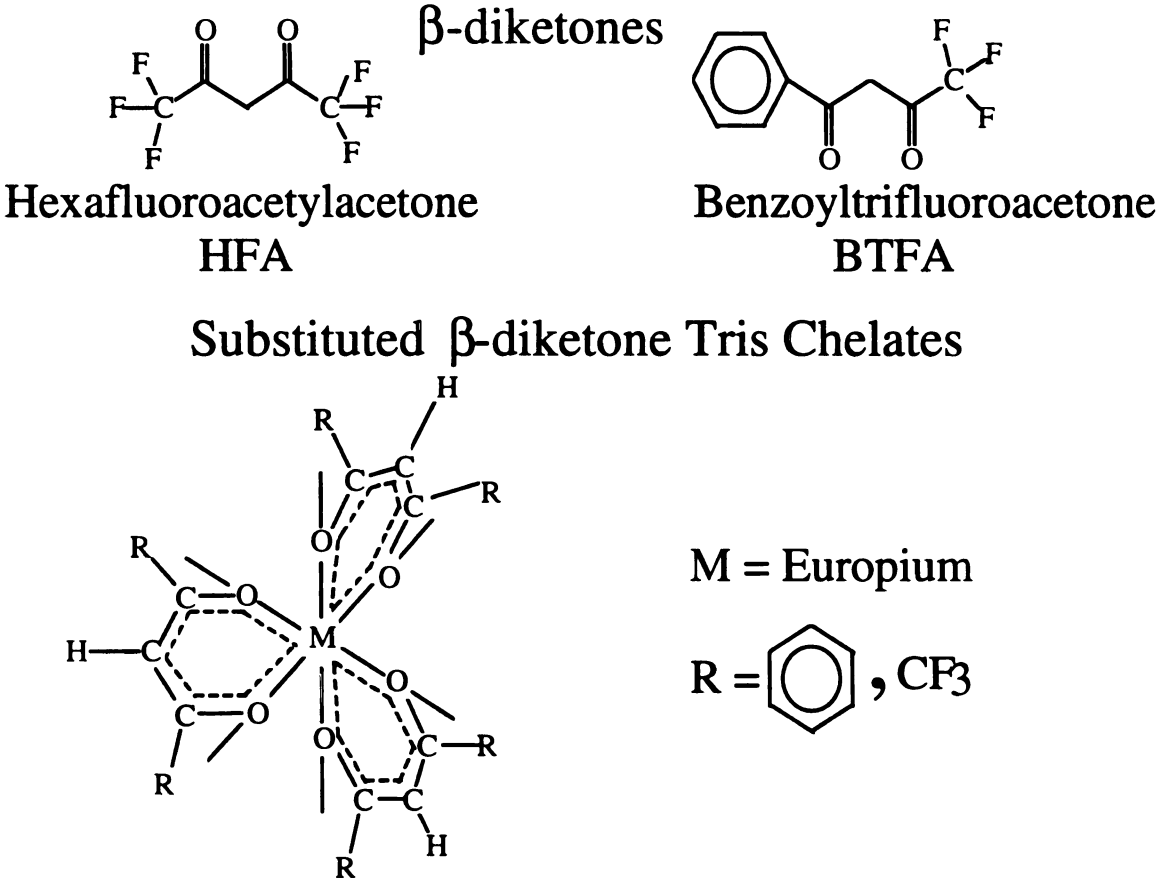

Figure VIII.1. *The structure for the two lanthanide* β*-diketone chelates, Eu(btfa)$_3$ and Eu(hfa)$_3$.*

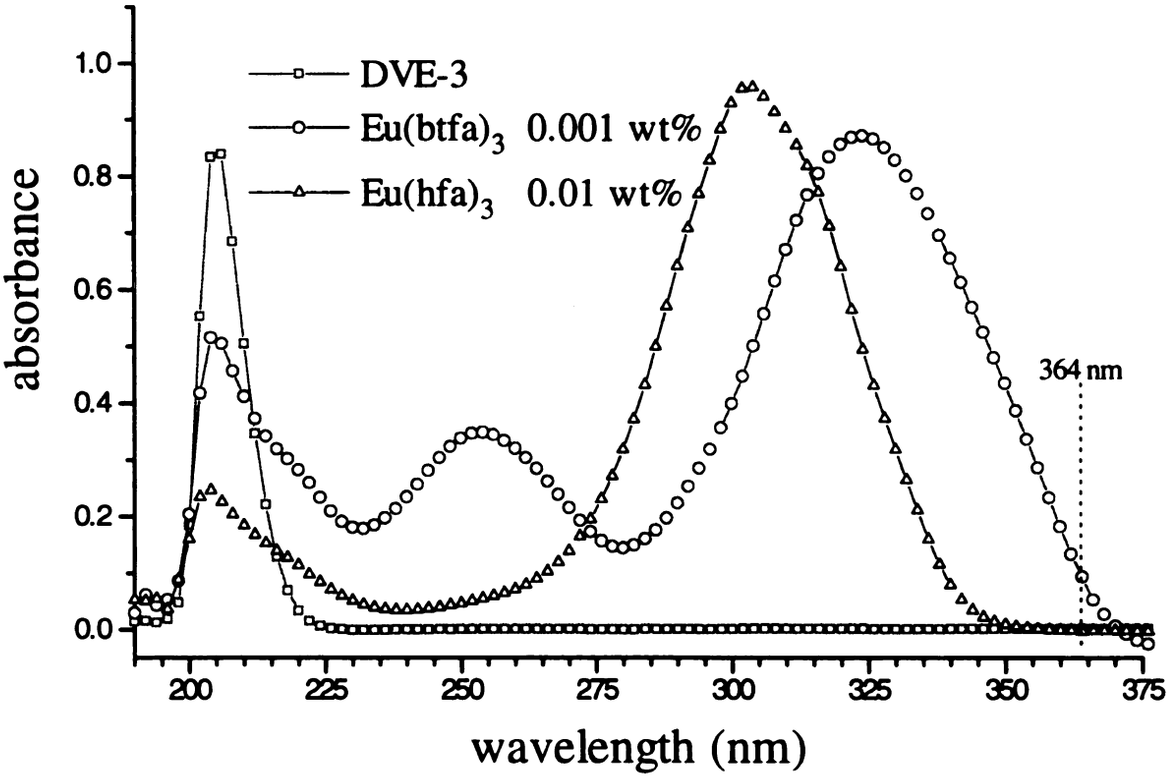

Figure VIII.2. *Absorption spectra of $Eu(btfa)_3$ (0.001 wt %), $Eu(hfa)_3$ (0.01 wt %), and DVE-3 in methanol.*

larger than that of $Eu(hfa)_3$. In addition, the $Eu(btfa)_3$ spectrum is shifted toward the red compared to the $Eu(hfa)_3$ spectrum, and absorbs much more strongly then $Eu(hfa)_3$ at 364 nm. While it may appear that the 364 nm $Eu(hfa)_3$ absorbance is too low to produce strong luminescence, $Eu(btfa)_3$ at 0.001 wt % and $Eu(hfa)_3$ at 0.01 wt % were found to have similar luminescence intensities (Figure VIII.3.). Due to its stronger absorption at 351 nm, the $Eu(hfa)_3$ emits a more intense signal when excited at this wavelength. Therefore the characterization of the cationic photopolymerizations was carried out using 351 nm as the excitation wavelength.

For the DVE-3 reaction system, it is important that the luminescence from the temperature probe does not overlap with the fluorescence signal from the anthracene photosensitizer (380-500 nm). For $Eu(btfa)_3$ and $Eu(hfa)_3$ the temperature sensitive emission peak occurs at around 620 nm (Figure VIII.3.), and therefore does not overlap with the anthracene peak. The fluorescence in the 375 nm range in Figure VIII.3. was attributed to the organic ligands and does not change with temperature. As described earlier, the energy transfer from the organic ligands to the metal center becomes less effective, and the luminescence of the metal center decreases, as the temperature of the system increases.

VIII.4.2. Temperature Studies

The temperature-dependent luminescence of $Eu(btfa)_3$ in the monomer is shown in Figure VIII.4. The figure illustrates that, as expected, an increase in the temperature leads to a decrease in the luminescence intensity. A plot of the luminescence intensity at

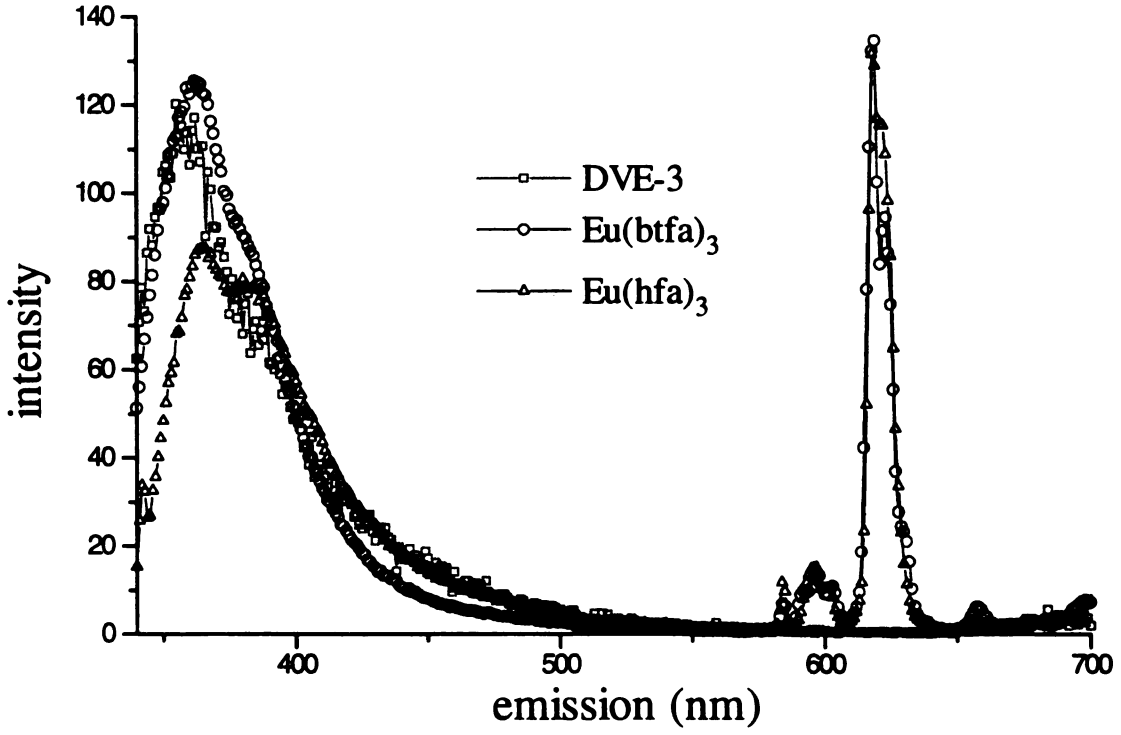

Figure VIII.3. *Luminescence spectra of $Eu(btfa)_3$ (0.001 wt %) and $Eu(hfa)_3$ (0.01 wt %) in DVE-3 and of DVE-3.*

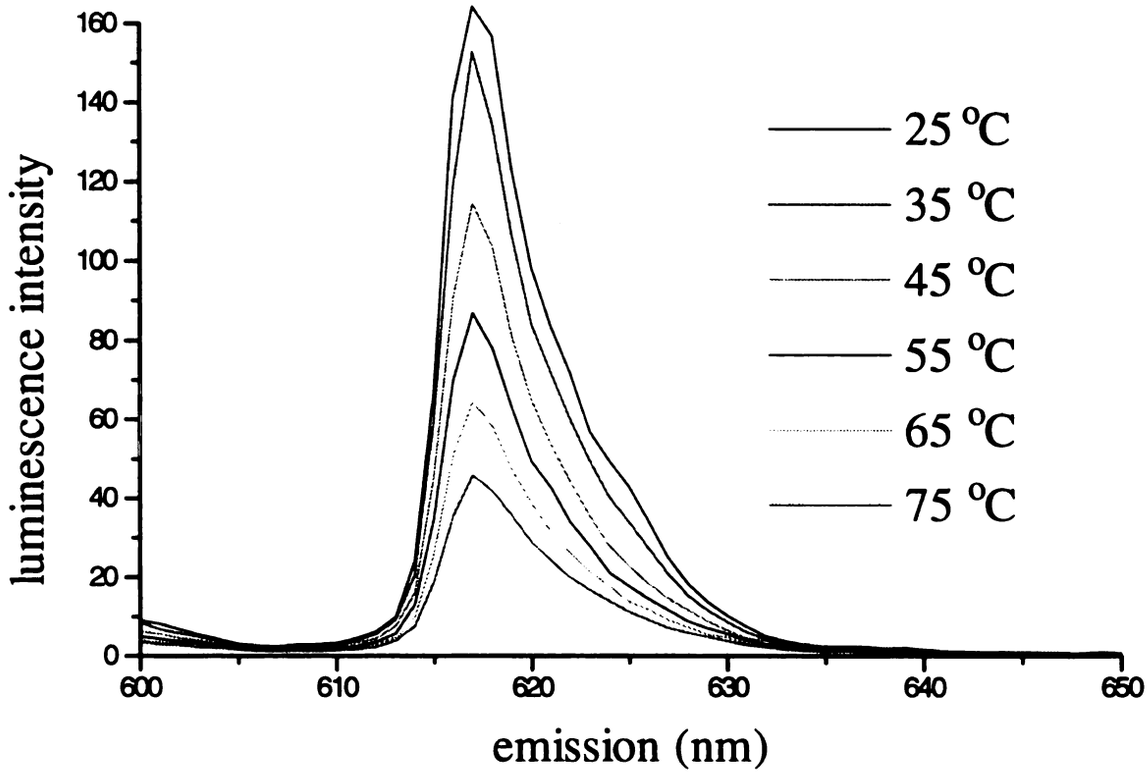

Figure VIII.4. *Luminescence spectra at varying temperatures for $Eu(btfa)_3$ at 0.001 wt % in DVE-3, excited at 364 nm.*

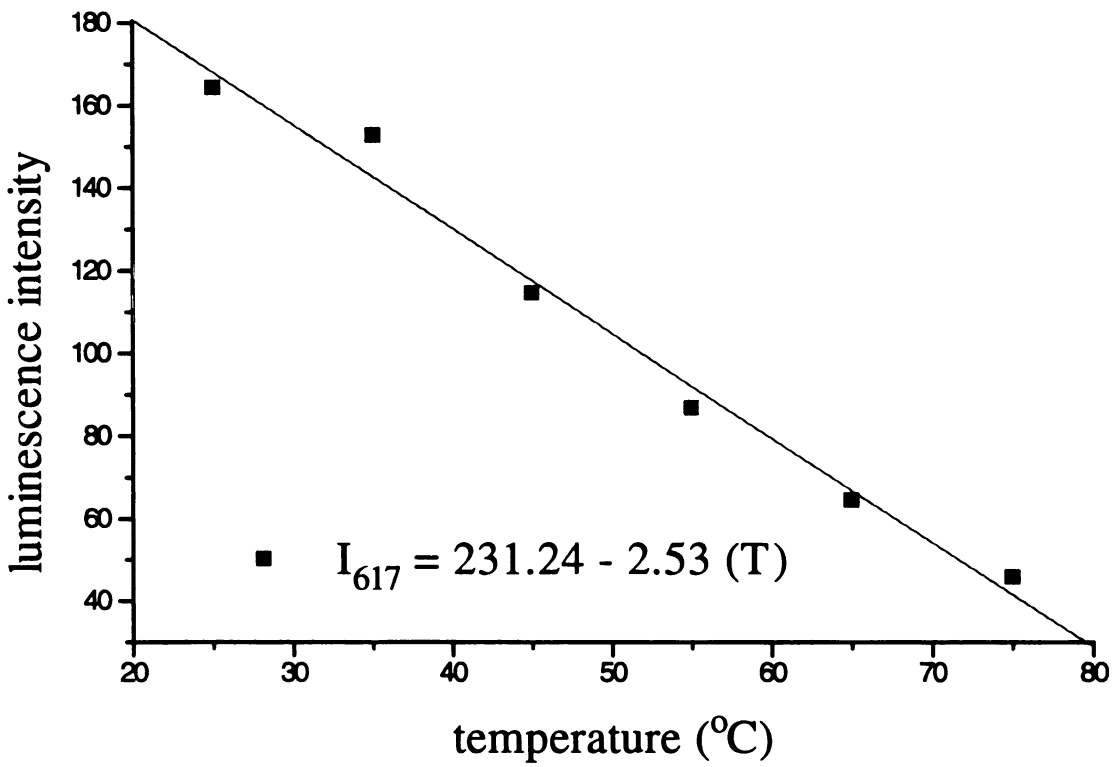

Figure VIII.5. *The luminescence intensity of $Eu(btfa)_3$ at an emission of 617 nm plotted at different temperatures, resulting in a linear calibration curve.*

618 nm (peak maximum) versus temperature, is shown in Figure VIII.5. This intensity varies linearly with temperature (the correlation coefficient is 0.9976) and may therefore be used to estimate the temperature of a system if the measurement is performed using the same experimental conditions (concentrations and instrument settings).

The temperature-dependent luminescence of $Eu(hfa)_3$ is shown in Figure VIII.6. Again, the luminescence intensity decreases with increasing temperature, however in contrast to the $Eu(btfa)_3$ profiles discussed above, the $Eu(hfa)_3$ luminescence exhibits two distinctive peaks centered at 618 and 622 nm. The intensities of these peaks undergo an inversion in relative intensity with the 622 nm peak exhibiting a larger intensity at low temperatures and the 618 nm peak exhibiting a higher relative intensity at high temperatures. Equations 1 and 2 illustrate the linear dependence of each peak intensity on temperature (the correlation coefficients are 0.99849 and 0.99788 for the 618 and 622 nm peaks respectively).

$$I_{618} = 150 - 1.6(T) \qquad \text{Eq. 1.}$$

$$I_{622} = 200 - 2.4(T) \qquad \text{Eq. 2.}$$

To take advantage of the inversion in the relative intensities of the two peaks, a detector-insensitive calibration was developed based upon an intensity ratio defined as the intensity of the 618 nm peak divided by the modified intensity of the 622 nm peak (see Figure VIII.7.). As shown in the figure, a plot of the resulting intensity ratio versus reciprocal temperature is linear with a correlation coefficient of 0.99997). This calibration curve is independent of operating conditions such as instrument settings since the peaks act as internal standards.

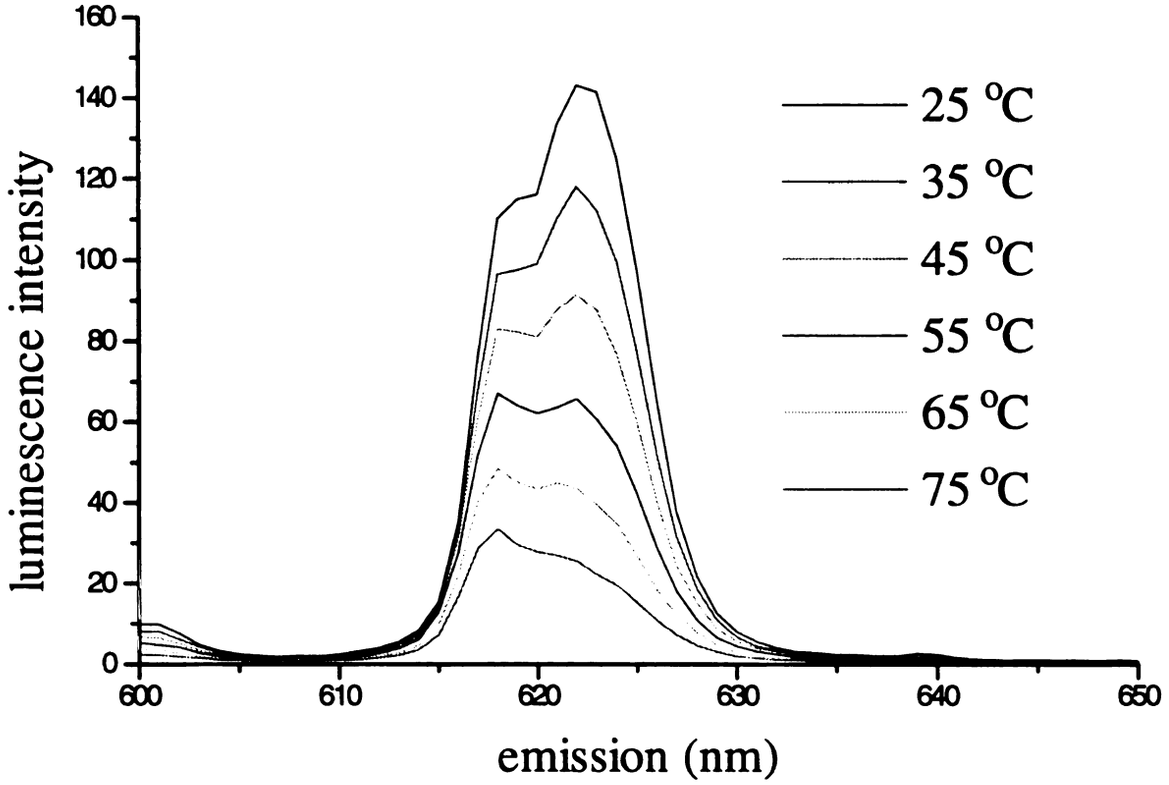

Figure VIII.6. *Luminescence spectra at varying temperatures for $Eu(hfa)_3$ at 0.01 wt % in DVE-3 excited at 340 nm.*

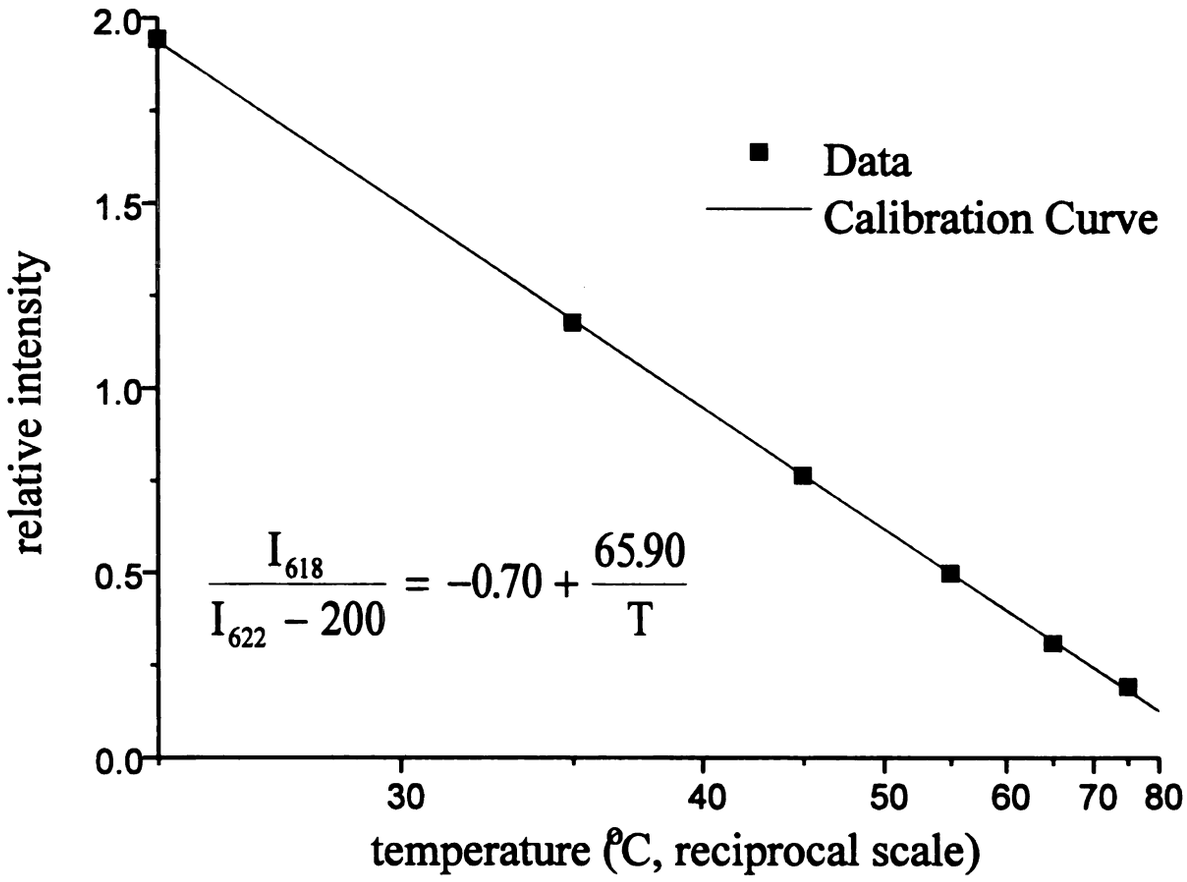

Figure VIII.7. *The relative intensity, referring to the intensity of the 618 peak divided by the modified intensity of the 622 peak, of $Eu(hfa)_3$ in DVE-3 (0.01 wt %) plotted versus reciprocal temperature.*

To investigate the effect of elevated temperature on the luminescence of the lanthanide chelates, a series of studies were performed for temperatures ranging from 30 to 130 °C. The resulting luminescence/temperature calibrations for $Eu(hfa)_3$ and $Eu(btfa)_3$ are shown in Figure VIII.8. As the figure illustrates, the $Eu(hfa)_3$ curve was best fit by a single straight line throughout the entire temperature range, while the $Eu(btfa)_3$ curve was best fit by an exponential decay. Therefore the $Eu(hfa)_3$ probe is better suited for the high temperature studies since it does not lose sensitivity as the temperature is increased. Theoretically this probe should be able to monitor much higher temperatures approaching its degradation temperature. However, since the luminescence intensity decreases as the temperature rises, the maximum measurable temperature is limited by the detector's low-level sensitivity. If the initial temperature is set to the maximum detector reading, the dynamic range of the detector limits the size of the temperature range. Therefore, the maximum effective temperature range is effectively limited by the dynamic range of the instrument.

VIII.4.3. Viscosity Independence

Many probes which exhibit temperature-dependent luminescence are also sensitive to changes in viscosity.[12] However, a viscosity-dependent response is unacceptable for a luminescent probe used for monitoring temperature during polymerization. These systems undergo a large change in viscosity, and any viscosity-dependent response will likely dominate the desirable temperature-dependence. Therefore, a series of studies were performed to determine whether the luminescence of

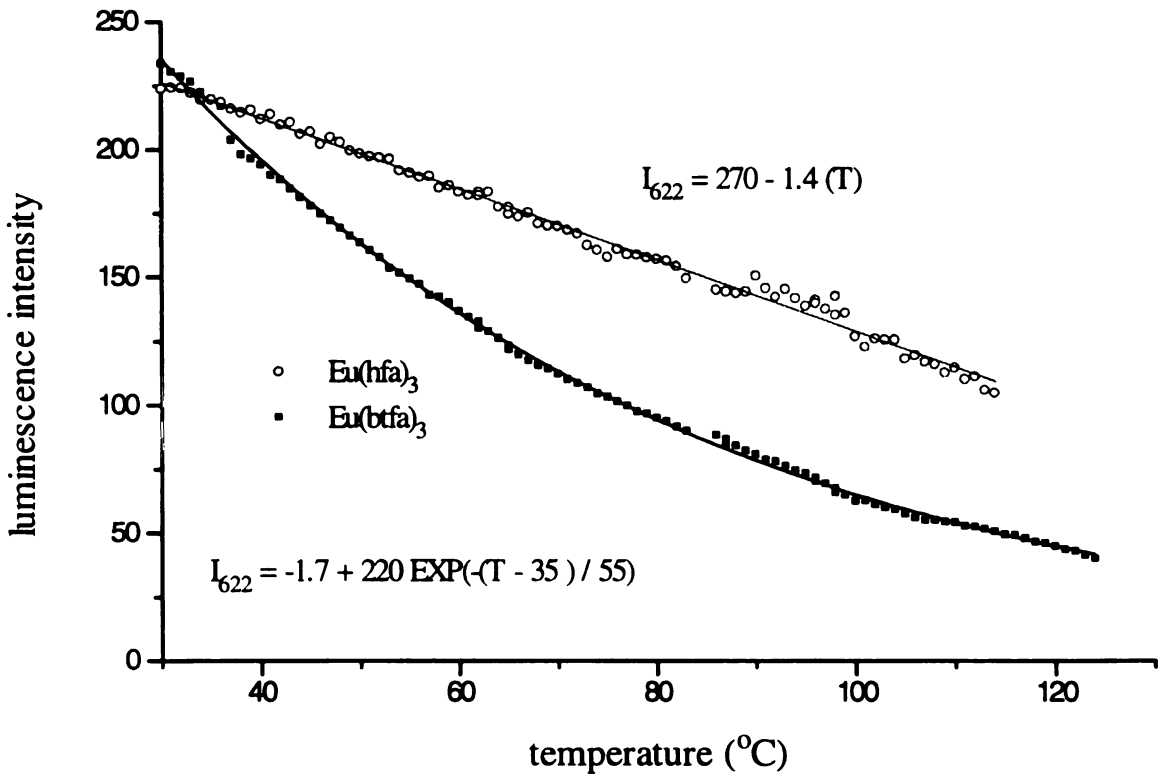

Figure VIII.8. *High temperature calibration curves for Eu(btfa)$_3$ and Eu(hfa)$_3$ excited at 364 nm and monitored at an emission of 620 nm.*

$Eu(hfa)_3$ and $Eu(btfa)_3$ were sensitive to viscosity. A calibration curve was produced for a liquid monomer system (~2 cps) and compared to a calibration for a solid polymerized system. Therefore, if the calibrations are the same for the two extremes of liquid and solid, the luminescence response is insensitive to viscosity.

A solution polymerization was chosen for preparing the solid samples to ensure optical clarity and permit easy removal of the polymer from the quartz cuvettes. DMF was chosen as the solvent due to its relatively high boiling point (153 °C) and because the resulting polymer was optically clear. A suitable ratio of monomer to solvent was found to be 40/60. The polymerizations were carried out at a temperature of 65 °C with an initiator concentration of 0.5 wt % and a β-diketone tris chelate concentration of 10^{-2} wt %.

Profiles of luminescence intensity versus temperature for the HEA/DMF system are shown in Figure VIII.9. When corrected for the presence of the AIBN initiator, the luminescence intensities show good agreement in both the liquid and solid state, indicating that the luminescence-temperature probe $Eu(hfa)_3$ is not sensitive to changes in viscosity. The viscosity independence of the europium probes is not surprising since the temperature dependent energy transfer is internal and should not be effected by the translational or rotational motion of the molecule. Equivalent viscosity experiments were performed with $Eu(btfa)_3$ yielding similar results.

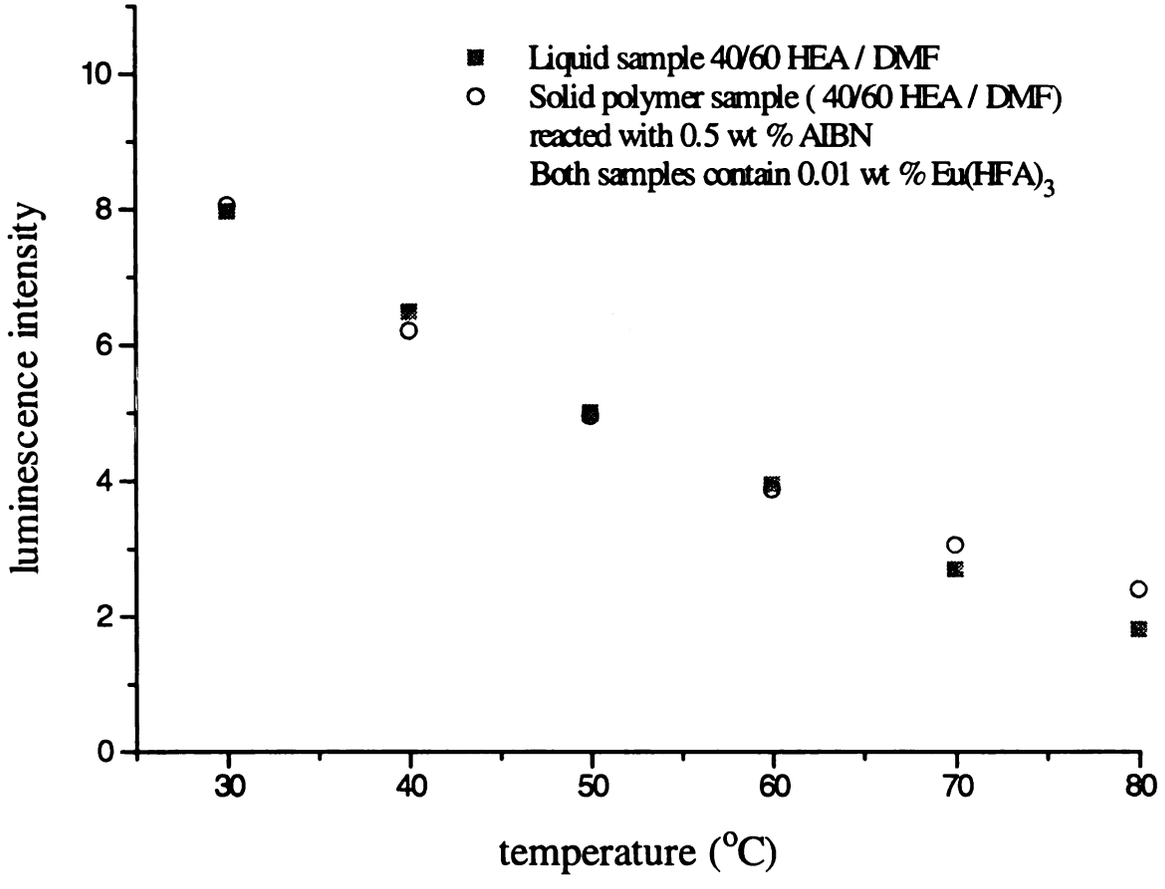

Figure VIII.9. *Temperature calibration curves for 0.01 wt % Eu(hfa)$_3$ excited at 351 nm in liquid and solid systems.*

VIII.4.4. Inherent System Limitations

The above discussion illustrates the utility of the lanthanide chelates for *in situ* temperature monitoring. These molecular-level probes exhibit a linear temperature dependence over a wide temperature range and, in the case of $Eu(hfa)_3$, may provide a detector-insensitive calibration. However, these systems have several inherent limitations. Perhaps the largest limitation arises from the sensitivity of the luminescent response to solvent. Because water effectively competes with the β-diketones for the coordination sites on the lanthanides, the luminescence is diminished in the presence of water. Therefore these probes cannot be used with any aqueous systems. In DVE-3, the luminescence intensity decreases over a period of days possibly due to the slow exchange of the ligand and the solvent. In addition, the shape of the luminescence spectra of the chelates is dependent on the solvent. For example, as shown in Figure 10, the two distinctive $Eu(hfa)_3$ peaks observed in DVE-3 are not present for experiments performed in methanol and methylene chloride. This dependence on solvent necessitates a calibration to be established for each system.

VIII.4.5. Temperature Profiles for the Cationic Photopolymerizations

Since the luminescence temperature probes were found to be sensitive to changes in temperature but insensitive to viscosity, they were investigated for use in monitoring the reaction temperature during the cationic photopolymerizations of DVE-3. A series of

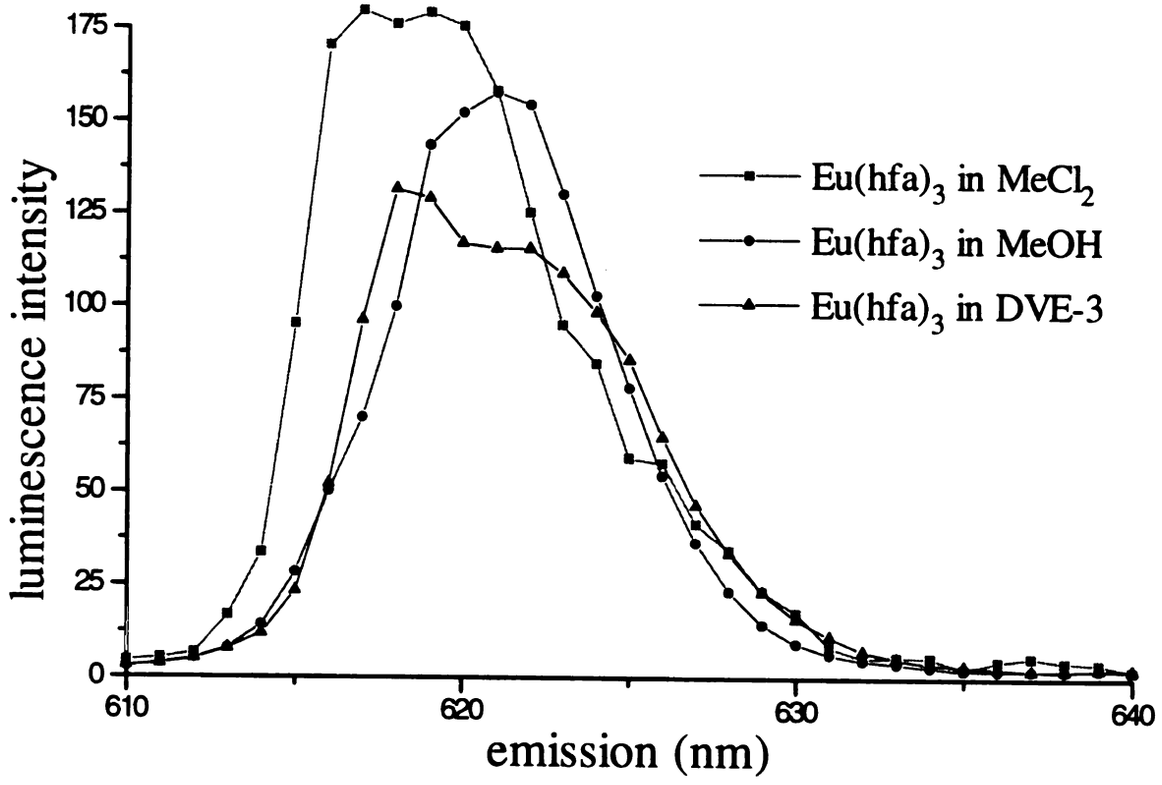

Figure VIII.10. *The luminescence of $Eu(hfa)_3$ (0.01 wt %) in methanol, methylene chloride, and DVE-3.*

studies were performed to ensure that the lanthanide probes did not affect the polymerization kinetics and that the presence of the initiator and photosensitizer did not disrupt the luminescence response of the temperature probes. The β-diketone tris chelates are electronically neutral, therefore they will not undergo electrostatic interactions with the propagating active centers. However it was anticipated that the lanthanide probes could possibly affect the reaction by interacting with the initiator or the anthracene photosensitizer.

A non-reacting system (a sample containing DVE-3, anthracene, and an europium probe) was tested to determine the time stability of the temperature-sensitive probe. No initiator was added to ensure that the system was non-reactive and remained isothermal when exposed to the beam from the argon ion laser. Essentially no change in luminescence was observed over the time scale of the experiment (30 sec) for both $Eu(hfa)_3$ and $Eu(btfa)_3$. Next, to investigate the effect of the initiator, the temperature-sensitive luminescence of a sample containing hexanol, anthracene, initiator, and an europium probe was monitored. Hexanol was chosen to approximate DVE-3 in this non-reactive system. The hexanol system was then exposed to the initiating wavelength causing the photosensitization to begin. For both probes ($Eu(hfa)_3$ and $Eu(btfa)_3$), there was no change in the temperature sensitive probe luminescence over a substantial period of time. This indicates that the temperature probes were not being consumed during the photosensitization reaction. By monitoring the anthracene fluorescence intensity as a function of time, the photosensitization reaction rate was found to be unaffected by the addition of the europium probes, indicating that the temperature probes are not adversely affecting the photosensitization reaction.

The cationic photopolymerizations were carried out in the MSU *LASER* laboratory, therefore calibration curves were generated using the Triplemate spectrometer and CCD detector. To produce the calibration curve, a non-reacting sample containing anthracene and a europium probe in DVE-3 was used. The sample tube was placed in a jacketed cell holder (as described in the experimental section), then the temperature was increased while the luminescence at 620 nm was measured (Figure VIII.11.).

In preliminary reaction-monitoring experiments, the europium luminescence at 620 nm was measured at 50 ms intervals, and the calibration curve was used to generate the temperature profile. The temperature reading at the start of the reaction was adjusted to match room temperature (25 °C). The luminescence from the europium probe indicated that the temperature increased gradually from ~25 to ~55 °C at which point the reaction temperature increased rapidly (Figure VIII.12.). Therefore these studies illustrate that, as expected, a marked increase in temperature is associated with the sudden increase in the reaction rate. The reaction temperature continues to increase; however, due to the instrumental dynamic range limitations mentioned above, higher temperatures were not able to be monitored in this system. In addition, at elevated temperatures the sample loses optical clarity. However, the important temperature at which the thermal runaway occurs (~55 °C for these specific reaction conditions) can be readily obtained from the temperature profile.

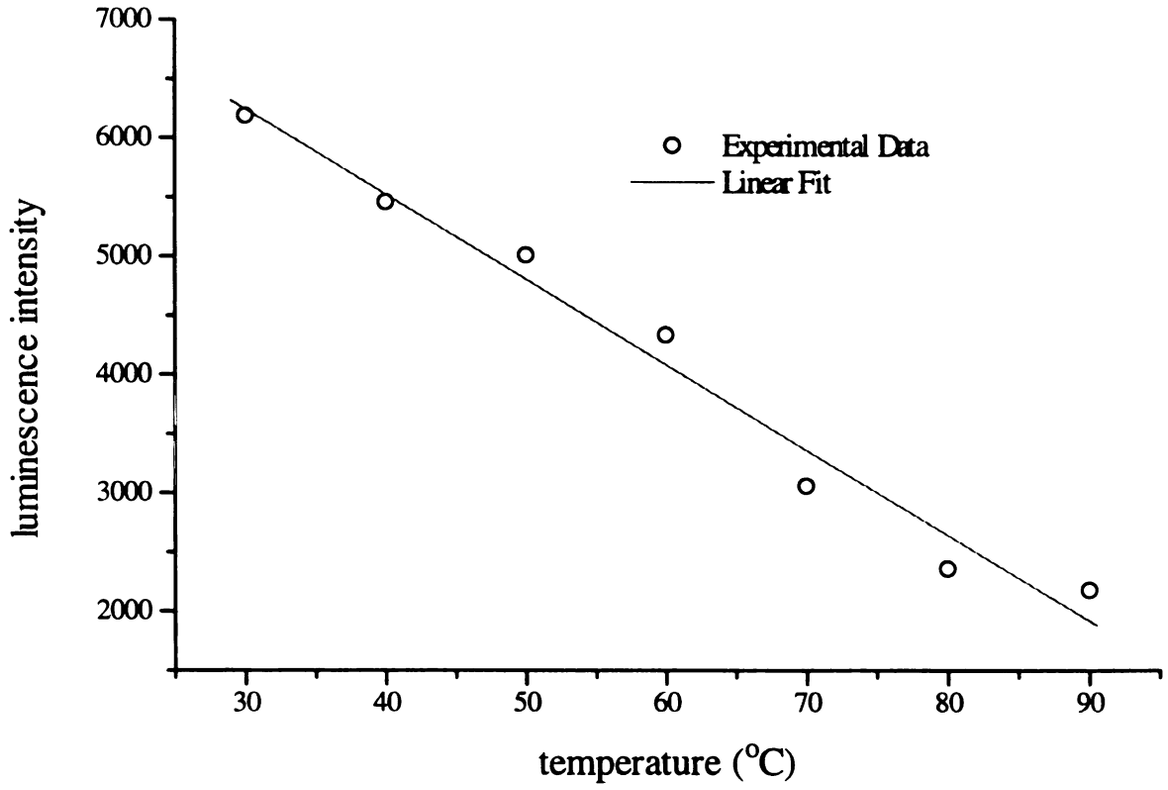

Figure VIII.11. *Temperature calibration for 1.6 x 10^{-2} wt % Eu(hfa)$_3$ in DVE-3 with 1.4 x 10^{-2} wt % anthracene excited with 15 mW at 351 nm using an argon ion laser.*

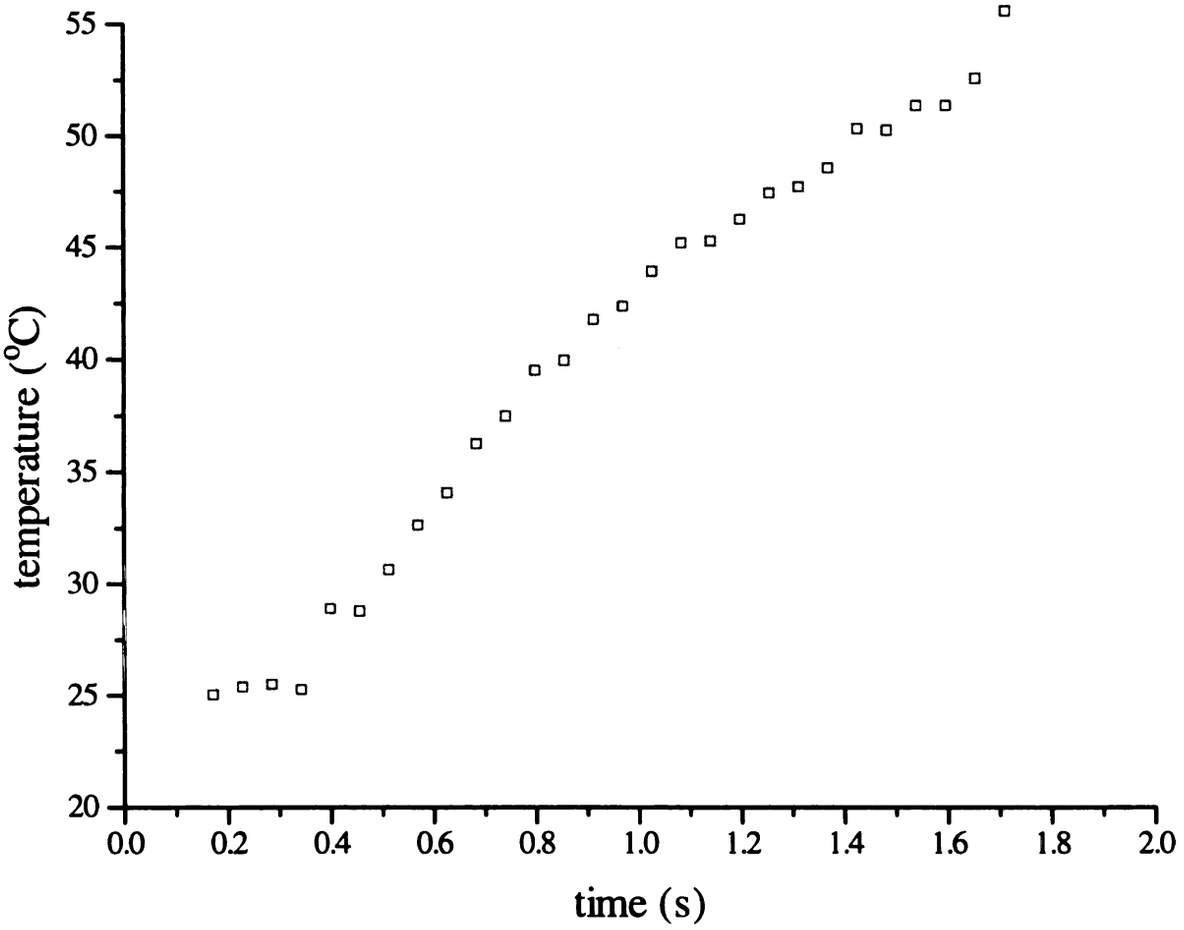

Figure VIII.12. *Temperature profile of the cationic polymerization of DVE-3 1.6 x 10^{-2} wt % anthracene and 1.0 wt % initiator monitored with 1.0 x 10^{-2} wt % Eu(hfa)$_3$.*

VIII.4.6. Further Applications

Due to their temperature dependence and viscosity insensitivity, the β-diketone tris chelates of europium may be attractive for temperature monitoring in a variety of systems. The technique could find application in any system in which an *in situ*, non-intrusive measurement of temperature is desired. Moreover, due to their viscosity insensitivity, the probes are appropriate for systems in which a change in phase occurs.

To illustrate the broader applicability of this technique in other reaction systems, the *in situ* luminescence during a free radical polymerization of 2-hydroxyethyl acrylate (HEA) was investigated for both probes. The reaction was a solution polymerization of 40/60 HEA/DMF in order to insure optical clarity during the reaction. The polymerizations were performed in 3.5 ml cuvettes heated to 65°C by a jacketed cell holder. AIBN was used as the initiator, and the lanthanide probes were present in concentrations of 10^{-2} wt %. Temperature excursions may occur due to the heat of polymerization, and the luminescence technique provides a temperature measurement which is averaged over the width of the cuvette. Luminescence measurements were easily performed in a standard luminescence spectrometer since the reaction takes minutes to complete as opposed to seconds in the case of cationic polymerizations.

Figure VIII.13. shows the temperature profile produced from the luminescence intensity at 620 nm (the peak maximum) during a free radical polymerization of HEA. A calibration curve was prepared using the procedures described previously for the cationic system. As the reaction proceeds the exothermic heat of polymerization will cause the

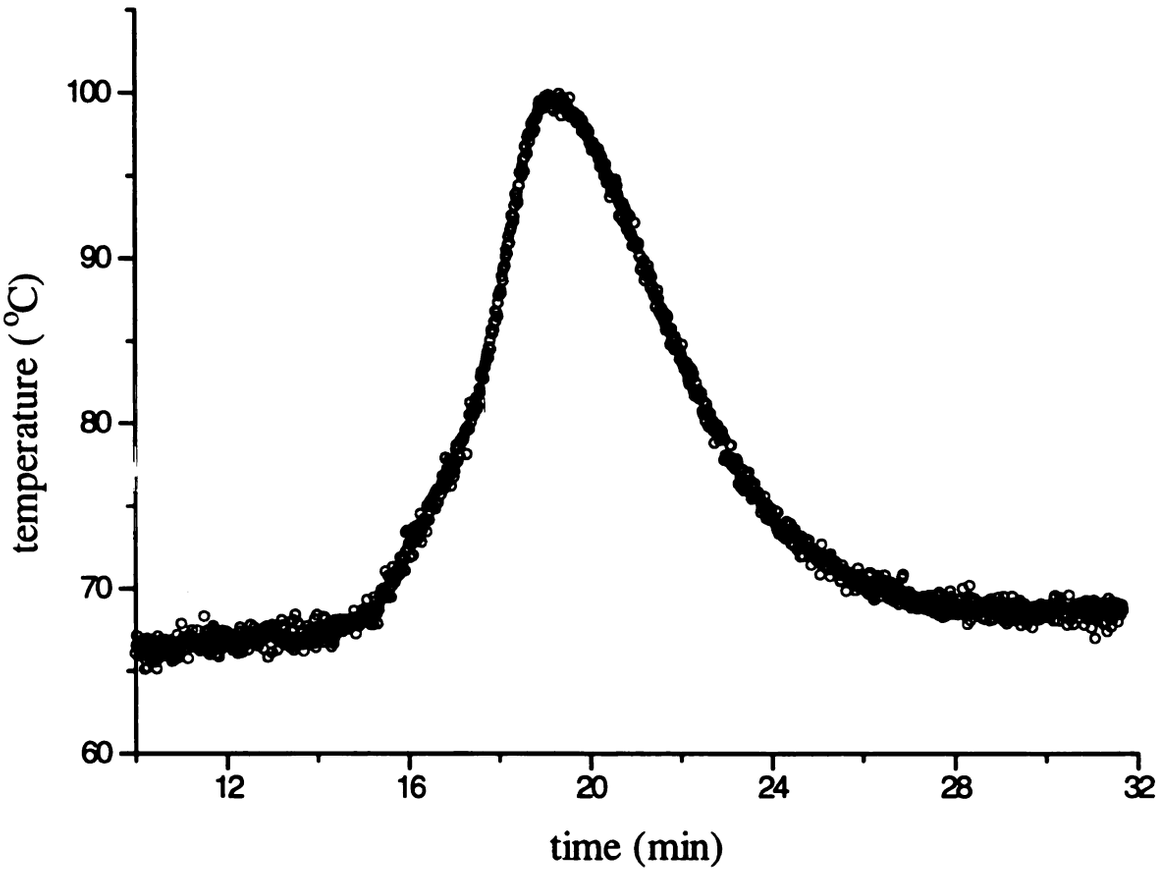

Figure VIII.13. *The temperature profile generated from the luminescence intensity of $Eu(hfa)_3$ in a free radical polymerization of HEA/DMF (40/60) with an initiator concentration of 0.2 wt %.*

system temperature to increase above the jacket temperature, if heat evolution rate is higher than the heat transfer rate. Therefore, a dramatic increase in the temperature was observed at ~15 minutes, corresponding to an increase in the reaction rate due to autoacceleration. After reaching a peak value of around 100 °C, the reaction is essentially complete and the temperature of the solution returns to that of the jacket (65°C). Therefore, the luminescence ultimately returns to approximately the same intensity as when the sample was a liquid (confirming that the luminescence is independent of viscosity). The profile shown in Figure VIII.13. has the well-characterized shape indicative of free radical polymerizations undergoing the gel effect,[13] thereby illustrating the broader applicability of these temperature probes.

VIII.5. Conclusions

In conclusion, luminescence can provide a novel *in situ*, non-destructive method for monitoring the temperature in high speed reactions. Molecular-level luminescent probes provide extremely rapid response without requiring a macroscopic probe to be imbedded in the sample. For temperature monitoring during photopolymerizations of vinyl ethers, two β-diketone tris chelates of europium [$Eu(hfa)_3$ and $Eu(btfa)_3$] were found to meet several stringent requirements. These probes exhibit a reproducible temperature dependence over a wide temperature range and, in the case of $Eu(hfa)_3$, may provide a detector-insensitive calibration. Calibration curves of luminescence intensity versus temperature were generated for the temperature range of interest (between 20 and 90 °C). In addition, these probes meet specific spectral requirements, such as excitation

in the 350 nm range and emission above 500 nm. Finally, the luminescence response of these probes was found to be independent of viscosity.

These temperature profiles for cationic photopolymerizations verified the importance of thermal effects in these high-speed polymerizations. The luminescence from the europium probe indicated that the temperature increased gradually from ~25 to ~55 °C, then increased dramatically in a period of a few hundred milliseconds. These results confirm that a thermal runaway effect is responsible for the large increase in polymerization rate, as previously postulated by Nelson *et al.*[4] While the temperature-sensitive probes appear to accurately monitor the temperature prior to thermal runaway, they are unable to determine the maximum reaction temperature due to detector dynamic range limitations and problems associated with the sample losing optical clarity. Furthermore, the luminescence of the probes was found to be sensitive to sample components (solvent, initiators, and water) and seemed to degrade at long times. However, this can be overcome with the use of system specific calibration curves and the use of fresh samples.

These studies have demonstrated the utility of the temperature-dependent luminescence of tris(β-diketone) europium chelates for characterizing the temperature during high-speed photopolymerizations that cannot be monitored using conventional techniques. However the applicability of these probes is not limited to this reaction system. These probes could find application in any system in which an *in situ*, non-intrusive measurement of temperature is desired. For example, due to their temperature dependence and viscosity insensitivity, the probes are appropriate for systems in which a change in phase occurs. The broader applicability of these probes was illustrated by our

studies of the HEA free radical polymerizations. Finally, a host of other lanthanide compounds could possibly be used as temperature sensitive fluorescent probes. For example, commercially available probes worthy of further study include tris(6,6,7,7,8,8,8-heptafluoro-2,2-dimethyl-3,5-octanedionato) europium and tris(2,2,6,6-tetramethyl-3,5-heptanedionato) europium.

VIII.6. List of References

1. J. V. Crivello, "Cationic Polymerization-Iodoium and Sulfonium Salt Photo-initiators", *Adv. Polym. Sci.*, **62**, 1 (1984).

2. J. V. Crivello, J. L. Lee, "Alkoxy-Substituted Diaryliodonium salt Cationic Photo-initiators", *J. Polym. Sci., Part A Polym. Chem.* **27**, 3951 (1989).

3. C. Decker, D. Decker, "Kinetic and Mechanistic Study of the UV-Curing O Vinyl Ether Based Systems," *RadTech 94 North American Proceedings*, RadTech International North America, 602, (1994).

4. E. W. Nelson, T. P. Carter, A. B. Scranton, "Fluorescence Monitoring of Cationic Photopolymerization: Divinyl Ether Polymerizations Photosensitized by Anthracene Derivatives," *Macromolecules*, **27**, 1013-1019 (1994).

5. W. F. Sager, N. Filipescu, F. A. Serafin, "Substituent Effects on Intramolecular Energy Transfer. I. Absorption and Phosphorescence Spectra of Rare Earth β-Diketone Chelates," *J. of Phys. Chem.*, **69** (4), 1092-1100 (1965).

6. F. Halverson, J. S. Brinen, and J. R. Leto, "Luminescence of Europium and Hexafluoroacetylacetonate," *J. of Chem. Phys.*, **40** (10), 2790-2792 (1964).

7. B. Alpha, R. Ballardini, V. Balzani, J-M. Lehn, S. Perathoner, N. Sabbatini, "Antenna Effect in Luminescent Lanthanide Cryptates: A Photophysical Study," *Photo-chemistry and Photobiology*, **52** (2), 299-306 (1990).

8. A. M. Murray, L. A. Melton, *Appl. Opt.*, **24**, 2783-2787 (1985).

9. M. F. Richardson, W. F. Wagner, D. E. Sands, "Rare-Earth Trishexafluoro-acetylacetonates and Related Compounds," *J. Inorg. Nucl. Chem.*, **30**, 1275-1289 (1968).

10. S. Sato, M. Wada, "Relations between Intramolecular Energy Transfer Efficiencies and Triplet State Energies in Rare Earth β-Diketone Chelates," *Bulletin of the Chemical Society of Japan*, **43**, 1955-62 (1970).

11. E. J. Schimitschek, J. A. Trias, "IR and Raman Spectra of Europium(III) β-Diketonates," *J. Inorgan. Nucl. Chem.*, **32**, 811-831 (1970).

12. K. F. Schrum, A. M. Williams, S. A. Haerther, D. Ben-Amotz, "Molecular Fluorescence Thermometry," *Anal. Chem.*, **66**, 2788-2790 (1994).

13. G. Odian, *Principles of Polymerization*, John Wiley & Sons, Inc.: New York, NY, 1991 p. 286.

CHAPTER IX. CONCLUSIONS AND RECOMMENDATIONS

The work reported in this thesis has contributed to the understanding of the kinetics and mechanisms of cationic photopolymerizations of divinyl ethers. The fundamental experimental and theoretical investigation of these UV-initiated cationic polymerizations presented in this thesis complement the more macroscopic studies currently in the literature, and are imperative if the potential of these reactions is to be realized. Furthermore, novel cure and temperature monitoring methods have been developed to characterize these high speed polymerization reactions. These new methods and techniques are general in their ability to monitor cure and temperature and will be widely applicable in high speed polymerization reactions. In this chapter, some general conclusions and suggestions for further work will be presented.

IX.1. Summary of Results

This research has provided the first detailed picture of the kinetics, structure, and properties of model cationic photopolymerization systems, and has resulted in the development of a host of analytical techniques which may now be used to characterize a broader set of cationic photopolymerizations. Several distinct aspects of the photo-polymerizations were investigated: 1) A series of fluorescence cure monitoring studies

based upon a novel experimental technique were used to investigate the effects of several reaction variables; 2) A series of studies, including fluorescence and phosphorescence lifetime measurements, were performed to characterize the photosensitization mechanism by anthracene and its derivatives; 3) A series of *in situ*, isothermal reaction studies were performed using Raman spectroscopy to directly monitor propagation; 4) A series of isothermal and dark-cure photo-differential scanning calorimetry studies were performed to characterize the reaction kinetics; and 5) A novel time-resolved, *in situ* temperature monitoring scheme was developed based upon β-diketone trischelates of lanthanide salts. Results of each of these studies are briefly described below.

IX.1.1. Fluorescence Cure Monitoring

Cationic photopolymerizations of vinyl ethers were investigated using in situ, time resolved fluorescence spectroscopy. Due to its short intrinsic timescale, fluorescence spectroscopy provides a means to characterize these polymerizations which proceed too rapidly to be monitored by traditional methods. The fluorescence intensity of the photosensitizer (anthracene or its derivatives) was monitored as a function of time with spectra collected in intervals as short as 2 milliseconds. An observed reduction in fluorescence intensity was attributed to consumption of the photosensitizer, providing a means to monitor the production of active cationic centers. The reaction rate increased as the initiator or photosensitizer concentrations were increased. Also, reactions photo-sensitized by anthracene and 9,10-dimethylanthracene produced the fastest rates, followed by 9-vinylanthracene. The polymerization rate for 9,10-diphenylanthracene was

considerably slower due to steric hindrance or resonance effects. These results illustrated the tremendous potential of in situ, time-resolved fluorescence spectroscopy for monitoring polymerizations.

IX.1.2. Characterization of the Photosensitization Mechanism

The photosensitization mechanism for cationic polymerizations initiated by diaryliodonium salts photosensitized by anthracene was investigated using fluorescence and phosphorescence spectroscopy. *In situ* photosensitizer fluorescence measurements confirmed that the photosensitization reaction proceeds by an electron transfer process. Transient phosphorescence studies demonstrated that electron transfer occurred from the triplet excited state of anthracene to the initiator. Further evidence for the role of the triplet state was provided by an observed 7-fold decrease in the polymerization rate upon addition of a triplet state quencher. Finally, numerical solution of the photophysical kinetic equations indicated that the triplet state concentration was approximately three orders of magnitude higher than that of the singlet state, and that 94-96 % of the active cationic centers are produced by reaction of the initiator with the triplet state. These results indicate that the electron transfer occurs primarily from the triplet state of anthracene, with the singlet state providing only a minor contribution to the photosensitization reaction.

IX.1.3. In Situ Raman Studies

Raman spectroscopy was used to monitor cationic photopolymerizations of a model divinyl ether. Using this technique complete spectra of approximately 1000 cm^{-1} were collected *in situ* during the cationic photopolymerization. Since molecular vibrations associated with the vinyl bonds are measured, the Raman technique offers a direct method for monitoring vinyl bond conversion, thereby allowing the reaction kinetics to be characterized at different temperatures and light intensities. Increases in the initiating light intensity or the reaction temperature resulted in an increased reaction rate and an enhanced limiting conversion. The apparent propagation constant exhibited an initial sharp increase and leveled off at a plateau value then decreased as a limiting conversion was reached. The propagation rate constant and activation energies obtained from the Raman studies were in good agreement with the results based upon photo-differential scanning calorimetry.

IX.1.5. Photo-Differential Scanning Calorimetry Studies

Photo-differential scanning calorimetry (PDSC) experiments were used to study a series of divinyl ether polymerizations at different temperatures. The apparent propagation rate constant, k_p, initially increased sharply, then maintained a plateau value until finally decreasing. The initial large increase in k_p was explained by a change in the reactivity of the carbocation species due to the decreased mobility of the large

hexafluoroantimonate counterion as the system viscosity increases. The separated ions are orders of magnitude more reactive than ion pairs dramatically increasing the apparent value of k_p. The final decrease in k_p arises from active center trapping which results in a limiting conversion for these highly crosslinked polymerizations.

IX.1.4. Temperature-Sensitive Luminescence Studies

The temperature-dependent luminescence of tris(β-diketone) chelates of europium was used for *in situ* temperature measurements during cationic photopolymerizations. These molecular-level luminescent probes provided a real-time, noninvasive method for monitoring temperature during these high-speed polymerizations. Two specific probes, tris(benzoyl-1,1,1-trifluoroacetone) europium and tris(1,1,1,5,5,5-hexafluoroacetyl-acetone) europium met several stringent spectral and performance requirements for application in our system. The luminescence from these probes exhibits a reproducible temperature dependence over a wide temperature range and is not sensitive to changes in viscosity. *In situ* temperature profiles obtained using this novel technique verified the importance of thermal effects during these highly exothermic photopolymerizations. These studies have demonstrated the utility of the of the europium chelates for characterizing the temperature during high-speed photopolymerizations that cannot be monitored using conventional techniques.

IX.2. Suggestions for Future Work

The experimental and analytical techniques developed for a model vinyl ether polymerization can now be used to characterize a broader range of systems which could find application as industrially relevant solvent-free coatings. Since the methods described in this thesis allow a large amount of information to be collected in a short period of time, a wide range of monomers, initiators, and photosensitizers can now efficiently and systematically be studied. To date a majority of the research on cationic photopolymerizations has focused on the development of new monomers and initiators, and there are now a wide variety of both commercially available monomers, thermally stable initiators, and photosensitizers. However, many of these cationic polymerization systems have received only cursory kinetic investigations.

To address both the scientific and industrial objectives of cationic photo-polymerizations for high speed coating systems, two criteria can be used for the selection of monomers: i) to provide fundamental information about the underlying relationships between the monomer structure and the characteristics of the polymerizations, sets of monomers whose molecule structures differ in a systematic manner were identified and ii) monomers which were deemed most promising for industrial applications. As described in detail below, future research performed in the following areas would aid in understanding cationic photopolymerizations: i) characterization of the initiation and photosensitization mechanisms for new initiator/photosensitizer combinations; ii) determination of the relationships between the monomer structure and the reaction

kinetics; iii) studies of the relationships between the monomer structure and the properties of the resulting polymers; and iv) investigations of the propagation reactions based upon linear polymerizations of monofunctional monomers.

IX.2.1. Characterization of the Photosensitization Mechanism

Several commercial cationic initiators are now available and should be investigated. These included iodonium and sulfonium salts, iron-arene complexes, and pyridinium complexes. These initiators are available commercially from a variety of sources including G.E. Silicones, Union Carbide, and Ciba Geigy. The choice of the counter ions may have a dramatic influence on the rate of the propagation reaction and the properties of the polymer film. Typical counter ions used for these systems include SbF_6, AsF_6, PF_6, and BF_4, and all four should be included in these studies. The size and acidity of the counter effects the actual propagating species during the cationic polymerization. The counter ion that produces the fastest reaction rates of is the hexafluoroantimonate, however there are potential environmental concerns associated with the heavy metal counterions (moreover, in microelectronics applications the presence of charged metal ions can have a detrimental effect on the performance of the device). Therefore, alternative counter-ions which due not contain heavy metals will be emphasized in our research. Available metal-free counter ions include trifluoro-methanesulfonate and terakis(pentafluorophenyl) borate.

Using the experimental methods described previously, the effects of the identities of the initiator and the counter ion on the observed polymerization kinetics can be

examined. In many cases differences in the observed polymerization rate are actually caused by differences in the rate of active center generation, and the efficiency of the initiator (at the wavelength of interest) is an important parameter. Since these cationic photoinitiators absorb light primarily in the deep-UV region of the spectrum, photosensitization is commonly used to shift the initiating wavelength to the near-UV or visible region. Photosensitization may occur by one of many possible mechanisms, including energy transfer, or electron transfer form the singlet or triplet excited states. An understanding of the operative photosensitization mechanism is important for both scientific and practical purposes since these reactions determine the rate of active center generation, and thereby play a pivotal role in the polymerization process.

In Chapter V, a complete set of photophysical studies demonstrated that photosensitization of diaryliodonium salts by anthracene occurs by electron transfer from the triplet excited state of the photosensitizer to the initiator. In future research, these studies could be expanded to other important initiation systems. For example, fluorescence and phosphorescence lifetime studies combined with photophysical rate calculations can now be used to characterize the photosensitization of sulfonium salts by anthracene and its derivatives. Due to the less favorable reduction potential of the sulfonium salts, the results for these systems should differ substantially form those for the iodonium salts. Measurement of the anthracene fluorescence and phosphorescence lifetimes in the presence and the absence of the initiator allow the intrinsic rates constants from these states to be determined. These rate constants, when combined with the photophysical rate expressions, allow the overall and individual rates of active center production to be determined. This analysis, which involves no adjustable parameters (all

kinetic constants are independently measured) exhibited remarkable agreement with experimental profiles of the anthracene concentration. Other photosensitizers such as pyrene and pereylene may be used to extend the initiation wavelength further into the red. Although these photosensitizers have received less attention than anthracene, they could provide important flexibility in the design of the initiating system (this flexibility may be important in systems containing dyes or pigments). Therefore, the mechanism and effectiveness of various photosensitizers can now be examined using the techniques described in previous chapters.

IX.2.2. Characterization of the Photopolymerization Reactions

Examination of the relationship between the monomer structure and the polymer characteristics by performing a series of integral studies will provide a comprehensive understanding of these complex reactions. Experiments performed in each of the following areas will provide detailed information about cationic photopolymerizations: i) the effect of the type of the reactive functionality by comparing studies performed with vinyl ethers, propenyl ethers, silicone-containing monomers, and vinylphenoxy alkanes; ii) for multifunctional monomers, the role of the chain length between reactive groups can be characterized by considering a homologous series of monomers; iii) to provide information about the propagation reaction as well as potential competing reactions, linear polymerizations of monovinyl ethers can now be performed so that the resulting polymers may be analyzed in detail using techniques that require dissolution. For each of these experiments the polymerizations kinetics will be characterized using *in situ*

fluorescence, Raman and Photo-Differential Scanning Calorimetry (PDSC) methods describe previously in this thesis, and the polymer properties can be characterized using standard techniques.

IX.2.3. Relationships between the Monomer Structure and the Reaction Kinetics

Three of most exciting classes of monomers which undergo cationic photopolymerizations are vinyl ethers, propenyl ethers, and silicone-containing monomers (epoxides and vinyl ethers). Studies with each of these monomers to determine the precise role of the reactive group on the polymerization kinetics can now be performed. While it is clear that each of these groups polymerize very rapidly, detailed kinetic studies are currently unavailable for most of these monomers. Fundamental studies of highly purified systems can eliminate the effects of impurities (if present these impurities could obscure the comparisons between monomers). In addition, for industrially-relevant systems studies can be performed without additional purification to characterize the reaction kinetics under typical industrial conditions. Together these studies will allow the kinetic effects of any of residual impurities to be determined.

Directly monitoring the consumption of the reactive (unsaturated) functionalities using *in situ* Raman spectroscopy, is ideally suited for these studies not only because it is a direct method, but also because it offers appropriate time resolution and allows the sample temperature to be controlled. In addition, because the technique provides a spectrum rather than the intensity at a single wavelength, information may be obtained from more than one spectral feature. For each monomer under consideration, Raman cure

profiles can now be obtained at a series of temperatures as described in Chapter VI. These Raman experiments provide a direct measure of conversion as a function of time and may be combined with the photosensitizer studies (which provide active center concentration as a function of time) to evaluate the effective propagation rate constant throughout the reaction. These studies provide fundamental kinetic information which may be applied in a variety of reaction conditions, including industrial processes. Using the thermostated sample cell, studies can be performed at a variety of temperatures, and the activation energies for overall polymerization, propagation, and photosensitization determined. These investigations would provide important information on the influence of the monomer structure on the activation energies. This is particularly important due to the highly exothermic nature of these reactions.

IX.2.4. Effect of Multifunctional Monomer Structure on Limiting Conversions

In polymerizations of multifunctional monomers a limiting conversion significantly less than unity is typically observed due to the restricted mobility of the pendent functionalities and the associated trapping of active centers. This limiting conversion can have a substantial effect on the polymer properties, therefore it is important to understand and control this effect. In future work, two different approaches can be used to characterize and control the limiting conversion. First, for homo-polymerizations of multifunctional monomers, the role of the chain length between reactive groups may be characterized by considering several homologous series of

monomers. In these studies three distinct systems would be characterized: a series of oligomeric ethylene glycol divinyl ethers, a series of alkylvinyl ethers, and a series of bis(vinylphenoxy)alkanes. In a second set of studies copolymerizations of multi-functional monomers with monofunctional monomers (containing one polymerizable moiety) will be investigated. The addition of the monofunctional monomers will increase the maximum attainable conversion due to the enhanced mobility in these systems.

In this thesis, the homopolymerizations of the monomer 3,6,9,12-tetra-oxatetradeca-1,13-diene (DVE-3) has been extensively characterized. This monomer contains two polymerizable vinyl ether functionalities separated by a chain of three ethylene glycol groups. A series of DVE monomers containing two to six ethylene glycol units between the reactive functionalities is now commercially available. This homologous series of monomers would allow the role of the chain length between reactive groups to be characterized. It is anticipated that the maximum attainable conversion will increase as the separation between reactive functionalities is increased (due to the enhanced mobility of the pendent functionality), and may influence the reaction kinetics as well. These studies will be performed using the Raman scattering technique described previously, and the results obtained from the spectroscopic techniques will be compared with results obtained using photo-differential scanning calorimetry (PDSC) in order to corroborate the results. In addition, similar studies can be performed for two other homologous series of cationically polymerizable monomers: bis(vinylphenoxy)alkanes (alkoxy-styrene units connected by alkane units of varying lengths[55]); and alkylvinyl ethers (divinyl ethers in which the reactive functionalities are separated by alkyl chains).

In the second set of studies, copolymerizations of multifunctional monomers with monofunctional monomers may be investigated using the Raman scattering technique. The maximum attainable conversion of mixtures of mono and di-functional monomers should increase due to the more flexible network structure, and may create a substantial effect on the overall polymerization kinetics. Monomers such as cyclohexanedimethanol monovinyl ether (CVE) and 1,4-bis[vinyloxy methyl]-cyclohexane (CHVE) should have very similar intrinsic reaction rates and should therefore provide information on limiting conversion due to changes in monomer structure. This strategy could provide an industrially feasible method for controlling the limiting conversion.

IX.2.5. Relationships between the Monomer Structure and Polymers Properties

In addition to the kinetic studies described above, experiments can be performed to establish the relationship between the monomer structure and the properties of the resulting polymer films. A complete characterization of the thermal properties of the polymer films may be obtained using the differential scanning calorimeter (DSC), thermal gravimetric analysis (TGA), and thermal mechanical analysis (TMA) instruments available at the Composite Materials and Structures Center (CMSC) at Michigan State University. These experiments will allow the glass transition temperature (if any) the degradation temperature, and the expansion coefficient of each film to be established. The mechanical properties of the films can be thoroughly investigated using a Rheometrics RMS 800 Dynamic Mechanical Analyzer (again available at the CMSC). Using standard procedures, this technique may be used to measure the loss and storage

moduli of the films for a spectrum of frequencies. The results of these experiments will be correlated with the kinetic studies to establish the effects of polymerization conditions, and polymer characteristics such as residual vinyl bond concentration, on the thermal and mechanical properties of the polymers.

IX.2.6. Investigations of the Propagation Reactions Based upon Linear Polymerizations

Further insight into the characteristics of these cationic photopolymerizations can be provided by a series of experiments performed with linear polymerizations of monofunctional monomers. Crosslinked polymers cannot be characterized using many traditional experiment techniques which require dissolution of the sample. However the linear polymerizations of the monofunctional monomers produce polymers which may be analyzed using traditional techniques such as gel permeation chromatography (GPC) and solution-state NMR. These techniques may allow mechanistic questions such as the extent of chain transfer, and the occurrence of possible side reactions to be answered. For example, the GPC analysis of the resulting linear polymers will allow the primary chain length to be determined and will provide information about the extent of chain transfer (which results in shorter chain lengths). One possible side reaction is acetal formation in cationic polymerizations of vinyl ethers. Solution-state NMR can be used to determine the extent of acetal formation in these systems. Several monofunctional vinyl ether monomers have recently become commercially available and can now be used for these

studies. These monomers include propenyl ether of propylene carbonate (PEPC), cyclohexanedimethanol monovinyl ether (CVE) and hydroxybutyl vinyl ether (HBVE).

IX.2.7. Effect of Light Source and Intensity

The rate of cationic photopolymerization of divinyl ethers has been shown to be very sensitive to the intensity of the initiation source. However, more detailed systematic studies of this effect need to be performed. Since the number of active centers produced per unit time may influence the network structure, the intensity of initiation will effect the overall performance of the coating material. Therefore, the kinetic monitoring techniques described in this work can be used to investigate the effect of intensity on different monomer, initiator and photosensitizer systems.

IX.2.8. Swelling Studies

The swelling properties and chemical resistance of each film may be thoroughly characterized using a variety of solvents, including water, methanol and methyl ethyl ketone. The equilibrium weight fraction of each solvent absorbed by the films can be determined. Any change in the properties of the films upon exposure to the solvents may then be thoroughly characterized. Furthermore, the extractable weight fraction of each sample should be determined. These experiments involve swelling the polymers in solvent for several days or even weeks to allow any extractable fraction to diffuse out of the polymer network, then drying the samples to constant weight. Upon removal of the

extractables, the thermal and mechanical properties of the films can again be characterized to monitor any changes.